An Investigation of the Properties of Bacteriophage M13 and the Implications for Its Large-Scale Bioprocessing

A thesis submitted to University College London
for the degree of Doctor of Philosophy

By Steven David Branston

2009

Department of Biochemical Engineering
University College London (UCL)
Torrington Place
London
WC1E 7JE

I, Steven David Branston, confirm that the work presented in this thesis is my own. Where information has been derived from other sources, I confirm that this has been indicated in the thesis.

Signed…………………..……

Date………………..…………

Acknowledgements

Abstract

Bacteriophage are a diverse class of viruses that infect bacterial cells. As a result of over 60 years of molecular biology advances, bacteriophage today feature as candidates for vaccination, gene therapy, biomaterial and antibacterial purposes. Consequently, scientific, commercial and public awareness of bacteriophage is growing rapidly. There is now an increasing need for the establishment of strong biochemical engineering foundations to serve as a guide for future bacteriophage bioprocessing. It has been the purpose of this study to contribute towards this knowledge base, by understanding the properties of the filamentous bacteriophage M13. Ultimately, this work has aimed to allow for the more efficient assembly of a large-scale production process.

By the application of well-understood small-scale predictive techniques, it has been found that bacteriophage M13 should not be severely damaged by hydrodynamic shear forces of the duration and magnitude imparted by fermentation, pumping or continuous centrifugation operations. Thus, it may well be possible to manufacture on the large-scale using existing large-scale equipment designs.

Amongst bacteriophage, the reproduction strategy of M13 is unusual in that propagation occurs by the non-lethal extrusion of progeny through the cell wall of the *E. coli* host. Investigation of bacteriophage M13 propagation indicated that growth in a medium that increased host cell density concomitantly increased bacteriophage yield; a four-fold increase to 2×10^{12} pfu ml^{-1} was achieved. At the end of culture, concentrations of supernatant DNA and protein contaminants were found to vary amongst three *E. coli* strains studied.

Post-fermentation, bacteriophage M13 can be precipitated from the cell-free process fluid by as little as 2 % (w/v) PEG 6 000 plus 25 mM magnesium sulphate, or by isoelectric precipitation. Purification factors in excess of 100 were achieved by PEG-salt precipitations with regards to the reductions in DNA and protein concentrations.

Methods used in this study have increased the processing knowledge of bacteriophage M13 and have a broader applicability to both derivatives of M13 and other bacteriophage.

Table of Contents

List of Figures

16

List of Tables

Nomenclature

A_{260}	Absorbance at 260 nm
bp	Base pairs
cfu	Colony forming units
C_0	Initial viable bacteriophage concentration (pfu ml^{-1})
C_t	Viable bacteriophage concentration at time t (pfu ml^{-1})
CER	Carbon dioxide evolution rate (mmol l^{-1} hr^{-1})
ds	Double-stranded (DNA)
Da	Daltons
DCW	Dry cell weight (g l^{-1})
DOT	Dissolved oxygen tension (%)
g	Gravitational acceleration (m s^{-2})
I	Current (A)
K	Bacteriophage decay rate constant (min^{-1})
m	Linear gradient (Chapter 7, days^{-1})
MOI	Multiplicity of infection
N	Number of experimental repeats
OC	Open circular (DNA)
OD_{600}	Optical density at 600 nm
OUR	Oxygen uptake rate (mmol l^{-1} hr^{-1})
P	P value (probability)
P	Power input (W)
pfu	Plaque forming units
pK_a	Acid dissociation constant
pK_b	Base dissociation constant
r	Disc radius (m)
rps	Revolutions per second
r_t	Disk radius at the laminar-turbulent flow transition
R	Disc radius (m)
Re	Reynolds number
RF1	Bacteriophage M13 DNA, Replicative Form 1 (double-stranded, supercoiled)
RO	Reverse osmosis water
ss	Single-stranded (DNA)
SC	Super-coiled (DNA)

t	Time (mins)
T	Applied torque (kg m^2 s^{-2})
$T_{0.5}$	Half-life (days)
V	Voltage (V)
V_b	Volume of the boundary layer (m^3)
Z	Net protein charge

Greek letters

δ	Boundary layer thickness (m)
δ_{lam}	Laminar flow boundary layer thickness (m)
δ_{max}	Maximum boundary layer thickness (m)
δ_{turb}	Turbulent flow boundary layer thickness (m)
ε	Energy dissipation rate (W kg^{-1})
ε_{max}	Maximum energy dissipation (W kg^{-1})
μ	Fluid viscosity (Pa s)
ν	Kinematic viscosity (m^2 s^{-1})
ρ	Density (kg m^{-3})
π	Pi (3.141)
θ	Angle (radians)
ω	Angular velocity (rad s^{-1})
τ_{max}	Maximum shear stress (Pa)
υ_{∞}	Tangential tip velocity (m s^{-1})

1   Introduction

1.1   Project Significance

Bacteriophage-based products offer promise of a new generation of antimicrobial treatments, vaccines and gene therapy. There have been numerous discoveries and proof-of-concept demonstrations in recent years (Hagens *et al.*, 2006; Lankes *et al.*, 2007; Lee *et al.*, 2009; Solomon, 2008; Wright *et al.*, 2009), and several companies exist in the UK and aboard to commercialize many of these findings (Housby and Mann, 2009). But the industry is very much in its infancy. On the road from discovery to market, a key challenge is the application of biochemical engineering principles to translate production of novel therapeutics from the laboratory to the large-scale process (Levy *et al.*, 2000b). To be effective, a production process must manufacture bacteriophage in a rapid, robust and cost-effective manner whilst maintaining the quality of the product. Furthermore, an understanding of the process at a fundamental level is becoming ever more crucial, as regulatory bodies such as the USA Food and Drug Administration and the European Medicines Agency (EMEA) increase pressure on the industry to fully understand their processes, and for early stage material to be more representative in quality to that of final manufacture (Lionberger *et al.*, 2008; Rathore and Winkle, 2009).

The filamentous bacteriophage M13 features as a tool in several lines of investigation (Hagens and Blasi, 2003; Lee *et al.*, 2009; Meola *et al.*, 1995; Solomon, 2008), but if these concepts were to come to fruition, limited literature currently exists specifically contributing towards its large-scale manufacture (Grieco *et al.*, 2009; Ling *et al.*, 2004; Smith and Gingrich, 2005). There is therefore much to understand about the large-scale production of this bacteriophage and its processibility at a fundamental level. Work to contribute towards the biochemical engineering knowledge of these entities would be timely.

Bacteriophage are relatively novel bioproduct entities and vary enormously in physical form and biological action. Understanding their form and manner of replication is fundamental to bioprocess design. This thesis concerns bacteriophage M13, which will be described in terms of its physical structure and replication strategy in the following pages. The relevance of bacteriophage as bioproducts will be discussed: today, bacteriophage-based therapeutics cover a broad spectrum of applications. Focusing on the manufacturing considerations of bacteriophage M13, an outline of potential strategies for its upstream production and downstream purification will be introduced. Drawing together the information presented thus far, the objectives of this thesis will be described.

1.2 Introduction to Bacteriophage

Bacteriophage are a class of viruses whose hosts are bacterial cells. Like all viruses, bacteriophage exist in a metabolically inert extracellular state and reproduce only upon infection of a suitable host cell. Their discovery is credited to two researchers, Twort and d'Herelle, who independently identified these agents of bacterial lysis in the early twentieth century (d'Herelle, 1917; Twort, 1915). Like bacteria, bacteriophage are ubiquitous in the environment, and, for every prokaryote group identified, almost invariably a corresponding bacteriophage has been isolated. Bacteriophage exhibit a variation and versatility as great as their hosts: therefore a level of caution is necessary when making generalisations about their behaviour.

1.2.1 Bacteriophage structural diversity

All bacteriophage carry a genome encased within a protein coat, although genomes may consist of single or double-stranded DNA or RNA, and may be circular or linear in form. Similarly, the protective protein coat (or capsid) displays a high level of morphological variety. As may be expected, bacteriophage classification is somewhat difficult and is chiefly defined by the physical morphology of the particle and the nature of the genome present (Ackermann, 2005). Broadly, bacteriophage are grouped into "tailed" or "tail-less" categories, referring to a common virion structure. The physical appearance of three bacteriophage which share *Escherichia coli* as a host is shown in Figure 1.1. The diversity of their physical forms is apparent: whereas bacteriophage R17 and λ both possess an icosahedral capsid, only λ displays a tail structure. In contrast, bacteriophage M13 appears as a semi-flexible tube several times longer than either R17 or λ.
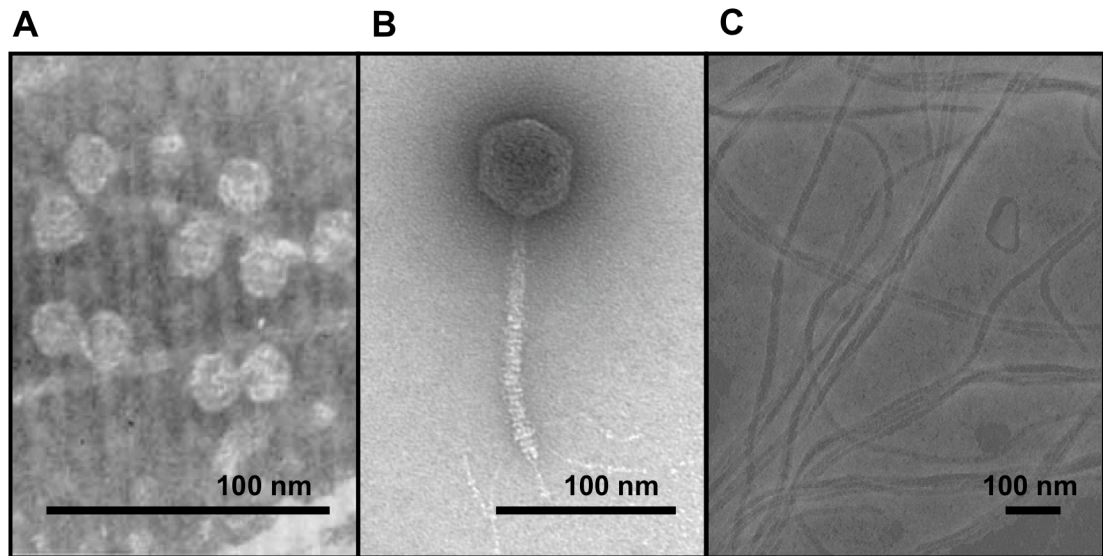
Figure 1.1 Transmission electron micrographs of three bacteriophage of *E. coli*. (A) shows a cluster of bacteriophage R17 attached to an *E. coli* F pilus, reproduced from Schmidt (1966). (B) shows a single bacteriophage λ, image available online (Inman, 2005). (C) shows the long thin filamental structure of several bacteriophage M13, image by this author.

1.2.2   The filamentous structure of bacteriophage M13

Bacteriophage M13 was first discovered in the sewers of Munich in 1963 (Hofschneider, 1963). It is one of several related filamentous bacteriophage, the other most commonly encountered being fd and f1. The genomic differences between M13, fd and f1 are slight and the particles are indistinguishable in appearance (Russel *et al.*, 2004). Collectively, they are known as Ff bacteriophage. Each M13 particle contains a 6.6 kb single-stranded DNA genome containing nine genes which encode for eleven proteins. Five of these proteins (pIII, pVI, pVII, pVIII, pIX) form the bacteriophage coat, the other six being required for DNA replication and bacteriophage assembly (Table 1.1). As noted in Figure 1.1, the defining characteristic of M13 is its filamentous appearance: 900 nm in length and 6.5 nm in diameter (Berkowitz and Day, 1976; Model and Russel, 2006). Figure 1.2 shows a schematic diagram of an M13 particle, where each of the five coat proteins is labelled. The bulk of the coat is made from approximately 2 700 copies of pVIII, a 5 kDa protein which has been shown to be arranged in an overlapping helical-pitched cylinder about the single-stranded DNA core (Overman *et al.*, 1996). The DNA genome runs almost the entire length of the particle (Makowski, 1992). Each end of the particle is "capped" by other coat proteins. Approximately five copies each of pVII (approximately 3.6 kDa) and pIX (3.5 kDa) form the so-called "distal" tip of the virus, while five each of pIII (approximately 45 kDa) and pVI (13 kDa) form the "proximal" tip (Endemann and Model,

1995; Russel *et al.*, 2004). It is the proximal tip of bacteriophage M13 that interacts with the *E. coli* cell wall to initiate infection.

Table 1.1 The nine genes of Ff filamentous bacteriophage encode for eleven proteins. Five proteins form the bacteriophage coat whilst six are required for DNA replication and bacteriophage assembly. The location of each protein in the *E. coli* host or on the bacteriophage particle are given. Adapted from Russel *et al.* (2004).

Gene	Protein	Function	Location
gI	pI	Assembly	Inner membrane
	pXI	Assembly	Inner membrane
gII	pII	Replication (nickase)	Cytoplasm
	pX	Replication	Cytoplasm
gIII	pIII	Coat component	Proximal tip
gIV	pIV	Assembly (exit channel)	Outer membrane
gV	pV	Replication (ssDNA bp)	Cytoplasm
gVI	pVI	Coat component	Proximal tip
gVII	pVII	Coat component	Distal tip
gVIII	pVIII	Coat component	Virion filament
gIX	pIX	Coat component	Distal tip
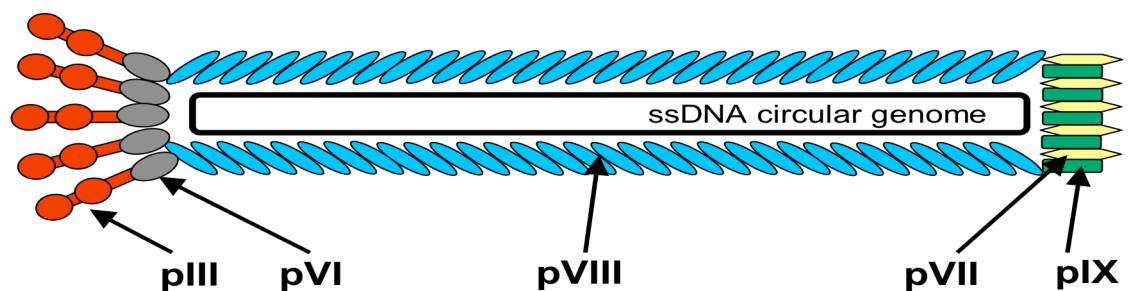
Figure 1.2 A schematic diagram of a single M13 bacteriophage. The labels indicate the location of each of the five proteins that constitute the bacteriophage coat. Packaged within the coat is a circular single stranded (ss) DNA genome.

1.2.3 General principles of bacteriophage replication

The replication cycles of bacteriophage are very different to their bacterial hosts and can typically be characterised by four distinct phases: adsorption, infection, multiplication and release (Guttman *et al.*, 2005). The adsorption phase is dependent on the presence of specific receptors on the surface of the bacterial host cell, to which the bacteriophage can attach (Kutter *et al.*, 2005). The bacteriophage is brought to the host receptor by random diffusion. Following adsorption, the infection phase occurs as the bacteriophage genome passes into the host cell by a mechanism likened to injection (Kutter *et al.*, 2005). Post-infection, the onset of the multiplication phase is dependent on the bacteriophage species. In the so-called lytic replication cycle (that is, bacteriophage production will culminate in the lysis of the host cell), the multiplication phase begins immediately. Normal host metabolism ceases as replication of the bacteriophage genome and synthesis of virion proteins occupy the host cell's synthetic machinery (Guttman *et al.*, 2005). Progeny virion particles are systematically assembled in controlled stages inside the host cytoplasm (Shors, 2008). When this process is complete the final "release" phase occurs, where the host cell is lysed from within to release the newly constructed progeny bacteriophage in a single burst.

The temperate cycle (also known as lysogeny) is an alternative replication strategy that also begins with adsorption and infection, but instead of entering the multiplication phase the bulk of bacteriophage-specific transcription slows to a halt whilst the bacteriophage DNA is maintained within the host cell as the cell divides and multiplies (Birge, 2000). The bacteriophage DNA can become integrated into the host genome and persist there indefinitely, replicating alongside the host cell genome as a heritable DNA segment (Campbell, 2006). An environmental trigger can induce the expression of the bacteriophage lytic genes from the bacteriophage DNA, through (for example) stimulation of the host cell SOS response (Little, 2006). The replication cycle therefore enters the multiplication phase, producing progeny as described in the lytic pathway. The well-studied bacteriophage λ has the ability to undergo the lytic and temperate cycles (Little, 2006).

The replication strategy of M13 and other filamentous bacteriophage is an exception because the bacteriophage undergo neither a lytic nor a temperate cycle. As in the lytic cycle, bacteriophage multiplication begins immediately upon infection (Calendar and Inman, 2005). Crucially however, normal host cell processes are not shut down upon infection and progeny are not released in a single cell lysis event. Instead, progeny bacteriophage are continually assembled at, and extruded through, the cell wall into the milieu (Russel *et al.*, 2004). The host cell is not killed and in fact continues to divide, albeit at a reduced rate (Salivar *et al.*, 1964). Figure 1.3 shows a transmission electron micrograph of an *E. coli* cell infected with the

filamentous bacteriophage ZJ/2, a relative of bacteriophage M13. Many progeny bacteriophage can be observed in the process of being extruded through the cell wall (Bradley and Dewar, 1967).
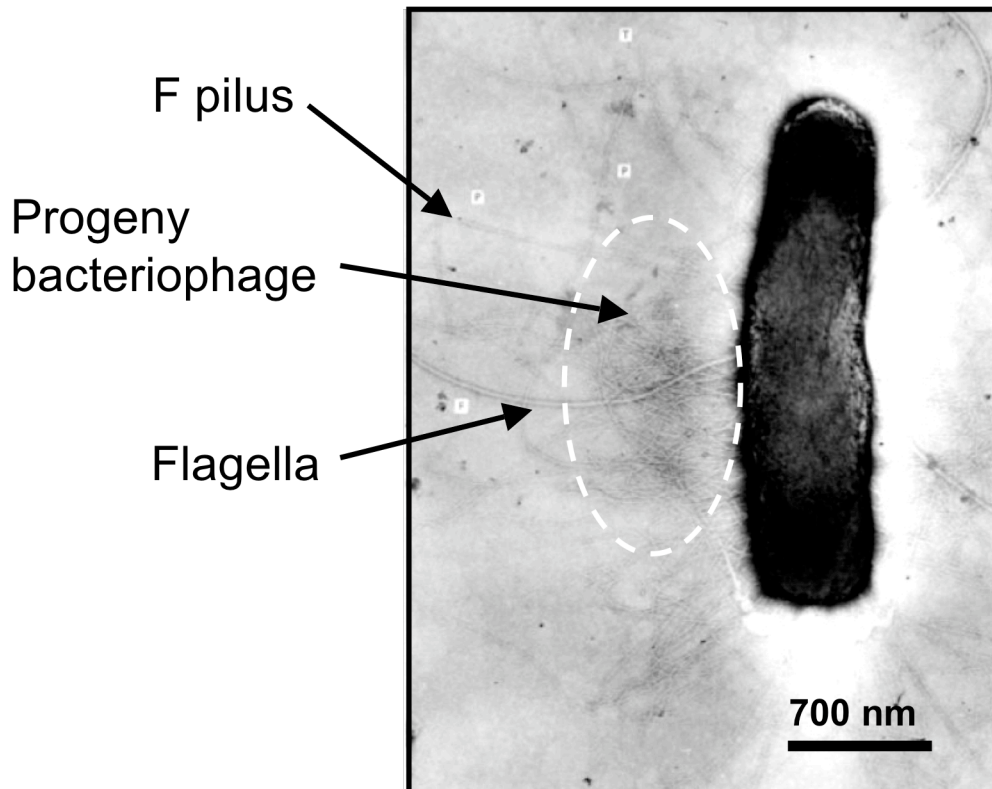
Figure 1.3 A transmission electron micrograph of an *E. coli* cell infected with filamentous bacteriophage ZJ/2, a close relative of bacteriophage M13. The largest filaments observed are flagella, the thinner ones F pili. The shorter, thin filaments clustered around the bacterium are the bacteriophage. Reproduced from Bradley and Dewar (1967).

1.2.4   The replication of bacteriophage M13

A schematic diagram summarising the essential steps of bacteriophage M13 replication is shown in Figure 1.4. The absorption phase of M13 replication begins upon the diffusion of an infective particle to the tip of an *E. coli* F pilus. Only *E. coli* cells holding the F-plasmid express the F pilus, therefore bacteriophage infection is limited to those cells. It is the pIII protein at the proximal end of the bacteriophage particle that adsorbs onto the tip of the F pilus, which is then retracted by a mechanism that is not yet fully understood (Model and Russel, 2006). Upon reaching the cell wall the pIII protein interacts with the bacterial Tol protein complex, allowing bacteriophage protein coat depolymerisation and injection of DNA into the cytoplasm (Pommier *et al.*, 2005). Thus the infection phase occurs.

The multiplication phase begins with the conversion of the single-stranded M13 DNA (the "positive" or "+" strand) into a supercoiled double-stranded replicative form (RF) by host RNA and DNA polymerases and topoisomerase (Russel *et al.*, 2004). The RF serves as the template for bacteriophage gene expression, which is necessary for further replication (particularly the synthesis of bacteriophage protein pII). M13 DNA replication proceeds by a modified rolling circle mechanism, beginning with a nick on the + strand origin by bacteriophage protein pII (a site-specific nicking-closing enzyme). Extension of the 3' end of the nick is made by *E. coli* DNA polymerase III using the negative (−) strand as a template. The original + strand is displaced by *E. coli* Rep helicase as the new is synthesised, and when the process is complete the displaced positive strand is recircularised by pII and converted into more RF DNA. Thus, as this process is repeated for all newly synthesized RFs, the level of RF, and consequently synthesized bacteriophage protein, increases (Russel, 1995).

The accumulation of RF DNA continues until critical concentrations of proteins pX and pV are reached. In particular, several copies of pV bind to newly generated + strands to form single-stranded DNA-pV complexes, blocking their conversion to RF DNA. The sequestered + DNA strands are earmarked for bacteriophage assembly at the *E. coli* cell membrane (Birge, 2000).

The release phase of bacteriophage M13 replication can be described as progressing in five stages: pre-initiation, initiation, elongation, pre-termination and termination. Pre-initiation encompasses the formation of an assembly site at the cell wall; a composition of three bacteriophage proteins pI, pXI and pIV at a point where the cytoplasmic and outer membranes are in close contact. The channel (through which the assembling bacteriophage passes) is formed by protein pIV (Russel *et al.*, 2004). Initiation occurs when the assembly site, a single-stranded DNA-pV complex and distal coat proteins pVII and pIX are present (Feng *et al.*, 1999). It is thought that an exposed region of DNA from the single-stranded DNA-pV complex (known as the "packing signal", or PS) interacts with the membrane-bound bacteriophage proteins pVII and pIX to initiate assembly and form the distal end of the bacteriophage particle (Russel and Model, 1989). During the elongation stage the single-stranded DNA genome translocates the cell wall. On the cytoplasmic side, pV is progressively shed from the DNA as it enters the pIV channel, whilst pVIII proteins are added in a helical array to form the bulk of the bacteriophage protein coat (Webster and Lopez, 1985). The pre-termination stage occurs once translocation of the DNA is almost complete. Five copies each of proteins pIII and pVI are incorporated to form the proximal end of the extruded bacteriophage particle. The complete M13 virus is then released from the cell wall.
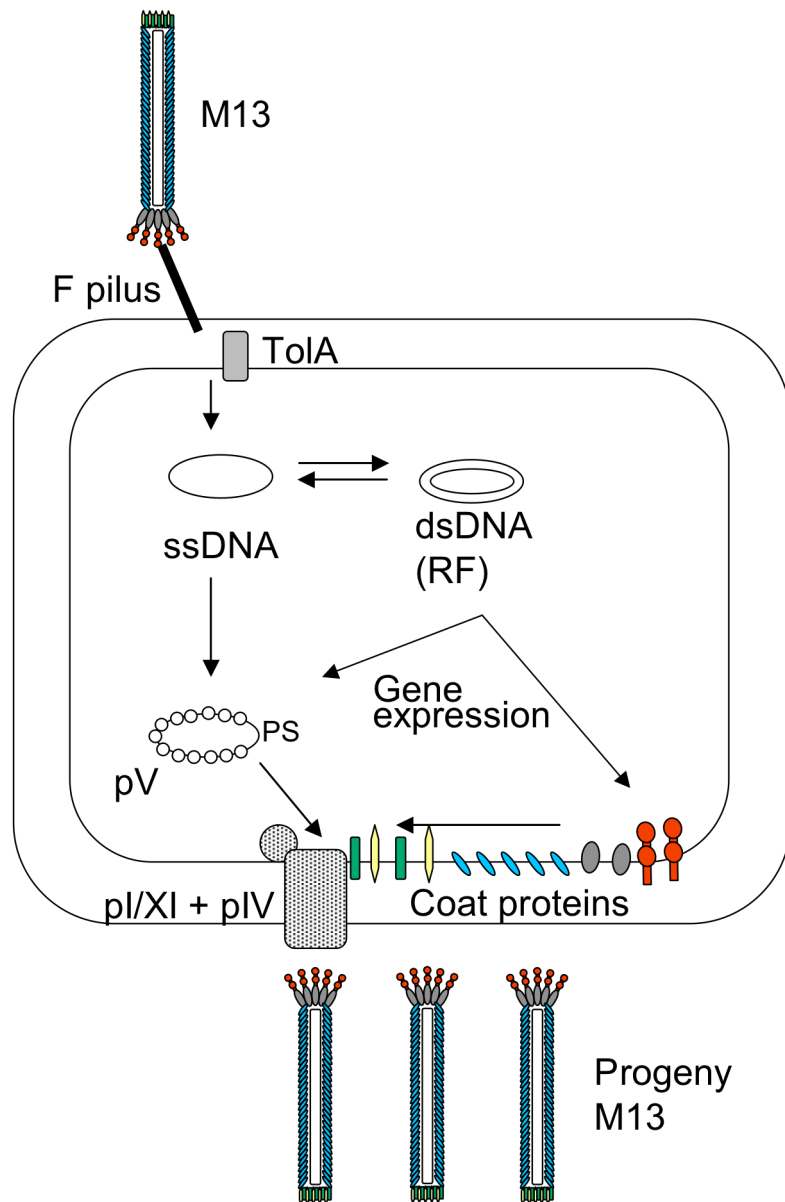
Figure 1.4 A schematic drawing outlining the lifecycle of the M13 bacteriophage. Infection begins with the binding of the pIII coat protein to the tip of an F pilus, causing retraction, followed by interaction with the Tol protein complex. Accumulation of bacteriophage protein and RF DNA then occurs until sufficient pV is synthesized to sequester newly generated ssDNA from further RF DNA creation. The packing signal (PS) – a region of DNA protruding from ssDNA-pV complex – interacts with bacteriophage coat proteins pVII and pIX at the assembly site (pI/XI and pIV) to initiate bacteriophage assembly. Progeny bacteriophage are produced and continuously extruded in a non-lethal mechanism.

1.3 Techniques Underpinning Bacteriophage Use as Bioproducts

The exploitation of bacteriophage as antimicrobial bioproducts first occurred soon after their discovery in the early 20th century. However, potential applications of bacteriophage today spread far beyond antimicrobial use, built upon over 60 years of advances made in the field of molecular biology. Therefore, the techniques underpinning modern bacteriophage-based bioproducts display diversity too.

1.3.1 Bacteriophage use in infection control: bacteriophage therapy

Since bacteriophage infection typically results in the death of the host bacterial cell, their use as antimicrobial agents has long been recognised. Indeed, the first known applications of bacteriophage to treat bacterial disease are reported to date back to within five years of their discovery (Sulakvelidze *et al.*, 2001).

The treatment of bacterial disease by bacteriophage is known as phage therapy. Early work focused on the treatment of humans (Asheshov *et al.*, 1937; Burnett *et al.*, 1930; Walker, 1929), although modern studies have demonstrated bacteriophage antimicrobial action in animals (Smith *et al.*, 1987), aquaculture (Nakai and Park, 2002), food products (Carlton *et al.*, 2005) as well as humans (Sulakvelidze and Kutter, 2005). Almost all trials utilize naturally occurring *lytic* bacteriophage for treatment, although success with genetically modified variants has been demonstrated (Fairhead *et al.*, 2009; Westwater *et al.*, 2003).

The route of bacteriophage application is as varied as the uses themselves. Surface microbial decontamination of food and animals has been simply accomplished by bacteriophage solution wash or spray (Carlton *et al.*, 2005; Smith *et al.*, 1987) whilst intraperitoneal or intramuscular injection into animals has been conducted (Barrow *et al.*, 1998; Nakai and Park, 2002). Meanwhile, phage therapy treatment of humans has included the topical, oral and intravenous routes (Sulakvelidze and Kutter, 2005).

A defining characteristic of phage therapy is that the quantity of bacteriophage required for successful microbial control can be many times less than the number of target organisms: bacteriophage replication can occur *in vivo*, and is self-limiting (Smith and Huggins, 1982). That is, once the target bacteria are all infected and lysed, replication ceases and remaining bacteriophage are removed by the immune system. However, the host immune response to systemic bacteriophage (as opposed to oral or topical) has raised important questions concerning the repeated applicability of bacteriophage therapy intravenously: bacteriophage are immunogenic and therefore elicit an antibody response (van Houten *et al.*, 2006). Consequently, debate exists as to whether *in vivo* bacteriophage therapy can be used repeatedly or for prolonged periods for each patient (Clark and March, 2006). Perhaps accordingly, many modern

studies have focused on the topical or oral application of bacteriophage (Bruttin and Brussow, 2005; Wright *et al.*, 2009) or agriculture situations where repeated dosage is unlikely (Fiorentin *et al.*, 2005; Wagenaar *et al.*, 2005).

A second important characteristic distinguishing phage therapy from antibiotics use is the specificity that bacteriophage exhibit for a target bacteria (Birge, 2000). This specificity is quite unlike the broad spectrum action of antibiotics. Therefore, phage therapy often uses so-called bacteriophage *cocktails*, where more than one bacteriophage type is applied concurrently (Smith and Huggins, 1983; Wright *et al.*, 2009).

1.3.2   Bacteriophage as molecular biology tools

Scientific understanding of the structure and lifecycle of bacteriophage was pioneered in the middle of the 20th century (Doermann, 1952; Ellis and Delbruck, 1939; Luria, 1945), and laid the basis for the development of molecular biology. Bacteriophage have subsequently been exploited as model systems, aiding our primary understanding of DNA, the genetic code and the molecular mechanisms of gene regulation (Summers, 2005). Bacteriophage-derived enzymes including DNA polymerase (bacteriophage T4, T7) RNA polymerase (T3, T4, SP6) and DNA ligase (T4) are now widely and routinely exploited as molecular biology tools (Marks and Sharp, 2000). Further advances in molecular biology have resulted in the development of bacteriophage as expression vectors for the display of foreign gene products on the bacteriophage surface. This so-called *phage display* technique was first demonstrated in 1985 (Smith) on bacteriophage M13, although the technique has been successfully applied to bacteriophage λ and others (Cicchini *et al.*, 2002; Danner and Belasco, 2001; Heal *et al.*, 1999). The expression of foreign gene products (such as antibody fragments) on the bacteriophage coat confers whole new functionalities to these molecules, and as a result this technology now underpins many of the modern applications of bacteriophage.

1.3.3   Phage display technology

A phage display construct is generated by the insertion of DNA encoding for a foreign (heterologous) protein into the bacteriophage genome. This DNA is added as a transcriptional fusion to one of the coat protein genes, meaning that progeny bacteriophage subsequently express the heterologous protein as a surface fusion to the corresponding coat protein.

For bacteriophage M13, this technique has allowed the display of heterologous proteins on all five coat proteins, although by far the most commonly used are coat proteins pVIII and pIII (Russel *et al.*, 2004). A fusion to these coat proteins is not consequence-free, however: peptides longer than six residues fused to every pVIII heavily decreases phage viability (Iannolo *et al.*,

1995), while substantial fusions to pIII can reduce infectivity. Nevertheless the pIII coat protein can generally tolerate much larger phage display fusions, up to 100 residues (Baek *et al.*, 2002).

A common approach to solve both these issues is to supply an excess of wild-type coat proteins to the host cell, usually via the superinfection of the host cell by a *helper* bacteriophage. The foreign DNA-coat protein fusion is instead expressed from a *phagemid* vector within the infected host, which contains both plasmid and bacteriophage replication origins, but no other bacteriophage genes (Russel *et al.*, 2004). The resulting progeny bacteriophage have only a few copies (and sometimes none) of the fused coat protein each. Due to their smaller genome packaged within, the progeny are also shorter in length than wild-type bacteriophage M13 (Khalil *et al.*, 2007). The mainly wild-type protein coat confers greater stability to the phage particle and allows the display of larger polypeptides: for pVIII the maximum fusion size increases from 7-8 residues to beyond 25 kDa (Corey *et al.*, 1993; Intasai *et al.*, 2003).

The phage display technique is closely associated with the generation of random peptide "libraries", where DNA of interest is fragmented and randomly cloned into phagemid vectors, again as transcriptional fusions to a bacteriophage coat protein (Mullen *et al.*, 2007). Subsequent screening of the library allows for the selection of bacteriophage with fusions that exhibit binding to specific antibodies, receptors or even inorganic materials of interest (Frenkel *et al.*, 2003; Poul and Marks, 1999; Whaley *et al.*, 2000). Further, DNA sequencing of the insert to the bacteriophage genome then allows for the rapid identification of the amino acid sequence of the fusion of interest.

As mentioned previously, the phage display technique is not limited to filamentous bacteriophage such as M13. Other bacteriophage successfully displaying proteins on their surfaces include bacteriophage λ (Cicchini *et al.*, 2002), T7 (Danner and Belasco, 2001) and MS2 (Heal *et al.*, 1999).

1.3.4   Gene delivery utilizing bacteriophage

Developed using the technique of phage display, bacteriophage (both filamentous and lytic) now show applicability in the field of gene delivery (Hart *et al.*, 1994; Larocca *et al.*, 2001; Liang *et al.*, 2006; Zanghi *et al.*, 2005). Phage display enables the expression of specific surface molecules on bacteriophage that cause binding to mammalian receptors (Legendre and Fastrez, 2002). The scientific advance lies in the additional insertion of mammalian promoter and reporter genes into the bacteriophage genome for transcription within the mammalian cell: successful internalisation and expression of reporter genes GFP (Poul and Marks, 1999) and luciferase (Lankes *et al.*, 2007) have been demonstrated. In a related approach not necessarily requiring phage display, the use of bacteriophage as vehicles for DNA vaccine delivery has

been reported (Clark and March, 2004a; March *et al.*, 2004). Here, bacteriophage uptake is by antigen-presenting cells. Once engulfed and the protein coat broken down, the DNA is freed and the vaccine expression cassette is transcribed, resulting in vaccine protein expression.

1.4 Examples of Bacteriophage-Based Bioproducts

Clinical and food-related investigations of bacteriophage technology can be broadly categorised into the major areas of antibacterial action, vaccination and gene therapies. Further niche applications of bacteriophage include use as groundwater tracers (Harvey, 1997), as bio-defence agents and as bacterial diagnostic tools (Petrenko and Vodyanoy, 2003). Although many of the technologies described are in early stages of development, the breadth and depth of innovation in the field suggest that studies contributing the large-scale production of these entities are timely.

1.4.1 Bacteriophage therapy

Bacteriophage therapy became a major area of research interest the early 20th century (Asheshov *et al.*, 1937; Burnett *et al.*, 1930; Walker, 1929), some way before a thorough scientific understanding of bacteriophage structure and lifecycle was gained (Doermann, 1952; Ellis and Delbruck, 1939; Luria, 1945). Many early studies correspondingly reported failure (Davison, 1922; Morrison, 1932), and it is thought that a poor understanding of bacteriophage behaviour contributed to the mixed results achieved (Barrow, 2001; Chanishvili *et al.*, 2001; Marks and Sharp, 2000). Chiefly, the concept of the lytic and temperate replication cycles was unheard of (thereby precluding the selection of effective, lytic bacteriophage), and the utilisation of broader host-range bacteriophage was not understood. Finally, poor experimental planning and quality control were also thought to have been responsible for several disappointing trials (Summers, 2005). As a result, research interest in bacteriophage therapy was already waning by the time antibiotics were introduced in the middle of the 20th century (Carlton, 1999).

The situation has been quite different in the former Soviet countries of Eastern Europe, where research into bacteriophage therapy continued. Recently, effort has been expended to translate historical studies published in the region into English, although it has been found that with regards to control data, experimental methodology has been frequently flawed (Alisky *et al.*, 1998; Chanishvili *et al.*, 2001). Therefore, such studies will not provide a shortcut to the rigorous proof of efficacy required of bacteriophage therapy today.

In recent years interest in bacteriophage as antibacterial agents has been somewhat revived as the limitations of antibiotic therapy have become apparent. With a thorough understanding of

bacteriophage biology, many of the issues described as afflicting early studies in the 20th century can now be avoided. Modern, controlled studies have successfully demonstrated microbial control by bacteriophage in a variety of settings. Advanced examples are the commercial control of *Listeria monocytogenes* on food by bacteriophage (Carlton *et al.*, 2005) and their use as antibacterial "pesticides" on commercial tomato and pepper crops (Balogh *et al.*, 2003). Clinical trials of bacteriophage-based therapies for human use include treatment of chronic *Pseudomonas aeruginosa* infections of the ear (Wright *et al.*, 2009) and against *Staphylococcus aureus* infections (Fairhead, 2009; Housby and Mann, 2009). The former utilizes a cocktail of naturally-occurring lytic bacteriophage to kill bacteria, whilst the latter uses genetically modified bacteriophage as a vector to deliver lethal genes to the target cells: in effect a form of gene delivery.

Other demonstrations of "gene delivery phage therapy" detail the use of the normally non-lethal bacteriophage M13 to deliver genes encoding for lethal agents to *E. coli* (Hagens and Blasi, 2003; Westwater *et al.*, 2003), and bacteriophage Pf3 to *Pseudomonas aeruginosa* (Hagens *et al.*, 2004). These inventions are yet to be commercialised, however. An advantage of these gene delivery methods lies in the prevention of bacterial lysis: the cells are killed but not lysed by bacteriophage infection. The release of endotoxin from lysed Gram-negative cells has the potential to provoke a strong (negative) biological response in patients, so this could be usefully avoided (Gorbet and Sefton, 2005).

A further alternative method to control microbial infection has been to apply bacteriophage-derived lytic enzymes rather than whole bacteriophage. These have been shown effective *in vivo* against *Streptococcus pneumoniae* infections of mice (Entenza *et al.*, 2005).

With the increasingly widespread development of antibiotic-resistant pathogenic bacteria, the need for new antibiotics and new strategies to control microbial infection is of rapidly increasing importance; the cost of antibiotic resistant infections has been estimated at $7.7 billion in the United States alone, a figure which does not include the wider costs to the community (Reed *et al.*, 2002).

With clinical trials in progress against *P. aeruginosa* and *S. aureus*, and successful animal-model demonstrations of bacteriophage therapy treatments against *S. aureus* (Matsuzaki *et al.*, 2003), *C. difficile* (Ramesh *et al.*, 1999) as well as *E. coli* and *S. pneumoniae*, bacteriophage therapy may yet have a renewed role to play in the treatment of infection. This may be as either as a single treatment or in conjunction with antibiotics – these therapies need not be mutually exclusive (Hagens *et al.*, 2006).

1.4.2   Bacteriophage as vaccination tools

Bacteriophage have been demonstrated to have a dual ability to act as tools for vaccine delivery. Firstly, using phage display, they can display vaccine antigens as fusions to their coat proteins, which elicit the desired immune response (Wang and Yu, 2004). Secondly, the bacteriophage particle can be used as a gene delivery vehicle to deliver a DNA vaccine expression cassette to eukaryotic cells (March *et al.*, 2004).

Reflecting their predominant use in phage display, filamentous bacteriophage such as M13 have been commonly used to display vaccine antigens. Examples include hepatitis B mimotopes (Meola *et al.*, 1995; Wan *et al.*, 2001), *Plasmodium vivax* (a protozoal parasite responsible for some types of malaria) surface protein mimotopes (Demangel *et al.*, 1998) and segments of β amyloid peptides (Frenkel *et al.*, 2003). The latter study investigated the use of filamentous bacteriophage to immunize against Alzheimer's Disease (AD). It is thought that progression of AD results from the increased production of β amyloid peptides (AβP) and their progressive accumulation as plaques in the brain of sufferers (Hawkes and McLaurin, 2007). Treatments have therefore focused on the promotion of plaque disaggregation. A randomly generated phage display library was screened with a specific anti-AβP antibody (which promotes plaque disaggregation), which preferentially selected clones displaying a sequence of four characteristic peptides (EFRH). This sequence corresponded to the N-terminal region of AβP (Frenkel *et al.*, 1998). Subsequent intranasal immunisation of AD transgenic mice with the selected bacteriophage clones rapidly provoked an anti-AβP antibody response. The amyloid plaque burden reduced and cognitive ability improved, suggesting that a filamentous bacteriophage-based immunization procedure could potentially offer a treatment to AD sufferers (Frenkel *et al.*, 2003; Solomon, 2008). This discovery is particularly significant when it is considered that the worldwide cost of Alzheimer's Disease and dementia combined has been estimated in excess of $300 billion (Wimo *et al.*, 2007).

Overall, the antigen-displaying bacteriophage vaccination therapy is thought to offer several potential advantages over recombinant protein, carbohydrate or peptide carrier protein fusions (Clark and March, 2004b). Chiefly, the ability to select displayed peptides from a phage display library against the specified antiserum means one need not have prior knowledge of the antigens themselves (Frenkel *et al.*, 1998). Further, once isolated, it is straightforward to reproduce the bacteriophage for eventual manufacture. Finally, although the immunogenic nature of bacteriophage themselves is a cause for concern in the bacteriophage therapy arena (Section 1.3.1) in terms of vaccination efficacy, the bacteriophage scaffold may have a useful immuno-stimulatory "adjuvant" effect (van Houten *et al.*, 2006).

Meanwhile, investigations into the use of bacteriophage as DNA vaccine candidates primarily utilize lytic bacteriophage (as opposed to non-lytic M13), and are a more recent innovation compared to antigen-displaying bacteriophage methods (Clark and March, 2004a; March *et al.*, 2004). Studies on bacteriophage λ expressing hepatitis B surface antigen have suggested that such vectors are more effective (that is, provoke a stronger antibody response) in mouse (Clark and March, 2004a) and rabbit (March *et al.*, 2004) models than equivalent plasmid DNA constructs.

1.4.3   Bacteriophage as vectors for gene delivery

The wider field of bacteriophage-based gene delivery field is in its infancy. As noted earlier, successful demonstrations of gene delivery to mammalian cells have thus far been limited to the expression of reporter genes such as GFP (Larocca *et al.*, 2002; Poul and Marks, 1999) by filamentous bacteriophage systems or luciferase by bacteriophage λ (Lankes *et al.*, 2007). Work has instead focused on improving levels of gene expression (Burg *et al.*, 2002; Liang *et al.*, 2006).

In general terms there are several available technologies for gene delivery, the most advanced being naked (or plasmid) DNA-based vectors and eukaryotic-based viral vectors. Of the gene therapy clinical trials monitored worldwide in 2009 (Edelstein *et al.*, 2009), the three most common vectors in use were adenovirus (n=377), retrovirus (n=329) and naked DNA-based vectors (n=281). No individual bacteriophage-based gene therapy trials are yet listed.

More research is needed to determine the commercial viability of bacteriophage-based vaccination and gene therapy technologies. But with the total biopharmaceutical market expected to reach an overall value of $70 billion within four years (Walsh, 2006), the potential rewards are high.

1.4.4   Bacteriophage M13 as a biomaterial

Away from the pharmaceutical arena, considerable interest has been expressed in exploiting the physical properties of bacteriophage M13 and its close relations. Phage display has been extensively utilized to generate bacteriophage particles displaying surface peptides with functionality towards inorganic materials. For example, peptides promoting the nucleation of semiconducting and magnetic crystals have been demonstrated to create bacteriophage-based "nanowire" structures (Huang *et al.*, 2005; Mao *et al.*, 2004). Further work has harnessed the natural ability of bacteriophage M13 to form liquid crystal structures at high concentrations (Dogic and Fraden, 2006; Graf *et al.*, 1993) together with the selection of bacteriophage displaying peptides with affinities for specified inorganic crystal surfaces. The result has been the creation of 2-D composite materials (Lee *et al.*, 2002; Yoo *et al.*, 2006). Most recently, the

formation of multilayered structures has culminated in the demonstration of functional bacteriophage M13-based lithium-ion batteries. (Lee *et al.*, 2009; Nam *et al.*, 2006). A performance comparison with existing lithium-ion battery technology was broadly positive. If bacteriophage-based batteries proved economically feasible to produce, they would compete in a lithium-ion battery market worth in excess of $3 billion in the United States alone (Balakrishnan *et al.*, 2006).

1.5   Considerations Concerning Bacteriophage Bioproducts

1.5.1   The regulatory perspective

The regulatory hurdles a potential bacteriophage therapeutic must clear are dependent upon its intended use. Understandably, the controls on a bacteriophage-based therapeutic intended for clinical use (classified as a drug) are more stringent that those for food use (classified as a food additive). In turn, the application of bacteriophage to entirely non-pharmaceutical or food uses (such as a biomaterial) requires less regulation.

For any product to be released onto the food or health markets it must receive approval from the relevant regulatory authorities in the country of release, such as the USA Food and Drug Administration (FDA) and the European Medicines Agency (EMEA). In order to achieve this, it must be shown to be efficacious and safe for use. A number of regulatory issues have arisen surrounding bacteriophage-based products intended for *clinical* use, in part due to the unique nature of these therapies. One (still current) example (Withington, 2001) is a guideline from the International Conference on Harmonisation of Technical Requirements for Registration of Pharmaceuticals for Human Use (ICH), concerning the test procedures and acceptance criteria for a biotechnological or biological product (ICH, 1999). The guideline specifically differentiates between certain products resulting from recombinant or non-recombinant cell culture: protein and peptide products (guideline applicable), and antibiotic, DNA and conventional vaccine products (guideline not applicable). The question arises: which guideline applies to bacteriophage? Are they a protein or a DNA product? Will the relevant guidelines applicable to a bacteriophage-based therapeutic depend on its final application? Close co-ordination between regulators and bacteriophage-therapeutic companies will be required to clarify such situations over the next few years.

The greatest advances in regulatory approval (and subsequent commercial use) of bacteriophage products have been in the agriculture and food industries. In 2005 the EPA registered the first pesticide product containing bacteriophage against *Xanthomonas campestris* pv. vesicatoria and *Pseudomonas syringae* pv. tomato, for use on tomato and pepper crops (EPA, 2005). As of 2009 the proprietor of the product, Onnilytics, Inc., claims to have sold over 200 000 litres. In

2006 the FDA approved a cocktail of bacteriophage for use as an antimicrobial agent against *Listeria monocytogenes* contamination in ready-to-eat meat and poultry products (FDA, 2006b). This was the first time that a bacteriophage preparation has been approved as a food additive, and since then a competing bacteriophage product against *Listeria monocytogenes* has received GRAS (Generally Regarded as Safe) status for all food products by the FDA (FDA, 2006a). Most recently, the USDA Food Safety and Inspection Service (FSIS) issued no objection letters for use the of bacteriophage against *E. coli* O157:H7 (USDA/FSIS, 2008a) and *Salmonella* (USDA/FSIS, 2008b; USDA/FSIS, 2008c) on live animals prior to slaughter. It is hoped that the repeated confirmation of the regulatory view that bacteriophage are safe for human use will assist the commercialisation of bacteriophage-based products for wider human applications (Housby and Mann, 2009).

1.5.2   Commercialisation of bacteriophage

Bacteriophage are being commercialised in several areas, typically by smaller enterprises (Table 1.2). Intellectual Property (IP) has been filed for their use as antimicrobial agents in food and agricultural products, as gene and vaccine delivery vehicles as well as their use in antimicrobial human therapy. It is of note that much of the commercial development of bacteriophage for human use has been on oral or topical applications, where the regulatory hurdles are anticipated to be lower (and fewer), thereby reducing the time to market (Housby and Mann, 2009).

However, as well as regulatory uncertainty it has been considered that the relatively slow development of bacteriophage therapy products for clinical use may be due to a perceived difficulty in obtaining intellectual property (IP) rights to protect product value (Clark and March, 2006; Parfitt, 2005). The absence of large pharmaceutical companies in human bacteriophage therapy development may reflect this. In traditional pharmaceutical product development terms, it is inexpensive to isolate any number of effective (and unrelated) bacteriophage against a bacterial strain, although rigorous clinical trials to gain approval for their use would still be required. The current model of an expensive drug development period (between $0.5 and $2bn) (Adams and Brantner, 2006) followed by many years of patent protection may not therefore be directly applicable to the development of bacteriophage therapy products.

Table 1.2 A selection of companies active in the commercialisation of bacteriophage-based products and therapies.

Company	Location	Primary product	Development stage
BigDNA Ltd.	Edinburgh, UK	Oral/ intravenous bacteriophage DNA vaccination	R&D
Biocontrol Ltd.	Nottingham, UK	*Pseudomonas aeruginosa* infections of the ear	Phase III
Cambrios Technologies Corp.	Sunnyvale, USA	Filamentous bacteriophage-derived materials for the electronic industry.	R&D
EBI Food Safety	Wageningen, The Netherlands	Listex^{TM} P100 bacteriophage preparation against *Listeria monocytogenes* in food	Market
Intralytix, Inc.	Baltimore, USA	Bacteriophage cocktail against *Listeria monocytogenes* in food	Market
NeuroPhage, Inc.	Boston, USA	Filamentous bacteriophage-mediated Aβ plaque disaggregation	R&D
Onmilytics, Inc.	Salt Lake City, USA	AgriPhage^{TM} crop pesticide, bacteriophage preparations against *E. coli, Salmonella* on live animals	Market
Phico Therapeutics Ltd.	Cambridge, UK	Lethal bacteriophage-mediated DNA delivery to *Staphylococcus aureus*	Phase I

1.5.3 Considerations for the large-scale production of bacteriophage

The requirements of a large-scale production process of a bacteriophage-based therapeutic will depend on the nature of the final application. Key issues are the scale of the manufacturing process and the necessary purity of the final product. Both strongly dictate the equipment required for, and the overall cost of, production.

Of the potential applications of bacteriophage described, it is probable that one of the most price sensitive would be in the biomaterial industry; that is, the manufacturing costs are critical to competitiveness. Whilst at a very early development stage, the quantities of bacteriophage required for lithium-ion cell production are potentially huge if one scales from the quantity of bacteriophage used in the pilot study. Here, the quantity of bacteriophage M13 loaded for a single 2- 4 volt lithium-ion battery cathode was approximately 2 mg cm^{-2} of cathode (Lee *et al.*, 2009). The mass of an individual M13 virus is approximately 3×10^{-17} g, which equates to about 7×10^{13} viruses cm^{-2}. Considering that the yield of bacteriophage M13 from shakeflask production in the laboratory is often of the order 5×10^{11} viruses ml^{-1} (Reddy and McKenney, 1996), the potential need is for an efficient high-yield, large-scale process, scaleable to the order of thousands of litres.

In the pharmaceutical arena, the quantity of bacteriophage required for each therapeutic application varies widely. Estimates range from 10^6 to 10^{13} bacteriophage per patient per day of treatment; the overall requirement therefore being a function of treatment duration too (Bujanover, 2004). Bacteriophage propagation typically results in 10^9 to 10^{12} viruses ml^{-1} by the end of standard batch culture. However, it can be deduced that up to 10 litres of fermentation culture may still be required per treatment dose, suggesting that large-scale bacteriophage production in the pharmaceutical arena may also be essential for many therapies.

The issue of product purification is of particular relevance for the large-scale manufacture of pharmaceutical-grade bacteriophage products. While it is relatively straightforward to produce high-titre, high-purity bacteriophage on the laboratory-scale, many of the standard purification processes are unfavourable on the large-scale. One example is caesium-chloride density centrifugation, which due to its batch nature and high equipment costs has substantial drawbacks for large-scale processing (Smith and Gingrich, 2005). A second is the common addition of chloroform to remove precipitants added in the course of concentrating the bacteriophage product. However, chloroform is a toxic chemical of known carcinogenic effect (Watts *et al.*, 2004), and requires some handling care (McKetta, 1993). Therefore, the development of a bacteriophage production process will involve the translation of laboratory-scale techniques to the large-scale, and the utilization of alternative scaleable processes.

The task of scale-up is hindered by the relative lack of published data on large-scale bacteriophage production. Where available, studies detailing the large-scale *deep-culture* fermentation of lytic bacteriophage are typically over 20 years old (Husimi and Keweloh, 1987; Sargeant, 1970; Sargeant *et al.*, 1968; Siquet-Descans *et al.*, 1973) – although the principles still hold – and a recent study on the fermentation of filamentous bacteriophage-derived phagemids virtually stands alone in the field (Grieco *et al.*, 2009). Similarly, studies primarily focusing on

scaleable bacteriophage purification processes are sparse, but include purification by monolith chromatography (Smrekar *et al.*, 2008), hydroxyapatite column chromatography (Smith and Gingrich, 2005) and expanded bed anion chromatography (Ling *et al.*, 2004). Of assistance here is that in many processing respects, a bacteriophage may be expected to perform as a large protein complex, and principles applying to recombinant protein production will be applicable to bacteriophage processing. Hence a much greater pool of processing knowledge can be tapped. However, a difficulty common to the assembly of all biological production processes remains: although many generalities apply, often the exact conditions required will be dependent on the molecule (or bacteriophage) of interest (Sargeant, 1970).

1.6   Production of Bacteriophage M13 as a Therapeutic

As described in Sections 1.2.1 and 1.2.3, the physical structures and replication cycles can vary considerably between bacteriophage species. That said, almost all of the general principles of production outlined here will be at least partly applicable to the production of all bacteriophage, not just M13. The main exception, as described earlier, is the characteristic of filamentous bacteriophage (such as M13) not to lyse their bacterial hosts, but extrude into the fermentation medium. The result is a distinct post-fermentation process fluid.

A number of large-scale fermentation and so-called "downstream processing" options are available for the production of bacteriophage M13. The sequence of large-scale production stages generally mirror those on the laboratory-scale: that is, a typical production process will begin with the generation of bacteriophage biomass by bacterial fermentation. Subsequently, downstream processing begins at the point of harvest. The first step would be the separation of cells from the fermentation medium, and, since bacteriophage M13 will be located in the extracellular environment, the cell-free fermentation medium would be taken forward for further processing. A volume reduction step is likely to follow to concentrate the bacteriophage, and ideally simultaneously achieve some purification. Given the stringent regulatory specifications required of a human therapeutic (Levy *et al.*, 2000b), the bacteriophage product is still in an impure state and would require further, higher resolution purification for such uses. At the laboratory scale this may involve caesium-chloride density centrifugation or small scale chromatographic separation followed by various small scale "polishing" steps to remove residual contaminants (Smith and Gingrich, 2005). At the large-scale several chromatographic separation stages are likely, each stage ideally exploiting a different physicochemical attribute of the bacteriophage molecule to enact separation from contaminants (Atkinson *et al.*, 1987). Finally, the pure bacteriophage product will be formulated in the manner in which it will be stably stored. The steps in this generalised production process are summarised in Figure 1.5.

```
                    Bacteriophage
                     and E. coli
                       inocula
                          │
                          ▼
                 ┌─────────────────┐
                 │  Fermentation   │
                 └─────────────────┘
                          │
                          ▼
                 ┌─────────────────┐       Cell
                 │      Cell       │────▶  paste
                 │    removal      │
                 └─────────────────┘
                          │
                          ▼
                 ┌─────────────────┐       Excess liquid,
                 │  Bacteriophage  │────▶  some contaminants
                 │  concentration  │
                 └─────────────────┘
                          │
                          ▼
                 ┌─────────────────┐       Remaining
                 │ High resolution │────▶  contaminants
                 │   purification  │
                 └─────────────────┘
                          │
                          ▼
                 ┌─────────────────┐
                 │  Polishing and  │
                 │   formulation   │
                 └─────────────────┘
                          │
                          ▼
                        Pure
                    bacteriophage
                       product
```
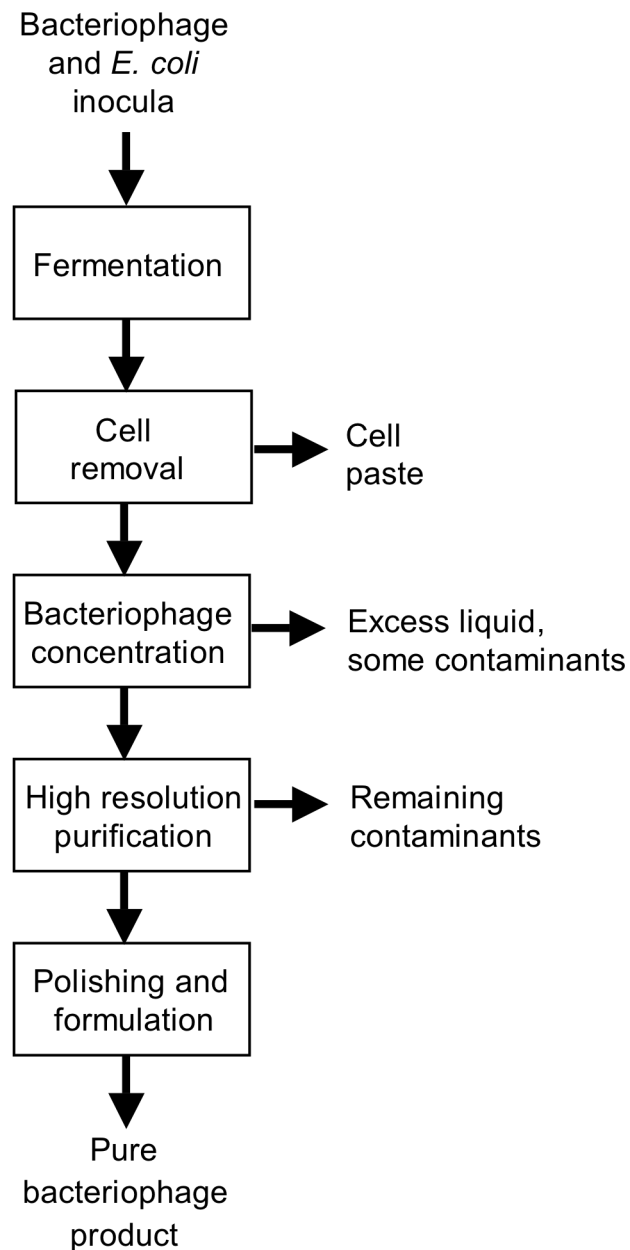
Figure 1.5 A general outline of the essential production stages of bacteriophage M13 for high-purity applications.

1.6.1   The upstream process: the fermentation of M13 infected *E. coli* cells

The primary function of the fermentation stage is to maximise bacteriophage M13 productivity in *E. coli*, where productivity is defined as the quantity of bacteriophage produced per unit volume per unit time. It would also be desirable to produce a post-fermentation process fluid allowing for the simplest downstream process possible.

Many factors can potentially affect the resulting yield of bacteriophage M13 from fermentation. These include the growth medium, the maintained dissolved oxygen tension (DOT), the infecting ratio of bacteriophage to *E. coli*, the infection time, the bacterial strain, the fermentation temperature, pH and the fermentation (feeding) strategy (Grieco *et al.*, 2009; Reddy and McKenney, 1996). Frustratingly for the biochemical engineer, there is no overall scheme for the maximisation of production within *E. coli*, be the product plasmid, recombinant protein or indeed bacteriophage (Harrison and Keshavarz-Moore, 1996). For example, in the specific case of plasmid expression, productivity differences between *E. coli* strains have been found to depend on the plasmid in question (Yau *et al.*, 2008). That is, one *E. coli* strain may show an excellent level of productivity for one plasmid, but a relatively poor level for another. Instead, optimisation of product yield will require at least some experimentation with *E. coli* expressing the product of interest, although that is not to say that several broad principles do not apply, such as the positive effects of maintenance of near-neutral pH and DOT above 30 % saturation (Garcia-Arrazola *et al.*, 2005).

The versatility of fermentation lies in the ability to monitor, control and amend the conditions within the fermenter to meet the nutritional needs of the cells during growth. As such, a fermentation can usually be expected to result in a more productive culture than that achieved by small-scale shakeflask experimentation (Grieco *et al.*, 2009). Further, dedicated sampling ports reduce the likelihood of contamination, and off-gas analysis can be utilised as an immediate, online measure of the state of the culture. Finally, and perhaps most importantly, fermenters are scaleable unit operations (Doran, 1999). Therefore, even experimentation in small sub-litre fermentations is generally able to predict the performance within large-scale fermenters, using standard biochemical engineering scale-up criteria.

1.6.2 Downstream process considerations

The objective of an efficient downstream process is the purification of the product whilst maximising recovery (i.e. minimising losses at each stage) at minimum cost (Wenzig *et al.*, 1993). Assembly of the process is governed by the following core criteria (Petrides, 2003; Wheelwright, 1987):

1. Separate the most plentiful impurities first
2. Select conditions that exploit the greatest differences in the properties of the product and the impurities
3. Use as highly selective step as early as possible
4. Employ separation processes based on different properties
5. Conduct the most difficult or expensive separations last

It can be seen from these criteria that to design the downstream process, it will be necessary to know both the composition of the post-fermentation process fluid and the physicochemical properties of the product and contaminants.

1.6.2.1 Separation of biomass

The two leading large-scale methods of solids separation are centrifugation and microfiltration. Centrifugation separates solid/liquid or liquid/liquid systems on the basis of density and size differences. Separation is effected by the application of centrifugal forces by high speed rotation. Centrifuges are routinely used in the biotechnology industry to remove intact cells, cell debris and protein aggregates from the liquid phase. Therefore, in the downstream processing of bacteriophage M13 they may well be appropriate for both the removal of intact *E. coli* cells from the post-fermentation fluid as well as the capture of precipitated bacteriophage particles (i.e. the bacteriophage concentration step outlined in Figure 1.5).

The centrifuges used in industry are usually of the continuous type as opposed to the standard batch centrifugation used in the laboratory. Here, the feed stream is continually fed into the rotating centrifuge chamber, where solids capture occurs. Clarified process fluid continually flows out. Depending on the type of centrifuge, the discharge of solids (sediment) can occur either intermittently (some designs requiring a temporary halt to centrifugation) or continuously. The most commonly used continuous centrifuges are the disk-stack, multichamber bowl and tubular bowl designs (Boychyn *et al.*, 2004).

Continuous centrifuges can process large volumes of process fluid. Large-scale disk-stack designs can separate whole cells at flow rates up to 3 000 to 5 000 litres hr^{-1} (Asenjo and Patrick, 1990). However, they do have limitations. The capital cost is often high, and 100 % cell removal cannot be obtained. A filtration step is usually required to protect subsequent stages – such as chromatography – that are prone to fouling. Further limitations include heat, noise, aerosol generation and containment issues (Tinnes and Hoare, 1992).

Microfiltration is often used for solids removal, most commonly after centrifugation to remove any remaining biomass. Less commonly, principally due to the issue of fouling, it is employed for total solids removal alone. In the biotechnology industry, cross-flow micro-filtration is often employed, where the process fluid flows tangentially to the filter membrane. The use of a sufficiently high flow rate reduces the issue of fouling by a self-scouring action (Mackay, 1996). Such filters may exhibit cross-membrane volumetric fluxes of the order 15 to 50 litres $m^{-2} hr^{-1}$ with a pore size of 0.22 or 0.45 μm (Brocklebank, 1986), large enough to allow extracellular protein (or bacteriophage) to pass through. The capital cost of microfiltration equipment is less than continuous centrifuges, and they offer better process stream clarification.

1.6.2.2 Primary purification and bacteriophage concentration

The volume reduction stage (i.e. bacteriophage concentration) is consistent with the guiding principles of downstream processing outlined at the start of Section 1.6.2, particularly if one considers water as a particularly plentiful "impurity" which should therefore be removed early on. Various competitive concentration steps exist, the most common being ultrafiltration and precipitation.

If the pore sizes are small enough, a membrane filter could be used to concentrate bacteriophage from the dilute cell-free medium. This is the principle behind ultrafiltration, where the membranes are rated in terms of their molecular weight (MW) cut offs (Busby and Ingham, 1980). The industrial technique of ultrafiltration is similar to that of microfiltration. That is, flow is generally tangential to the membrane to reduce fouling. In theory, the achievable protein concentration on the large-scale is high, and the process usefully allows for buffer changes to be made ("diafiltration") (Eykamp, 1997).

From a modern perspective, the traditional methods of protein precipitation may be considered unfavourable relative to ultrafiltration. In particular, salt fractionation via the additions of ammonium sulphate has been widely used due to its high solubility and low price, but at the cost of poor selectivity for the protein of interest. However, work exhibiting the fractional precipitation of proteins and plasmid DNA by CTAB (Lander *et al.*, 2002; Tomanee *et al.*, 2004), polyethylene glycol (Tsoka *et al.*, 2000) and spermine (Murphy *et al.*, 1999) illustrate the selective ability of precipitation, as well as its capacity to concentrate. This dual ability is particularly useful prior to higher resolution purification stages (such as chromatography) again because these are prone to fouling by excess contaminants (Prazeres and Ferreira, 2004).

1.6.2.3 High resolution purification

Chromatographic separations can rightly be considered the longstanding workhorses of downstream processing (Przybycien *et al.*, 2004). Differing chromatographic matrices can select on the basis of charge (ion exchange), size and shape (gel filtration), hydrophobicity (hydrophobic interaction) and affinity for a specific ligand (affinity chromatography) (Atkinson *et al.*, 1987). The application of a combination of these techniques to the process stream allows for the high-resolution purification of the bacteriophage product for high-purity applications.

Chromatographic separations are not without their drawbacks, however, the most oft-cited being high cost, batch operation and complex scale-up (Przybycien *et al.*, 2004; Thommes and Etzel, 2007). Consequently, alternatives to chromatography are being explored, including selective precipitation (Lander *et al.*, 2002), membrane chromatography (Teeters *et al.*, 2003),

and monolith separations (Smrekar *et al.*, 2008). Monoliths in particular have been demonstrated as a viable high-resolution purification strategy for large particles such as bacteriophage (Etzel and Riordan, 2009; Jungbauer and Hahn, 2008).

1.6.2.4   Polishing and formulation

The final stages of downstream processing would focus on the formulation of the purified bacteriophage product into a form in which it can be stably stored, most likely in a buffered solution state. If necessary a diafiltration step may be employed to change the suspension buffer (Eykamp, 1997).

1.6.3   Whole bioprocess considerations: GMPs, validation and containment

If bacteriophage-based therapeutics are to be administered to humans or animals, then they must be manufactured in accordance with current Good Manufacturing Practices (GMP), as stated by FDA guidelines on the preparation of investigational new drug products (FDA, 1991). GMPs cover all aspects of drug product manufacture, from raw materials, utilities, packaging and transferral of the final product to the clinic (Kletch, 1997). In essence, the manufacturing process needs to be defined and controlled. Therefore, if any part of the procedure from manufacture to clinic is not in conformity with GMP, the product is "adulterated" and cannot legally be approved (Doblhoff-Dier and Bliem, 1999).

The process of validation has been introduced to assure product consistency, and is therefore an essential provision of GMPs (Eckman, 1997). It requires the establishment of documented evidence that any product, process, procedure, system, equipment or software used in the process of manufacture consistently meets predetermined specifications. Thus, in a downstream process each unit operation must be validated to prove that it is capable of the consistent removal of the impurities to level required (Sofer, 1995). The validation process also extends to the cleaning of each piece of equipment. The process of validation is beneficial to the finalised downstream process: reduced process variability means fewer failed batches and reduced costs (Kozlowski and Swann, 2006).

A basic demand of GMP is the avoidance of product impurity, be it by foreign matter or indeed cross-contamination (Sherwood, 1996). Therefore, the bioprocessing of a bacteriophage-based therapeutic raises important issues regarding containment, largely dependent on whether the bacteriophage product is biologically infective. The ability of an infective bacteriophage to propagate means carefully considered containment measures will need to be implemented to prevent the cross-contamination of fermentations in the manufacturing area, particularly if the facilities are of mixed use. Conversely, non-infectious bacteriophage particles can be considered simply as a DNA or RNA-protein product. When designing a bacteriophage-therapeutic facility,

aspects of equipment and plant design from the dairy industry may be applicable, where bacteriophage control is a longstanding issue (McGrath *et al.*, 2007; Moineau, 1999). As expected, practical approaches to contamination control include adapted plant design, ventilation and sanitation (Sherwood, 1996; Whyte, 1991).

1.6.4   Techniques for the prediction of bioprocess performance

At the early design stages of a bioprocess, the quantity of available material is often extremely limited, so the ability to experiment on small quantities of material is important. The conventional approach to scaled-down process development is experimentation with correspondingly scaled-down process equipment into the litre-sized range. Alternatively, the development of "ultra scale-down" (USD) techniques has allowed for the performance prediction of unit operations using only millilitres of material. The USD technique combines the use of standard laboratory equipment with custom-made devices to mimic the engineering environment within large-scale equipment. Upon verification of a particular USD method to mimic conditions, it can be used to great effect in process development and understanding at an earlier point in the discovery process. USD methods have been developed to mimic several process steps including depth filtration (Reynolds *et al.*, 2003), filtering centrifugation (Boulding *et al.*, 2002), continuous centrifugation (Boychyn *et al.*, 2004) and chromatography (Wenger *et al.*, 2007).

The response of the target molecule (bacteriophage in this study) to the frequently intense fluid flow environment imposed by large-scale equipment has been of particular concern to biochemical engineers. Over the course of an entire bioprocess, the cumulative exposure to hydrodynamic *shear forces* can be significant. Continuous centrifuges are known to be particularly damaging to sensitive biological materials, which is why substantial attention has focused on the development of USD mimics of the feed-zone of this unit operation (Biddlecombe *et al.*, 2007; Boychyn *et al.*, 2001; Chan *et al.*, 2006; Hutchinson *et al.*, 2006; Levy *et al.*, 1999a). Within a continuous centrifuge, the feed-zone is the point at which the process fluid first enters the rotating centrifuge chamber. Consequently, the shear forces within this region are high. At the laboratory-scale, where early experimentation and manufacture occurs, conditions are benign and little physical damage is caused. Therefore, standard laboratory-scale techniques are often a poor prediction of the quality of product that may be achieved on the large-scale.

1.7   Aims and Objectives

It has been demonstrated that bacteriophage M13 (as well as its close relations and derivatives) features as a candidate in several promising biotechnological areas. However, it has also been explained that of all bacteriophage types, limited biochemical engineering literature currently exists to support large-scale filamentous bacteriophage manufacture. If this state of affairs persists, the assembly of production schemes for these future therapies will be hindered.

With a focus on the fundamental properties of bacteriophage M13, the principal objective of this thesis is to contribute towards the processing knowledge of bacteriophage M13, its relations and derivatives. Ultimately, this work aims to pave the way for the assembly of a more efficient large-scale production process. Within this framework, five areas of research were undertaken, utilizing wild-type bacteriophage M13 as a model system. Each of the areas investigated corresponds to one of the results chapters presented of this thesis. The five goals of thesis are therefore:

1. **Evaluate the effect of hydrodynamic shear on the filamentous bacteriophage particle (Chapter 3).**

   Unit operations such as fermentation, continuous centrifugation and ancillary pumps will all impart flow conditions on the process fluid up to several orders of magnitude greater in energy than that imparted by standard laboratory processing. It is therefore important to assess the response of bacteriophage M13 to high-energy hydrodynamic shear conditions. However, since so little is known about the response of bacteriophage M13 to any of these environments, a general approach will be undertaken using a USD rotating disk shear device. As described in Section 1.6.4, USD techniques allow for the rapid assessment of a range of shear conditions, using only millilitres of fluid. The fragility of bacteriophage M13 will be assessed upon exposure to fluid flows of varying intensity, and the effect of the fluid of suspension shall also be studied. Bacteriophage M13 will be compared to other complex molecules in terms of their relative resistances to hydrodynamic shear. Finally, experimentation to elucidate some of the mechanisms of damage will be studied. The potential implications for the large-scale bacteriophage M13 processing will then be assessed.

2. **Investigate the fermentation and harvesting of bacteriophage M13 (Chapter 4).**

   The efficient planning of a downstream process is dependent on knowing the concentration of the product and major contaminants in the process stream. The composition of the post-fermentation process fluid will therefore be examined. The *E. coli* host strain and growth medium will be investigated for improvements in

bacteriophage M13 yield and the effects on the resulting post-fermentation process stream. Experimentation will be conducted at the shakeflask and bioreactor scales.

3. **Evaluate the effect of hydrodynamic shear on *E. coli* cell integrity (Chapter 5).**
   Using USD techniques, the response of the *E. coli* host to high-energy hydrodynamic shear conditions will be determined. The effects of M13 infection and culture age on the *E. coli* cells will be assessed in terms of the observed alterations in cell fragility. The implications for large-scale processing will be assessed: increased cell damage could result in increased process stream contamination by intracellular components. Downstream processing may therefore be hindered.

4. **Investigate the primary purification of bacteriophage M13 (Chapter 6).**
   Effective precipitants of bacteriophage M13 will be determined in pure as well as post-fermentation fluid systems. Studies in pure systems will allow the fundamental characteristics of the precipitants to be evaluated. Precipitation of bacteriophage M13 from post-fermentation fluid will allow for the comparison of selected precipitants in terms of the achieved bacteriophage yield and purification.

5. **Consider the issues concerning the introduction of bacteriophage M13 to a mixed-use production facility (Chapter 7).**
   The resistance of bacteriophage M13 to several physical and chemical challenges will be examined, each relevant for the assessment of its safe introduction to a mixed-use facility. This will include exposure to common disinfection agents as well as extremes of temperature, pH and desiccated conditions. An effective disinfectant agent will also be determined against *E. coli* cells. The consequences of accidental bacteriophage M13 release will be discussed. Standard operating procedures for the propagation of bacteriophage M13 at the 20 L scale in the UCL fermentation suite will be derived and discussed.

While focus of this thesis is undoubtedly upon bacteriophage M13, many of the techniques used are general and will therefore be of use in the investigation of the properties of other bacteriophage types.

2   Materials and Methods

2.1 Buffers, Solutions and Media

All solutions and media were prepared using reverse osmosis (RO) water by Elga Option 4 water purifier. Sterilisation was by autoclaving at 121 °C, 1 bar pressure for 15 minutes.

2.1.1   Tris EDTA (TE) buffer pH 7.5

TE buffer contained 10 mM Tris-HCl (pH 7.5 at 25 °C) and 1 mM EDTA suspended in RO water and autoclaved.

2.1.2   3 x Loading buffer

Loading buffer contained 40 % (w/v) sucrose, 100 mM EDTA and 150 μg ml^{-1} bromophenol blue suspended in sterile RO water.

2.1.3   Tris-Borate-EDTA electrophoresis buffer (TBE)

Supplied as pre-mixed powder (Fisher) giving a 1 x concentration of 89 mM Tris, 89 mM boric acid, 2 mM EDTA suspended in RO water.

2.1.4   2 x Laemmli loading buffer

Laemmli loading buffer contained 4 % SDS, 130 mM Tris-HCl (pH 6.8 at 25 °C), 18 % (v/v) glycerol and 60 ug ml^{-1} bromophenol blue suspended in sterile RO water. Immediately prior to use dithiothreitol was added to an aliquot of loading buffer to a concentration of 200 mM.

2.1.5   Running buffer for SDS-PAGE

SDS-PAGE running buffer contained 25 mM Tris, 29 mM glycine and 0.1 % (w/v) SDS suspended in RO water.

2.1.6   Nutrient Broth Number 2 (NB2), agar (NB2A) and overlay agar (NB2OA)

NB2 powder 25 g l^{-1} (containing 10 g l^{-1} meat-derived "Lab-Lemco" powder, 10 g l^{-1} meat-derived peptone, 5 g^{-1} l sodium chloride, Oxoid) was suspended in RO water and autoclaved for NB2 broth, or supplemented with granulated agar (Difco) 1.4 % (w/v) prior to autoclaving for NB2A. For NB2OA, NB2 powder 25 gl^{-1} was supplemented with granulated agar (Difco) 0.7 % (w/v). NB2

2.1.7   Fermentation medium

Fermentation medium contained 10 g l^{-1} yeast extract (Difco), tryptone peptone (Difco), sodium chloride (BDH) and glycerol (BDH) suspended in RO water and autoclaved (Doig *et al.*, 2001).

2.1.8   Thiamine supplemented minimal agar

Plain agar was prepared by autoclaving 130 ml of RO water with granulated agar (Difco) 1.4 % (w/v). Molten 55 °C plain agar was supplemented with M9 salts 1 x concentration, $CaSO_4$ 0.1 mM and $MgSO_4$ 6 mM (BDH). Each individual stock was sterilised by autoclaving prior to addition. Further supplement was by glucose 0.8 % (w/v) (BDH) and thiamine 5 μg ml^{-1}, each stock filter sterilised (0.22 μm Millipore). The resulting minimal media was immediately poured to produce agar plates.

2.1.9   DNAse Test Agar with Methyl Green

DNAse Test Agar with Methyl Green powder 42 g l^{-1} (Difco) was suspended in RO water, boiled by microwave for 1 minute to dissolve, then autoclaved.

2.1.10   Antibiotic stocks

2.1.10.1   Tetracycline

Tetracycline (Sigma) was dissolved in ethanol to give 5 mg ml^{-1} and stored at -20 °C as a stock solution. The typical working concentration was 5 μg ml^{-1}.

2.1.10.2   Ampicillin

Ampicillin (Sigma) was dissolved in sterile RO water to give 100 mg ml^{-1}, filtered (0.22 μm Millipore), and stored at -20 °C as a stock solution. The typical working concentration was 100 μg ml^{-1}.

2.1.10.3   Kanamycin

Kanamycin (Sigma) was dissolved in sterile RO water to give 20 mg ml^{-1}, filtered (0.22 μm Millipore), and stored at -20 °C as a stock solution. The typical working concentration was 50 μg ml^{-1}.

2.1.11   5-bromo-4-chloro-3-indoyl-βD-galactopyranoside (X-gal)

X-gal (Sigma) was dissolved in dimethyl sulphoxide (Sigma) to give a 40 mg ml^{-1} stock solution. Where appropriate, the stock solution was added post-autoclaving to molten agar (55 °C) to a final concentration of 40 μg ml^{-1}.

2.1.12   Isopropyl β-D-1-thiogalactopyranoside (IPTG)

IPTG (Sigma) was dissolved in sterile RO water to give a 20 mg ml^{-1} stock solution. Where appropriate, the stock solution was added post-autoclaving to molten agar (55 °C) or growth media to a final concentration of 20 μg ml^{-1}.

2.2 Bacteria and Bacteriophage Strains

All bacteria and bacteriophage strains used in this study are listed in Tables 2.1 and 2.2.

Table 2.1 Names and genotype of bacterial strains used.

Strain	Genotype	Source/ Reference
Escherichia coli JM107	F′[*tra*D36 *lac*I^q Δ(*lac*Z)M15 *pro*A+B+] e14– (*Mcr*A–) Δ(*lac-pro*AB) *thi gyr*A96 (Nal^r) *end*A1 *hsd*R17 (r^k– mk$^+$) *rel*A1 *gln*V44	Yanisch-Perron *et al.* (1985)
Escherichia coli TOP10F'	F′[*lac*I^q, Tn*10*(Tet^R)] *mcr*A (*mrr-hsd*RMS-*mcr*BC) φ80*lac*ZΔM15 Δ*lac*X74 *rec*A1 *ara*Δ139 Δ(*ara-leu*)7697 *gal*U *gal*K *rps*L (Str^R) *end*A1 *nup*G	Invitrogen Ltd.
Escherichia coli W1485	F′ λ-	NCIMB[1] 9481 Lederberg

Table 2.2 Names of bacteriophage used.

Strain	Source/ Reference
M13	ATCC[2] 15669B1

[1]NCIMB- National Collection of Industrial, Marine and Food Bacteria

[2]ATCC- American Type Culture Collection

2.3 Cultivation of *E. coli* and Propagation of Bacteriophage

2.3.1 Preparation of working *E. coli* cultures

Working liquid *E. coli* cultures were routinely prepared at the 5 ml scale as described below. Cultures were assumed to be in the stationary phase after overnight growth at 37 °C with shaking. Relative standard deviations in OD$_{600}$ values between similarly prepared 5 ml cultures were <2 %.

2.3.1.1 JM107

Cultures of JM107 were prepared by streaking a loopful of stock culture onto a minimal agar plate (Section 2.1.7) and incubated overnight at 37 °C. Working liquid cultures were then prepared by inoculating 5 ml NB2 with a loopful of cells taken from an isolated colony on the minimal agar plate and incubated overnight at 37 °C with shaking.

2.3.1.2 Top10F'

Cultures of Top10F' were prepared by streaking a loopful of stock culture onto an NB2A plate supplemented with 5 μg ml^{-1} tetracycline and incubated overnight at 37 °C. Working liquid cultures were then prepared by inoculating 5 ml NB2 supplemented with 5 μg ml^{-1} tetracycline with a loopful of cells taken from an isolated colony on the NB2A plate and incubated overnight at 37 °C with shaking. When larger culture volumes were required, 1 ml of working Top10F' culture was inoculated into 50 ml NB2 (in a baffled 250 ml shakeflask) supplemented with 5 μg ml^{-1} tetracycline and incubated overnight at 37 °C.

2.3.1.3 W1485

Cultures of W1485 were prepared by streaking a loopful of stock culture onto an NB2A plate and incubated overnight at 37 °C. Working liquid cultures were then prepared by inoculating 5 ml NB2 with a loopful of cells taken from an isolated colony on the NB2A plate and incubated overnight at 37 °C with shaking.

2.3.2 *E. coli* cultivation

Larger *E. coli* cultures were prepared by inoculating 400 ml NB2 or fermentation medium (Section 2.1.7) in a two-litre baffled shake flask (Nalgene) with 5 ml of overnight working culture (Section 2.3.1), equating to 1 x 10^{10} colony forming units (cfu). Appropriate antibiotic selection was used if the culture was to be further propagated. Flasks were incubated at 37 °C with shaking (200 rpm).

2.3.3 Propagation of bacteriophage M13

Stocks of bacteriophage M13 were prepared by inoculating 400 ml NB2 in a two-litre baffled shake flask (Nalgene) with 1 x 10^{10} colony forming units (cfu) of stationary phase Top10F' (Section 2.3.1.2) and 2 x 10^{11} plaque forming units (pfu) of M13. Following overnight incubation at 37 °C with shaking (200 rpm), a bacteriophage concentration of mid-10^{11} pfu ml^{-1} was routinely achieved. Each 400 ml culture was divided between two 250 ml Sorvall centrifuge bottles (Thermo Scientific Ltd). Centrifugation was by Sorvall GSA rotor at 14 000 $\times$ g (RCF$_{max}$) for 15 minutes at 4 °C, and the supernatants decanted. M13 concentration was achieved by polyethylene glycol (PEG) precipitation (Yamamoto *et al.*, 1970). Briefly, M13 was precipitated from the supernatants by the addition of 3.3 % (w/v) polyethylene glycol 6000

and 330 mM NaCl and incubated at 4 °C overnight. Precipitated M13 particles were pelleted by centrifugation, again in 250 ml Sorvall centrifuge bottles. Centrifugation was by Sorvall GSA rotor at 14 000 × g (RCF_{max}) at 4 °C for 10 minutes, and resuspended in 4 ml 10 mM Tris (pH 7.5 at 25 °C) per 250 ml bottle. Resuspended bacteriophage pellets were filtered through a 0.22 μm filter and stored at 4 °C.

2.4   Caesium Chloride Density Centrifugation

Purification of bacteriophage was performed by caesium chloride density gradient centrifugation. Caesium chloride (0.4 g ml^{-1}) was added to each M13 bacteriophage preparation (10^{12} pfu ml^{-1} M13). M13 solutions were ultracentrifuged at 110,000 x g (RCF_{max}) for 23 h at 15 °C in a Beckman ultracentrifuge using a Ti 70.1 rotor. The caesium chloride purified bacteriophage were visualized as a thin blue-tinted band within each tube. After removing each centrifuge tube cap, bacteriophage were recovered by piercing the tube wall with a hypodermic needle (1.0 mm x 16 mm) attached to a 2 ml syringe at the base of the band and drawing off the bacteriophage. The resulting concentrated bacteriophage suspensions were dialysed against three litres of 10 mM Tris (pH 7.5 at 25°C) using 10 000 MWCO dialysis tubing (Pierce, Rockford, IL, USA) for 24 hours. Dialysis solution was changed once. The resulting bacteriophage were then enumerated (Section 2.5.2) and stored at 4 °C.

2.5   Enumeration of Bacterial and Bacteriophage Suspensions

2.5.1   Enumeration of bacterial suspensions

Unless otherwise stated, *E. coli* bacteria were enumerated using the spread plate technique. Here, the bacterial suspension was ten-fold serially diluted to 1 x 10^{-8} in 10 mM Tris (pH 7.5). Typically, each dilution involved adding a 20 μl sample to 180 μl diluent. Triplicate volumes (100 μl) of each dilution were spread onto NB2A plates. The plates were then incubated at 37 ºC for 12- 24 hours before examining for colony formation. Dilutions giving rise to 30 – 300 colonies were used for enumeration. The number of cfu per 100 μl of suspension was calculated by multiplying the mean number of colonies by the reciprocal of the dilution factor. This figure was then multiplied by 10 to convert to cfu ml^{-1}.

2.5.2   Enumeration of bacteriophage suspensions

All bacteriophage were enumerated using the surface droplet technique, based on the protocol devised by Miles and Misra (Miles and Misra, 1938) for bacterial suspension enumeration. Briefly, the bacteriophage suspension was ten-fold serially diluted using an appropriate buffer, typically 10 mM Tris. Typically, each dilution involved adding a 20 μl sample to 180 μl diluent.

Lawns of Top10F' were prepared by mixing 2×10^8 pfu cells (Section 2.3.1.2) with 5 ml molten (50 °C) NB2OA and pouring onto a solidified NB2A plate. The agar lawns were inoculated with triplicate 10 µl drops of each dilution and left to air dry for 20 min. The plates were then incubated at 37 ºC overnight before examining for plaque formation. Dilutions giving rise to 3 – 30 plaques were used for enumeration. The number of pfu per 10 µl of undiluted solution was calculated by multiplying the mean number of plaques by the reciprocal of the dilution factor. This figure was then multiplied by 100 to convert to pfu ml^{-1}.

2.6   Storage of Bacterial and Bacteriophage Stocks

Stocks of each *E. coli* strain were propagated from the original sources as described in Section 2.3.1. Each culture was supplemented with sterile glycerol 15 % (w/v) and stored at -20 ºC in 5 ml polystyrene tubes. Agar plates streaked from the *E. coli* stocks were stored at 4 ºC for up to one week. Short and long term storage of bacteriophage was at 4 ºC in sterile polypropylene tubes.

2.7   Analysis of Bacterial and Bacteriophage DNA and Protein

2.7.1   Spectrophotometric DNA quantification

Where appropriate, DNA quantification was determined by absorbance at 260 nm by NanoDrop ND-1000 spectrophotometer (Thermo Scienific). Extinction coefficients were taken as 50 and 33 ng cm µl^{-1} for double-stranded and single-stranded DNA respectively.

2.7.2   Agarose gel electrophoresis

Agarose (1.2 g, Bio-Rad) was added to 150 ml of 1 x TBE buffer (Fisher) in a Pyrex conical flask and dissolved completely by microwave heating for 2- 3 minutes at 800 W (Panasonic). Following cooling of the molten agarose to approximately 50 °C, ethidium bromide (10 mg ml^{-1} stock, Sigma) was added to a final concentration of 0.27 µl ml^{-1} and gently mixed. The molten agarose was poured into a casting tray of suitable size and allowed to set. Typically, 30 well combs (5 mm diameter per well) were used. DNA samples were mixed with 0.33 volumes of 3 x loading buffer (Section 2.1.2). λ/*Hin*dIII (0.1 mg ml^{-1} DNA, Fermentas) and 1 kb (0.15 mg ml^{-1} DNA, Bioline HyperLadder 1) markers were used where appropriate. Gels were electrophoresed in $1 \times$ TBE buffer at approximately 80 V for 1 hour. All gels were scanned and analysed using a UV transilluminator gel doc system (Syngene Gene Genius) with GeneSnap acquisition software (Syngene).

2.7.3 Polyacrylamide gel electrophoresis (SDS-PAGE)

Acrylamide gels (12 % (w/v)) were prepared for SDS polyacrylamide gel electrophoresis (SDS-PAGE), based on the method of Sambrook et al. (2001). Gels of thickness 0.75 mm were cast and run using the Bio-Rad Mini-PROTEAN 3 system. For a single 5 ml gel, 1.3 ml 1.5 M Tris (pH 8.8 at 25 °C, Sigma), 50 μl 10 % (w/v) SDS solution (BDH), 2.0 ml 30 % (w/v) acrylamide/ 0.8 % (w/v) methylene bisacrylamide solution (National Diagnostics) was added to 1.6 ml sterile RO water. Ammonium persulphate (50 μl, 10 % (w/v), BDH) and 2 μl tetramethylethylenediamine (TEMED, Amresco) were added simultaneously and the mixture gently swirled. This was immediately poured between the glass casting plates to a level 0.5 - 1 cm below the furthest reach of the gel comb. Isopropanol was pippetted on top of the gel, which was subsequently allowed to polymerise for 20 minutes. The isopropanol was poured off and all remaining traces removed with blotting paper. A single 3 ml stacking gel was prepared by adding 0.38 ml 1.0 M Tris (pH 6.8 at 25 °C), 30 μl 10 % (w/v) SDS solution, 0.5 ml 30 % (w/v) acrylamide/ 0.8 % (w/v) methylene bisacrylamide solution to 2.1 ml sterile RO water. Ammonium persulphate (30 μl, 10 % (w/v)) and 3 μl TEMED were added simultaneously and the mixture gently swirled. This was immediately poured on top of the cast gel to the top of the glass plates and a 10 well comb inserted. The gel was allowed to polymerise for at least a further 30 minutes. Samples were mixed with one volume 2 x Laemmli loading buffer (Section 2.1.4) and incubated at 95 °C for 5 minutes. A 2- 212 kDa broad range protein marker was used (P7702S, NEB) at 1, 5 or 10 x dilutions in 1 x Laemmli loading buffer and incubated 95 °C for 5 minutes. All samples were centrifuged for 30 seconds, 13 000 x g, room temperature, before loading. Gels were electrophoresed in running buffer (Section 2.1.5), at 200 V for 45 minutes. Gels were either silver-stained by kit, according to the manufacturer's instructions (Owl Separation Systems), or by SYPRO Ruby gel stain (Invitrogen). Briefly, gels to be stained by SYPRO Ruby were first fixed by two 15 minute incubations in a 50 ml 50 % (v/v) methanol 7 % (v/v) acetic acid solution. Gels were each stained overnight in 50 ml SYPRO Ruby stain and destained for 30 minutes in 100 ml 10 % (v/v) methanol 7 % (v/v) acetic acid solution. All SYPRO Ruby stained gels were scanned and analysed using a UV transilluminator gel doc system (Syngene Gene Genius) with GeneSnap acquisition software (Syngene). All silver-stained gels were scanned and analysed using a backlit visible light gel doc system (Syngene Gene Genius) with GeneSnap acquisition software (Syngene).

2.7.4 Analysis of agarose and acrylamide gels

Quantitative analysis of DNA in agarose gels and protein in acrylamide gels were performed using GeneTools analysis software (Syngene). The absolute intensity of each band was measured and the local background intensity manually subtracted. Sample DNA quantification was achieved by comparison with the band intensities of the relevant DNA ladders. SYPRO

Ruby stained protein gels were quantified in relative terms by comparing the intensity of each lane to a control lane.

2.7.5 Bradford assay

Quantitative analysis of protein concentration in solution was performed by the Bradford assay (Bradford 1976). Coomassie protein assay reagent (Sigma) was diluted five-fold in sterile RO water and filtered (0.22 μm Millipore). An aliquot (1 ml) of this working reagent was added to each 30 μl sample in a 1 ml semi-micro cuvette (Sarstedt), mixed, and incubated at room temperature for 5 minutes. The absorbance of all samples at 565 nm was read within 5 minutes on a Hitachi U-1800 spectrophotometer. A 1 mg ml^{-1} bovine serum albumin (BSA) standard (Sigma) was 0.66 x serially diluted. Absorbance at 595 nm was linear in the range 13- 225 μg ml^{-1} BSA. Samples were analysed in triplicate.

2.8 Molecular Biology Techniques

2.8.1 Preparation of bacteriophage M13 single-stranded DNA

Naked single-stranded DNA was prepared from intact M13 bacteriophage by phenol-chloroform extraction. An equal volume of phenol- chloroform- isoamyl alcohol (of ratio 25: 24: 1) was added to the M13 solution and vortexed for 20 seconds. Following centrifugation for three minutes at 17 000 x g, room temperature, the aqueous layer was removed and the process repeated. An equal volume of chloroform was added to the resulting aqueous layer and gently mixed. Following a further three minute centrifugation at 17 000 x g, room temperature, the aqueous layer was removed and the DNA precipitated on ice by two volumes -20 ºC 100 % ethanol/ 0.1 volumes room temperature 4 M sodium acetate for 15 minutes. DNA was pelleted by centrifugation for 20 minutes, 13 000 x g at 4 ºC. The supernatant was removed; the pellet washed by addition of 200 μl -20 ºC 70 % (v/v) ethanol, and then centrifuged for 10 minutes, 13 000 x g at 4 ºC. The supernatant was removed and the pellet dried at 50 ºC for 5 minutes. The pellet was resuspended in TE, and DNA concentration quantified by absorbance at 260 nm (Section 2.7.1).

2.8.2 Large-scale preparation of bacteriophage M13 double-stranded DNA

Naked double-stranded DNA was prepared from infected *E. coli* cells by alkaline/SDS lysis (Birnboim and Doly, 1979), using a Qiagen Maxiprep kit (Qiagen). Cultures (400 ml) were prepared as described in Section 2.3.3 except that the bacterial pellets were kept. Cell paste (0.5 g) was resuspended in 10 ml buffer P1 (50 mM Tris-HCl (pH 8.0), 10 mM EDTA, 100 μg ml^{-1} RNase A), before the addition of 10 ml buffer P2 (200 mM NaOH, 1 % (w/v) SDS). The cell suspension was vigorously inverted 4- 6 times, and incubated at room temperature for 5

minutes. A total of 10 ml 4 ℃ buffer P3 (3.0 M potassium acetate (pH 5.5) was then added and the mixture vigorously inverted 4- 6 times and immediately applied to a QIAfilter Maxi cartridge. The lysate was incubated for 10 minutes at room temperature, and cleared by filtration through the QIAfilter Maxi cartridge. The clarified supernatant was immediately applied to the anion-exchange resin of a Qiagen-tip 500 column, which had been pre-equilibrated by the addition of 10 ml buffer QBT (750 mM NaCl, 50 mM MOPS (pH 7.0), 15 % (v/v) isopropanol, 0.15 % (v/v) Triton X-100), and allowed to empty under gravity flow. The column was then washed by the application of two 30 ml volumes of buffer QC (1.0 M NaCl, 50 mM MOPS (pH 7.0), 15 % (v/v) isopropanol), before eluting the bacteriophage DNA by the addition of 15 ml buffer QF (1.25 M NaCl, 50 mM Tris-HCl (pH 8.5), 15 % (v/v) isopropanol). The nucleic acid was precipitated from the eluate by the addition of 0.7 volumes of room temperature isopropanol, and recovered by centrifugation for 30 minutes at 15,000 x g, 4 °C. The DNA pellet was then washed with 5 ml of room temperature 70 % (v/v) ethanol, centrifuged again (15,000 x g, 15 min, 4 °C) and the pellet air dried for 5 minutes at 50 °C. The pellet was resuspended in a suitable volume of TE buffer, and DNA concentration quantified by absorbance at 260 nm (Section 2.7.1).

2.8.3 Small-scale preparation of plasmid DNA

Plasmid DNA was isolated from 5 ml *E. coli* cultures (Section 2.3.1) by alkaline/SDS lysis (Birnboim and Doly, 1979), using Qiagen Miniprep kit (Qiagen). Cells were pelleted by centrifugation at 4 500 × g (RCF_{max}) for 15 minutes at 4 °C, and the supernatant discarded. The cells were resuspended in 250 µl buffer P1 (Section 2.8.2). 250 µl of buffer P2 (Section 2.8.2) was added and the cell suspension was gently inverted 4- 6 times. A total of 350 µl 4 ℃ buffer P3 (Section 2.8.2) was then added and the mixture gently inverted 4- 6 times. The lysate was then centrifuged at 17 000 x g for 10 minutes, room temperature. The supernatant was immediately applied to the anion-exchange resin of a Qiagen QIAprep spin column, and centrifuged at 17 000 x g for 1 minute. The flow-through was discarded. The column washed by the successive application of 500 µl buffer PB (proprietary composition) and 750 µl buffer PE (proprietary composition), each followed by centrifugation at 17 000 x g for 1 minute and the flow-through discarded. All traces of buffer PE were removed by a further 1 minute centrifugation. The plasmid DNA was eluted into a sterile 1.5 ml polypropylene tube by addition of a suitable volume of buffer EB (10 mM Tris-HCl, pH 8.5) to the centre of the spin column, incubation for 1 minute at room temperature and centrifugation at 17 000 x g for 1 minute.

2.9   Preparation and Transformation of Competent *E. coli* Cells

2.9.1   Preparation of CaCl$_2$ competent *E. coli* cells

A 5 ml *E. coli* culture was first prepared as outlined in Section 2.3.1. A 20 ml NB2 solution, supplemented with 20 mM MgCl$_2$ post-autoclaving, was prepared in a 50 ml polypropylene tube and warmed to 37 °C. This was inoculated with the 5 ml overnight culture and incubation at 37 °C with shaking for 1 hour. The culture was cooled on ice for 10 minutes to arrest growth, and the cells pelleted by centrifugation at 4 500 × g (RCF$_{max}$) for 10 minutes at 4 °C. The supernatant was discarded, and the pellet held on ice. The pellet was resuspended in 2 ml ice-cold sterile 15 % (v/v) glycerol, 75 mM CaCl$_2$ solution by brief vortexing before being returned to ice. The cell suspension was divided into 100 µl aliquots in pre-cooled 1.5 ml polypropylene tubes on ice and stored at -80 °C.

2.9.2   Transformation of CaCl$_2$ competent *E. coli* cells

Transformations were performed by adding approximately 50 ng ice cold DNA (prepared by Section 2.8.3) to 100 µl of thawed competent cells on ice, and incubating for 45 minutes. The cells were subsequently heat shocked for 2 minutes at 42 °C and returned to ice for a further 2 minutes. A 5 ml quantity of sterile NB2 was inoculated with all the cells, and grown for 90 minutes at 37 °C with shaking. Transformants were typically selected by plating 100 µl of the incubated transformation culture onto appropriate antibiotic- supplemented NB2A plates. Where appropriate, further supplementation of NB2A with X-gal (Section 2.1.11) and IPTG (Section 2.1.12) facilitated blue/white colony screening. Where intact bacteriophage M13 or its derivatives were the target, incubated transformation culture cells were pelleted by centrifugation at 4 500 × g (RCF$_{max}$) for 10 minutes at 4 °C. A 100 µl aliquot of supernatant was then mixed with 2×10^8 pfu of appropriate plating cells (Section 2.3.1.2) and 5 ml molten (50 °C) NB2OA and poured onto a solidified NB2A plate. Both base and overlay agars were supplemented with antibiotics (Section 2.1.10) and X-gal/ IPTG as required. All plates were incubated at 37 °C for a minimum of 18 hours (overnight).

2.10   Electron Microscopy

Caesium chloride purified bacteriophage M13 (Section 2.4) was visualised by transmission electron microscopy (TEM) at the Electron Microscopy Unit within the UCL Department of Anatomy and Developmental Biology. Each carbon grid (carbon film supported on 3 mm 400 mesh copper grid, Agar Scientific) was placed mesh-side down onto a 50 µl droplet of 10^9 pfu ml^{-1} bacteriophage sample for twenty seconds and removed. The excess was removed with absorbent paper. Each grid was then placed onto a 50 µl droplet of uranyl acetate (0.25 % w/v) for 10- 20 seconds, then immediately placed on a 50 droplet of sterile RO water for 1 minute.

The excess was removed with absorbent paper and the grid allowed to air dry. Samples were imaged by JEOL 100CX electron microscope.

2.11 Viscosity Measurement

Sample fluid viscosity was determined by cone and plate viscometer (DV-II+, Brookfield) according to the manufacturer's instructions. Briefly, 0.5 ml samples were subject to increasing shear rates within the viscometer and the corresponding shear stresses recorded. At least four different shear rates were tested per sample. Sample viscosity was determined as the gradient of the linear relationship between shear stress and shear rate. Therefore samples were assumed to be Newtonian. Viscosity measurements were conducted in duplicate.

2.12 Techniques Used to Study the Effects of Hydrodynamic Shear

2.12.1 Sonication of bacteriophage M13

Caesium chloride purified bacteriophage M13 (Section 2.4) were 100-fold diluted in sterile 10 mM Tris (pH 7.5 at 25 °C) to give 25 ml of concentration of 10^{11} pfu ml^{-1}. A 20 ml aliquot of this bacteriophage suspension was measured into a sterile 50 ml polypropylene tube. The tube was clamped over an ice-water slurry in a Soniprep 150 (Sanyo Gallenkamp) ultrasonic disintegrator, fitted with a 9.5 cm probe of transformation ratio 5.5:1. The probe was immersed 1 cm below the bacteriophage suspension surface, and the tube was held to avoid touching the probe. The solution was sonicated for two minute periods. Samples (500 µl) were taken at 0, 2, 4, 6, 8 and 10 minutes. The zero timepoint was sampled in triplicate. The entire experiment was repeated three times. Ultrasound amplitudes of 1, 5 and 10 µm were tested. The viability of bacteriophage M13 in each sample was determined by the surface droplet technique (Section 2.5.2).

2.12.2 Ultra scale-down (USD) shear device operation

Turbulent hydrodynamic shearing was performed by a custom-built device consisting of a single rotating stainless steel disk of diameter 40 mm, thickness 0.14 mm, mounted centrally in a 20 ml capacity stainless steel cylindrical chamber (Figure 2.1). The temperature within the chamber was controlled by a surrounding cooling water jacket, through which 4 °C water was circulated. Initial experiments were conducted with an electrically-driven brushed DC motor attached to the shaft assembly, which could be operated at a maximum of 350 revolutions per second (rps). Shaft rotation speed was detected by optical sensor. Similar equipment has been used by Levy *et al.* (1999b) to study the effects of shear on plasmids and Boychyn et al. (2001) to model the shear stresses within continuous centrifuges. Higher speed operation required the

use of updated equipment, including the use of an electrically- driven brushless motor attached to the shaft assembly, which could be operated at a maximum of 533 rps. Shaft rotation speed was detected by phase sensor. Temperature was also monitored by a thermocouple bonded to the underside of the chamber by thermally conductive adhesive. Updated equipment also included a power analyser (Medusa Research), which allowed for the direct calculation of power input to the motor during operation (Figure 2.2). Each experimental run consisted of completely filling the chamber with the test solution and rotating the disk within the chamber at the required speed for the required time. Within each experimental run, direct samples of 500 µl were taken at the specified time-points. All experiments were performed at room temperature. The zero timepoint was sampled in triplicate. Between shearing runs, the chamber was completely filled with 1 % Virkon solution for 10 minutes, and rinsed with five changes of sterile RO water. The entire experiment was repeated three times.
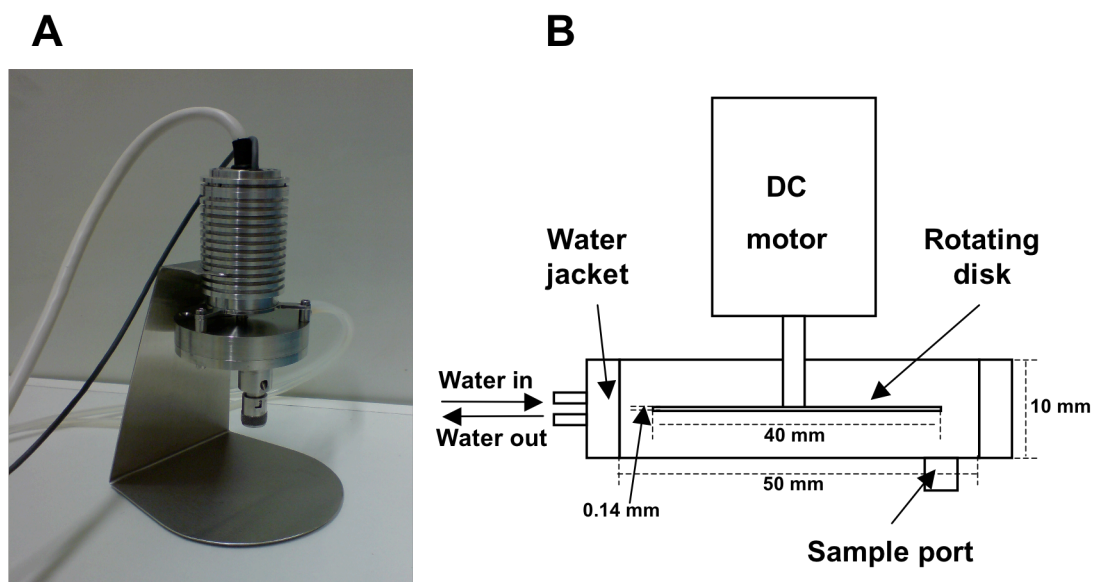
Figure 2.1 Photograph of the USD rotating disk shear device (A) together with a schematic diagram of the device chamber (B). A stainless steel disk of diameter 40 mm and thickness 0.14 mm was mounted centrally within the chamber. The stainless steel chamber was cooled by ice water flowing through a water jacket.
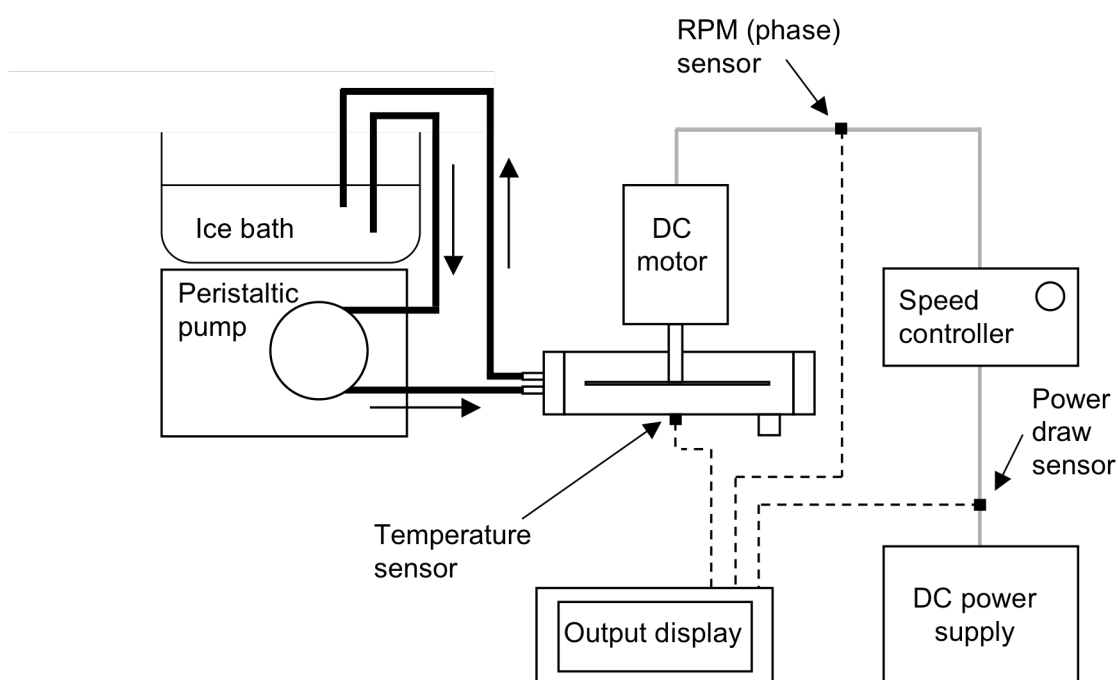
Figure 2.2 A schematic diagram of the USD rotating disk shear device with associated equipment. Ice water was supplied to the water jacket by flexible silicone tubing through a peristaltic pump. The power draw was calculated by voltage and current measurement from the DC power supply. Temperature was measured by thermocouple. DC motor rotation speed was measured by RPM (phase) sensor.

2.12.3 Cavitation Detection

The level of cavitation within test fluids subject to sonication (Section 2.12.1) and turbulent shear (2.12.2) was determined by Weissler's reaction (Weissler *et al.*, 1950). That is, the generation of hydroxide and peroxyl radicals by cavitation in aqueous solution can be detected by the presence of potassium iodide. The free radicals oxidize the iodide anion (I^-) to liberated iodine of the form (I_3^-) with a zero order rate law (Wayment and Casadonte, 2002). This change is measured by the change in absoption at 350 nm. Potassium iodide (Alfa Aesar) solution of concentration 3 M in RO water was subject to sonication exactly as described in Section 2.12.1, and turbulent shear in Section 2.12.2, where samples were taken at 0, 5, 10, 15, 20 and 25 minutes, subject to 32 000 rpm disc rotation. Triplicate non-sonicated and non-sheared negative controls were present in each case. The change in absorbance at 350 nm was measured on a Hitachi U-1800 spectrophotometer with disposable UV-clear acryl-cuvettes (Sarsedt). The Beer- Lambert relationship was then used to calculate I_3^- concentrations using an extinction coefficient of 2.6×10^4 M^{-1} cm^{-1} (Wayment and Casadonte, 2002). All experiments were repeated three times.

2.13   Bacteriophage M13 Fermentation Techniques

2.13.1   Shakeflask experimentation

Three overnight 5 ml starter cultures of Top10F' were prepared in NB2 with antibiotic selection as described in Section 2.3.1, and the OD_{600} values measured following dilution in fresh NB2 media (CO8000 Cell Density Meter, WPA-Biochrom). Three pre-warmed baffled shakeflasks (250 ml) containing 50 ml sterile NB2 were inoculated with 1 ml of starter culture each and incubated at 37 °C with shaking (200 rpm). When M13 infection was required 2.3 x 10^8 pfu of bacteriophage were added to each flask. Samples (1ml) were removed at 0 minutes, 30 minutes and 1 hour and then at hourly intervals afterwards. The OD_{600} value was recorded and 50 μl removed for cell and bacteriophage enumeration (Sections 2.5.1 and 2.5.2). Samples for enumeration were stored on ice until needed. The remainder of every sample was centrifuged at 17 000 x g for 3 minutes to pellet the cells. Supernatants were carefully decanted and stored at - 20 °C until needed.

2.13.2   Two-litre batch fermentation

Laboratory scale fermentations were performed in a 2 litre (working volume 1.5 litre) LH 210 series fermenter (Bioprocess Engineering Services) fitted with three equally spaced top driven six bladed turbines and four diametrically opposed baffles. pH was measured by a steam sterilisable Mettler Toledo pH probe (Mettler Toledo) and controlled at pH 7 ($\pm$ 0.05) by the metered addition of 500 mM sodium hydroxide and 1 % (v/v) sulphuric acid. The dissolved oxygen tension (DOT) was measured by a polarographic oxygen electrode (Mettler Toledo). The inlet and exhaust gases were filtered through 0.2 μm PTFE filters (Millipore) and the oxygen and carbon dioxide levels in the exhaust gas were determined by Tandem gas analyser (Adaptive Biosystems). Data logging and exhaust gas measurements were recorded by Squirrel 1600 data logger (Grant).

The fermenter was sterilized by autoclaving (121 °C for 20 minutes) with 1.35 litres of all media components (excluding antibiotics, IPTG, or calcium chloride supplements, if required) and antifoam present (0.2 ml l^{-1} polypropylene glycol 2000. BDH). Non-autoclaved supplements were added immediately prior to inoculation and sterilized by 0.2 μm filtration. After adjustment of vessel conditions to 37 °C and pH 7.0, the DOT was set to 100 %. The vessel was then inoculated with 150 ml of shake flask culture grown overnight (10 % (v/v) inoculum). Inoculum cultures were prepared as described in Section 2.3.2 with matching media for the fermentation. Where necessary, the culture was inoculated with caesium chloride purified bacteriophage M13 (Section 2.4). Bacteriophage M13 inoculation occurred at either the zero timepoint (1.3 x 10^{11} pfu) or three hours into the fermentation (2 x 10^{11} pfu), as appropriate for the experiment.

The fermentation was carried out at a minimum DOT of 30 % of air saturation. Throughout fermentation, DOT was maintained above this level by increasing the rate of stirring, up to a maximum of 1 500 rpm. The agitation rate was initially set at 750 rpm, and increased when necessary. The vessel was aerated at a rate of 1 L min^{-1} (0.67 vvm). Growth was monitored regularly by absorbance at 600 nm at hourly intervals, plus an extra sample at 30 minutes. Samples were suitably diluted with fresh media and absorbances measured in triplicate (CO8000 Cell Density Meter, WPA-Biochrom). Viable cells were enumerated as described in Section 2.5.1. Bacteriophage were enumerated as described in Section 2.5.2.

2.13.3 Dry cell weight determination

Triplicate 0.5 ml aliquots of each sample were measured into 1.5 ml polypropylene tubes. All tubes had been pre-dried at 60 °C for 24 hours and weighed. Cells were pelleted by centrifugation at 17 000 x g, 3 minutes, room temperature, and the supernatants discarded. Pellets were dried at 60 °C for 48 hours and the tubes reweighed. The dry cell weight was then calculated in g l^{-1}.

2.14 Primary Purification Techniques

2.14.1 Precipitation of pure bacteriophage M13 in a 1 ml qualitative screen

Stocks of 10 % (w/v) cetyl trimethylammonium bromide (CTAB), 5 M sodium chloride (BDH), 100 mM spermidine (Sigma), 1M calcium chloride (BDH), 500 mM managanese sulphate (BDH), 50 % (w/v) ammonium suphate (BDH) were prepared in sterile RO water. Except for CTAB, every stock plus 500 ml of sterile RO water was adjusted to pH 7.0 prior to use with 1 % (v/v) sulphuric acid/ 500 mM sodium hydroxide (Seven Easy pH meter, Mettler-Toledo). Each 1 ml precipitation reaction was performed in a 1.5 ml polypropylene tube. Appropriate amounts of each stock were added to each tube to give the desired final concentration in 1 ml, plus sterile RO water up to 0.99 ml. Finally, 10 μl caesium chloride purified bacteriophage M13 (Section 2.4) of concentration 4 x 10^{13} pfu ml^{-1} was added and the tubes inverted 4- 6 times to mix. All tubes were incubated for 15 minutes at room temperature and then centrifuged at 8 000 x g for 10 minutes at room temperature to pellet the bacteriophage. The exception was the ammonium sulphate reactions, which were left overnight at room temperature and centrifuged for 10 minutes at 17 000 x g (Rossomando and Zinder, 1968). Tubes were inspected for a white pellet of bacteriophage. The pH of reactions at the extremes of precipitant concentration was checked with indicator strips to confirm neutrality (BDH). The experiment was repeated twice.

2.14.2 Precipitation of pure bacteriophage M13 by polyethylene glycol (PEG) in a 10 ml quantitative screen

Stocks of 15 % (v/w) polyethylene glycol (PEG) of average molecular weights 600 (Fluka), 2 000 (Fluka), 6 000 (BDH), 8 000 (Fluka), 12 000 (Fluka) and 20 000 (Fluka) were prepared in RO water and autoclaved. Stocks of 5 M sodium chloride, 1 M magnesium chloride and 1 M sodium sulphate were prepared in RO water and autoclaved. Every stock plus 500 ml of sterile RO water was adjusted to pH 7.0 prior to use with 1 % (v/v) sulphuric acid/ 500 mM sodium hydroxide (Seven Easy pH meter, Mettler-Toledo). Each 10 ml precipitation reaction was performed in a 15 ml polypropylene tube. Appropriate amounts of each stock were added to each tube to give the desired final concentration in 10 ml, plus sterile RO water up to 9.9 ml. Finally, 100 µl caesium chloride purified bacteriophage M13 (Section 2.4) of concentration 4 x 10^{13} pfu ml^{-1} was added and the tubes inverted 4- 6 times to mix. Typically, tubes were incubated on ice for 1 hour. All tubes were centrifuged for 10 minutes, 8 000 x g, 4 °C and the supernatants decanted into fresh 15 ml tubes (Yamamoto *et al.*, 1970). Pellets were resuspended in 10 ml 20 mM Tris (pH 7.5 at 25 °C) by vortexing. Supernatants were also vortexed. The bacteriophage concentration in the pellets and supernatants was determined by the surface droplet technique (Section 2.5.2). Each precipitation experiment had a positive control of 3.3 % (w/v) PEG 6 000, 330 mM NaCl, and a negative control of sterile RO water. All experiments were repeated three times.

2.14.3 Precipitation of pure bacteriophage M13 by isoelectric precipitation in a 10 ml quantitative screen

The effect of pH was investigated first. Eight 30 ml aliquots of sterile RO water in 50 ml polypropylene tubes were each inoculated with 300 µl caesium chloride purified bacteriophage M13 (Section 2.4) of concentration 4 x 10^{13} pfu ml^{-1}. The pH of each was adjusted with 1 % (v/v) sulphuric acid/ 500 mM sodium hydroxide to give pH readings of 3.7, 3.9, 4.1, 4.3, 4.5, 4.7, 4.9 and 7.0 at room temperature (Seven Easy pH meter with three point calibration, Mettler-Toledo). A 15 ml quantity of each 30 ml aliquot was transferred to a fresh 50 ml tube on ice. All samples were incubated for 2 hours and the pH of each checked and adjusted back to target. A 10 ml quantity of each sample was then transferred to a fresh 15 ml polypropylene tube and incubated for a further 22 hours to allow the bacteriophage to precipitate (Bachrach and Friedmann, 1971). The pH of each sample was then checked and all samples centrifuged at 15 000 x g for 8 minutes. Samples incubated on ice were centrifuged at 4 °C, samples incubated at room temperature were centrifuged at 25 °C. Supernatants were decanted into fresh 15 ml tubes, to which 100 µl Tris (pH 8.07 at 25 °C) was added to arrest precipitation. Pellets were resuspended in 10 ml 20 mM Tris (pH 7.5 at 25 °C) by vortexing. Supernatants were also vortexed. The bacteriophage concentration in the pellets and supernatants was determined by the surface droplet technique (Section 2.5.2). The experiment was repeated three times.

The precipitation time was also investigated. Two 45 ml aliquots of sterile RO water in 50 ml polypropylene tubes were each inoculated with 450 µl caesium chloride purified bacteriophage M13 (Section 2.4) of concentration 4×10^{13} pfu ml^{-1}, and cooled on ice. The pH of each was adjusted with 1 % (v/v) sulphuric acid/ 500 mM sodium hydroxide to give pH readings of 4.3 and 7.0 at approximately 2- 4 °C (Seven Easy pH meter, Mettler-Toledo). A 10 ml sample of each 45 ml aliquot was transferred to a fresh 15 ml tube and centrifuged at 15 000 x g, 8 minutes, 4 °C, and the supernatant decanted into a fresh 15 ml tube. After 1 hour's incubation, the pH of each remaining sample was checked and adjusted back to target. A second 10 ml sample of each remaining 35 ml aliquot was transferred to a fresh 15 ml tube and centrifuged at 15 000 x g, 8 minutes, 4 °C, and the supernatant decanted into a fresh 15 ml tube. The same process was repeated after 2 and 24 hour's incubation on ice. After decanting, 100 µl Tris (pH 8.07 at 25 °C) was added to every supernatant to arrest precipitation. Pellets were resuspended in 10 ml 20 mM Tris (pH 7.5 at 25 °C) by vortexing. Supernatants were also vortexed. The bacteriophage concentration in the pellets and supernatants was determined by the surface droplet technique (Section 2.5.2). The experiment was repeated three times.

2.14.4   Precipitation of pure bacteriophage M13 by divalent and polyvalent cation precipitation in a 10 ml quantitative screen

Stocks of 1 M calcium chloride and 5 M sodium chloride were prepared in RO water and autoclaved. A 100 mM stock of spermidine was prepared with sterile RO water. Precipitation reactions at the 10 ml scale were conducted as described in Section 2.14.2, except incubation was at room temperature for 15 minutes only, and post-centrifugation, 100 µl 5 M sodium chloride was added to each supernatant to arrest precipitation. Each precipitation experiment was repeated three times.

2.14.5   Precipitation of bacteriophage M13 from broth in a 10 ml qualitative screen

A 400 ml culture of *E. coli* Top10F' in NB2 was prepared as described in Section 2.3.2, and was infected with 2×10^{9} pfu ml^{-1} caesium chloride purified bacteriophage M13 prior to overnight incubation. The culture was centrifuged at 14 000 $\times$ g (RCF$_{max}$) for 10 minutes at 4 °C, and the bacterial pellet discarded. The supernatant was filtered by 0.2 µm Steritop GP Express Plus (Millipore) to remove remaining biomass.

Stocks of 1 M calcium chloride, 5 M sodium chloride, 1 M magnesium sulphate, 15 % (v/w) PEG 6000 and 100 mM spermidine were prepared in sterile NB2. Every stock plus filtered culture was adjusted to pH 7.0 prior to use with 1 % (v/v) sulphuric acid/ 500 mM sodium hydroxide (Seven Easy pH meter, Mettler-Toledo). Precipitation reactions (10 ml each) were conducted as described in Sections 2.14.2, 2.14.3 and 2.14.4, except that the addition of caesium

chloride purified bacteriophage M13 was unnecessary, and tubes were inspected for bacteriophage pellets post-centrifugation. In the isoelectric precipitation reaction, 15 ml of culture was adjusted to pH 4.3 and incubated for 1 hour on ice. Reactions giving successful precipitation at the lowest precipitant quantities were further investigated by bacteriophage enumeration using the surface droplet technique (Section 2.5.2). These experiments were repeated twice.

2.14.6 Precipitant comparison in terms of bacteriophage M13 purification

Filtered chilled culture (Section 2.3.2) was adjusted to pH 7.0 prior to use with 1 % (v/v) sulphuric acid/ 500 mM sodium hydroxide. Dry precipitants were added directly to culture supernatant of final volume 40 ml in sterile 50 ml polypropylene tubes. Precipitants were dissolved by incubation at room temperature with gentle shaking for 5 minutes, and the pH checked with indicator strips to confirm neutrality (BDH). The pH of 40 ml culture subject to isoelectric precipitation was adjusted by concentrated sulphuric acid to pH 4.3. All reactions were incubated on ice for 1 hour to precipitate the bacteriophage, and the pH of the isoelectric precipitation culture re-checked. Tubes were centrifuged for either 10 minutes, 8 000 x g, 4 °C or 8 minutes, 15 000 x g, 4 °C (isoelectric precipitation only) and the supernatants decanted into fresh 50 ml tubes. Pellets were resuspended in 800 μl 20 mM Tris (pH 7.5 at 25 °C) by gentle rocking and brief vortexing. Supernatants were also vortexed. Pellets, supernatants and untreated culture were analysed by SDS-PAGE (Section 2.7.3), agarose gel electrophoresis (Section 2.7.2), Bradford assay (Section 2.7.5) and surface droplet bacteriophage enumeration (Section 2.5.2) to determine the purification of bacteriophage M13 achieved by each precipitation method. The experiment was repeated three times.

2.15 Bacteriophage and *E. coli* Characterisation Studies

2.15.1 Determination of an effective decontamination agent

2.15.1.1 Effect of Tego on bacteriophage M13 viability

The liquid amphoteric surfactant Tego 2001 (proprietary composition based on 1-alkyl-1,5-diazapetane in aqueous solution. Johnson Diversey) was tested for efficacy against caesium chloride purified bacteriophage M13 at concentrations of 0, 1, 2 and 10 % (v/v). The typical working concentration was 2 % (v/v) at room temperature. Solutions (9 ml) of Tego in sterile RO water were made in sterile 50 ml polypropylene tubes, to which 1 ml of bacteriophage were added, making the appropriate Tego concentration in 10 ml. Tubes were briefly mixed, and duplicate 20 μl samples were taken for bacteriophage enumeration (Section 2.5.2) after 10 second, 1, 5, 10 and 20 minute incubations at room temperature. Samples were immediately ten-fold serially diluted to 10^{-2} of their original concentration. A control of 10 % Tego solution

alone was also serially diluted and plated onto Top10F' overlay agar plates. The experiment was repeated three times.

2.15.1.2 Effect of Solquest on bacteriophage M13 viability

The liquid surfactant Solquest (proprietary composition based on 10- 30 % (w/v) tetrasodium EDTA, 5- 10 % (v/v) amino-tri(methylene phosphonic acid), 5- 10 % (w/v) sodium hydroxide, Arrowmight Biosciences) was tested for efficacy against caesium chloride purified bacteriophage M13 at concentrations of 0, 0.5, 1 and 5 % (v/v) at 50 °C and 70 °C. The typical working concentration was 1 % (v/v) in "hot" water. Solutions (900 µl) of Solquest in sterile RO water were made in sterile 1.5 ml polypropylene tubes and incubated at the appropriate temperature for 20 minutes in a pre-warmed heat block (Thermomixer Comfort, Eppendorf). Caesium chloride purified bacteriophage (100 µl) were added to each, making the appropriate Solquest concentration in 1 ml. Tubes were briefly mixed, and duplicate 20 µl samples were taken for bacteriophage enumeration (Section 2.5.2) after 10 second, 1, 5, 10 and 20 minute incubations. Samples were immediately ten-fold serially diluted to 10^{-2} of their original concentration. A control of 5 % Solquest solution alone was also serially diluted and plated onto Top10F' overlay agar plates. All experiments were repeated three times.

2.15.1.3 Effect of Virkon on bacteriophage M13 viability

The oxidising disinfectant powder Virkon (proprietary composition based on < 50 % (w/w) pentasodium bis(peroxymonosulphate) bis(sulphate), 5- 10 % (w/w) sulphamidic acid, 5- 15 % (w/w) sodium dodecylbenzenesulfonate, <2 % (w/w) dipotassium peroxdisulphate, DuPont) was tested for efficacy against caesium chloride purified bacteriophage M13 as 0, 0.01, 0.1 and 1 % (w/v) solutions. The typical working concentration was 1 % (w/v) at room temperature. A 2 % (w/v) stock was prepared. Solutions (9 ml) of Virkon in sterile RO water were made in sterile 50 ml polypropylene tubes, to which 1 ml of bacteriophage were added, making the appropriate Virkon concentration in 10 ml. Tubes were briefly mixed, and duplicate 20 µl samples were taken for bacteriophage enumeration (Section 2.5.2) after 10 second, 1, 5, 10 and 20 minute incubations at room temperature. Samples were immediately ten-fold serially diluted to 10^{-2} of their original concentration. A control of 1 % Virkon solution alone was also serially diluted and plated onto Top10F' overlay agar plates. The experiment was repeated three times.

2.15.1.4 Effect of Virkon on *E. coli* viability

A 150 ml baffled shake flask containing 50 ml NB2 was inoculated with 1 ml of *E. coli* W1485 working culture (Section 2.3.1.3), and incubated at 37 ºC with shaking, overnight. The oxidizing disinfectant powder Virkon (DuPont) was tested for efficacy against *E. coli* W1485 as 0, 0.1, 0.5 and 1 % (w/v) solutions. The typical working concentration was 1 % (w/v) at room temperature. A 2 % (w/v) stock was prepared. Solutions (10 ml) of Virkon in sterile RO water

were made in sterile 50 ml polypropylene tubes of concentration 0, 0.2, 1 and 2 % (w/v), to which 10 ml of culture was added, making the appropriate Virkon concentration in 20 ml. Tubes were briefly mixed, and duplicate 20 μl samples were taken for *E. coli* enumeration by the surface droplet technique (Section 2.5.2). Samples were taken after 10 second, 1, 5, 10 and 20 minute incubations at room temperature. Samples were immediately ten-fold serially diluted to 10^{-2} of their original concentration. The experiment was repeated three times.

2.15.2 The effect of desiccation on bacteriophage M13 and *E. coli*

2.15.2.1 Preparation of *E. coli* cultures

Two 150 ml baffled shake flasks containing 50 ml NB2 were inoculated with 1 ml *E. coli* Top10F' working culture (Section 2.3.1.2). One flask was also inoculated with 2×10^{9} pfu ml^{-1} caesium chloride purified bacteriophage M13 (Section 2.4), and both flasks incubated at 37 ℃ with shaking, overnight. This procedure was repeated three times.

2.15.2.2 Preparation of bacteriophage M13

Caesium chloride purified bacteriophage M13 (4 ml) (Section 2.4) was combined with 1 ml 5x NB2 to give 1×10^{13} pfu ml^{-1} in 1x NB2. An aliquot of this solution (500 μl) was subsequently 10-fold serially diluted in 4.9 ml amounts of NB2 to an M13 concentration of 1×10^{4} pfu ml^{-1}. The serial dilution process was repeated three times.

2.15.2.3 Preparation for desiccation

Desiccation was conducted in polystyrene round-bottomed 96-well plates (Sterilin). Two hundred microlitre quantities of each *E. coli* culture (infected and non-infected with M13) and M13 dilutions of 10^{13}, 10^{10}, 10^{7} and 10^{4} pfu ml^{-1} were loaded. Each 96-well plate held all three experimental repeats. Twenty-four 96-well plates were loaded. The wells of eight plates were sealed with self-adhesive impermeable tape (Fisher) as non-desiccated controls. All uncovered plates were placed under a fume hood until dry. The relative humidity of the fume hood was recorded (H-2 humidity meter, Testo).

2.15.2.4 Desiccation

Once dry, eight 96-well plates were immediately placed, uncovered, in a laboratory desiccator filled with anhydrous silica gel crystals (BDH). The desiccator was placed in a cupboard to protect the samples from light and draughts. Eight 96-well plates were placed alongside the desiccator, also uncovered, together with the eight sealed control plates. One plate was removed from each condition on days 0, 1, 3, 6, 12, 20, 30 and 47 post commencement of desiccation. The relative humidity within the desiccator and in the laboratory was recorded twice-weekly.

2.15.2.5   Enumeration of viable bacteriophage M13 and *E. coli*

At each time-point the cells and bacteriophage in the removed 96-well plates were rehydrated with 200 µl 20 mM Tris (pH 7.5 at 25 °C) per well. Plates were incubated for 20 minutes at room temperature, and the cells and bacteriophage gently pipetted to resuspend. After a further 10 minute incubation and pipetting, cells and bacteriophage were enumerated by the surface droplet technique (Section 2.5.2).

2.15.3   The effect of extremes of pH on bacteriophage M13

Caesium chloride purified bacteriophage M13 suspension (640 µl) (Section 2.4) was combined with 160 µl 5 x NB2 to give 1 x 10^{13} pfu ml^{-1} in 1 x NB2. Aliquots (15 ml) of sterile RO water were adjusted with 10 % (v/v) sulphuric acid/ 4 M sodium hydroxide to give pH readings of 1.0, 3.0, 7.0, 11.0 and 13.0 at room temperature (Seven Easy pH meter, Mettler-Toledo). The volumes were then each adjusted to 9.9 ml, and 100 µl of bacteriophage M13 solution added. Each tube was briefly inverted to mix and the pH checked with indicator strips (BDH). Samples of 400 µl were taken after 1, 5, 10 and 20 minute incubations. A total of 400 µl 1 M Tris (pH 7.5 at 25 °C) was immediately added to every sample to neutralize the solution. pH was checked with indicator strips to confirm neutrality (BDH). Similarly, 100 µl of bacteriophage M13 solution was added to 9.9 ml each of 10 % sulphuric acid, 4 M sodium hydroxide, and another pH 7.0 control. Each tube was briefly inverted to mix, and 400 µl samples were again taken after 1, 5, 10 and 20 minute incubations. Acidic samples were neutralised with 370 µl 4 M sodium hydroxide, 150 µl 1 M Tris (pH 7.5 at 25 °C) and 80 µl sterile RO water. Alkaline samples were neutralised with 450 µl 10 % sulphuric acid, 150 µl 1 M Tris (pH 7.5 at 25 °C). 450 µl sterile RO water and 150 µl 1 M Tris (pH 7.5 at 25 °C) was added to the pH 7.0 control. pH was again checked with indicator strips to confirm neutrality (BDH). Bacteriophage in all samples were then enumerated by the surface droplet technique (2.5.2). The entire experiment was repeated three times.

2.15.4   The effect of temperature on bacteriophage M13

One millilitre of caesium chloride purified bacteriophage M13 (Section 2.4) was combined with 2 ml 5 x NB2 and 7 ml sterile RO water to give a stock of 1 x 10^{12} pfu ml^{-1} in 1 x NB2. Each experimental run consisted of eight 50 µl aliquots of M13 stock in 500 µl polypropylene PCR tubes, evenly spaced along the centre row of Techne TC- 512 PCR block (VWR- Jencons). The lid temperature was always set at 105 °C to prevent condensation. Timing began once the PCR block reached within 0.5 °C of the specified temperature, a process typically taking less than 10 seconds. A sample tube was then removed after a 1, 5, 10, 20, 30, 40, 50 and 60 minute incubation time. The removed sample was immediately cooled in 10 °C water. Incubation temperatures of 99, 95, 90, 80, 70, 60, 50, 40, and 25 °C were tested, together with a room temperature control not incubated within the device. A 20 µl quantity of each sample was

enumerated for bacteriophage by the surface droplet technique (2.5.2). A further 20 μl of each sample was directly plated onto Top10F' overlay agar plates to serve as a 10^0 dilution. The entire experiment was repeated three times.

2.16   Data Transformation and Statistical Analysis

All statistical analyses were performed using GraphPad InStat software (version 3.0) and Microsoft Excel for Mac (version 11.5.5). Unless otherwise stated all bacterial and bacteriophage titres were transformed to $\log_{10}$ values prior to the application of the statistical tests. In all data sets containing three or more data groups, a single factor analysis of variance (ANOVA) test was applied. Where the determination of significant differences between samples was required, a derivative of the ANOVA test was used (Wardlaw, 1999). The Dunnett statistical analysis test was used to compare values in a data set against a standard control value, and determined which values in the data set were significantly different from the control value only. The Tukey test allowed the comparison of each value in a data set to each of the other values where there was no control value. The confidence interval was set at 95 %. In all data sets containing two data groups, or groups of non-equal size, a Student's t test ("t-test") was applied of two-tailed, two-sample equal variance type. It was assumed that data sets possessed a normal distribution. Standard error analysis was performed alongside all statistical tests and was displayed graphically with every experiment or shown as a "±" figure in tables.

3 The Effect of Hydrodynamic Shear on the Filamentous Bacteriophage Particle

3.1 Introduction

It was noted in Section 1.2.2 that bacteriophage M13 and its close relations are filamentous in structure. They appear as extremely long protein-coated tubes, 900 nm in length but only 6.5 nm in diameter, and are semi-flexible in nature. In effect the filamentous bacteriophage are macromolecular complexes of molecular weight 16.4 MDa (Schmidt *et al.*, 2000), which is 200-400 times that of the average globular protein and equivalent in mass to a 30 kb plasmid. In terms of size, the bacteriophage contour length is also significantly greater than the average 8-12 nm antibody protein (Biddlecombe *et al.*, 2007) and is comparable to the 1.2 μm characteristic dimensions of a 20 kb plasmid (Arulmuthu *et al.*, 2007). This is important since it has been shown that both antibody proteins and 20 kb plasmids are sensitive to high-energy turbulent shear conditions (Biddlecombe *et al.*, 2007; Levy *et al.*, 1999b). Thus, would the large bacteriophage molecule combine shear-sensitive aspects of each? The investigation of shear sensitivity is relevant for bacteriophage large-scale processing, since unit operations such as fermentation, continuous centrifugation and ancillary pumps all impart flow conditions on the process fluid up to several orders of magnitude greater in energy than that imparted by standard laboratory processing (Yim and Shamlou, 2000). Since little is known about the response of bacteriophage M13 to any of these environments, it was considered that a general approach should be undertaken to examine its fragility. Thus, the primary aim of this chapter was to examine the effect of turbulent fluid flows of varying energy intensity on bacteriophage M13 by use of a rotating-disk ultra scale-down (USD) device (described in the Materials and Methods, Section 2.12.2).

A shear resistance comparison between bacteriophage M13 and double-stranded DNA is particularly important since both entities have been studied for their effectiveness as vectors for gene therapy and vaccination (Kutzler and Weiner, 2008; Larocca *et al.*, 2002; Wan *et al.*, 2001). As "competing" technologies, it would be of significant interest if one construct proved substantially more resilient to hydrodynamic shear forces than another. Therefore, the relative resistances of M13 bacteriophage, single-stranded and supercoiled double-stranded DNA to turbulent shear conditions were investigated. All three molecules were of the same genome size to allow for an equal basis of comparison.

Over the course of a purification scheme the composition of the process fluid would alter considerably as contaminants are progressively removed, buffers changed and chemicals added. Since the shear resistance of both protein and DNA complexes have been shown to depend on the nature of the process fluid (Harrison *et al.*, 1998; Levy *et al.*, 1999a; Levy *et al.*, 1999b), the

shear resistance of bacteriophage M13 in several process fluid environments was consequently examined.

This chapter begins with the revisiting of an early method determining the fragility of filamentous bacteriophage to ultrasonication. The rotating disk USD shear device is then introduced, and the theory of describing the imposed conditions discussed. The resistance of bacteriophage M13 to a range of shear conditions is first examined, followed by the comparison with single and double-stranded DNA molecules. The effect of solution conditions is then shown. Two experiments are presented which aimed to clarify some of the mechanisms of damage within the device. Finally, a comparison is made between bacteriophage M13 and existing data for various other complex macromolecules tested within the USD shear device. The implications of these results for the large-scale bioprocessing of bacteriophage M13 are then discussed.

3.2   The Effect of Ultrasonication on Bacteriophage M13

An early reference to filamentous bacteriophage fragility was made in 1963, where the severe sensitivity of bacteriophage fd to the shear imparted by sonication was described. This newly discovered bacteriophage was found be much more sensitive to these conditions relative to smaller, more spherical bacteriophage molecules (Marvin and Hoffman-Berling, 1963). Since bacteriophage M13 is closely related to fd, it was expected that a severe sensitivity would also be noted.

3.2.1   The effect on bacteriophage viability

The effect of sonication on the viability of caesium chloride purified bacteriophage M13 in 10 mM Tris (pH 7.5 at 25 °C) was investigated as described in the Materials and Methods (Section 2.12.1). The concentration of bacteriophage was 3×10^{11} pfu ml^{-1}, similar to that achieved by the end of fermentation (Section 2.3.3). The decay in bacteriophage viability upon exposure to 1, 5 and 10 μm amplitudes was recorded. The experiments were repeated three times.

The resulting decay profiles were each plotted as fractional concentrations of viable bacteriophage relative to non-sonicated controls. A severe loss of bacteriophage viability was recorded upon exposure to sonication of 5 and 10 μm amplitudes (Figure 3.1). This is illustrated by the viability losses in the first two minutes: at the 10 μm amplitude 98 % of bacteriophage M13 had already been inactivated, and at the 5 μm amplitude 81 % of bacteriophage M13 had lost viability. However, there was no significant loss of viability at 1 μm amplitude over the course of the ten minute experiment (P>0.05, Dunnett). The decay profiles at the 5 and 10 μm

amplitudes showed a linear decrease on the semi-log plot of Figure 3.1. This was indicative of a first order decay process represented by the general form shown in Equation (1), below:

$$\ln \frac{C_t}{C_0} = Kt \qquad\qquad (1)$$

where C_t is the concentration of viable bacteriophage at time t, C_0 the initial viability prior to shearing and K the decay rate constant (representing a proportional loss in bacteriophage viability per minute). The decay constant was -0.87 at 5 μm amplitude (R^2=0.99) and -1.71 at 10 μm amplitude (R^2=0.96).
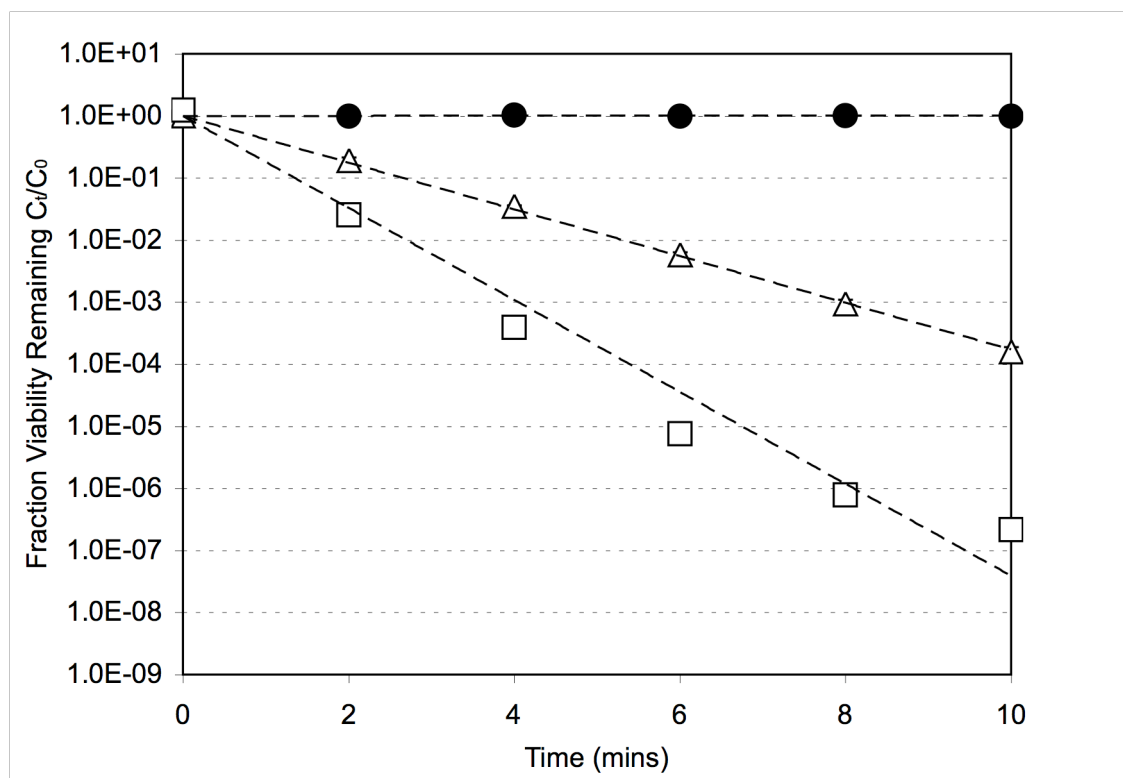
Figure 3.1 Fraction of viable bacteriophage M13 at sonication amplitudes 1 μm (●), 5 μm (△) and 10 μm (□) as a function of time. The initial bacteriophage concentration (C_0) was 4 x 10^{11} pfu ml^{-1}. Viability was determined by the surface-droplet technique (Section 2.5.2). Error bars represent the standard error of the mean fractions, N=3.

3.2.2   Visualisation of sonication damage by electron microscopy

The extent of the physical damage caused by sonication was further investigated by transmission electron microscopy. Bacteriophage samples were prepared and visualised as described in the Materials and Methods (Section 2.10). The non-sonicated control was compared with the effect of sonication at the 10 μm amplitude for 10 minutes.

It was found that the severe decline in bacteriophage viability noted in Section 3.2.1 correlated with severe damage to the particle structure (Figure 3.2). Very few intact bacteriophage particles were visible post-sonication. It was assumed that the abundant particulate matter observed after sonication was bacteriophage fragments.
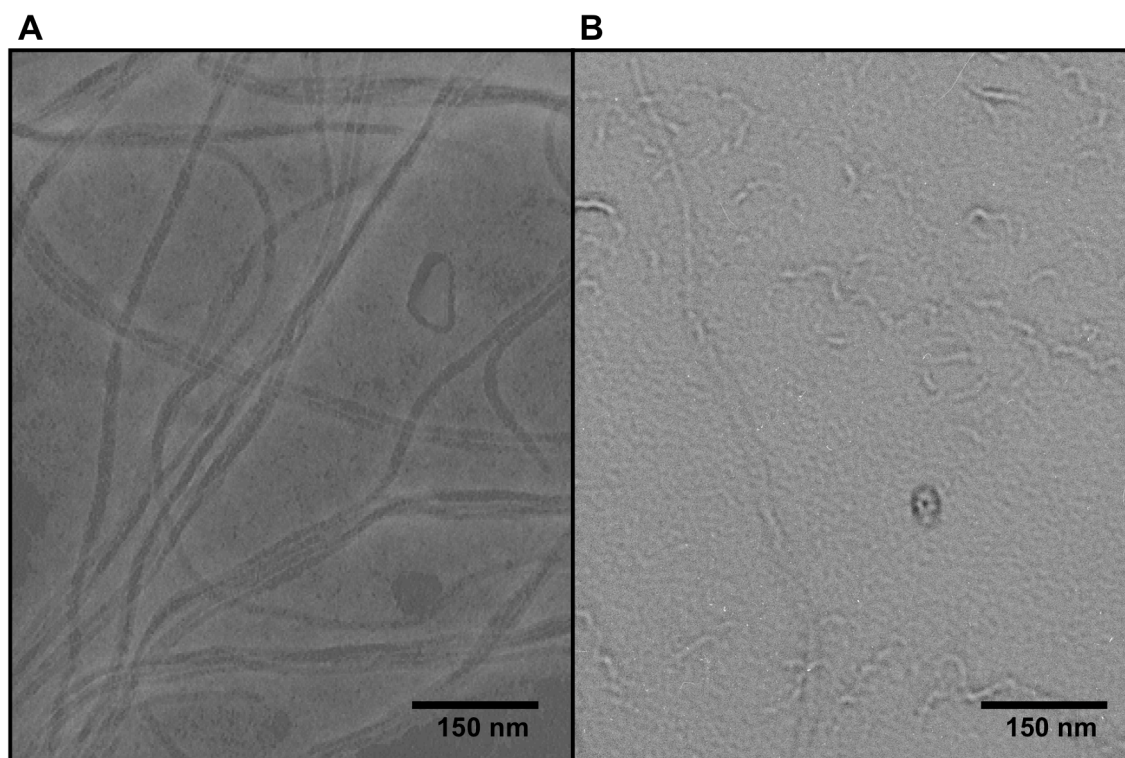
Figure 3.2 Transmission electron microscope (TEM) image of several non-sonicated intact M13 bacteriophage (A), and bacteriophage of the same concentration subject to 10 μm amplitude sonication for 10 minutes (B). Samples were negatively stained with 0.25 % (w/v) uranyl acetate.

3.3   The Effect of Hydrodynamic Shear on Bacteriophage M13

3.3.1   Theoretical aspects: the calculation of energy dissipation within the rotating disk boundary layer

A detailed description of the USD rotating disk shear device equipment can be found in the Materials and Methods, Section 2.12.2. In this thesis, the conditions within the shear device chamber were described in terms of the imposed maximum energy dissipation rate, a key parameter used extensively in the literature (Boychyn *et al.*, 2001; Boychyn *et al.*, 2004; Hutchinson *et al.*, 2006). The maximum energy dissipation rate serves as a basis of comparison between the small-scale experimentation and large-scale unit operations. Substantial literature exists on the estimation of the maximum energy dissipation rates within large-scale unit operations (Mollet *et al.*, 2004; Yim and Shamlou, 2000).

Analytical predictions of the maximum energy dissipation rate within the USD shear device were previously described by Boychyn *et al.* (2001) by the application of flat-plate boundary layer theory to the rotating disk and the assumption that breakage of particles occurs by fluid stresses prevailing in this region. Alternatively, in this chapter rotating-disk boundary layer theory was applied, where the Reynolds number (used to determine the prevailing flow regime) in the rotating disk system was calculated at a radius r (m) by $Re = r^2\omega/v$, where ω is the rotational speed (rad s^{-1}) and v the kinematic viscosity (m^2 s^{-1}). In the laminar flow regime the boundary layer thickness can be estimated for a rotating disk by (Schlichting, 2000):

$$\delta_{lam} = 5.5\sqrt{\frac{v}{\omega}} \qquad (2)$$

where δ_{lam} is the laminar boundary layer thickness (m). The laminar boundary layer thickness is independent of r. Lingwood (1995) observed that the transition from laminar to turbulent flow over rotating disks occurs as an abrupt axisymmetric phenomenon at a defined radius. Assuming a rapid transition from laminar to turbulent flow, the turbulent boundary layer thickness was estimated by (Schlichting, 2000):

$$\delta_{turb} = 0.52 r^{\frac{3}{5}}\left(\frac{v}{\omega}\right)^{\frac{-1}{5}} \qquad (3)$$

where δ_{turb} is the turbulent boundary layer thickness (m), which is dependent on r. The volume of the boundary layer was thus calculated from the integration of boundary layer expressions (2) and (3) over the areas of the disk within which each regime prevailed:

$$V_b = 2\pi r_t^2 \delta_{lam} + 2\int_{r_t}^{R} dr \int_0^{2\pi} r d\theta \int_0^{\delta_{max}(r)} d\delta \qquad (4)$$

where r_t is the disk radius at which the laminar- turbulent transition occurs, and V_b is the volume of the boundary layer (m^3). Finally, the energy dissipation rate was calculated:

$$\varepsilon = P/\rho V_b \qquad (5)$$

where ρ is the liquid density (kg m^3) and P the power input into the ungassed system (W).

The power input P was calculated by more than one method. In initial experiments (Section 3.3.2, below), it was estimated as described by Boychyn *et al.* (2001), from $P=2\pi\omega T$, where T is the applied torque to the disk (kg m^2 s^{-2}):

$$T = 0.664\pi\mu\upsilon_\infty\left(\frac{\rho\upsilon_\infty}{\mu}\right)^{\frac{1}{2}}\left(\frac{16R^{\frac{5}{2}}}{15}\right) \qquad (6)$$

where μ is the solution viscosity (Pa s), υ_∞ the tangential tip velocity (m s^{-1}) and R the disk radius (m). However, in further experimentation (Section 3.3.3, below), it was possible to calculate the power input directly from the electrical power draw of the attached motor, $P=VI$, where V is the voltage (V) and I the current (A). A maximum efficiency of 88 % for the motor was assumed according to the manufacturer's specifications. Thus, the maximum energy dissipation rate in the region of the boundary layer was estimated as a function of the rotational speed and compared with established data for various unit operations.

3.3.2   Initial USD shear device experimentation

Initial experiments were conducted with rotating disk shear device powered by an electrically-driven brushed DC motor (see Materials and Methods, Section 2.12.2). The maximum disk rotation speed was 350 revolutions per second (rps); similar equipment has been used by Levy *et al.* (1999b) to study the effects of shear on plasmids and Boychyn *et al.* (2001) to model the performance of pilot-scale continuous centrifuges. Here, the power input to the device could not be measured directly so was estimated using Equation (6).

A suspension of caesium-chloride purified bacteriophage M13 of concentration 3 x 10^{11} pfu ml^{-1} in 10 mM Tris (pH 7.5 at 25 °C) was prepared and processed within the device at 350 rps for a total of 60 seconds, the maximum possible for the equipment. In addition to triplicate time zero samples, a timed non-sheared control was conducted within the device. This ensured that any observable declines in viability over time were due to shear effects alone. The experiment was repeated three times.

The measured concentration of viable bacteriophage post-shearing was expressed as a fraction of the viable concentration in the non-sheared controls (Table 3.1). It was found that over the course of 60 seconds there was no significant fractional decrease in viability in either the sheared or non-sheared samples in the device.

Table 3.1 The viability of bacteriophage M13 expressed as a fraction of the initial non-sheared viability (C_t/C_0) after 60 seconds within the USD shear device at 350 rps and 0 rps. The equivalent maximum energy dissipation rate (ε_{max}) was estimated as described in Section 3.3.1. Uncertainties represent the standard error, N=3.

Condition	Equivalent ε_{max} x10^5 (W kg^{-1})	C_t/C_0 after 60 seconds	P value (t-test)
350 rps	1.6	0.95 ± 0.12	0.53
0 rps	0	0.97 ± 0.06	0.66

3.3.3   High-speed USD shear device experimentation

Since no significant bacteriophage damage was observed in Section 3.3.2, the USD shear device was developed to operate reliably at significantly higher rotation speeds. An electrically-driven brushless DC motor system was developed as described in Section 2.12.2. The updated equipment was capable of a maximum speed of rotation of 533 rps, and direct measurement of the power draw of the motor improved the accuracy of the maximum energy dissipation calculation. Otherwise, experimentation was consistent with that described previously (Section 3.3.2).

Solutions of caesium-chloride purified bacteriophage M13 of concentration 3 x 10^{11} pfu ml^{-1} in 10 mM Tris (pH 7.5 at 25 °C) were prepared and processed within the device at rotation speeds of 300, 400, 467, 500 and 533 rps for 25 minutes (Section 2.12.2). Triplicate non-sheared controls were present. All treatments were repeated three times.

The maximum energy dissipation rate at each rotation speed was calculated as described in Section 3.3.1. The power input to the system was estimated from the torque applied to the disk (Equation (6)) and calculated from the power draw of the motor (Table 3.2), and the two methods compared. The power input as estimated from the torque applied to the disk was found to be up to 4-fold higher than the *actual* electrical energy input. Therefore the energy dissipation rates calculated using Equation (6) were significant overestimates relative to those employing the measured power draw of the motor, which were used for all further calculations. These maximum energy dissipation rates ranged from 8.9 x 10^4 to 3.1 x 10^5 W kg^{-1}, and were found to vary with the disk rotation speed as a power law relationship (Figure 3.3). The "tip speed" of the rotating disk, shown in Table 3.2, is an alternative expression of the rotation speed of the device used in the literature (Biddlecombe *et al.*, 2007; Boychyn *et al.*, 2004). It is a general parameter that allows for the comparison of conditions between shear devices of differing disk diameters.

Table 3.2 Relationship between disk rotation speed and maximum energy dissipation rate (ε_{max}), calculated by DC motor power draw and applied torque methods.

Rotation speed (rps)	Tip speed (m s^{-1})	Power input measured by DC motor power draw		Power input estimated from applied torque, Equation (6)	
		Power input (W)	ε_{max} x10^5 (W kg^{-1})	Power input (W)	ε_{max} x10^5 (W kg^{-1})
300	37.7	120	0.9	345	2.9
400	50.3	209	1.8	708	6.0
467	58.6	277	2.4	1041	8.9
500	62.8	323	2.8	1237	10.6
533	67.0	353	3.1	1454	12.6
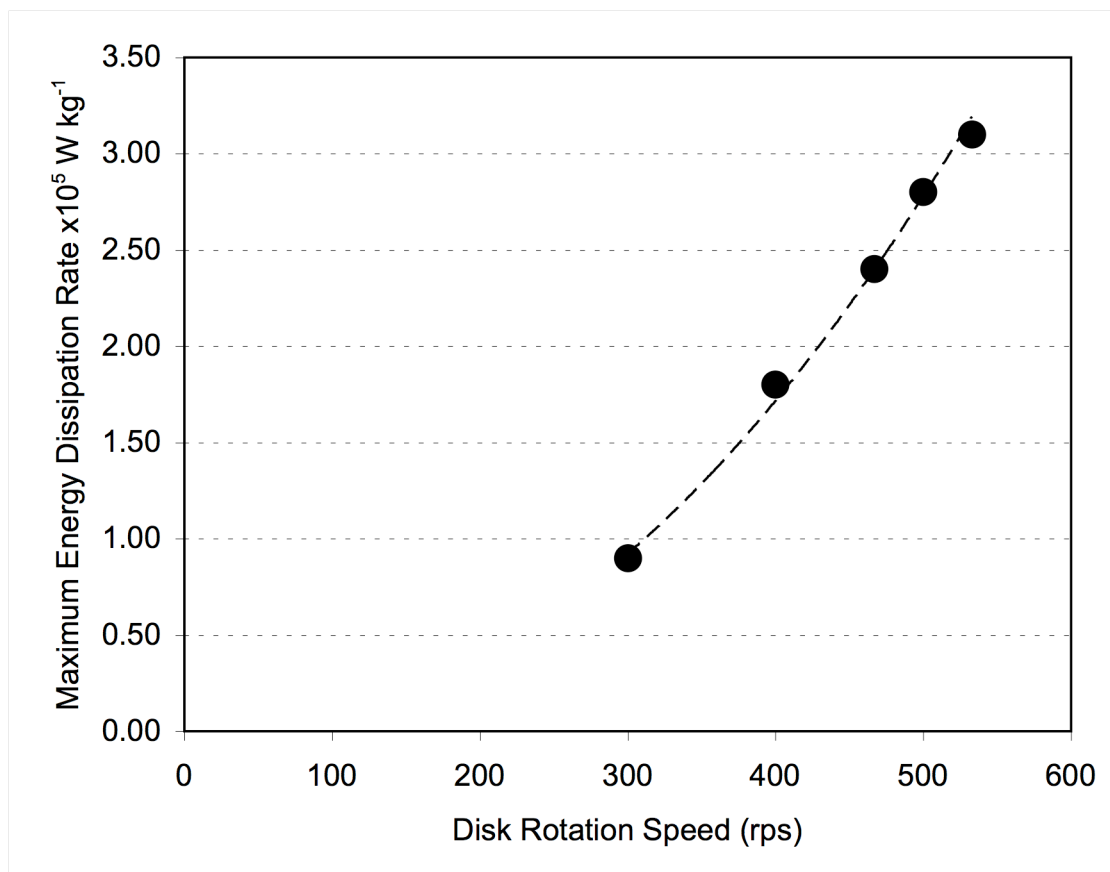
Figure 3.3 Maximum energy dissipation rate (W kg^{-1}) calculated as a function of USD shear device disk rotation speed (rps). The R^2 value for the power law trend was >0.99. The maximum energy dissipation rate was calculated using the power draw of the DC motor.

There was no detectable effect on bacteriophage M13 viability following a 25 minute subjection to shear at 300 and 400 rps within the device at 25 °C (Figure 3.4). At 467 rps, the drop in viability was small and diverged significantly from a non-sheared control only after the full 25 minutes exposure (P= 0.001, t-test). However, exposure to 500 and 533 rps resulted in much greater rates of viability decay (Figure 3.5). Indeed, at 533 rps the M13 viability had decreased by 62 % over the 25 minute period of study.
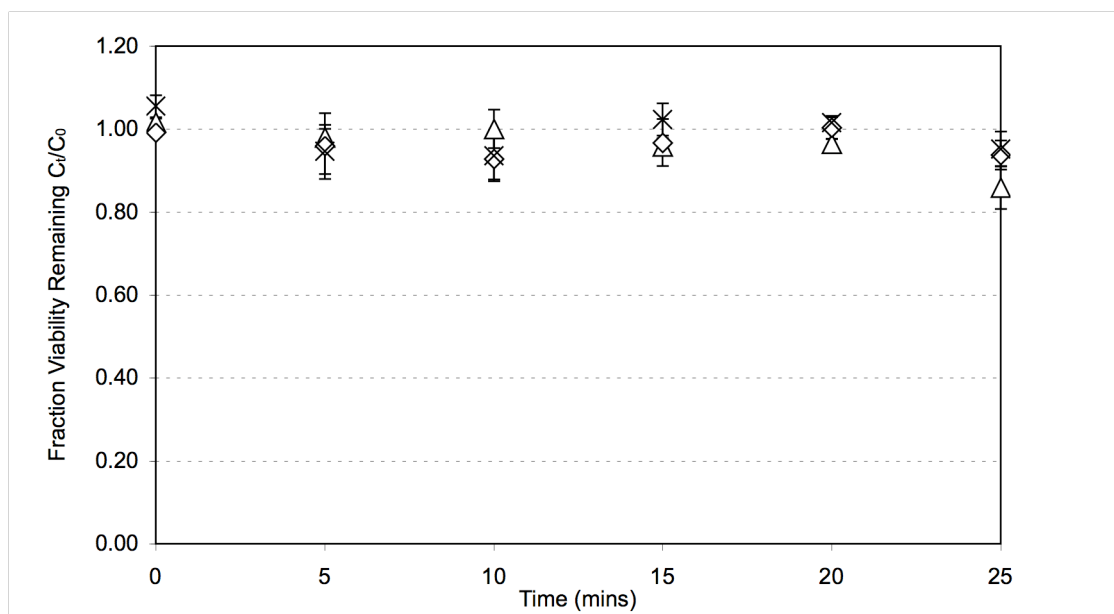
Figure 3.4 Concentration fraction of bacteriophage M13 viability remaining at disk rotation speeds 300 (×), 400 (◇) and 467 rps (△) as a function of time. The initial bacteriophage concentration (C_0) was 3 x 10^{11} pfu ml^{-1}. Error bars represent the standard error of the mean fractions, N=3.

Figure 3.5 Concentration fraction of bacteriophage M13 viability remaining at disk speeds 467 rps ($\triangle$), 500 rps ($\square$) and 533 rps ($\bullet$) as a function of time. The initial bacteriophage concentration (C_0) was 3×10^{11} pfu ml^{-1}. Error bars represent the standard error of the mean fractions, N=3.

Each set of data in Figure 3.5 was fitted to a first order decay process represented by the general form shown in Equation 1. Each decay rate constant (K, representing the proportional loss in bacteriophage viability per minute) was plotted against the corresponding maximum energy dissipation rate for the conditions tested (Figure 3.6). As expected, K was found to increase with maximum energy dissipation. This was found to be an exponential relationship:

$$K = (1 \times 10^{-6})e^{(3 \times 10^{-5})\varepsilon} \qquad \qquad (7)$$

where ε is the energy dissipation rate, in W kg^{-1}.
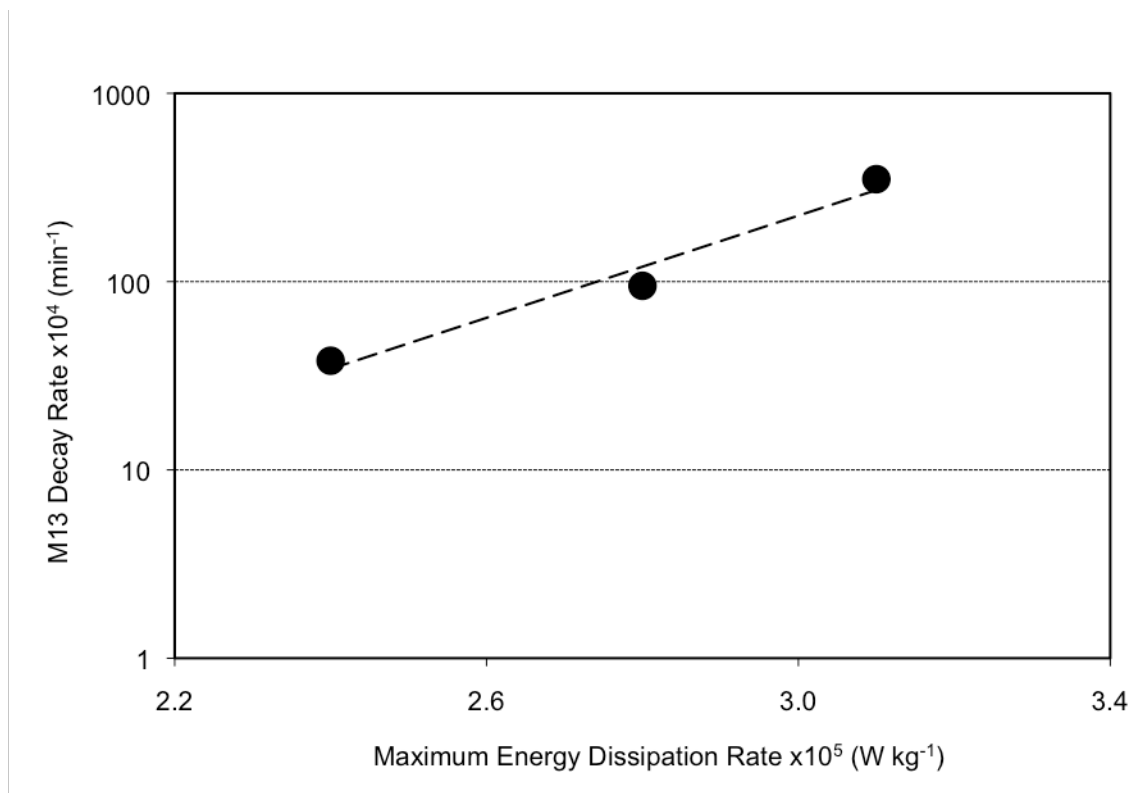
Figure 3.6 The effect of the maximum energy dissipation rate (W kg^{-1}) on the bacteriophage rate of decay, K (min^{-1}). The R^2 value for the exponential trend was 0.98.

3.3.4 The relative shear resistance of bacteriophage M13 and naked DNA

Packaged bacteriophage M13, naked supercoiled double-stranded (ds)DNA (6.6 kb) and naked open circular single-stranded (ss)DNA (6.6 kb) in TE buffer were subject to turbulent shear at 533 rps with the intention of comparing the relative resistances of these macromolecules.

As described in Chapter 1 (Section 1.2.4), once infected by bacteriophage M13 an *E. coli* cell contains many copies of the M13 genome in a "non-packaged" supercoiled double-stranded form (Replicative Form 1, or RF1). Effectively, the RF1 form has the structure of a plasmid, and so was used for the relative robustness comparison between intact "packaged" M13 bacteriophage and supercoiled dsDNA. M13 infected Top10F' cultures were cultivated as described in Section 2.3.3. The RF1 DNA was extracted from the cells by Qiagen MaxiPrep kit (Section 2.8.2). The DNA concentration was determined according to absorbance at 260 nm. The DNA was subsequently diluted in TE buffer to an equivalent concentration of 3 x 10^{11} molecules ml^{-1} prior to shearing.

Single-stranded DNA was prepared directly from caesium-chloride density gradient purified M13 bacteriophage, as described in Section 2.8.1. Again, the DNA concentration was

determined according to absorbance at 260 nm. The DNA was subsequently diluted in TE buffer to an equivalent concentration of 3×10^{11} molecules ml^{-1} prior to shearing.

Post-shearing, all DNA samples were subsequently concentrated ten-fold by ethanol precipitation (Section 2.8.1). Analysis was by 0.8 % (w/v) agarose gel electrophoresis (Section 2.7.2) and densitometric scanning (Section 2.7.4). All experiments were performed three times at room temperature. Shear damage to supercoiled dsDNA was determined in terms of the decrease in supercoiled form, while shear damage to ssDNA was determined in terms of the decrease in open circular form.

The proportion of supercoiled (SC) dsDNA was observed to decrease as shearing progressed over 25 minutes (Figure 3.7). Over the same period, the decrease in intact ssDNA was much more marked (Figure 3.7). Densitometric scanning of these gels allowed for the plotting of the relative decline in integrities, where they were compared with the viability data for packaged bacteriophage M13 particles (Figure 3.8). The degradation rate of supercoiled dsDNA was substantially less than that of both ssDNA and packaged bacteriophage particles. After 25 minutes the proportion of remaining supercoiled DNA was 0.67, the proportion of intact ssDNA was 0.45 and the proportion of viable M13 bacteriophage 0.38.
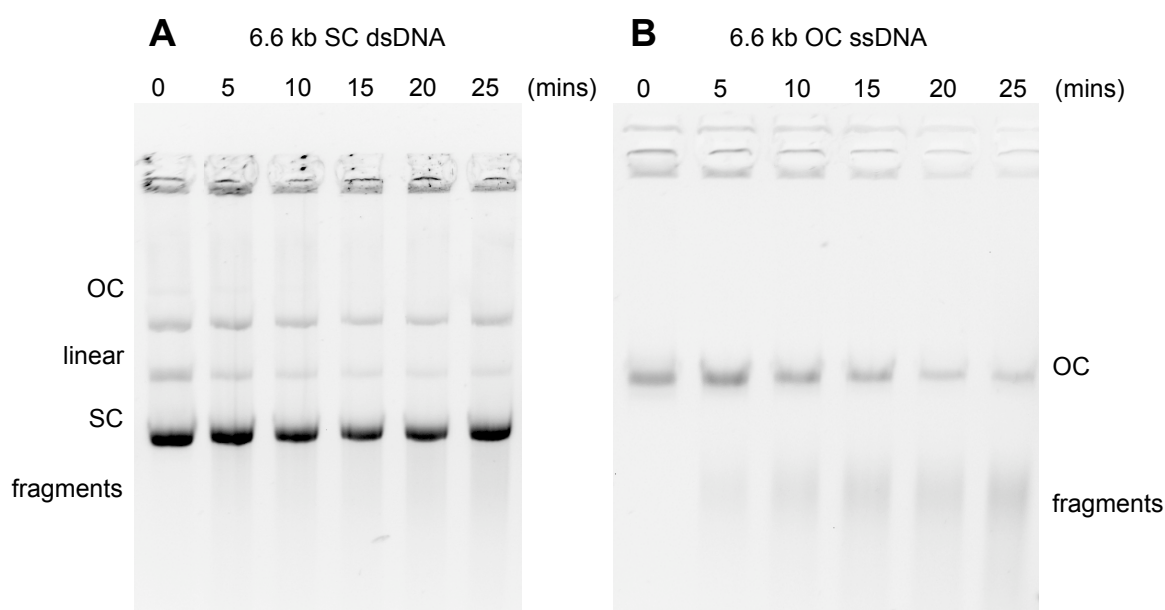
Figure 3.7 Agarose gel electrophoresis of ethanol precipitated double-stranded M13 RF1 DNA (6.6 kb) is shown in (A), and single-stranded M13 DNA (6.6 kb) in (B). Samples were taken at 0, 5, 10, 15, 20 and 25 minute timepoints at 533 rps. Densitometric scanning of the gels was performed as outlined in Materials and Methods. Abbreviations: OC, open circular, SC, supercoiled.
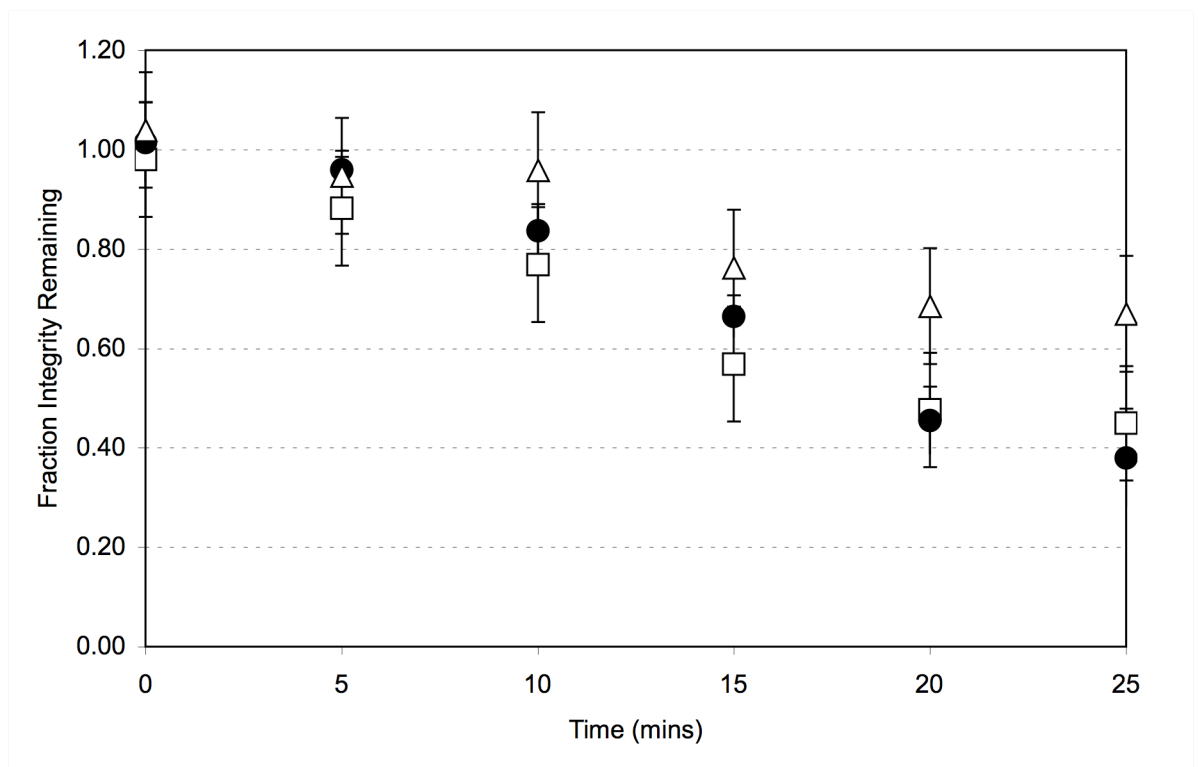
Figure 3.8 Declines in the proportions of intact SC double-stranded DNA ($\triangle$), intact OC single-stranded DNA ($\square$) and viable M13 bacteriophage ($\bullet$) as a function of time at 533 rps. Declines are calculated relative to the quantities measured in non-sheared controls. Error bars represent the standard error of the mean fractions, N=3.

3.3.5 The effect of process fluid conditions on bacteriophage M13 decay profiles

Bacteriophage M13 was suspended in four process fluids representative of probable key processing stages, and each was subject to turbulent shear at 533 rps within the USD device. The conditions were:

1. In post-shakeflask fermentation culture with *E. coli* Top10F' cells, prepared as described in Section 2.3.3. Cultures were supplemented with 0.2 g l^{-1} of PPG 2 000 antifoam (BDH). The average OD_{600} value was 2.9.

2. In post-shakeflask fermentation culture supernatant. Cells had been removed by centrifugation at 14 000 × g for 15 minutes at 4 °C (Section 2.3.3).

3. In post-shakeflask fermentation culture supernatant with 3.3 % (w/v) PEG 6 000 and 330 mM NaCl to precipitate the bacteriophage. Samples were incubated on ice for 1 hour prior to shearing to complete precipitation (Section 2.3.3).

4. Caesium-chloride purified bacteriophage M13 suspended in 10 mM Tris (pH 7.5 at 25 °C), of concentration 3 x 10^{11} pfu ml^{-1}.

In particular, in a large-scale scheme the process fluid under conditions (1.) and (3.) (above) may be subject to the high-energy turbulent shear feed-zone of a continuous centrifuge to remove the *E. coli* cells and capture the bacteriophage, respectively.

All fluids were prepared and processed within the USD device at a rotation speeds 533 rps for 25 minutes (Section 2.12.2). Triplicate non-sheared controls were present. All experiments were repeated three times.

The decline in bacteriophage viability over time under each condition (1.- 4.) is shown in Figure 3.9. After 25 minutes exposure, the viable fraction of bacteriophage ranged from 0.12 in culture supernatant to 0.39 in culture. However, there were apparent differences in the patterns of decline. The viability of M13 in culture decreased in a trend consistent with first order decay kinetics. Under culture supernatant, precipitated and 10 mM Tris conditions, M13 displayed degradation patterns consistent with resistance to shear for up to 10 minutes before entering phases of increased susceptibility to shear. This trend was particularly marked in culture supernatant after 15 minutes shearing time.
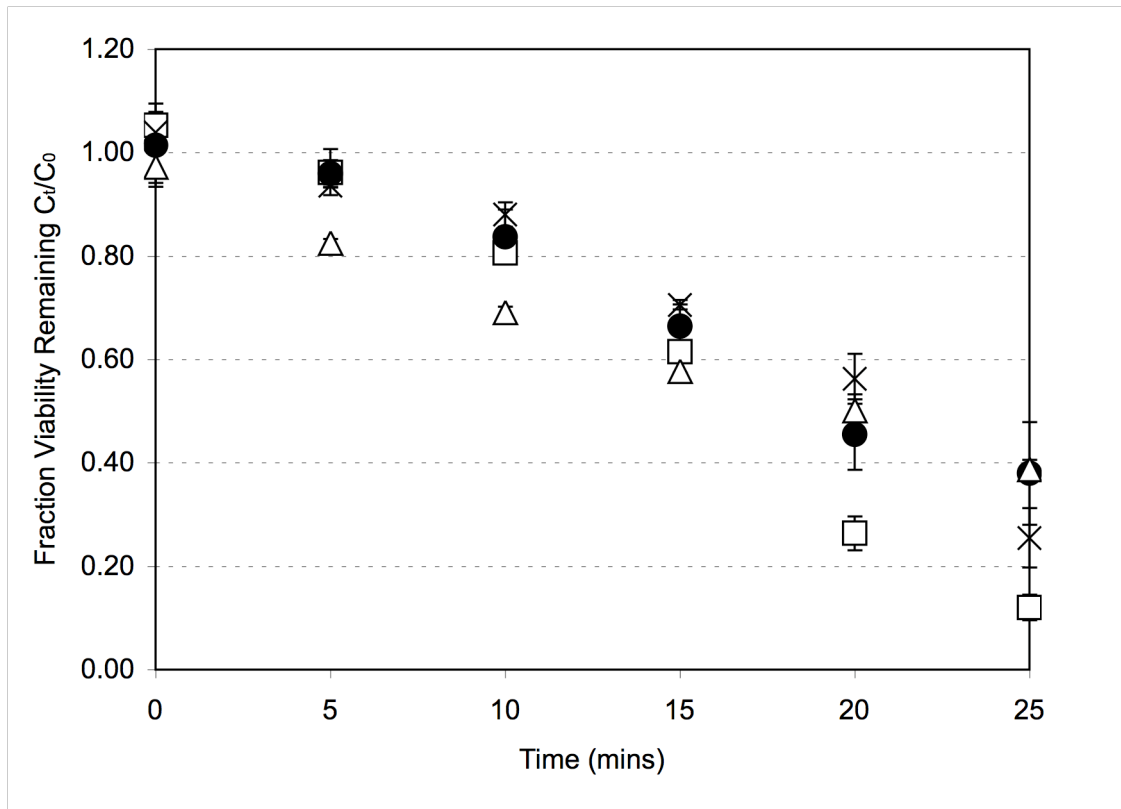
Figure 3.9 The fractional concentration decline in M13 viability in four process fluid conditions as a function of time. The conditions were: fermentation culture ($\triangle$); culture supernatant ($\square$); culture supernatant with PEG and NaCl added ($\times$); purified M13 in 10 mM Tris buffer ($\bullet$). All samples were subjected to disk speed of 533 rps. Error bars represent the standard error of the mean fractions, N=3.

3.3.6   Calculation of maximum energy dissipation rate for each process fluid condition

The maximum energy dissipation rate was calculated for each process fluid subjected to 533 rps within the USD shear device to determine if variances in the M13 decay rate could be attributed to differences in the maximum energy dissipation rate, the calculation of which depends on the fluid viscosity (Section 3.3.1). The viscosity of each fluid described in Section 3.3.5 was measured in duplicate as described in the Materials and Methods (Section 2.11) using a cone and plate viscometer at 25 °C. A linear relationship existed between shear stress and shear rate (Figure 3.10); therefore every fluid was Newtonian and the viscosity (μ, Pa s) could be measured as the gradient of the line. The measured viscosity of the water control (μ= 1.04 mPa s) was in line with that expected at 25 °C (Perry *et al.*, 1998).
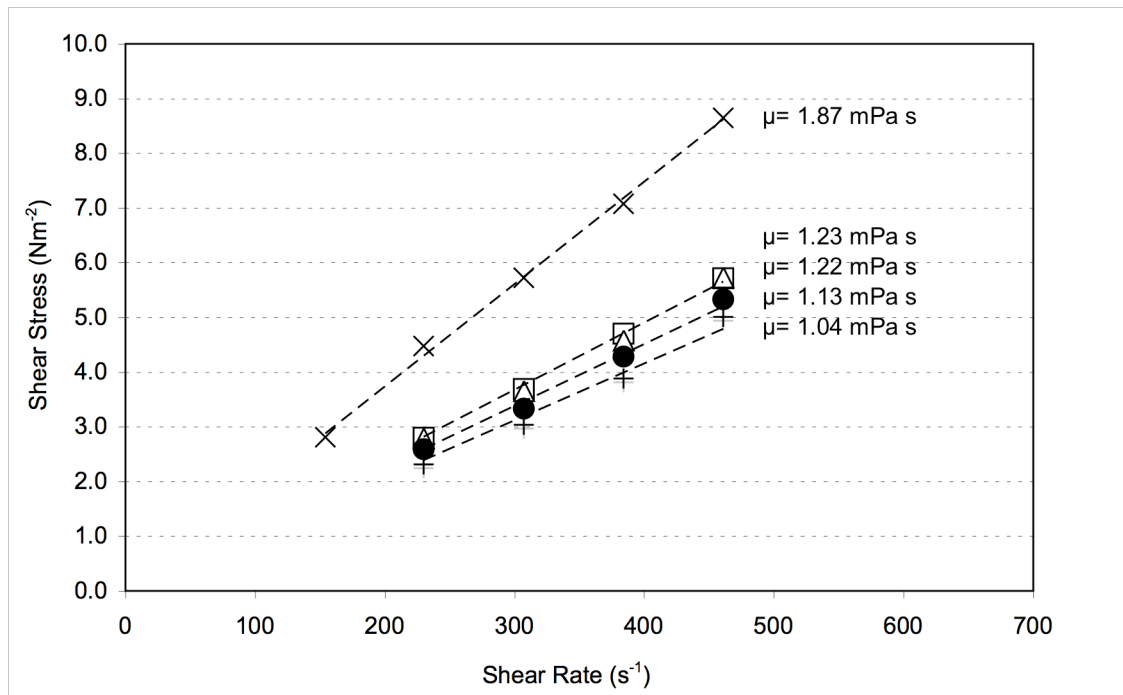
Figure 3.10 The viscosity measurement of four process fluid solutions. Viscosity (μ) was calculated from the gradient of each line. The conditions were: fermentation culture ($\triangle$); culture supernatant ($\square$); culture supernatant with PEG and NaCl added ($\times$); purified M13 in 10 mM Tris buffer ($\bullet$). A control of RO water was also tested ($+$). N=2.

The energy dissipation rates were subsequently calculated using the measured viscosities and average power draw of the DC motor. The fluid density was assumed to remain at 1 000 kg m^{-3}. Despite variations in viscosity and power input between fluids, the calculated energy dissipation rates were similar (Table 3.3). That is, the differences in viscosity and power input between fluids resulted in a less than 10 % difference in maximum energy dissipation rate. It was therefore concluded that the differences in M13 decay profiles between process fluids was not chiefly due to differences in energy dissipation rate.

Table 3.3 The effect of solution viscosity on the power input and maximum energy dissipation rates calculated within the USD shear device at 533 rps.

Process fluid	Viscosity (mPa s)	Power input (W)	ε_{max} x10^5 (W kg^{-1})
Culture	1.22	363	3.1
Culture supernatant	1.23	348	3.0
Culture supernatant, 3.3 % PEG 6 000, 330 mM NaCl	1.87	392	3.3
10 mM Tris	1.13	353	3.1

3.3.7 The effect of air-liquid interfaces on bacteriophage M13

It was considered that the variation in decay profiles of bacteriophage M13 in Section 3.3.5 may have been the result of the action of more than one mechanism of damage, dependent on the process fluid. Since some bacteriophage and proteins are known to display a vulnerability to air-liquid interfaces (Thompson and Yates, 1999), it was surmised that air-liquid interfaces could be playing a part in the viability loss of M13. The main evidence for this lay in the apparent acceleration in decay rate as time increased in the culture supernatant, precipitated and 10 mM Tris environments (Figure 3.9), albeit to greater or lesser degrees in each. As time increased, 500 µl samples had been removed from the 20 ml device chamber at five minute intervals (Section 2.12.2), leading to an increasing amount of air in the chamber.

Four experiments were therefore conducted to determine if the sampling technique over time (each 500 µl sample represented 2.5 % of the total volume) was responsible for the accelerated decay rates by increasing the quantity of air-liquid interfaces within the device. Caesium-chloride purified bacteriophage M13 of concentration 3 x 10^{11} pfu ml^{-1} in 10 mM Tris buffer were subject to shear at 533 rps for 5 minutes without sampling in the first treatment, and 25 minutes without sampling in the second. In the third and fourth treatments the chamber was filled but then 2 ml of fluid removed, equivalent to a 10 % (v/v) air volume within the chamber and representative of the conditions between the standard 20 and 25 minute shearing times. The fluid was sheared for 5 minutes in the third treatment, and 25 minutes in the fourth. The experiment was repeated three times.

The decay profile of bacteriophage M13 with standard interval sampling at 533 rps in 10 mM Tris (from Figure 3.5) is re-shown in Figure 3.11, together with the new limits of shearing for

25 minutes with no sampling (i.e. the chamber was full), and 25 minutes with 10 % (v/v) air present. Shearing without sampling halved the rate of decay in M13 viability; the fraction of remaining viability was 0.78 after 25 minutes, rather than 0.38. Conversely, the fraction of remaining viability after 25 minutes shearing with 10 % (v/v) air was reduced to 0.29, but this was not significantly different from the drop experienced by the standard interval sampling (P=0.49, t-test).
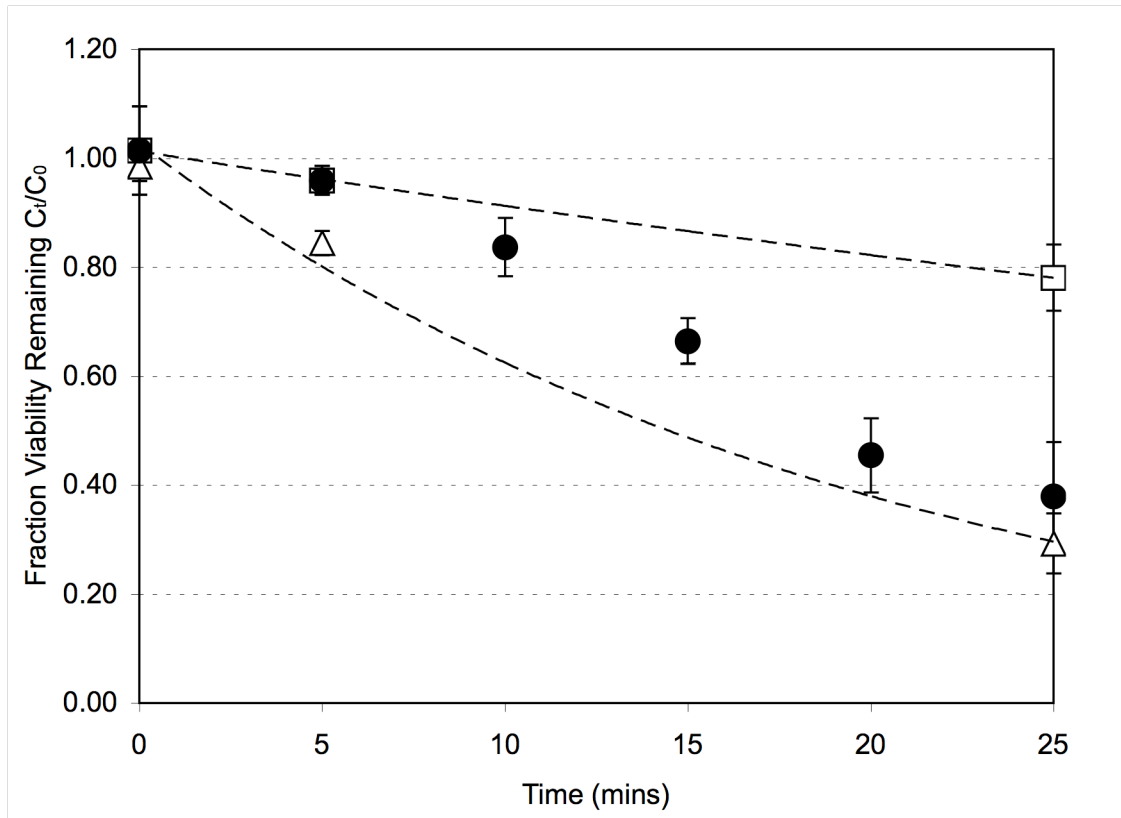
Figure 3.11 Concentration fraction of bacteriophage M13 viability remaining at disk speed 533 rps with standard interval sampling ($\bullet$), with no sampling ($\square$) and 10 % (v/v) air with no sampling ($\triangle$) as a function of time. The initial bacteriophage concentration (C_0) was 3 x 10^{11} pfu ml^{-1}. The no-sampling limits are fitted with first order decay trends, $R^2 > 0.99$ for each. Error bars represent the standard error of the mean fractions, N=3.

3.4 Detection of Cavitation within the Ultrasonicator and USD Shear Device

To further elucidate the mechanisms of bacteriophage M13 decay within the USD shear device, an assay for the detection of cavitation was applied to determine if significant levels of cavitation were occurring within the chamber at the highest rotation speed (533 rps). Exposure to cavitation causes a measurable change in absorbance (at 350 nm) of 3 M potassium iodide solution. The mechanism is described in the Materials and Methods (Section 2.12.3) and essentially involves the liberation of iodine (which reacts to form the triiodide ion, I_3^-) from the iodide (I^-) solution (Morrison *et al.*, 1971). The assay has been used to detect cavitation within large-scale homogenisation equipment (Lander *et al.*, 2000) and USD capillary shear equipment (Meacle *et al.*, 2004).

Firstly, 3 M potassium iodide alone was subject to identical ultrasonication conditions as solutions of bacteriophage M13 were (Section 3.2.1) to determine a correlation between bacteriophage decay (as shown in Figure 3.1) and iodine release. Sonication of a fluid is known to result in acoustic cavitation; essentially the formation and violent collapse of bubbles within the fluid gives rise to highly localised areas of intense temperature and pressure gradients (Didenko *et al.*, 1999). The experiment was conducted as described in Section 2.12.3. The amount of cavitation was expressed in terms of the μM concentration of I_3^- (Wayment and Casadonte, 2002).

A linear rise in I_3^- concentration over time was observed at the 5 μm amplitude (R^2=0.99), and a greater linear increase at 10 μm (R^2=0.97) (Figure 3.12). At 5 μm amplitude the I_3^- concentration increased at a rate of 0.14 μM min^{-1} and at 10 μm amplitude the rate was 0.20 μM min^{-1}. At the 1 μm amplitude, there was no detection of a significant rise in I_3^- concentration over ten minutes ($P>0.05$, Dunnett). Comparing the concentration increase of I_3^- (Figure 3.12) with the decrease in bacteriophage viability (observed earlier in Figure 3.1) showed that, as expected, the increased rate of I_3^- liberation was associated with an increased rate of M13 decay. At 1 μm amplitude, the undetectable level of cavitation by this assay correlated with an undetectable decay in M13 viability under the same conditions.
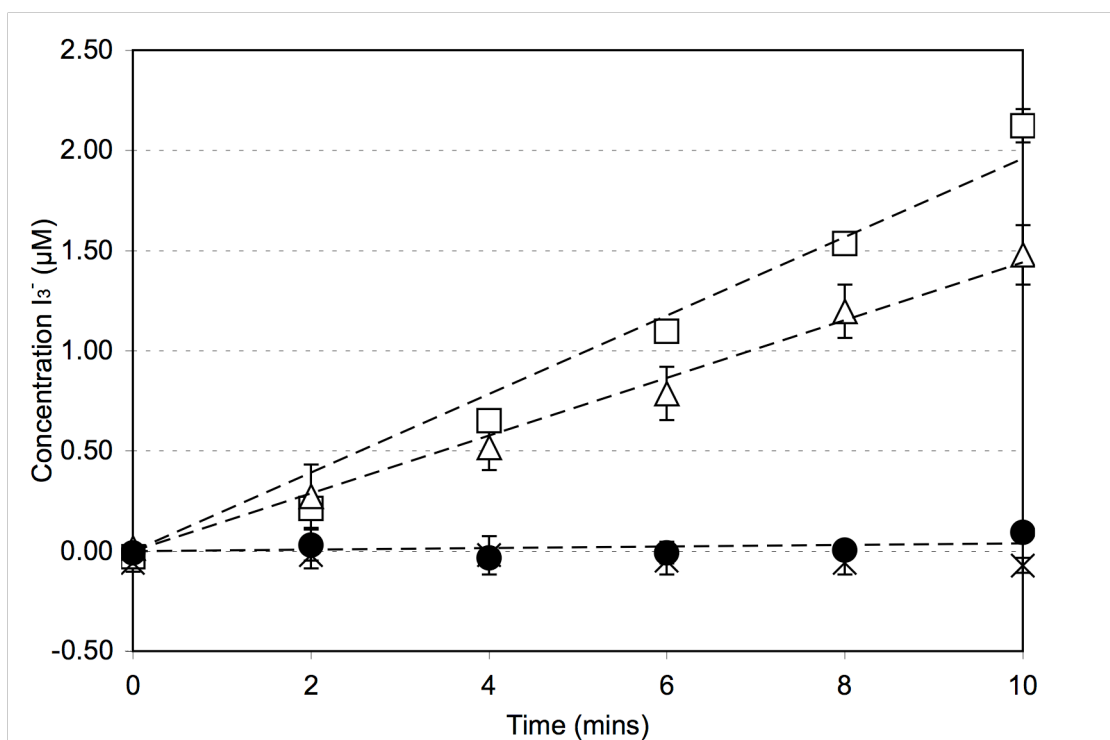
Figure 3.12 Concentration of liberated I_3^- at sonication amplitudes 1 µm (●), 5 µm (△), 10 µm (□) and non-sonicated (✕) as a function of time. I_3^- concentration was determined by absorbance at 350 nm. The R^2 values for the linear trends were 0.97 (10 µm), 0.99 (5 µm) and 0.22 (1 µm). Error bars represent the standard error, N=3.

Potassium iodide solution (3 M) was subsequently subjected to 533 rps within the USD rotating disk shear device. The device was operated as described in the Materials and Methods Section 2.12.2 and the cavitation assay conduced as described in Section 2.12.3. Upon subjection to 533 rps the detected concentration of I_3^- was found not to be significantly different from the non-sheared controls over the entire 25 minute experiment (P>0.05. Dunnett). The concentration of I_3^- remained close to zero (Figure 3.13).
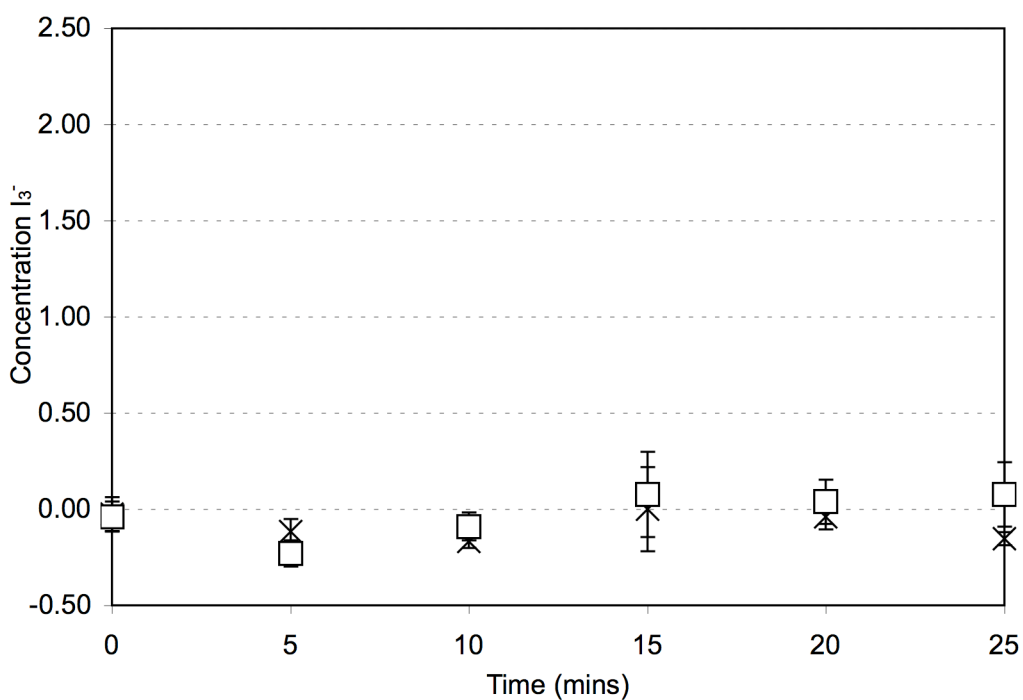
Figure 3.13 Concentration of liberated I_3^- at 533 rps within the rotating disk shear device (□) and non-sheared (×) as a function of time. I_3^- concentration was determined by absorbance at 350 nm. Error bars represent the standard error, N=3.

3.5 Comparison of the Hydrodynamic Shear Resistances of Several Macromolecules

Over several years many biological macromolecules have been subject to turbulent shear conditions within the USD rotating-disk shear device (Biddlecombe *et al.*, 2007; Boychyn *et al.*, 2000; Levy *et al.*, 1999a; Zhang *et al.*, 2007). A summary of some of these findings is found in Table 3.4 to provide context for the data gained for bacteriophage M13. The maximum energy dissipation rate associated with the shear device conditions in each study were calculated using expressions (4), (5) and (6). In Levy *et al.* (1999b) and Boychyn *et al.* (2001), a 30 mm disk was rotated at a maximum of 460 rps. In Biddlecombe *et al.* (2007), a 27 mm disk was rotated at a maximum of 250 rps. In this study, a 40 mm disk was rotated at a maximum of 533 rps. Solution viscosities were assumed to be of that of water. The complex macromolecules shown in Table 3.4 are diverse and varying in morphology, so the term "length scale" is difficult to define and therefore only approximate. For amorphous particles, this represents an average diameter. For the defined rod-shaped bacteriophage M13, this represents the contour length. Although direct comparisons between experiments is difficult (particularly due to differing exposure times to shear), it is noteworthy that particles of similar length scale to bacteriophage M13 – such as supercoiled plasmid DNA (20 kb) and protein precipitates – were found to be

severely damaged in only seconds upon exposure to conditions (1.4×10^5 W kg^{-1}) which had no significant affect on the viability of bacteriophage M13 over 25 minutes (Table 3.4 and Figure 3.4).

Table 3.4 A comparison of the turbulent shear resistance of biological macromolecules treated within versions of the USD rotating-disk shear device. Except for the yeast protein precipitate, all particles were suspended in low ionic strength buffer solution. The shear device conditions described in each study (disk speed and rotation) were expressed as maximum energy dissipation rates, calculated using expressions (4), (5) and (6).

Particle	Approximate Length Scale	Equivalent ε_{max} x10^5 (W kg^{-1})	Effect	Reference
IgG4 antibody	8- 12 nm	0.26	60 % monomer loss over 2 hours	Biddlecombe *et al.* (2007)
6.6 kb SC DNA (M13 RF1)	350 nm	3.1	33 % SC loss over 25 minutes	Present study
Bacteriophage M13 (6.6kb ssDNA)	900 nm	3.1	62 % viability loss over 25 minutes	Present study
20 kb SC plasmid DNA (pQR150)	1200 nm	1.4	95 % SC loss over 25 seconds	Levy *et al.* (1999b)
Homogenized yeast protein precipitate	1300 nm average	1.4	45 % reduction in average particle size over 20 seconds	Boychyn *et al.* (2001)

3.6   Discussion

The purpose of this chapter was to determine the fragility of the filamentous bacteriophage M13 upon exposure to high-energy hydrodynamic shear forces, using a USD shear device. The resistance of bacteriophage M13 was compared with single and double-stranded DNA molecules, and the effect of solution conditions demonstrated. Two experiments were conducted which aimed to clarify the mechanisms of damage within the USD shear device. Finally, a comparison was made between bacteriophage M13 and existing data for various other complex macromolecules tested within the USD shear device. Here, the implications of these results for large-scale bacteriophage M13 processing will also be discussed.

3.6.1   Description of the conditions within the USD shear device

In this thesis the conditions within the USD shear device are determined analytically and characterised in terms of the associated *maximum energy dissipation rate*. The analysis of flow

and energy dissipation patterns within both the USD shear device and indeed large-scale unit operations has been previously conducted by both computational fluid dynamics (CFD) and analytical calculations (Boychyn *et al.*, 2001; Levy *et al.*, 1999a; Zhang *et al.*, 2007). Both approaches have successfully predicted the response of fluids in large-scale unit operations by small-scale experimentation, by matching the conditions within the USD shear device disk and the identified critical region within the process equipment. The basis of comparison by other authors has also been described in terms of the maximum energy dissipation rate (Boychyn *et al.*, 2001; Boychyn *et al.*, 2004; Hutchinson *et al.*, 2006), but *average* energy dissipation rate (Levy *et al.*, 1999b), shear rate (Biddlecombe *et al.*, 2007; Harrison *et al.*, 1998) and most simply disk tip speed (Boychyn, 2000) have also been employed. More generally, substantial literature exists on the estimation of the maximum energy dissipation rates within large-scale unit operations (Mollet *et al.*, 2004). While precise estimation can still be difficult (Yim and Shamlou, 2000), many useful small-scale predictions of the response of novel biological macromolecules to high dissipation energy environments have been made.

Difficulties in the precise estimation of the conditions within the USD shear device itself were highlighted in Table 3.2, where alternative methods for the calculation of energy input resulted in four-fold differences in maximum energy dissipation rate. Nevertheless, the calculated maximum energy dissipation rates in this study (of the order 10^5 W kg^{-1}) were in the range of those predicted for the feed-zones of continuous centrifuges, cited as the most potentially damaging unit operations in downstream processing (Boychyn *et al.*, 2004; Yim and Shamlou, 2000). Although verification of USD predictions at scale is essential, this is an important consideration because the unusual non-lethal lifecycle of M13 (where progeny bacteriophage are translocated through the *E. coli* cell wall) means that virus particles will be free in the fermentation fluid for a considerable period and will not be protected from high energy shear conditions imposed on the process fluid.

3.6.2   Initial USD shear device experimentation

The work of Levy et al. (1999b) served as a reference point for the parameters of operation of the USD shear device on pure bacteriophage M13 in 10 mM Tris buffer (Section 3.3.2). Levy *et al.* (1999b) outlined the effect of subjecting pure plasmid DNA preparations of 20 kb size to turbulent shear for 25 seconds at an equivalent rotation speed of 350 rps and a maximum energy dissipation rate of 1.4 x 10^5 W kg^{-1}. Under these conditions, there was a 95 % drop in supercoiled plasmid DNA content (Table 3.4). Although the 20 kb plasmid and bacteriophage M13 were of similar characteristic length scales (1200 nm and 900 nm respectively) their shear resistances in buffer were very different: no significant damage to bacteriophage M13 was observed when subject to the same treatment over 60 seconds (Table 3.1). However, it was considered that only by finding the point at which M13 viability declined would it be possible to

assess the limits of its processability. To achieve this aim the USD shear device was hence upgraded to operate at the higher rotation speeds required (Section 3.3.3).

3.6.3   High-speed USD shear device experimentation

High-speed USD shear device experimentation found that there was no significant effect on the viability of bacteriophage M13 for up to 25 minutes at 400 rps (1.8×10^5 W kg^{-1}) (Figure 3.4). Moreover, even at 467 rps (2.4×10^5 W kg^{-1}) the drop in viability only diverged significantly from a non-sheared control after the full 25 minute exposure. However, the much greater rates of viability decay observed upon exposure to 500 and 533 rps (2.8×10^5 W kg^{-1} and 3.1×10^5 W kg^{-1}) suggested that a threshold resistance had been exceeded (Figure 3.5). Indeed, the degradation rate then increased in an exponential fashion (Figure 3.6). This result showed that the total loss of bacteriophage M13 from shear was a function of maximum energy dissipation rate as well as the time of exposure.

There are two implications for large-scale bacteriophage processing. Firstly, in the most damaging process equipment (such as continuous centrifuges) the exposure time to the critical high-energy dissipation areas is only of the order of a fraction of a second (Byrne *et al.*, 2002), hence total damage will probably be small. Secondly, although the overall cumulative exposure time in large-scale processing can be considerably longer than this (Zhang *et al.*, 2007), the highest maximum energy dissipation rates within mechanically agitated fermenters are typically only up to 10^3 W kg^{-1} and within pumps up to 10^5 W kg^{-1} (Yim and Shamlou, 2000). Since a maximum energy dissipation rate of 1.8×10^5 W kg^{-1} was found to result in no significant bacteriophage viability loss over 25 minutes, bacteriophage damage may be unlikely. These predictions would need to be verified by experimentation at scale.

3.6.4   The effect of process fluid conditions on bacteriophage M13 decay profiles

Of course, bacteriophage M13 will not be in buffer over the entire course of a production scheme. Instead, from raw fermentation culture the composition of the process fluid will alter considerably as contaminants are progressively removed, buffers changed and chemicals added. This was of concern since the shear resistance of both protein and DNA complexes have been shown to depend on the nature of the process fluid (Harrison *et al.*, 1998; Levy *et al.*, 1999a; Levy *et al.*, 1999b). The shear resistance of bacteriophage M13 in several process fluid environments was consequently examined, and it was found that the bacteriophage decay profile did depend on the fluid composition (Section 3.3.5). After 25 minutes exposure to turbulent shear at 533 rps, the fraction of viable bacteriophage increased in the order: culture supernatant (0.12) < culture supernatant plus PEG and NaCl (0.25) < 10 mM Tris (0.38)< culture medium with cells (0.39) (Figure 3.9). Furthermore, the decay profiles varied. While the viability of M13 in culture decreased in a trend consistent with first order decay kinetics, in the culture

supernatant, PEG precipitated and 10 mM Tris conditions, M13 displayed degradation patterns consistent with resistance to shear for up to 10 minutes before entering a phase of increasing rates of damage. This trend was particularly marked in culture supernatant conditions after 15 minutes shearing time. Similar decay profiles have been reported by other authors for both plasmids and proteins (Levy *et al.*, 1999a; Thomas *et al.*, 1979), but contrasts with a reported case of broth components providing protection for proteins relative to buffer (Harrison *et al.*, 1998). It was considered likely therefore, that the decay of bacteriophage viability was due to more than one mechanism of damage.

Firstly, calculation of the maximum energy dissipation rates (Section 3.3.6) showed that there was little variation between process fluids, so this effect was discounted. Secondly, the effect of air-liquid interfaces was examined (Section 3.3.7), since a possible explanation for this behaviour was that M13, in common with other bacteriophage and proteins, displayed a vulnerability to air-liquid interfaces (Thompson and Yates, 1999). It was found that shear damage to bacteriophage M13 was indeed enhanced by the presence of air-liquid interfaces, although the distribution of these interfaces within the device remained unknown (Figure 3.11). Of particular note was that the drop in viability when deliberately sheared for 25 minutes with 10 % air was not dramatically less than the standard sampling technique, which progressively increased the proportion of air within the chamber to 10 % (v/v) by the end of 25 minutes. This suggested that, in 10 mM Tris buffer at least, the effect of air-liquid interfaces began after the first sample point but did not substantially multiply after further sampling. This pattern could explain the noted decay trend of "resistance for a time followed by decay" in the buffer, culture supernatant and PEG precipitated environments (Figure 3.9). It is however an effect which depended on the process fluid, since protection was afforded when in culture but lost once the cells were removed.

3.6.5   Detection of cavitation within the ultrasonicator and USD shear device

The first part of this chapter (Section 3.2) revisited an early reference to the severe sensitivity of bacteriophage fd to the shear imparted by sonication (Marvin and Hoffman-Berling, 1963). Since bacteriophage M13 is closely related to fd, it was expected that a severe sensitivity would also be noted, and this was confirmed by experimentation (Figure 3.1). First order decay profiles were observed, which matched those reported for fd. Sonication damage to the bacteriophage particles in solution arose directly from the effects of cavitation. Cavitation in a fluid results in highly localised areas of intense temperature and pressure gradients (caused by the formation and violent collapse of bubbles within the fluid) (Didenko *et al.*, 1999), shear forces associated with these gradients (Kondo *et al.*, 1989) and also free radicals (McLean and Mortimer, 1988). This data was subsequently used to determine if bacteriophage viability loss within the USD shear device was due to cavitation effects (Section 3.4). The cavitation

detection assay showed that increased rates of cavitation by sonication were associated with an increased rate of bacteriophage M13 decay (Figure 3.1 and Figure 3.12). In the USD shear device, no I_3^- liberation was detected, which suggested that either cavitation was not present or was at very low levels undetectable by this assay. It was therefore considered likely that the decays in bacteriophage viability observed in the USD shear device were largely a result of turbulent shear (Section 3.3.3) and air-liquid interface effects (Section 3.3.7).

3.6.6   The relative shear resistance of bacteriophage M13 and naked DNA

A direct comparison of the shear resistances of M13 bacteriophage, ssDNA and SC dsDNA was made in the USD shear device at 533 rps. All three molecules were of the same genome size to allow for an equal basis of comparison. It was found that after 25 minutes exposure, the remaining proportion of intact molecules decreased in the order SC dsDNA (0.67) > ssDNA (0.45) > bacteriophage M13 (0.38) (Figure 3.7 and Figure 3.8). The difference in shear resistance between dsDNA and ssDNA molecules can be directly attributed to the differences in inherent molecular strength (Odell and Taylor, 1994), dsDNA being the stronger. But a study on the inherent strength of the M13 particle demonstrated its resistance to stretching forces that damage dsDNA (Khalil *et al.*, 2007). This measure is of relevance when understanding a particle's resistances to the turbulent conditions within the shear device; the fluid flow within the chamber can be described in terms of the *shear* and *elongational* strain rates imposed (Zhang *et al.*, 2007). Therefore, if the difference in behaviour between dsDNA and packaged M13 bacteriophage was not due to an inherently greater strength of dsDNA, then the greater resistance of dsDNA to these conditions could have been due to the very different morphologies of the two molecules. Naked DNA molecules are free to compact in solution while DNA packaged within a bacteriophage M13 particle is not due to the relative rigidity of the encapsulating protein coat. Consequently, the characteristic hydrodynamic diameter of the 6.6 kb SC dsDNA molecule in this study was approximately a third of the contour length of the packaged M13 particle (Arulmuthu *et al.*, 2007). USD shear device studies on SC plasmid dsDNA molecules of increasing genome size have demonstrated the critical effect the physical size of the DNA molecule has on its resistance to shear conditions (Levy *et al.*, 1999b; Meacle *et al.*, 2004). That is, the smaller molecules were more resistant. It is therefore possible that the significantly greater length scale of bacteriophage M13 resulted in the greater fragility than dsDNA of equivalent genome size, assuming damage was a result of mechanical effects. While it has been shown that this is not entirely the case– air-liquid interfaces enhanced the degradation rate of bacteriophage M13 (Figure 3.11)– similar effects have been demonstrated for SC plasmid dsDNA under similarly pure conditions (Levy *et al.*, 1999b).

Overall, there are likely to be several factors governing the difference in the rate of decay of dsDNA and packaged M13 particles. Particle size and inherent molecular strength are no doubt

important, but properties such as density, stiffness and relative reactivity may also have had a significant effect on the shear-resistance outcome. This is particularly true of bacteriophage, where viability can be abolished by damage solely to the protein coat, leaving the encapsulated DNA intact. In practical terms, however, it was important that each particle was assessed in terms of its own recognised standard. The quality of a (plasmid) dsDNA therapeutic is typically assessed as the proportion supercoiled (Eastman and Durland, 1998; Lander *et al.*, 2002; Levy *et al.*, 1999b), and this convention was adhered to in this study. It may be reasonable to expect that viability emerges as the standard measure of the quality of a bacteriophage-based therapeutic, since the particle must be intact to be infectious.

The comparison with plasmid DNA is particularly important since both have been studied for their effectiveness as vectors for gene therapy and vaccination, although plasmid-based technology is significantly more advanced (Kutzler and Weiner, 2008; Larocca *et al.*, 2002; Wan *et al.*, 2001). Whereas most early clinical trials have involved plasmids of 10 kb or less, it is predicted that in the future the production of larger plasmids of size 20 kb or more will be necessary (Levy *et al.*, 2000b), sizes which, as Table 3.4 indicated, are very susceptible to shear damage. The length of the bacteriophage M13 particle depends solely on the nucleotide count of the tightly packaged DNA within; there is a linear scaling of bacteriophage length to genome size. Future work could investigate the important relationship between bacteriophage M13 length and the impact on its susceptibility to shear damage.

3.6.7   Concluding remarks

This chapter described how a USD shear device was upgraded and used to evaluate the effect of hydrodynamic shear forces on bacteriophage M13. Within the device, conditions imposing a maximum energy dissipation rate up to 1.8×10^5 W kg^{-1} upon the therapeutic candidate bacteriophage M13 were shown not to cause a significant drop in bacteriophage viability. This implies that the shear imposed by bioprocessing steps such as fermentation and pumping may not have an adverse effect, although large-scale experimentation would need to verify these predictions. At higher energy dissipation rates, the relationship between viability decay and maximum energy dissipation rate was found to be non-linear. Over the course of the 25 minute shear experiment, the pattern of viability decay was found to be affected by the condition of the process fluid. The rate of bacteriophage decay in buffer was shown to be enhanced by the presence of air-liquid interfaces, and an assay for the detection of cavitation showed undetectable levels of cavitation within the device at the highest energy conditions imposed (3.1×10^5 W kg^{-1}). Under these same maximal conditions, the rate of decay of M13 was shown to be greater than SC plasmid DNA of the same genome size. However in practical terms, despite being noted in the literature as a fragile molecule, bacteriophage M13 appears to be largely resistant to high-energy turbulent shear conditions.

4 A Study of Bacteriophage M13 Fermentation and Harvesting

4.1 Introduction

In common with all other viruses, bacteriophage are parasitic and therefore dependent upon a host organism to propagate. For bacteriophage M13, this host is *E. coli*, a bacterium that is commonly used for the industrial production of recombinant proteins in industry (Baneyx, 1999; Schmidt, 2004; Swartz, 2001). Therefore, the manufacture of products based upon bacteriophage M13 has the distinct advantage of using a well characterised host organism. As with recombinant protein production, the yield of progeny bacteriophage is inextricably linked to the state of the *E. coli* (in terms of both their concentration and health), particularly since bacteriophage M13 infection does not result in the death of the cells (Chapter 1, Section 1.2.3). Cells continue to divide, albeit at a reduced rate (Salivar *et al.*, 1964), continually producing progeny M13 by an extrusion mechanism through the cell wall (Russel and Model, 1989). Amongst bacteriophage this reproduction strategy is unusual and limited to the filamentous bacteriophage group (*Inoviridae*), yet it is potentially advantageous. Propagation, in other classes of bacteriophage, is a lytic process where host cell division is halted upon infection and bacteriophage induced cell lysis is required to release the progeny bacteriophage. In avoiding cell lysis, the downstream processing of bacteriophage M13 could be assisted because contamination of the process stream with *E. coli* intracellular proteins, RNA and DNA would be greatly reduced. A key aim of this chapter, therefore, was to explore the composition of the post-fermentation process fluid (the culture supernatant fraction), since efficient planning of downstream recovery steps is dependent on knowing the concentration of the product and major contaminants in the process stream (Asenjo and Patrick, 1990).

Whilst downstream processing primarily focuses upon minimizing product losses by application of fewer (or more efficient) steps (Wenzig *et al.*, 1993), a defining characteristic of the fermentation step is the ability to increase the overall yield of a process. Limited studies currently exist on the optimisation of bacteriophage M13 yield from fermentation, although it is likely that productivity is a function of the physiological state of the host *E. coli* cells. What parameters allow the cells to be in the best state for bacteriophage replication and multiplication is uncertain, although it has been suggested that restriction of cell growth rate may increase bacteriophage yield (Salivar *et al.*, 1964), as may medium supplementation with magnesium ions (Reddy and McKenney, 1996). That said, it has been demonstrated that the overall yield of bacteriophage M13 is relatively insensitive to the multiplicity of infection (MOI) (Reddy and McKenney, 1996). The MOI is the initial ratio of bacteriophage to *E. coli* cells at the start of fermentation.

The role of medium richness in improving cell growth and therefore bacteriophage yield is unclear. For example, SOB medium (2 % (w/v) tryptone, 0.5 % (w/v) yeast extract, 10 mM NaCl, 2.5 mM KCl) has been shown to result in up a 60 % increase in bacteriophage M13 titre compared to LB medium (1 % (w/v) tryptone, 0.5 % (w/v) yeast extract, 80 mM NaCl) (Reddy and McKenney, 1996), whereas NYZ broth (1 % (w/v) NZ-Amine, 0.5 % (w/v) yeast extract, 85 mM NaCl) was unequivocally shown to result in a 3-fold higher bacteriophage titre over SB medium (50 mM MOPS, 3 % (w/v) tryptone, 2 % (w/v) yeast extract) (Grieco *et al.*, 2009). It is therefore likely that the bacteriophage productivity of *E. coli* is a complicated function, of which medium ion concentration and carbon source are just two factors.

It was nevertheless hypothesized that since bacteriophage production occurs concomitantly with *E. coli* growth (Brown and Dowell, 1968), conditions which support increased *E. coli* cell density could conceivably lead to an improved yield of bacteriophage M13.

It was also hypothesized that the choice of host *E. coli* cell would also impact upon the yield of bacteriophage as well as the quality of the process fluid. The *E. coli* strain used thus far in this thesis, Top10F', has been demonstrated in the literature to produce bacteriophage M13 adequately (Karlsson *et al.*, 2005). Further, in this thesis the typical yields of bacteriophage M13 resulting from the standard two-litre shakeflask fermentation (Section 2.3.3) are similar to that reported elsewhere (Reddy and McKenney, 1996; Sambrook and Russell, 2001). However, Top10F' is a cloning strain which is recombination deficient (*recA*⁻). As a result, and in common with other *recA*⁻ strains, a Top10F' culture will consist of three sub-populations of actively dividing, residually dividing and non-dividing cells (Capaldo *et al.*, 1974). Actively dividing cells typically represent only a 49 % fraction of the total population after 5 hours growth in a *RecA*⁻ host (Capaldo and Barbour, 1973). With regards to bacteriophage M13 manufacture, this implies that productivity could be hampered if such a large proportion of the cell population is non-viable. Hence, bacteriophage M13 propagation in *recA*⁺ strains was investigated in terms of product yield and process fluid contamination, and compared to Top10F'.

This chapter is structured in three parts. After selection of analyses to track contamination levels in 50 ml Top10F' culture (250 ml baffled shakeflasks), several *E. coli* strains were then compared at the same scale (in NB2) for bacteriophage yield and contaminant accrual. Thirdly, fermentation on the two-litre benchtop bioreactor scale was investigated with a medium shown to increase *E. coli* titre relative to NB2. Fermentations were also analysed in terms of bacteriophage yield and accumulated contamination.

4.2 Top10F' Culture and Selection of Analyses

4.2.1 Identification of available analyses

The post-fermentation process fluid will primarily consist of the M13 bacteriophage product, intact cells, some cell debris and medium components (chiefly ions, short chain soluble polypeptides and nucleotides). Some low level accumulation of cell debris is expected as a result of usual *E. coli* culture (Salivar *et al.*, 1964), which will include host chromosomal DNA, RNA, proteins, lipids, endotoxins and chemical residuals (Eastman and Durland, 1998; Prazeres and Ferreira, 2004). Several techniques are available for the detection of these contaminant components, each with varying specificity, sensitivity and cost (Bristow, 1990). For example, detection of free chromosomal DNA in the culture could be detected by agarose gel, A_{260} and qPCR assays; protein by colorimetric assay, or SDS-PAGE followed by immunoassay or sensitive staining techniques; and endotoxin by the Limulus amoebocyte lysate (LAL) assay. In this chapter the quantities of released DNA and protein were measured to represent the level of culture contamination. DNA was measured by agarose gel and A_{260}; protein by Bradford assay and SDS-PAGE with silver staining. These techniques were applied to 50 ml M13 infected and non-infected Top10F' cultures and their effectiveness compared.

4.2.2 M13 infected and non-infected Top10F' culture

All 50 ml NB2 cultures in 250 ml baffled shakeflasks were prepared and grown as described in the Materials and Methods (Section 2.13.1). Briefly, a loopful of frozen Top10F' stock culture was streaked on to an NB2A plate supplemented with 5 μg ml^{-1} tetracycline and incubated overnight at 37 °C. Working liquid *E. coli* cultures were then prepared by inoculation of five 5 ml aliquots of NB2 (supplemented with 5 μg ml^{-1} tetracycline) with a single loopful of cells each, individually taken from isolated colonies on the NB2A plate and incubated overnight at 37 °C with shaking. Three pre-warmed 50 ml NB2 cultures were subsequently inoculated with 1 ml of individual working *E. coli* culture at the zero time-point. When M13 infection was required 2.3 x 10^8 pfu (from a single caesium chloride purified stock) was also added at the zero time-point. No static infection period was conducted. Culture OD_{600}, cell and bacteriophage counts were recorded as described (Section 2.13.1). Cells were removed by centrifugation (17 000 x g for 3 minutes) and supernatants were analysed for DNA and protein. To expose all DNA (including bacteriophage M13 DNA), 400 μl of each supernatant sample was subject to phenol-chloroform extraction, of which 250 μl was subsequently ethanol precipitated and 10-fold concentrated (Section 2.8.1).

Agarose gel analysis (Section 2.7.2) of untreated supernatant, phenol-chloroformed and 10-fold concentrated samples was performed to observe free DNA (10 μl of sample per well). Quantification of DNA bands was as described in Section 2.7.4. Spectrophotometric DNA

quantification (A_{260}) was performed on 10-fold concentrated samples only (Section 2.7.1): prior phenol-chloroform treatment was necessary to remove protein absorption contaminants and ethanol precipitation to concentrate the DNA but also remove residual phenol, which is a strong absorber at 260 nm (Santella, 2006). Readings required 1.5 µl of sample (measured in triplicate). The Bradford assay was performed on untreated supernatant as directed (Section 2.7.5). SDS-PAGE was also performed as described in the Materials and Methods (Section 2.7.3) with 10 µl of sample (plus 10 µl loading buffer) loaded per well, followed by silver staining.

Growth as measured by OD_{600} ceased after four hours in M13 infected Top10F' cultures, attaining an OD_{600} value of 1.08 (Figure 4.1). This was less than that of non-infected cells (2.43), which ceased growing by six hours. Similarly, the viable cell count of non-infected Top10F' culture over time was consistently higher than M13 infected Top10F' culture (Figure 4.2). Viable cell counts were divided by OD_{600} value at every timepoint to ascertain whether the viability of Top10F' culture was decreased by bacteriophage M13 infection (Table 4.1). On this normalised OD_{600} basis the viable cell count of M13 infected Top10F' was lower than non-infected after two hours incubation.
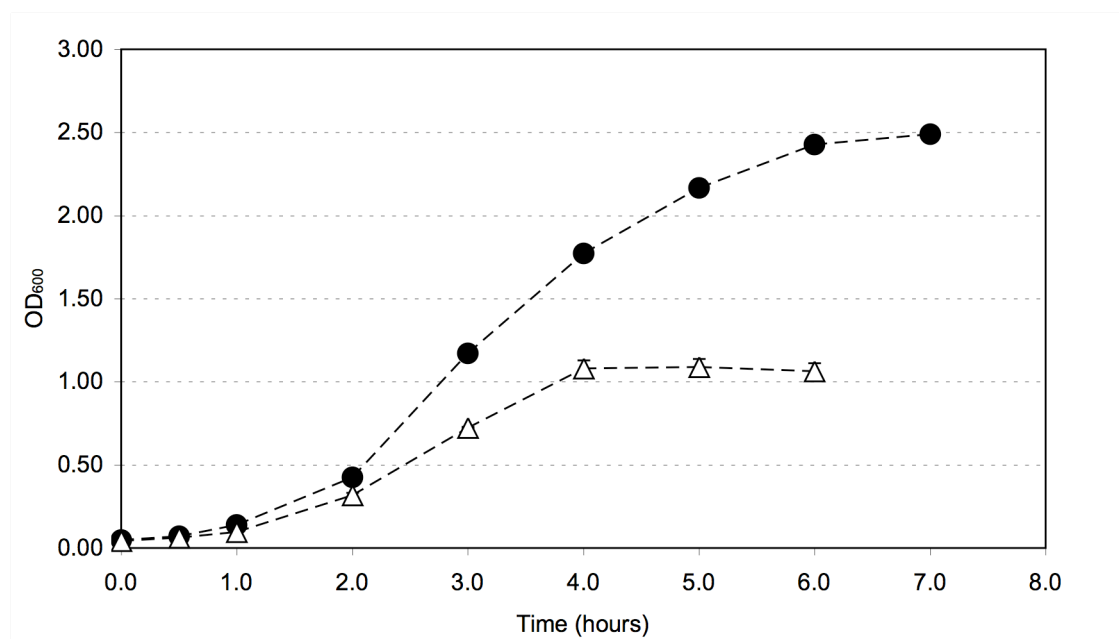
Figure 4.1 OD_{600} value of non-infected (●) and M13 infected (△) Top10F' culture as a function of incubation time. *E. coli* was infected with bacteriophage M13 at the zero hour timepoint. Error bars represent the standard error, N=3.
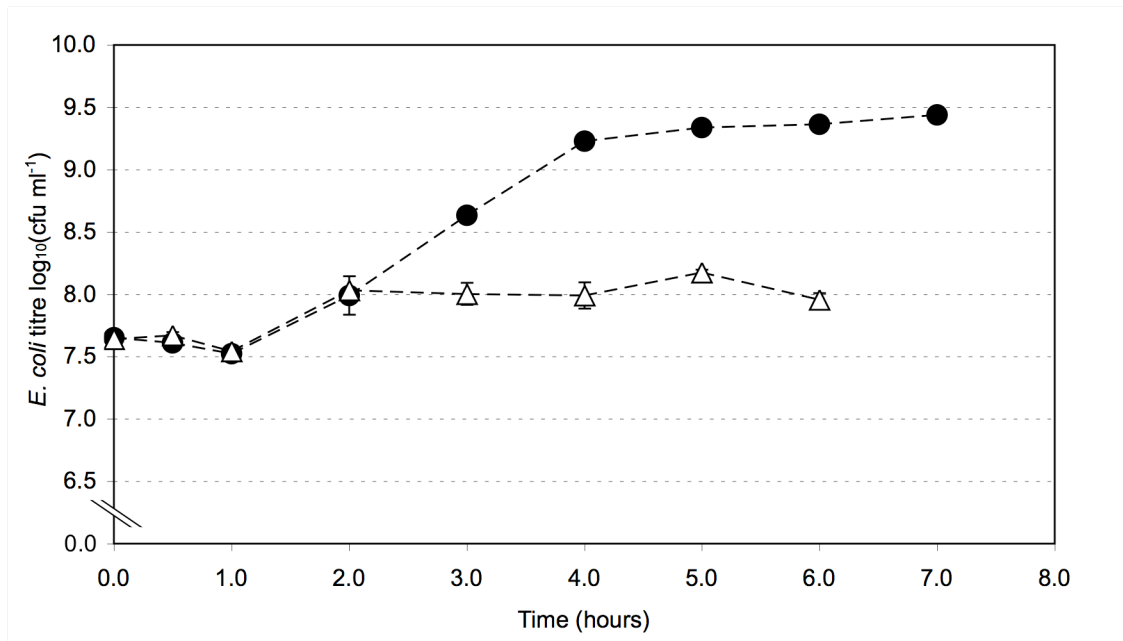
Figure 4.2 Viable cell count of non-infected (●) and M13 infected (△) Top10F' culture as a function of incubation time. Error bars represent the standard error, N=3.

Table 4.1 The viable Top10F' count per OD_{600} unit as a function of time for non-infected and M13 infected cells. Values were similar until two hours incubation, after which the counts of non-infected cells per OD_{600} unit were increasingly greater than infected cell values. Statistical analysis (t-test) was performed on log_{10}-transformed cell count data.

Incubation time	Viable cell count (cfu ml^{-1}) per OD_{600} unit		P value
	Non-infected Top10F'	M13 infected Top10F'	
0 hours	9.40×10^8	1.01×10^9	0.67
30 minutes	5.85×10^8	7.37×10^8	0.03
1 hour	2.40×10^8	3.58×10^8	0.04
2 hours	2.30×10^8	3.39×10^8	0.34
3 hours	3.67×10^8	1.39×10^8	0.02
4 hours	9.58×10^8	9.04×10^7	0.0007
5 hours	1.00×10^9	1.37×10^8	3.6×10^{-6}
6 hours	9.54×10^8	8.48×10^7	4.7×10^{-5}
7 hours	1.11×10^9	-	-

The titre of bacteriophage in infected Top10F' cultures ceased to increase significantly (P>0.05, Tukey) after four hours (Figure 4.3). The maximum titre achieved was 4.1×10^{11} pfu ml^{-1}, attained by 5 hours growth. The production of bacteriophage was noted to closely correlate with the increase in culture OD_{600} (Figure 4.1).
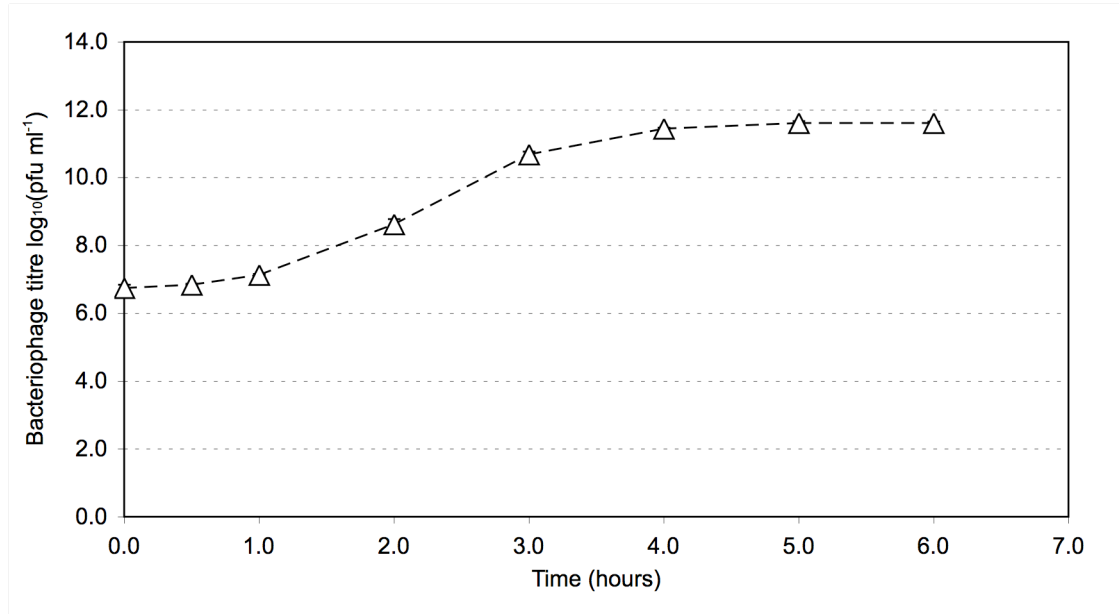
Figure 4.3 Bacteriophage concentration in M13 infected ($\triangle$) Top10F' culture as a function of incubation time. Error bars represent the standard error, N=3.

4.2.3   Quantification of DNA

The quantity of DNA in the culture supernatant increased over time, as culture density increased (Figure 4.4). A DNA band greater than 10 kb was observed in both infected and non-infected cultures, later measured to be at least 20 kb in size (Section 4.2.4). It was assumed this represented released *E. coli* chromosomal DNA. In M13-infected culture, a secondary band was observed post phenol-chloroform treatment, which was subsequently proven to be bacteriophage DNA (see Section 4.2.4). This finding was consistent with published data stating that bacteriophage DNA is not visible by ethidium bromide staining when encapsulated within the bacteriophage protein coat (Moses *et al.*, 1980). The amount of *E. coli* DNA in both infected and non-infected cultures was subsequently quantified at the 5 hour timepoint by densitometry, where bacteriophage M13 production has ceased and the culture would be harvested. This was achieved by running the untreated 5 hour timepoint culture supernatant samples in triplicate on a further agarose gel for the purposes of densitometry only.
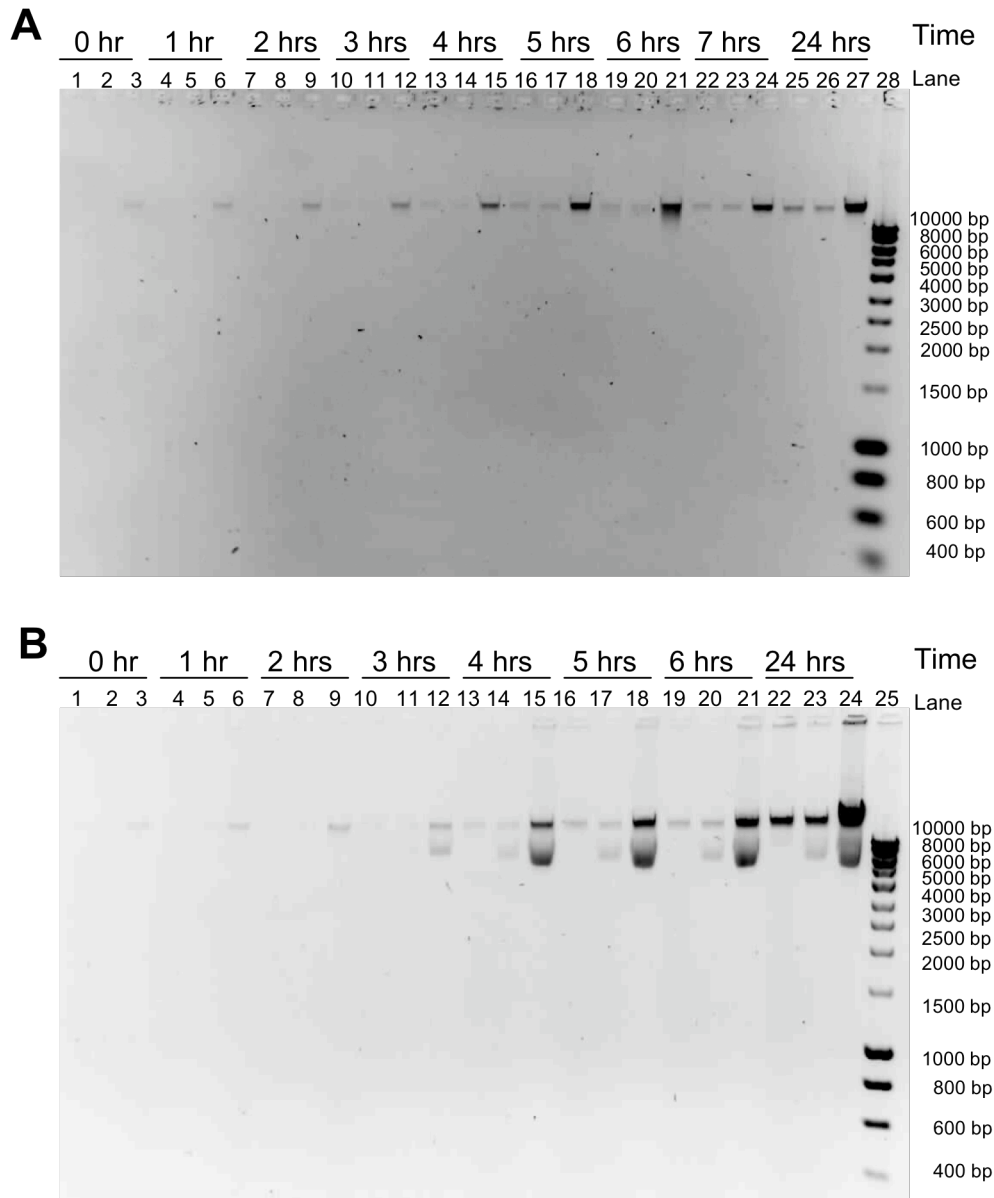
Figure 4.4 Agarose gels indicating the quantity of DNA in the culture supernatant. Gel (A) represents non-infected Top10F' culture. Lanes 1, 4, 7, 10, 13, 16, 19, 22 and 25 are untreated culture supernatant samples. Lanes 2, 5, 8, 11, 14, 17, 20, 23 and 26 are phenol-chloroform treated culture supernatant samples. Lanes 3, 6, 9, 12, 15, 18, 21, 24 and 27 are phenol-chloroform treated culture supernatant samples which have been 10-fold concentrated by ethanol precipitation. Lane 28 is Bioline HyperLadder 1. Gel (B) represents M13 infected Top10F' culture. Lanes 1, 4, 7, 10, 13, 16, 19 and 22 are untreated culture supernatant samples. Lanes 2, 5, 8, 11, 14, 17, 20, and 23 are phenol-chloroform treated culture supernatant samples. Lanes 3, 6, 9, 12, 15, 18, 21 and 24 are phenol-chloroform treated culture supernatant samples which have been 10-fold concentrated by ethanol precipitation. Lane 25 is Bioline HyperLadder 1.

Quantification of band intensities in the agarose gels was determined relative to the Bioline HyperLadder 1 (Section 2.7.4). The concentration of chromosomal DNA in the supernatant of non-infected culture was measured to be 0.24 µg ml^{-1}. In infected culture the concentration was 0.63 µg ml^{-1}, which was significantly higher (P=0.004, t-test).

While the concentration of chromosomal DNA in the supernatant was observed to increase concomitantly with *E. coli* growth by agarose gel electrophoresis, a contrary trend was observed by A_{260} readings of the (phenol-chloroform treated, ethanol precipitated) 10-fold concentrated supernatant samples (Figure 4.5). Of particular note was that fresh NB2 medium subject to the same treatment gave the greatest A_{260} readings of all samples. Assuming all phenol has been removed, it was surmised that the dominant contributor to absorbance readings was not therefore chromosomal (and bacteriophage M13) DNA but a consumable component of the NB2 medium, which is meat-extract derived. It was decided to not continue this analytical technique, principally because DNA quantification by agarose gel provided an effective alternative.
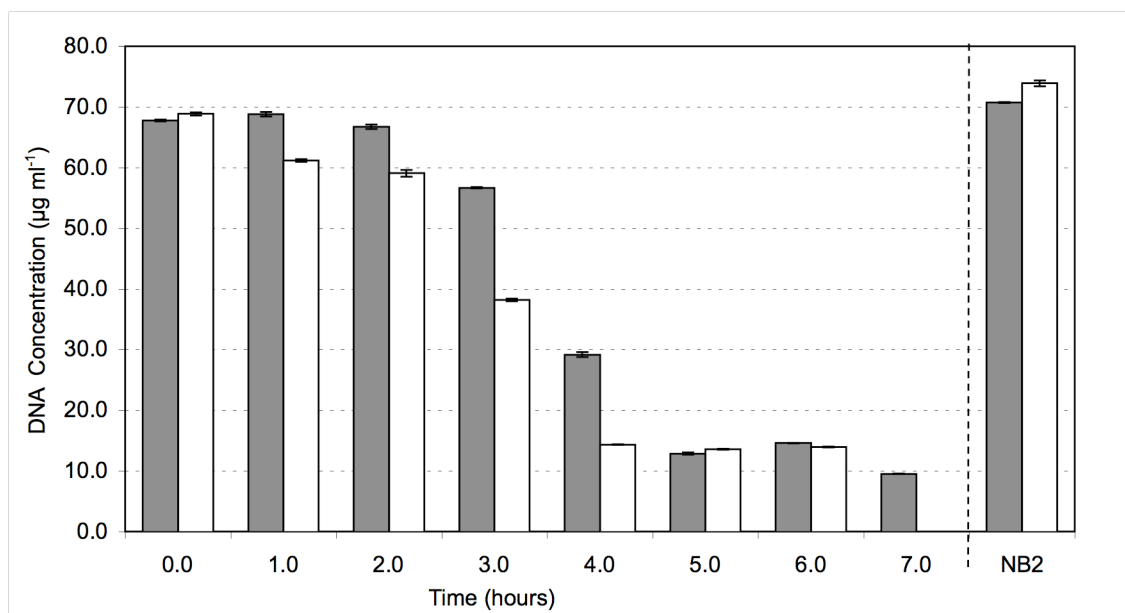
Figure 4.5 Concentration of DNA in non-infected (■) and M13 infected (□) culture supernatants as a function of time. DNA concentration was measured by A_{260} reading. Error bars represent the standard error, N=3.

4.2.4 Identification of agarose gel DNA bands

An experiment was conducted to confirm that the secondary band visible (post phenol-chloroform treatment) from M13 infected culture was indeed bacteriophage DNA. Two 30 µl aliquots were taken from the supernatants of infected and non-infected Top10F' cultures incubated for 24 hours at 37 °C. To each aliquot 1 µl of 100 mM MgCl$_2$ was added and the pH was confirmed to be above 6. To degrade all free DNA, 1 µl of Benzonase (Merck, Purity Grade II, approx. 20 000 U ml^{-1}) was added to one each of infected and non-infected aliquots. Every aliquot was subsequently incubated at 37 °C for 30 minutes, followed by 65 °C for 30 minutes to inactivate the Benzonase. To liberate bacteriophage DNA, 15 µl of each aliquot was then phenol-chloroform treated (Section 2.8.1). Loading buffer (3x concentrated, 5 µl) was added to 10 µl of every sample, each of which was then subject to agarose gel electrophoresis.

It was found that Benzonase treatment removed the DNA band suspected to be chromosomal DNA (Figure 4.6, Lanes 2 and 3 non-infected Top10F', Lanes 6 and 7 M13 infected Top10F'). However, in M13 infected cultures the secondary band still appeared post Benzonase and phenol-chloroform treatment (Lane 7). This suggested that the secondary band at 5-6 kb was indeed bacteriophage DNA which had been protected from Benzonase treatment by the bacteriophage protein coat. No secondary band was visible in non-infected cultures post phenol-chloroform treatment (Lane 5).
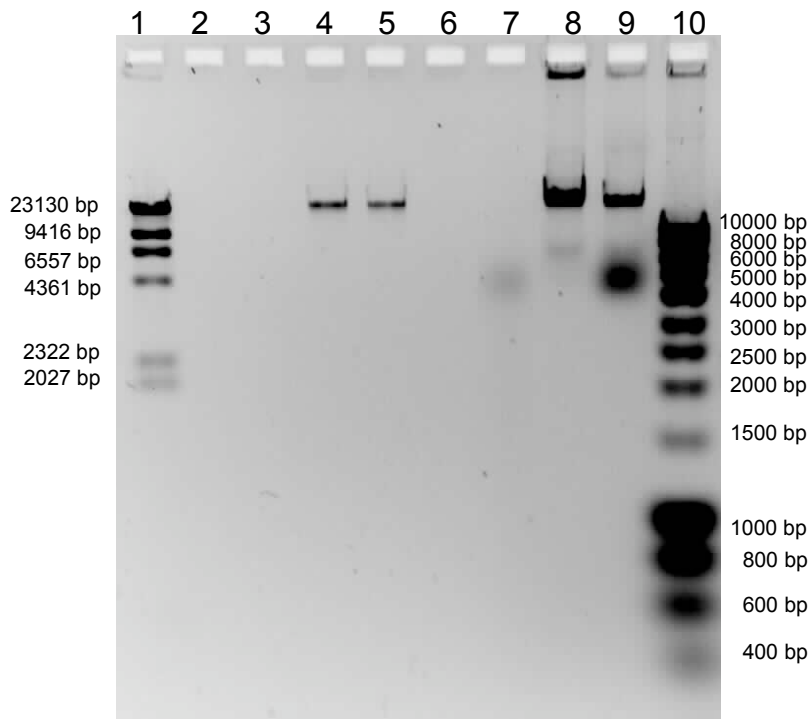
Figure 4.6 Agarose gel determining the nature of the visible DNA bands in Top10F' culture supernatant. Lane 1 is Fermentas λ/HindIII ladder. Lane 2 is Benzonase-treated non-infected Top10F' culture supernatant (no DNA visible cf. Lane 4). Lane 3 is Benzonase-treated non-infected Top10F' culture supernatant, then phenol-chloroform treated (no DNA visible cf. Lane 5). Lane 4 is non-infected Top10F' culture supernatant. Lane 5 is non-infected Top10F' culture supernatant, then phenol-chloroform treated. Lane 6 is Benzonase-treated M13 infected Top10F' culture supernatant (no DNA visible cf. Lane 8). Lane 7 is Benzonase-treated M13 infected Top10F' culture supernatant, then phenol-chloroform treated (no 20 kb DNA visible cf. Lane 9, secondary band visible). Lane 8 is M13 infected Top10F' culture supernatant. Lane 9 is M13 infected Top10F' culture supernatant, then phenol-chloroform treated (two bands visible). Lane 10 is Bioline HyperLadder 1.

4.2.5 Quantification of protein

The amount of protein in the culture supernatant increased as growth progressed, as observed qualitatively by silver staining of SDS-PAGE gels (Figure 4.7). A control lane was included, which contained caesium-chloride purified bacteriophage M13 of concentration 4×10^{11} pfu ml^{-1}, similar to that in the culture supernatant at the end of bacteriophage production. A single band was visible at approximately 60 kDa, which corresponded to bacteriophage coat protein pIII. The other four coat proteins were of molecular masses below the 20.0 kDa size limit of the 12 % acrylamide gels prepared, and so were not observed. Although the actual molecular weight of pIII is 42.6 kDa, it is known to run to the 60 kDa level (Gailus and Rasched, 1994;

Steiner *et al.*, 2006). Therefore it was concluded that the bands observed in culture supernatant samples were chiefly due to *E. coli* rather than bacteriophage proteins.
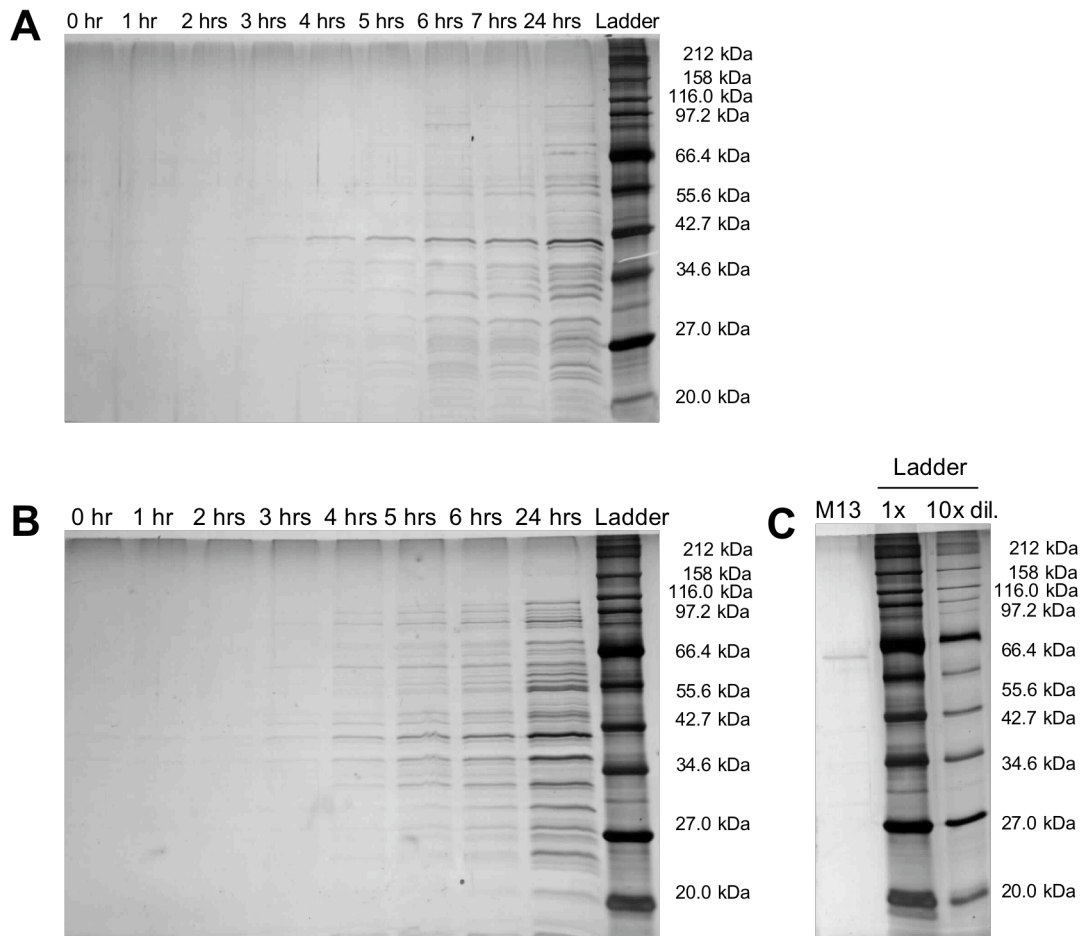
Figure 4.7 SDS-PAGE gels showing the visible supernatant proteins in culture supernatant of molecular weight 20-212 kDa. A total of 10 µl of sample (plus 10 µl loading buffer) was loaded in each well. Gel (A**)** shows the increase in supernatant protein as a function of time for non-infected Top10F' culture. Gel (B) shows the increase in supernatant protein as a function of time for M13 infected Top10F' culture. Gel (C) shows the control lane of 4 x 10^{11} pfu ml^{-1} of caesium-chloride purified bacteriophage M13. The bacteriophage coat protein pIII can be seen at approximately 60 kDa.

The amount of protein in the supernatant as measured by Bradford assay did not correlate with the trends observed by SDS-PAGE. Whilst the quantity of protein was observed to qualitatively increase over time by acrylamide gel analysis (Figure 4.7), the Bradford assay indicated that it did not (Figure 4.8). Similarly to the data determining DNA concentration by sample A_{260} reading, fresh NB2 medium gave one of the highest protein concentration readings. It was therefore assumed that the same pattern was occurring, i.e. the dominant contributor to the assay

readings was not released *E. coli* protein but a consumable component of the NB2 medium. The Bradford assay was consequently not used to track protein over time.

Henceforth, the Bradford assay was limited to being a measure of total protein at the point of culture harvest. From a downstream processing perspective, at the point of harvest both medium and free *E. coli* proteins may be considered as contaminants. Therefore, the assay has value as a general measure of protein concentration at this point. Comparing the quantity of total protein at the 5 hour timepoint when bacteriophage M13 production has ceased (Figure 4.8), it can be seen that the measured quantity of protein in the infected culture (30.5 µg ml^{-1}) was significantly higher (P=0.02, t-test) than that in the non-infected culture (20.6 µg ml^{-1}). A control of caesium-chloride purified bacteriophage M13 (in 10 mM Tris, pH 7.5 at 25 °C) of concentration 4 x 10^{11} pfu ml^{-1} showed that there was no contribution by bacteriophage coat proteins to the total measured quantity by Bradford assay (Figure 4.8).
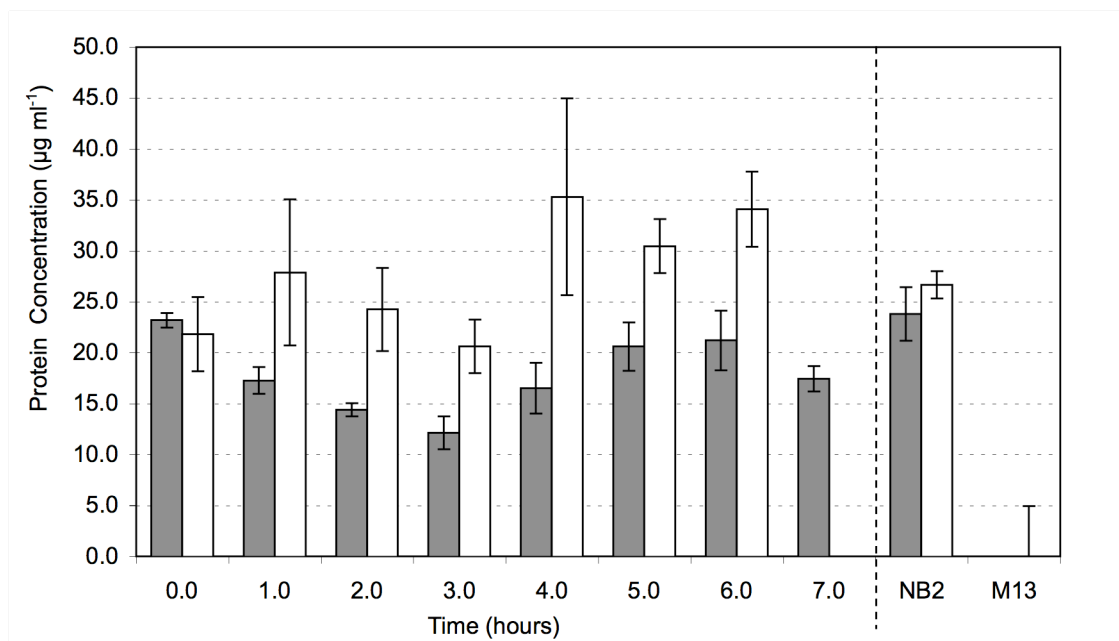
Figure 4.8 Concentration of protein in non-infected (■) and M13 infected (□) culture supernatants as a function of time. "NB2" was unused Nutrient Broth Number 2. "M13" was 4 x 10^{11} pfu ml^{-1} caesium chloride purified bacteriophage M13. Protein concentration was measured by Bradford assay. Error bars represent the standard error, N=3.

4.3   Comparison Between *E. coli* Top10F', JM107 and W1485 Culture

M13 infected cultures of Top10F', JM107 and W1485 were compared for bacteriophage yield and contaminant accrual. Generally speaking, it has proven difficult to correlate host cell genotype with recombinant protein or plasmid DNA productivity (Harrison and Keshavarz-Moore, 1996; Yau *et al.*, 2008), although the *recA* mutation may be an exception due to its far reaching effects (Capaldo and Barbour, 1973).

In this study, JM107 was selected as a representative $recA^+$ cloning strain, originally developed as a high transformation efficiency host for M13 derivatives (Yanisch-Perron *et al.*, 1985). Top10F' was selected as a representative $recA^-$ strain. In contrast, *E. coli* strain W1485 is close to wild-type, having only being cured of a λ lysogen by UV treatment (Jensen, 1993) and therefore possesses functioning restriction and modification systems. For all strain genotypes, see Section 2.2.

4.3.1   M13 infected *E. coli* culture

All strains were cultured as exactly described in Section 4.2.2 for Top10F' with the following exceptions: loopfuls of frozen JM107 stock culture were streaked on to a thiamine supplemented minimal agar plate (Section 2.1.8), whilst frozen W1485 stock culture was streaked onto NB2A plates (Section 2.1.6) without antibiotic selection. All were incubated overnight at 37 °C. Isolated colonies from these plates were then used to inoculate individual 5 ml aliquots of NB2 and incubated overnight at 37 °C with shaking. Subsequent shakeflask experimentation at the 50 ml scale was identical to that described for Top10F' (Section 4.2.2). Bacteriophage infection occurred at the zero timepoint by the addition of 2.3×10^8 pfu bacteriophage M13. The average MOI (multiplicity of infection) for each strain was calculated to be 6.0×10^{-2} for W1485, 7.1×10^{-2} for JM107 and 1.0×10^{-1} for Top10F' cultures.

Similarly to Top10F' culture, the OD_{600} value of M13 infected JM107 cells plateaued after four hours growth (Figure 4.9), albeit at a value of 0.88 rather than 1.08. In contrast, the OD_{600} of W1485 cells did not plateau until seven hours growth, at which point the cell density was substantially greater at 1.54. Enumeration of the viability of cells showed a different pattern (Figure 4.10): the viability count of Top10F' cells was consistently lower than that of JM107, although the OD_{600} was higher. Strikingly, the concentration of viable W1485 cells was measured to decrease in the first two hours of growth, from 7.8×10^7 cfu ml^{-1} at 0 hours, to only 2.6×10^7 cfu ml^{-1} at 2 hours. However, this was followed by a sustained period of viability increase.
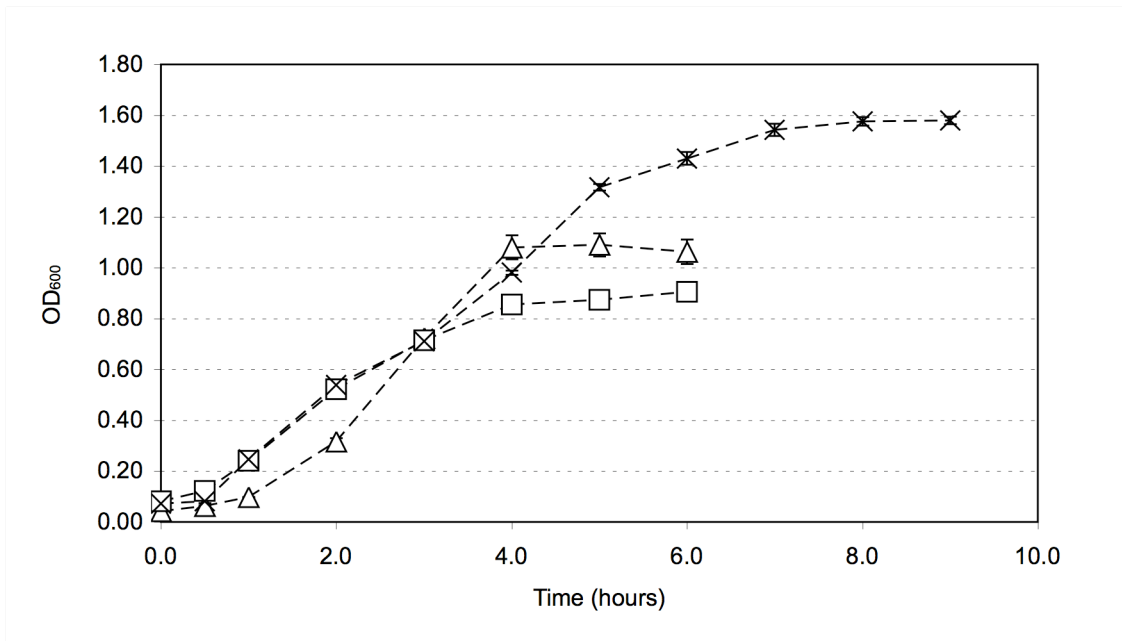
Figure 4.9 OD_{600} value of Top10F' ($\triangle$), JM107 ($\square$) and W1485 ($\times$) cultures as a function of incubation time. Error bars represent the standard error, N=3.
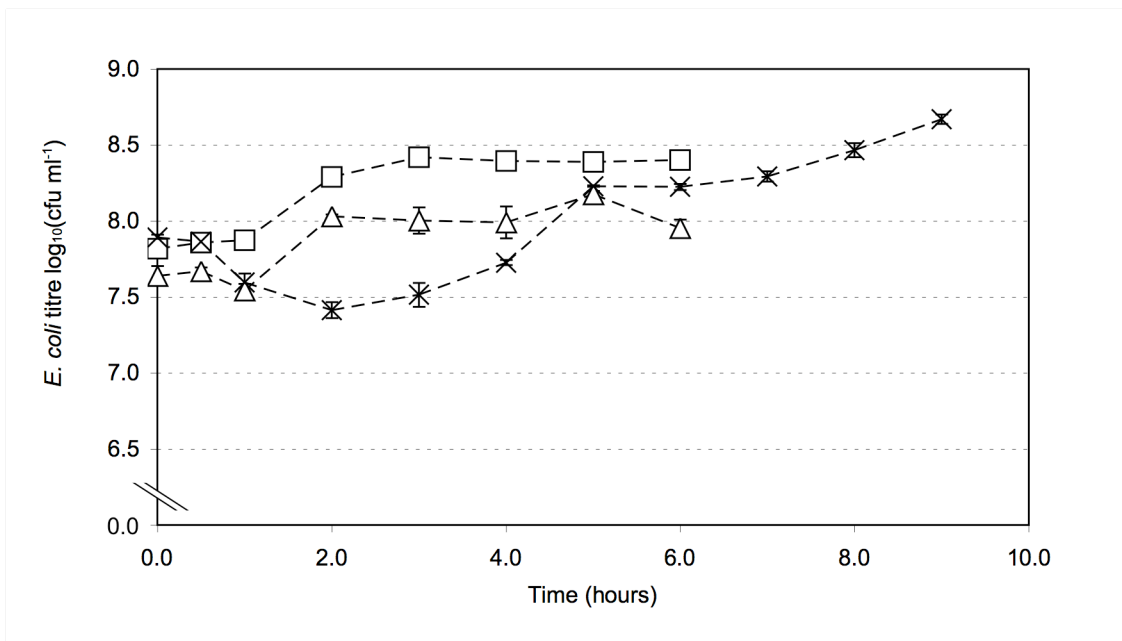
Figure 4.10 Viable cell counts of Top10F' ($\triangle$), JM107 ($\square$) and W1485 ($\times$) cultures as a function of incubation time. Error bars represent the standard error, N=3.

The maximum titre of bacteriophage was achieved by 5 hours growth in JM107 culture (3.9 x 10^{11} pfu ml^{-1}) which was similar to Top10F' (4.1 x 10^{11} pfu ml^{-1}) (Figure 4.11). The bacteriophage concentration in W1485 culture also plateaued after 5 hours growth (at 4.6 x 10^{11} pfu ml^{-1}) and did not significantly rise for a further three hours (P>0.05, Tukey). However, the titre of bacteriophage reached a maximum after 9 hours growth– 7.8 x 10^{11} pfu ml^{-1} – which was significantly higher than that after 5 hours (P<0.05, Tukey). Regardless of the OD_{600} and cell viability profiles, all three strains produced yields of bacteriophage M13 that were not significantly different from one another after five hours growth (P>0.05, Tukey).
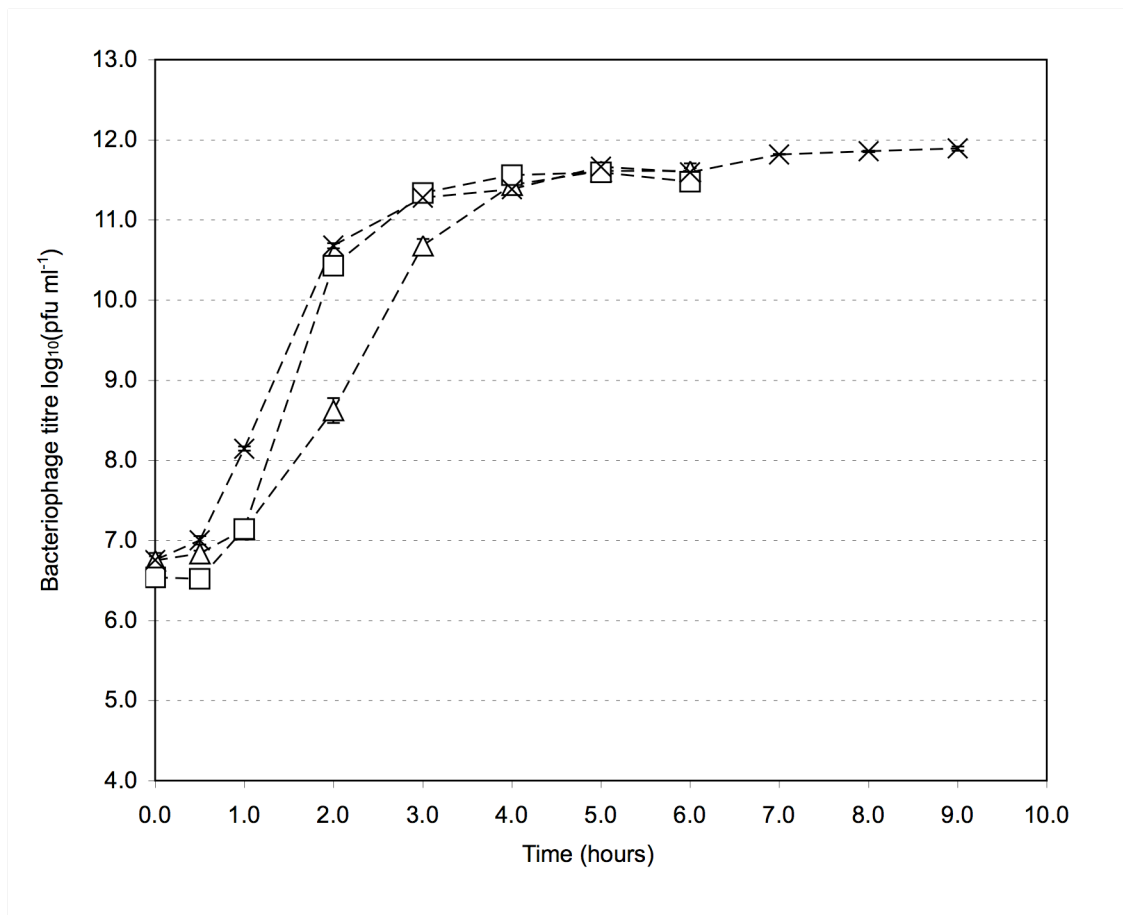
Figure 4.11 Bacteriophage concentration in Top10F' ($\triangle$), JM107 ($\square$) and W1485 ($\times$) cultures as a function of incubation time. Error bars represent the standard error, N=3.

After 24 hours incubation, the OD_{600} values, viable cell and bacteriophage concentrations were again measured for each *E. coli* strain. These were compared with the last recorded values of each growth curve to detect any secondary growth phase. It was observed that JM107 and W1485 cultures exhibited significant increases in OD_{600} value, and all three strains showed significant increases in viable cell counts, suggesting that a biphasic growth phenomenon occurred (Table 4.2). However, no culture experienced a significant rise in bacteriophage concentration.

Table 4.2 Comparing the OD_{600} values, viable cell and bacteriophage concentrations between the last recorded values of each growth curve and a 24 hour timepoint. Statistical analysis (t-test) was performed on log_{10}-transformed cell and bacteriophage count data.

Strain		OD_{600} value	Viable cell count (cfu ml^{-1})	Bacteriophage count (pfu ml^{-1})
Top10F'	6 hours	1.06	9.0×10^7	4.1×10^{11}
	24 hours	1.18	6.6×10^8	4.9×10^{11}
	P value	0.12	0.0003	0.40
JM107	6 hours	0.91	2.5×10^8	3.0×10^{11}
	24 hours	1.95	1.5×10^9	3.6×10^{11}
	P value	0.000006	0.01	0.30
W1485	9 hours	1.58	4.7×10^8	7.8×10^{11}
	24 hours	2.46	1.5×10^9	6.7×10^{11}
	P value	0.00006	0.001	0.14

4.3.2   Comparison of supernatant DNA concentration between strains

The accumulation of free DNA in JM107 and W1485 cultures was analysed by agarose gel electrophoresis (Figure 4.12 and Figure 4.13) as conducted for Top10F' (Figure 4.4). All cultures showed an increase in chromosomal DNA over time. The pattern observed in JM107 culture was identical to that for Top10F': chromosomal DNA appeared as a band of at least 20 kb in size. However, in W1485 culture this DNA appeared as a smear of increasingly small fragments as time progressed. All three strains showed that post phenol-chloroform treatment a secondary band of bacteriophage DNA was observed. The amount of chromosomal DNA in JM107 and W1485 cultures was subsequently quantified by densitometry (on a further agarose gel) of triplicate 5 hour timepoint samples and compared to Top10F' (Table 4.3). The average concentration of DNA in the supernatant of JM107 culture was 0.38 μg ml^{-1}, which was significantly lower than the 0.63 μg ml^{-1} in Top10F' culture (P=0.006, t-test). However, the amount of DNA in W1485 culture was quantified to be 5.7 μg ml^{-1}, which was considerably higher than both JM107 and Top10F'.
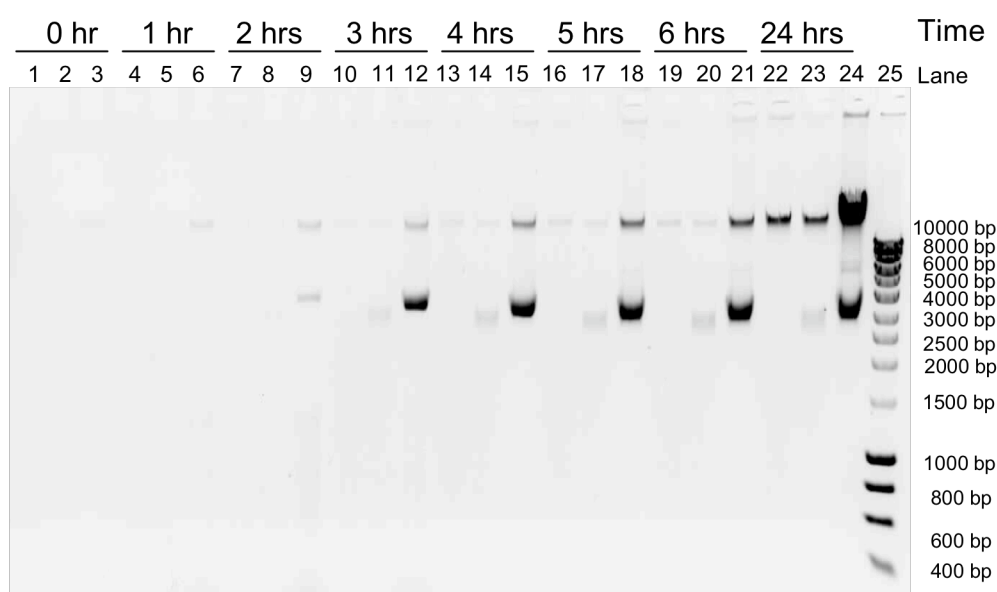
Figure 4.12 Agarose gel indicating the quantity of DNA in the JM107 culture supernatant. Lanes 1, 4, 7, 10, 13, 16, 19 and 22 are untreated culture supernatant samples. Lanes 2, 5, 8, 11, 14, 17, 20, and 23 are phenol-chloroform treated culture supernatant samples. Lanes 3, 6, 9, 12, 15, 18, 21 and 24 are phenol-chloroform treated culture supernatant samples which have been 10-fold concentrated by ethanol precipitation. Lane 25 is Bioline HyperLadder 1.
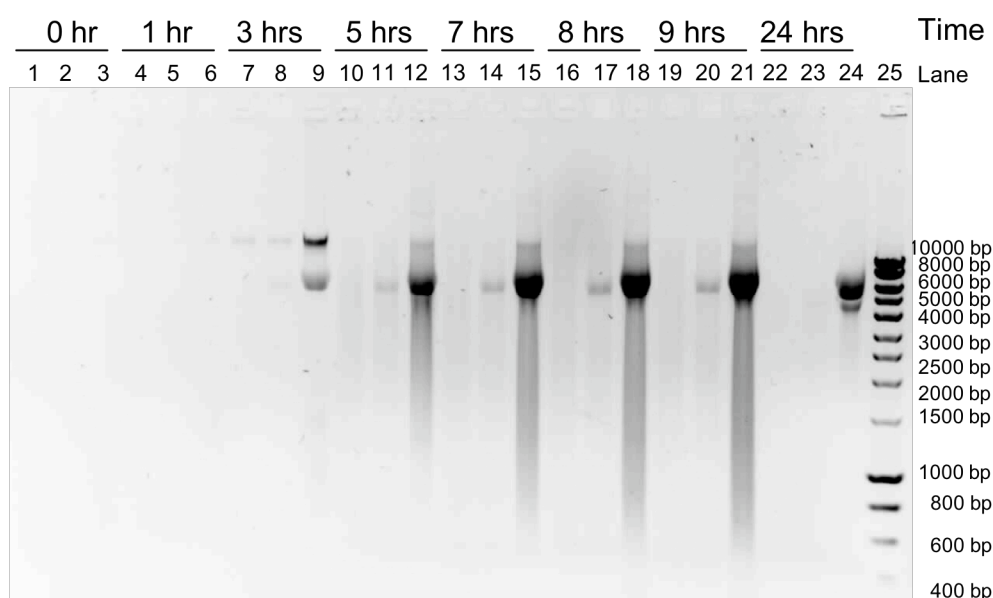
Figure 4.13 Agarose gel indicating the quantity of DNA in the W1485 culture supernatant. Lanes 1, 4, 7, 10, 13, 16, 19 and 22 are untreated culture supernatant samples. Lanes 2, 5, 8, 11, 14, 17, 20, and 23 are phenol-chloroform treated culture supernatant samples. Lanes 3, 6, 9, 12, 15, 18, 21 and 24 are phenol-chloroform treated culture supernatant samples which have been 10-fold concentrated by ethanol precipitation. Lane 25 is Bioline HyperLadder 1.

Table 4.3. Average DNA quantity in M13 infected Top10F', JM107 and W1485 culture supernatants, measured from agarose gels. Samples were quantified at the 5 hour timepoint. Uncertainties represent the standard error, N=3.

Quantity of DNA after 5 hours incubation ($\mu g \ ml^{-1}$)		
Top10F'	JM107	W1485
0.63 ± 0.03	0.38 ± 0.04	5.7 ± 1.2

4.3.3   Determination of endogenous nuclease activity

It was surmised that the degradation of free DNA in W1485 culture (Figure 4.13) was due to low levels of endogenous nucleases released into the culture medium. Non-nuclease-deficient *E. coli* strains have been demonstrated to partially degrade host nucleic acid under alkaline lysis conditions (Monteiro *et al.*, 1999). To test this hypothesis, M13 infected and non-infected cultures of Top10F', JM107 and W1485 were streaked on methyl green DNAse agar (Section 2.1.9) where the presence of DNAse activity was indicated by the formation of colourless zones in the previously green agar plate. Cultures (5 ml) were prepared as described in the Materials and Methods (Section 2.3.1). M13 infected cultures were inoculated with 2 x 10^6 pfu caesium chloride purified bacteriophage M13. All cultures were incubated for five hours at 37 °C with shaking. After streaking onto the DNAse agar, all plates were incubated at 37 °C overnight.

It was found that small zones of clearing were observed around colonies of all three strains, and were more pronounced when M13 infected (Figure 4.14). The strength of clearing around colonies were indistinguishable between Top10F' and JM107, but were visibly stronger on W1485. However, all zones of clearing were faint.
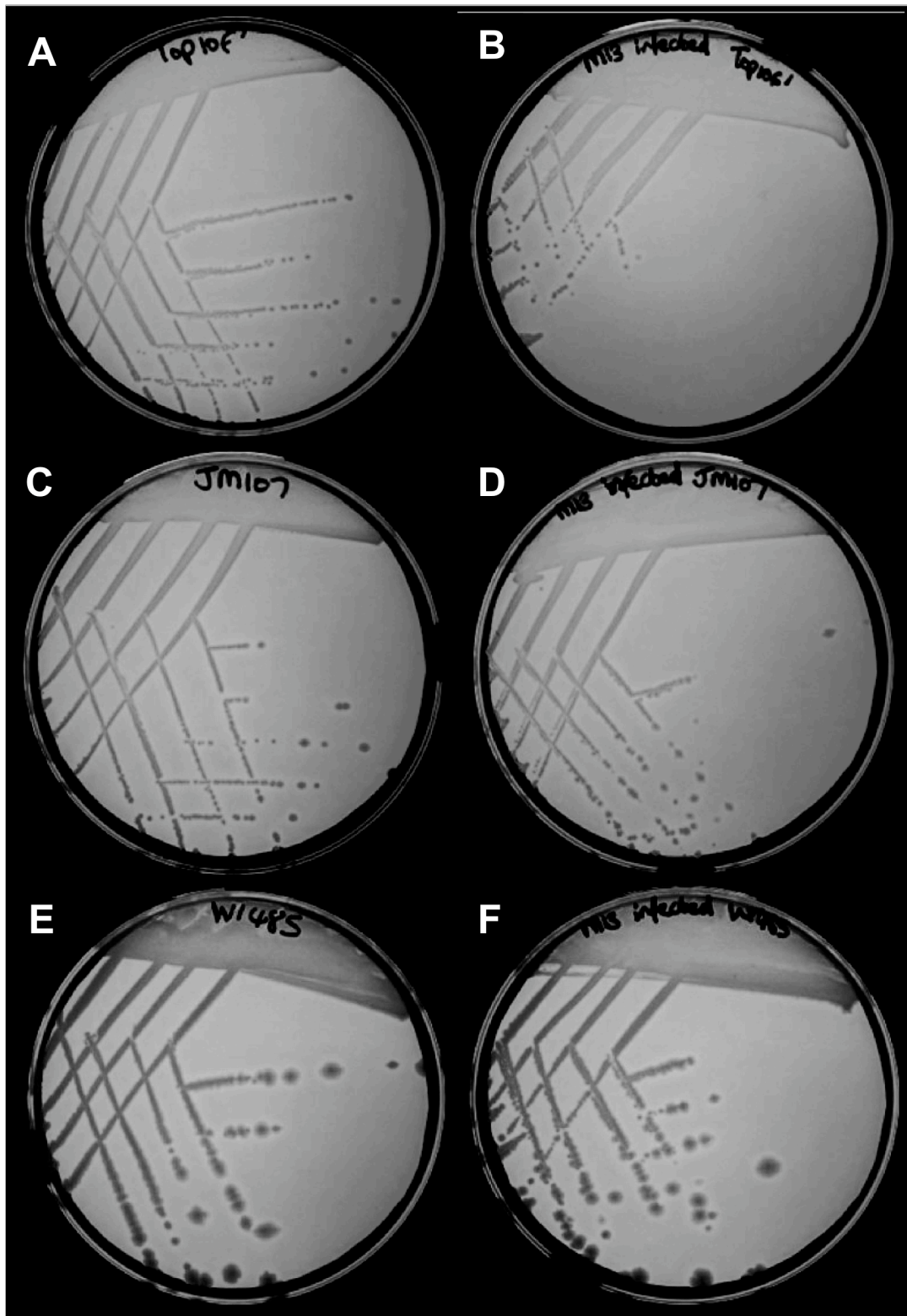
Figure 4.14 Methyl green DNAse agar plates streaked with non-infected and M13 infected Top10F', JM107 and W1485 cultures incubated overnight at 37 °C. Plate (A), Top10F'. Plate (B), M13 infected Top10F'. Plate (C), JM107. Plate (D), M13 infected JM107. Plate (E), W1485. Plate (F), M13 infected W1485. DNAse activity is indicated by a loss of green pigmentation. To highlight clearance zones, images were converted to greyscale and the contrast enhanced.

4.3.4 Comparison of supernatant protein concentration between strains

The concentration of protein in the JM107 and W1485 culture supernatants was observed to increase over time by SDS-PAGE and silver staining (Figure 4.15 and Figure 4.16) in a manner consistent with Top10F' (Figure 4.7). A further acrylamide gel was prepared to compare the three strains at the 5 hour timepoint (Figure 4.17). On a qualitative basis, the concentration of protein in the supernatant appeared to increase in the order JM107 < Top10F' < W1485, although this observation was of a single replicate. However, this pattern was matched by triplicate Bradford assay measurements of total protein at the harvest timepoint (Table 4.4), which increased in the order JM107 (22.1 µg ml-1) < Top10F' (36.8 µg ml-1)< W1485 (38.0 µg ml-1). The concentration of total protein in the supernatant of JM107 culture was significantly lower than that in Top10F' and W1485 cultures (P<0.001, Tukey). However, the concentration of protein in Top10F' and W1485 cultures was similar (P>0.05, Tukey).
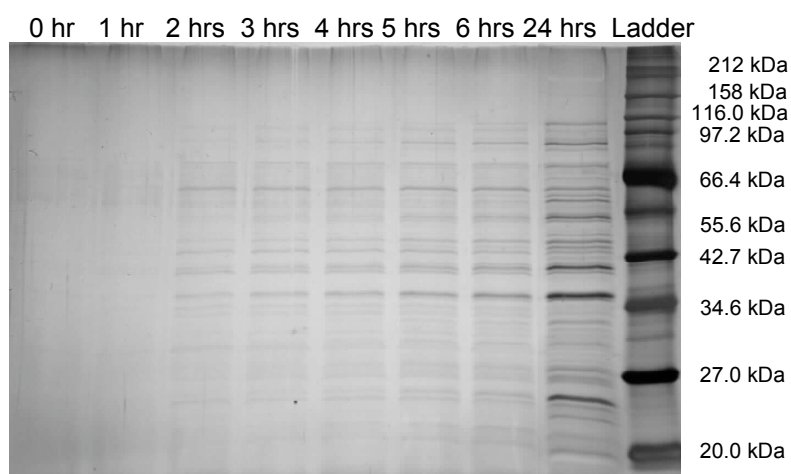
Figure 4.15 SDS-PAGE gel showing the visible supernatant proteins in JM107 culture supernatant of molecular weight 20-212 kDa. A total of 10 µl of sample (plus 10 µl loading buffer) was loaded in each well. The gel shows the increase in supernatant protein as a function of time.
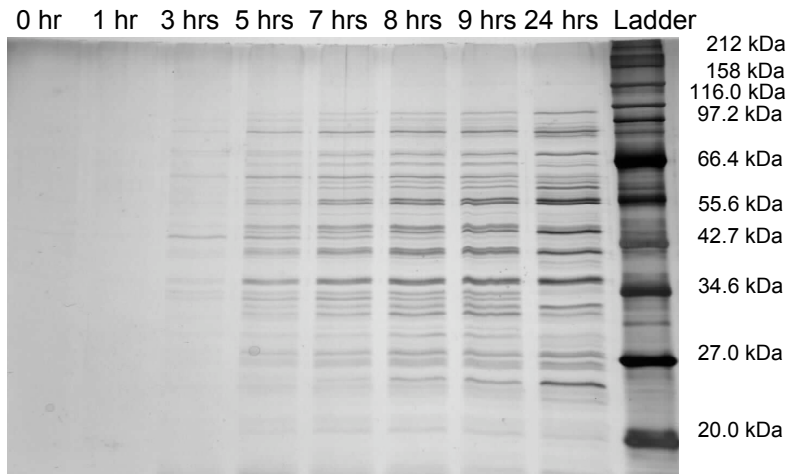
Figure 4.16 SDS-PAGE gel showing the visible supernatant proteins in W1485 culture supernatant of molecular weight 20-212 kDa. A total of 10 µl of sample (plus 10 µl loading buffer) was loaded in each well. Gel shows the increase in supernatant protein as a function of time.
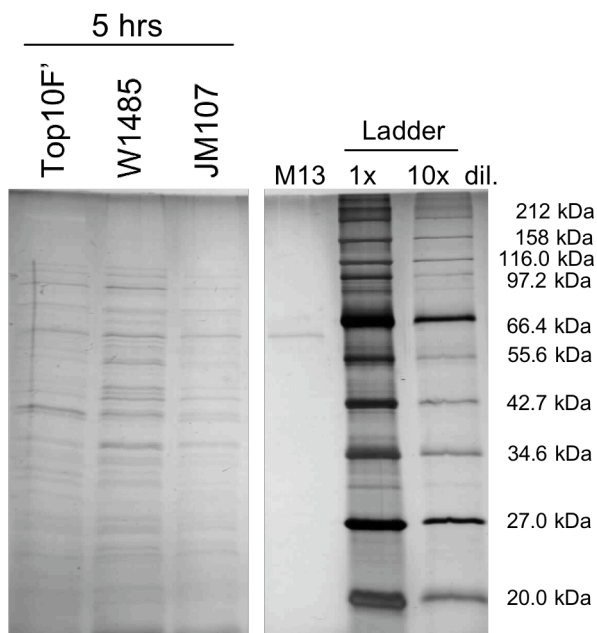
Figure 4.17 SDS-PAGE gels showing the visible supernatant proteins in culture supernatant of molecular weight 20-212 kDa. A total of 10 µl of sample (plus 10 µl loading buffer) was loaded in each well. The left hand portion of the gel shows the relative quantities of supernatant protein in M13 infected Top10F', JM107 and W1485 cultures after 5 hours growth. The right hand portion of the gel shows the control lane of 4×10^{11} pfu ml^{-1} of caesium-chloride purified bacteriophage M13. The bacteriophage coat protein pIII can be seen at approximately 60 kDa.

Table 4.4 Protein quantity in M13 infected Top10F', JM107 and W1485 culture supernatants, measured by Bradford assay. Samples were quantified at the 5 hour timepoint. Uncertainties represent the standard error, N=3.

Quantity of protein after 5 hours incubation ($\mu g\ ml^{-1}$)		
Top10F'	JM107	W1485
36.8 ± 2.1	22.1 ± 1.9	38.0 ± 2.7

Since the yield of bacteriophage M13 at the 5 hour harvest point was not significantly different between strains (Figure 4.11), it was concluded that *E. coli* JM107 was marginally preferable in terms of the quantity of protein and DNA released. Although partial degradation of DNA by W1485 was observed, it was incomplete, and total DNA and protein levels were higher.

4.4 Culture of an M13 Infected Top10F' Strain Producing a Recombinant Nuclease

4.4.1 Approach

The free *E. coli* chromosomal DNA detected in the culture supernatant is a contaminant of the bacteriophage M13 product. One strategy for its removal is to exploit physicochemical differences between DNA and bacteriophage to separate them in a downstream processing step. An alternative approach would be to selectively degrade the free DNA by enzymatic action, leaving the bacteriophage intact. The addition of exogenous nucleases, such as Benzonase (a commercially available form of the extracellular nuclease of *Serratia marcescens*), would achieve this aim (as successfully demonstrated in Section 4.2.4) but at a cost not viable at large scale (Cooke *et al.*, 2003). Instead, utilising a "biological" solution from the host strain may prove cost-effective. As noted in Section 4.3.3, the wholesale lysis of non-nuclease deficient *E. coli* results in partial nucleic acid degradation by endogenous nucleases (Monteiro *et al.*, 1999). However, since the extent of cell lysis in bacteriophage M13 production is comparatively small, such effects may be minor. Instead of relying upon endogenous nuclease activity, a more effective solution would be to modify the *E. coli* host strain to express a heterologous nuclease targeted to the periplasmic space. This would circumvent both the issues of cost and quality, and regulatory issues concerning the source of non-recombinant enzymes would also be avoided (Cooke *et al.*, 2003).

4.4.2   Transformation of a Staphylococcal nuclease-producing vector in Top10F'

A plasmid vector conferring nuclease activity to an *E. coli* cell has been previously constructed in our laboratory (Cooke, 2003). A *Staphylococcus aureus* (NCTC 8323) nuclease B (nucB) expression cassette was cloned into a pMMB67EH expression vector to give pMMBompnucB. nucB is expressed as a fusion to the ompA signal peptide, which targets the protein to the periplasmic space during growth (Suciu and Inouye, 1996). A 5 ml culture of JM107 *E. coli* holding the pMMBompnucB plasmid was prepared as described in Section 2.3.1, and the plasmid extracted by Qiagen Miniprep (Section 2.8.3). Chemically competent Top10F' cells were prepared as described in Section 2.9.1, and transformed with the pMMBompnucB vector as described in Section 2.9.2. Transformants were isolated from overnight incubation (37 °C) on methyl green DNAse agar plates (Section 2.1.9) supplemented with 100 µg ml^{-1} ampicillin.

4.4.3   Culture of M13 infected Top10F' cells holding pMMBompnucB plasmid

Top10F' cells holding the pMMBompnucB plasmid were cultured as described in Section 4.2.2. Starter cultures (5 ml) were supplemented with 5 µg ml^{-1} tetracycline and 100 µg ml^{-1} ampicillin. Two sets of growth curves (50 ml) were conducted in triplicate. In the first set nuclease production was not induced whereas in the second, nuclease production was induced by supplementation with 20 µg ml^{-1} IPTG.

The OD$_{600}$ value of M13 infected non-induced Top10F'-pMMBompnucB cells plateaued after four hours growth at a value of 1.11 (Figure 4.18), after which there was no significant increase ($P>0.05$, Tukey). This was very similar to the OD$_{600}$ value of 1.08 measured at the same timepoint in Top10F' cultures. In contrast, the OD$_{600}$ of induced Top10F'-pMMBompnucB cells plateaued an hour later, at a value of 0.82, which was significantly lower than the non-induced culture ($P=0.002$, t-test). Enumeration of viable cells showed that from one hour of growth onwards the viability of induced Top10F'-pMMBompnucB cells was consistently lower than that of non-induced Top10F'-pMMBompnucB and Top10F' cells (Figure 4.19).
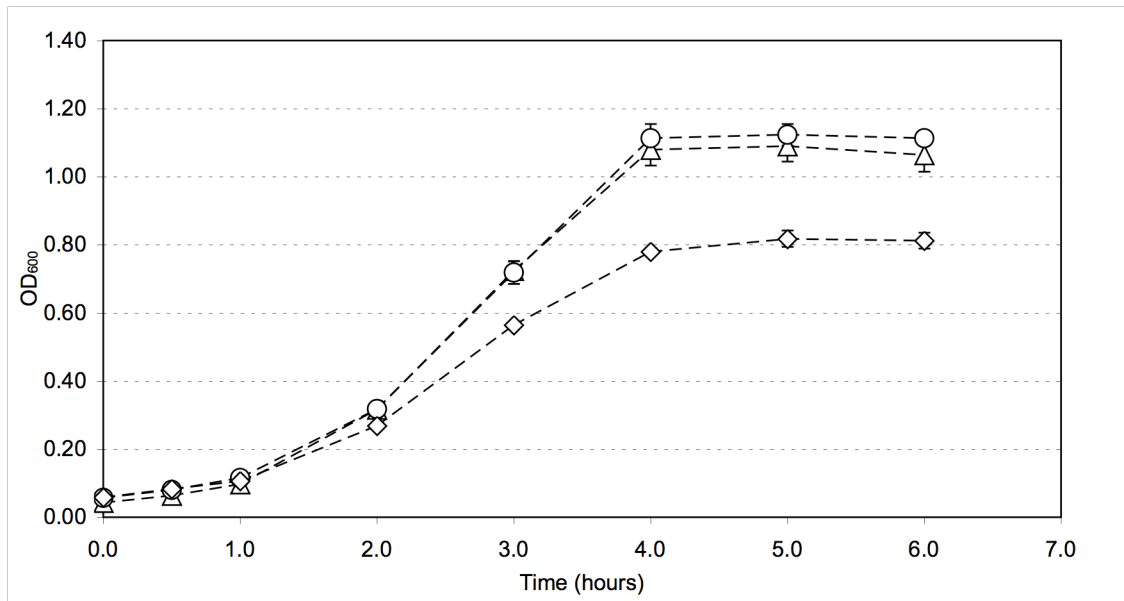
Figure 4.18 OD_{600} value of Top10F' ($\triangle$), non-induced Top10F'-pMMBompnucB ($\bigcirc$) and induced Top10F'-pMMBompnucB ($\diamondsuit$) cultures as a function of incubation time. All cultures were M13 infected at time zero. Error bars represent the standard error, N=3.
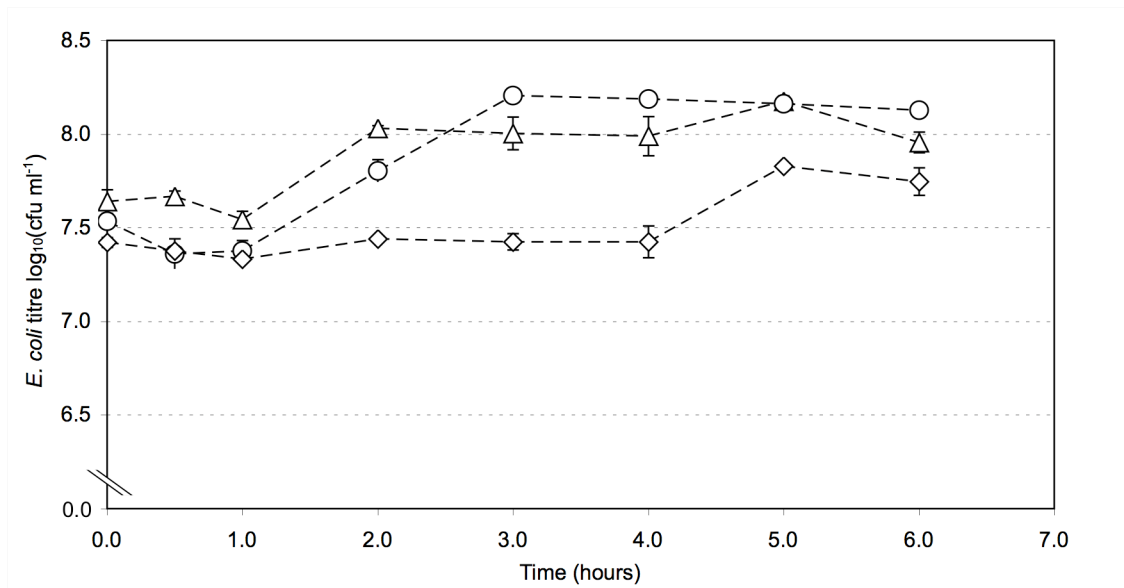
Figure 4.19 Viable cell counts of Top10F' ($\triangle$), non-induced Top10F'-pMMBompnucB ($\bigcirc$) and induced Top10F'-pMMBompnucB ($\diamondsuit$) cultures as a function of incubation time. All cultures were M13 infected at time zero. Error bars represent the standard error, N=3.

The maximum titre of bacteriophage was achieved by 5 hours growth in non-induced Top10F'-pMMBompnucB culture (4.4×10^{11} pfu ml-1), which was similar to Top10F' (4.1×10^{11} pfu ml^{-1}) (Figure 4.20). The bacteriophage concentration in induced Top10F'-pMMBompnucB culture reached a maximum an hour later, at a bacteriophage concentration of 3.0×10^{11} pfu ml^{-1}. These maximum bacteriophage titres were not significantly different from one another ($P>0.05$, Tukey).
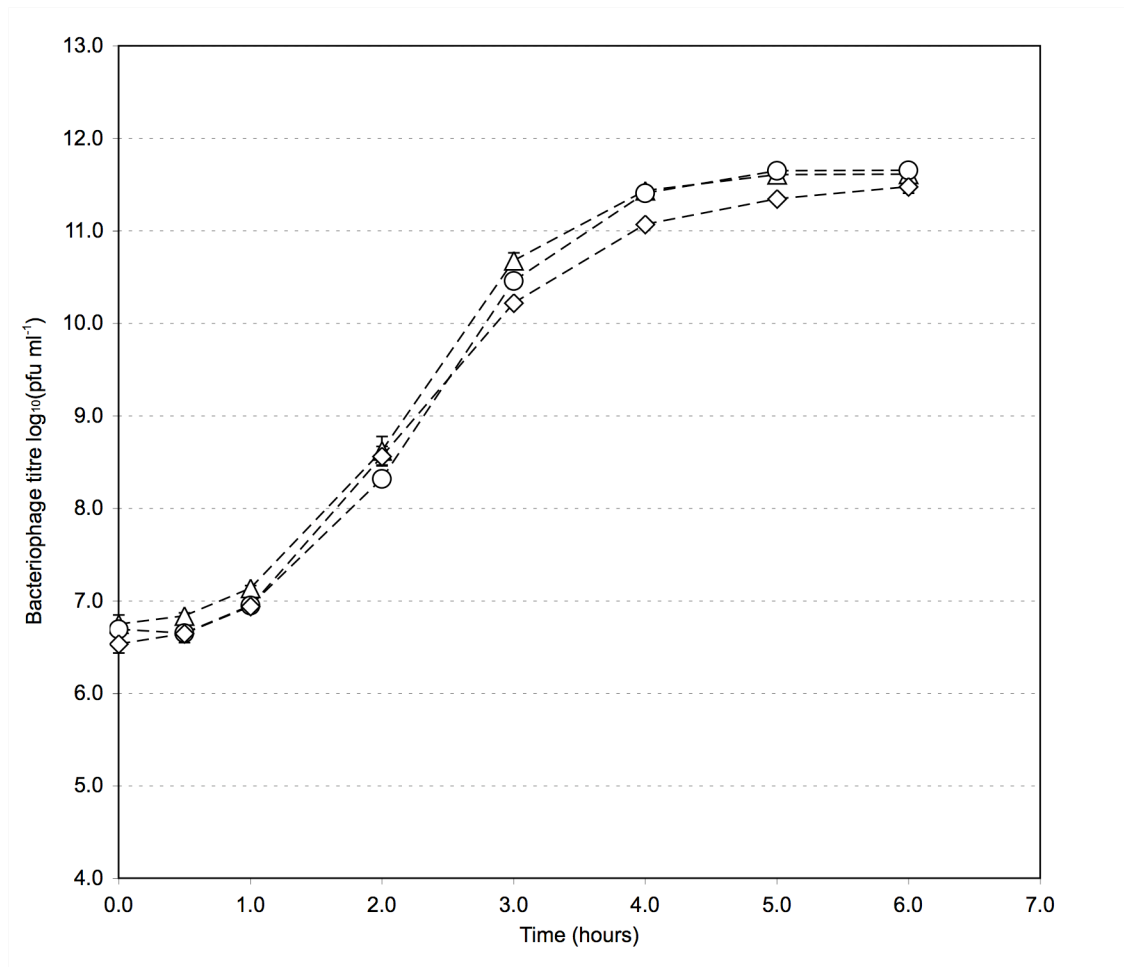
Figure 4.20 Bacteriophage concentration in Top10F' (△), non-induced Top10F'-pMMBompnucB (○) and induced Top10F'-pMMBompnucB (◇) cultures as a function of incubation time. All cultures were M13 infected at time zero. Error bars represent the standard error, N=3.

The accumulation of released DNA in (M13 infected) non-induced and induced Top10F'-pMMBompnucB cultures was analysed by agarose gel electrophoresis (Figure 4.21 and Figure 4.22) as conducted for Top10F' (Figure 4.4). Compared to M13 infected Top10F' supernatant samples (Figure 4.4), sufficient nuclease was produced and released in both induced and non-induced cultures to degrade all visible chromosomal DNA in untreated supernatant. A faint characteristic band of chromosomal DNA at >20 kb was only observed after 10-fold concentration by ethanol precipitation. Post-phenol chloroform treatment, the expected band of M13 DNA at 3-5 kb was visible.
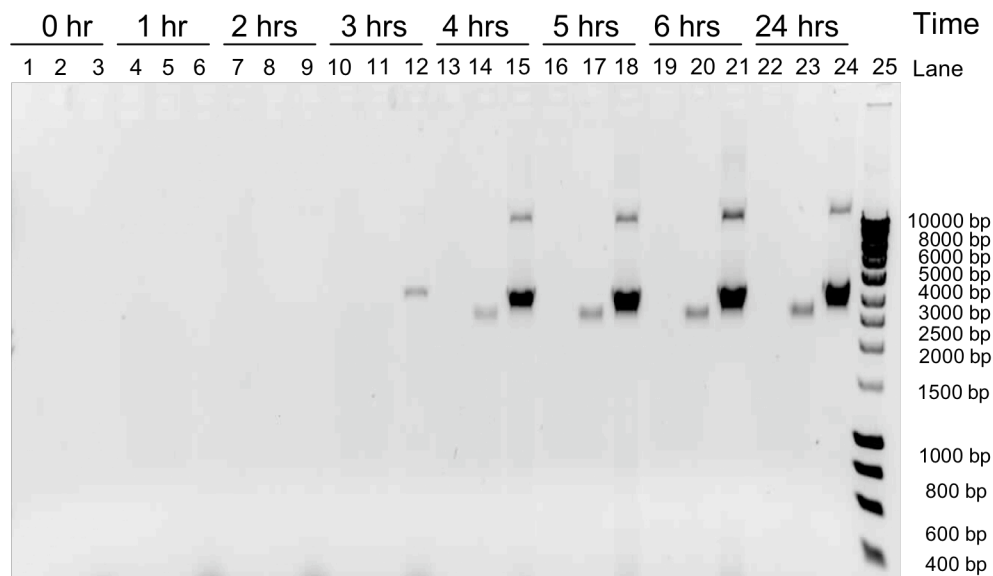
Figure 4.21 Agarose gel indicating the quantity of DNA in the (M13 infected) non-induced Top10F'-pMMBompnucB culture supernatant. Lanes 1, 4, 7, 10, 13, 16, 19 and 22 are untreated culture supernatant samples. Lanes 2, 5, 8, 11, 14, 17, 20, and 23 are phenol-chloroform treated culture supernatant samples. Lanes 3, 6, 9, 12, 15, 18, 21 and 24 are phenol-chloroform treated culture supernatant samples which have been 10-fold concentrated by ethanol precipitation. Lane 25 is Bioline HyperLadder 1.
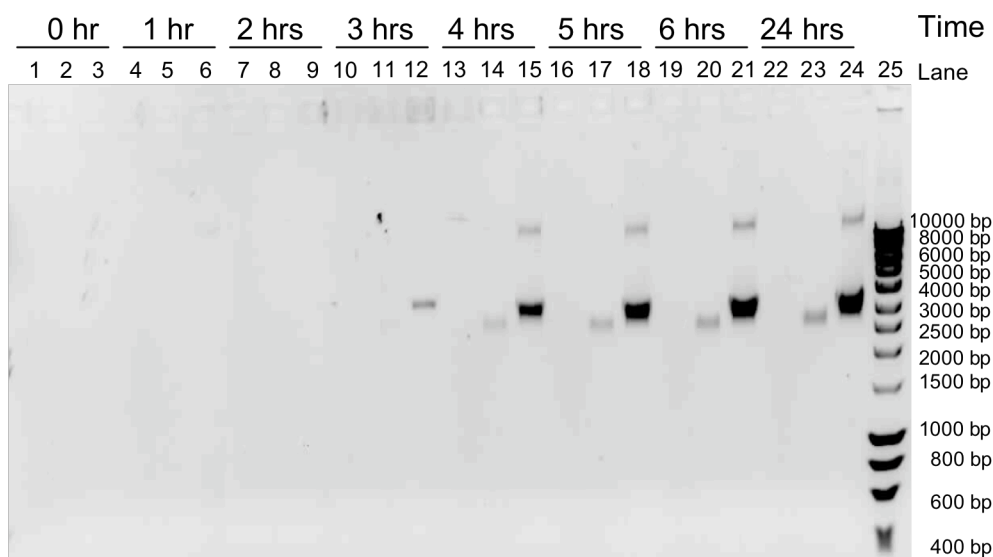
Figure 4.22 Agarose gel indicating the quantity of DNA in the (M13 infected) induced Top10F'-pMMBompnucB culture supernatant. Lanes 1, 4, 7, 10, 13, 16, 19 and 22 are untreated culture supernatant samples. Lanes 2, 5, 8, 11, 14, 17, 20, and 23 are phenol-chloroform treated culture supernatant samples. Lanes 3, 6, 9, 12, 15, 18, 21 and 24 are phenol-chloroform treated culture supernatant samples which have been 10-fold concentrated by ethanol precipitation. Lane 25 is Bioline HyperLadder 1.

To confirm nuclease activity, M13 infected and non-infected cultures of induced and non-induced Top10F'-pMMBompnucB were prepared and streaked on methyl green DNAse agar as described in Section 4.3.3. The DNAse agar was supplemented with 20 µg ml^{-1} IPTG for induced Top10F'-pMMBompnucB cells. After overnight incubation at 37 °C, large colourless zones were observed around induced and non-induced culture colonies (Figure 4.23) in comparison to very small zones of clearing around Top10F' colonies without pMMBompnucB plasmid (Figure 4.14). No visible difference was observed for M13 infected or non-infected cultures.
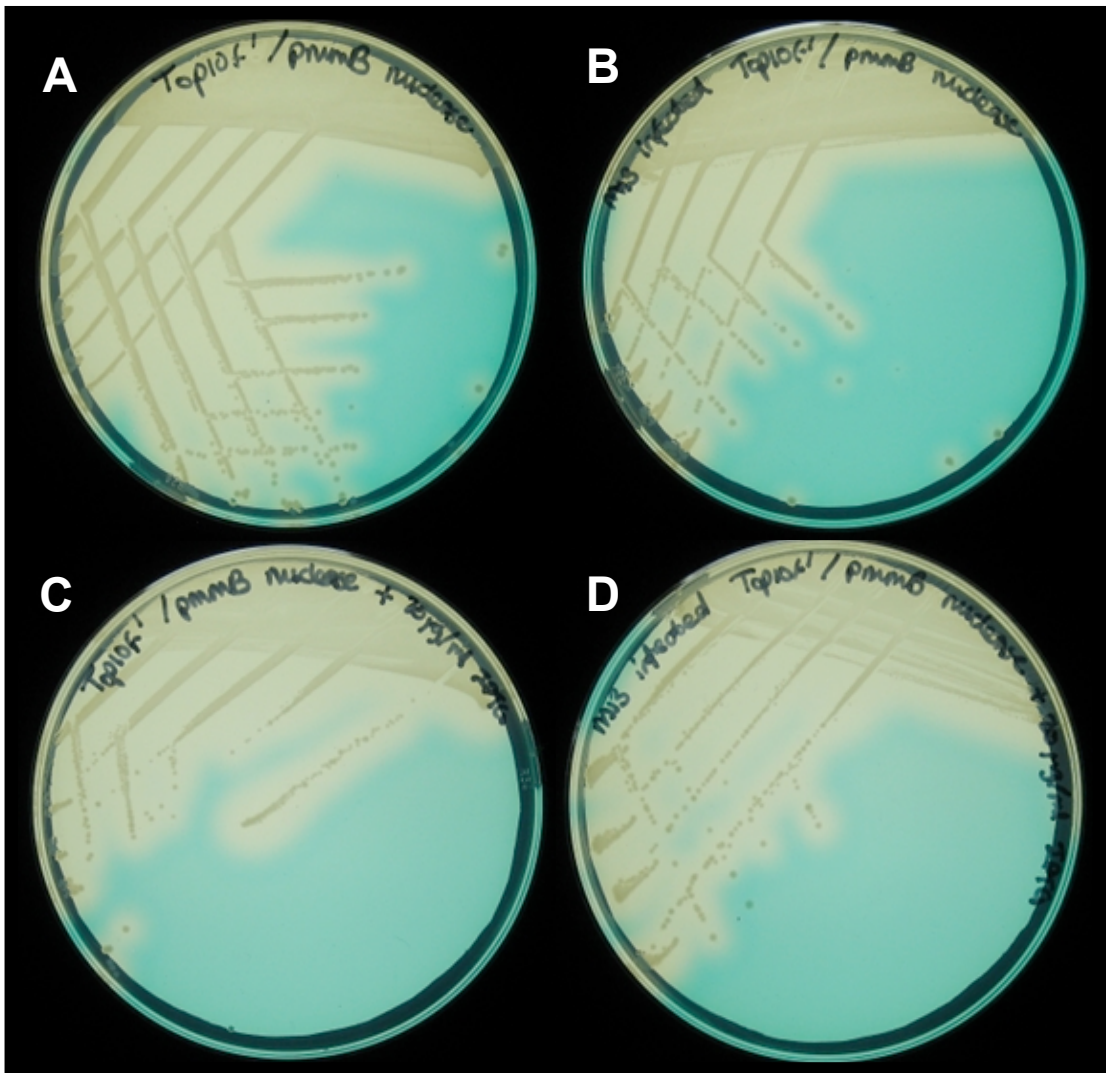
Figure 4.23 Methyl green DNAse agar plates. Plate (A), Non-induced Top10F'-pMMBompnucB. Plate (B), M13 infected non-induced Top10F'-pMMBompnucB. Plate (C), induced Top10F'-pMMBompnucB. Plate (D), M13 infected induced Top10F'-pMMBompnucB. DNAse activity is indicated by a loss of green pigmentation. No image manipulation to increase contrast was conducted.

At the point of maximum bacteriophage yield (and therefore the harvest point), the total amount of protein in the induced and non-induced Top10F'-pMMBompnucB cultures was measured in triplicate (i.e. three different cultures) by Bradford assay and compared to Top10F' (Table 4.5). The concentration of protein in the supernatant of induced Top10F'-pMMBompnucB cultures was significantly higher than that in Top10F' and non-induced Top10F'-pMMBompnucB cultures (P<0.001 and P<0.001 respectively, Tukey). However, the concentration of protein in Top10F' and non-induced Top10F'-pMMBompnucB cultures was similar (P>0.05, Tukey).

Table 4.5 Protein quantity in M13 infected Top10F', induced and non-induced Top10F'-pMMBompnucB culture supernatants, measured by Bradford assay. Samples were quantified at the timepoint where bacteriophage M13 production has ceased. Top10F' and non-induced Top10F'-pMMBompnucB cultures were therefore sampled at 5 hours, induced Top10F'-pMMBompnucB cultures were sampled after 6 hours incubation. Uncertainties represent the standard error, N=3.

Quantity of protein (μg ml^{-1})		
Top10F'	Non-induced Top10F' -pMMBompnucB	Induced Top10F -pMMBompnucB
36.8 ± 2.1	39.1 ± 1.4	45.5 ± 1.9

4.5   2 L Fermentation Study

Fermentations were preformed in a two litre (working volume 1.5 litres) LH 210 series bioreactor with pH control and exhaust gas data logging. Equipment details and method of operation are described in the Materials and Methods (Section 2.13.2). The *E. coli* inoculum formed 10 % (v/v) of the final working volume. Unless otherwise stated, M13 infection occurred at the zero timepoint in the bioreactor.

4.5.1   Fermentation of non-infected Top10F': medium comparison

The growth of non-infected Top10F' cells in NB2 and a richer fermentation medium (Section 2.1.7) was investigated at the 1.5 litre scale. Top10 cells previously grown in the fermentation medium in the same two litre capacity bioreactor (10 g l^{-1} each of yeast extract, tryptone peptone, sodium chloride and glycerol) have been reported to achieve OD_{600} values of at least 12 (Doig *et al.*, 2003).

At the 1.5 litre fermentation scale the yield of Top10F' cells in NB2 was low compared to the richer fermentation medium (Figure 4.24). In NB2 the maximum OD_{600} of 2.72 was achieved by five hours growth, which was consistent with OD_{600} values achieved by Top10F' culture at the 50 ml shakeflask (OD_{600}=2.49 after 7 hours, Figure 4.1) and 400 ml shakeflask (OD_{600}=2.80 after 5 hours, Table 5.2) scales. However, this was six-fold lower than the maximum OD_{600} value attained in the fermentation medium (18.45), which was achieved after six hours growth as was consistent with OD_{600} values reported in the literature for Top10F' (Doig *et al.*, 2003). Similarly, at the cessation of growth the titre of viable cells in NB2 culture was ten-fold lower than that in fermentation medium (Figure 4.25).
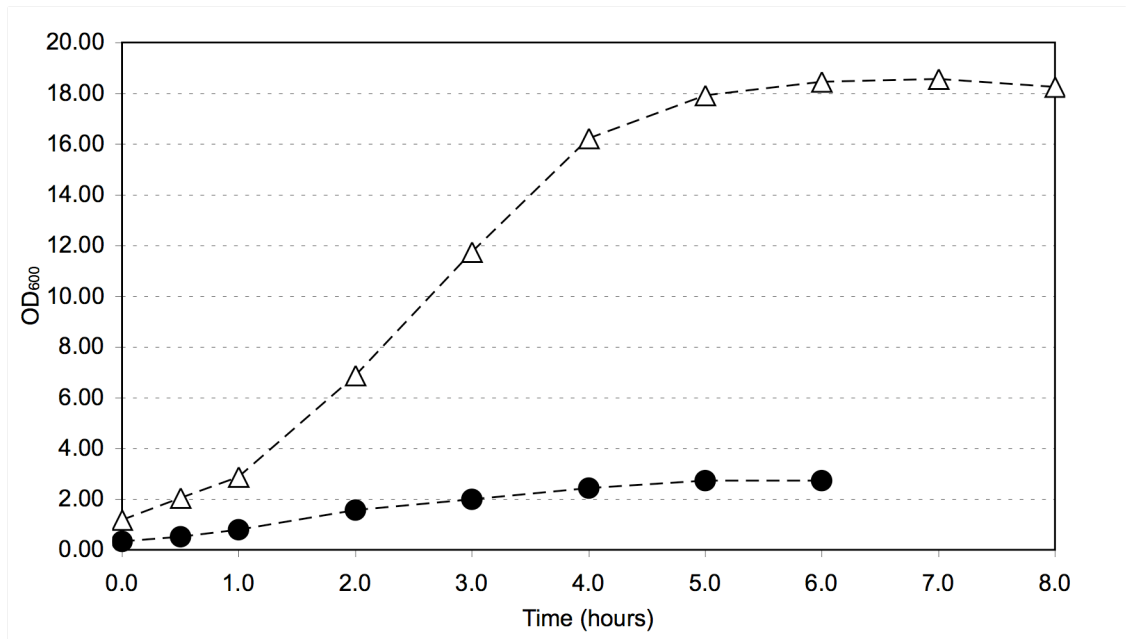
Figure 4.24 OD_{600} value of non-infected Top10F' culture in NB2 (●) and fermentation medium (△) as a function of incubation time. Cultures were inoculated with *E. coli* Top10F' at the zero timepoint.
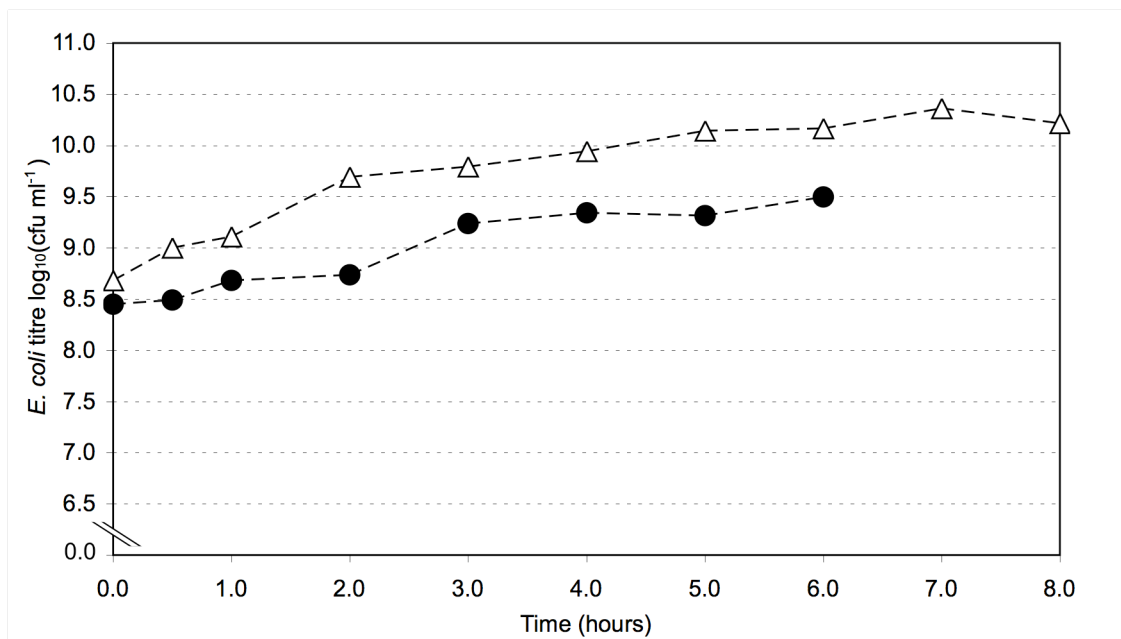
Figure 4.25 Viability count of non-infected Top10F' culture in NB2 (●) and fermentation medium (△) as a function of incubation time. Cultures were inoculated with *E. coli* Top10F' at the zero timepoint.

4.5.2 Fermentation of M13 infected Top10F'

The richer fermentation medium was investigated in detail to determine if improved Top10F' growth translated to an increase in bacteriophage yield. The fermentation and analyses (exhaust gas data, OD_{600} readings, bacteriophage counts, cell counts and dry cell weight) were conducted as described in Section 2.13.2 and Section 2.13.3. A limited study of M13 infected Top10F' culture in NB2 was then conducted for comparison, where culture OD_{600} and bacteriophage titre was measured once after five hours growth.

In Top10F' culture in fermentation medium, the increase in bacteriophage concentration over time was compared to the viable cell concentration, OD_{600}, dry cell weight and fermentation exhaust gas data (Figure 4.26). The aim was to determine which measurements correlated best with bacteriophage production. Since bacteriophage enumeration is an off-line process requiring the overnight incubation of agar plates (Section 2.5.2), an at-line (such as OD_{600}) or on-line measurement (such as dissolved oxygen tension (DOT), oxygen uptake rate (OUR) and carbon dioxide evolution rate (CER)) which could be used as a proxy for the cessation of bacteriophage production would be useful. In the fermentation medium a maximum bacteriophage concentration of 1.8×10^{12} pfu ml^{-1} was achieved after four hours growth (Figure 4.26). This was nearly 4-fold greater than the concentration achieved after 5 hours growth in NB2 (4.8×10^{11} pfu ml^{-1}, OD_{600}=2.21). Comparison of the bacteriophage concentration trend with the available on-line, at-line and off-line data shows that maximum bacteriophage titre correlated with the end of growth, similarly to that observed at the 50 ml scale (Sections 4.2, 4.3 and 4.4). Maximum bacteriophage concentration therefore coincided with a plateau in OD_{600} value (4.40) and dry cell weight (2.4 g l^{-1}). After reaching a maximum at 2 hours, the OUR decreased as growth slowed and stabilised at 9.24 mmol l^{-1} h^{-1} by 5 hours, as did the CER at 8.79 mmol l^{-1} h^{-1}. Conversely, the reduction in oxygen demand after 2 hours resulted in a rise in DOT to 82.7 % by 5 hours.

After the plateau in growth, further increases in OD_{600}, OUR and CER were observed between 5 and 8 hours growth. The viable cell concentration and dry cell weight also continued to rise, and the DOT dropped in response to the increased oxygen demand. This biphasic growth phenomenon did not result in an increase in bacteriophage M13 concentration (Figure 4.26).
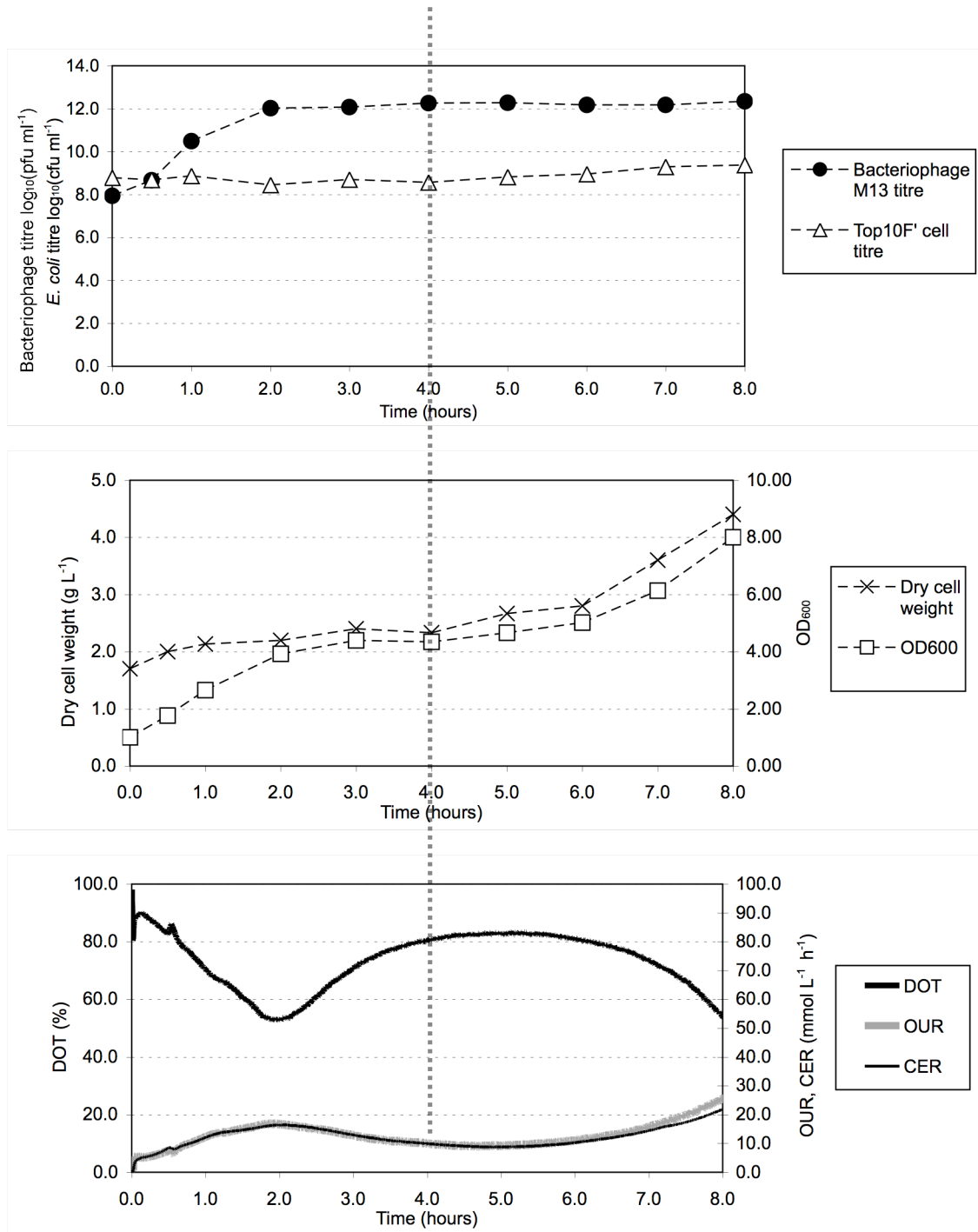
Figure 4.26 Recorded data from the 1.5 litre scale fermentation of M13 infected Top10F'. Bacteriophage and cell titres were off-line analyses, as well as dry cell weight. In this study, OD_{600} measurement was at-line. The DOT, OUR and CER values were on-line measurements. The dashed vertical line marks the time at which maximum bacteriophage titre was achieved (4 hours).

4.5.3   The effect of delayed infection on bacteriophage M13 yield

Thus far, Top10F' cells have always been infected with bacteriophage M13 at the start of fermentation. At end of growth, the resulting culture density was typically lower than for non-infected cells (Sections 4.2, 4.5.1 and 4.5.2). It was postulated that delaying the addition of the bacteriophage would result in a higher density of Top10F', which on infection with bacteriophage M13 would produce a greater bacteriophage concentration. Such a scheme resembled product manufacture by plasmid-based expression systems in *E. coli*, where cells are typically cultured to high density before induction to produce the desired product (Doig *et al.*, 2001; Tustian *et al.*, 2007; Zhao *et al.*, 2005).

Prior to bacteriophage infection, the increase in culture OD_{600} value closely matched that of the non-infected Top10F' culture (Figure 4.27). After 3 hours incubation (at an OD_{600} of 11.47) the bacteriophage inoculum (2×10^{11} pfu) was added, after which the optical densities diverged. One hour later the OD_{600} value of the infected culture was 2.82 units less than the non-infected. The culture reached a maximum OD_{600} value of 17.17 after 5 hours incubation, then decreased to 15.89 by 8 hours incubation. A maximum concentration of 4.58×10^{11} pfu ml^{-1} bacteriophage was achieved by 8 hours incubation, which was less than half the concentration achieved when bacteriophage infection occurred at the start of fermentation (Figure 4.28).
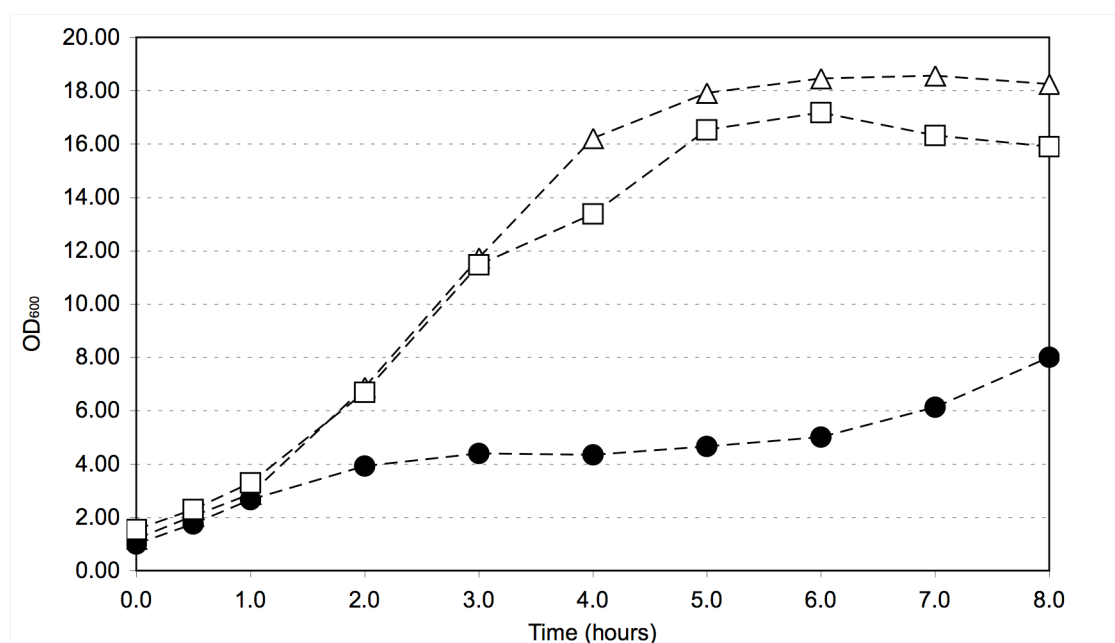
Figure 4.27 OD_{600} value of non-infected Top10F' ($\triangle$), M13 infected Top10F' at t= 0 hours ($\bullet$) and M13 infected Top10F' at t= 3 hours ($\square$) cultures as a function of incubation time.
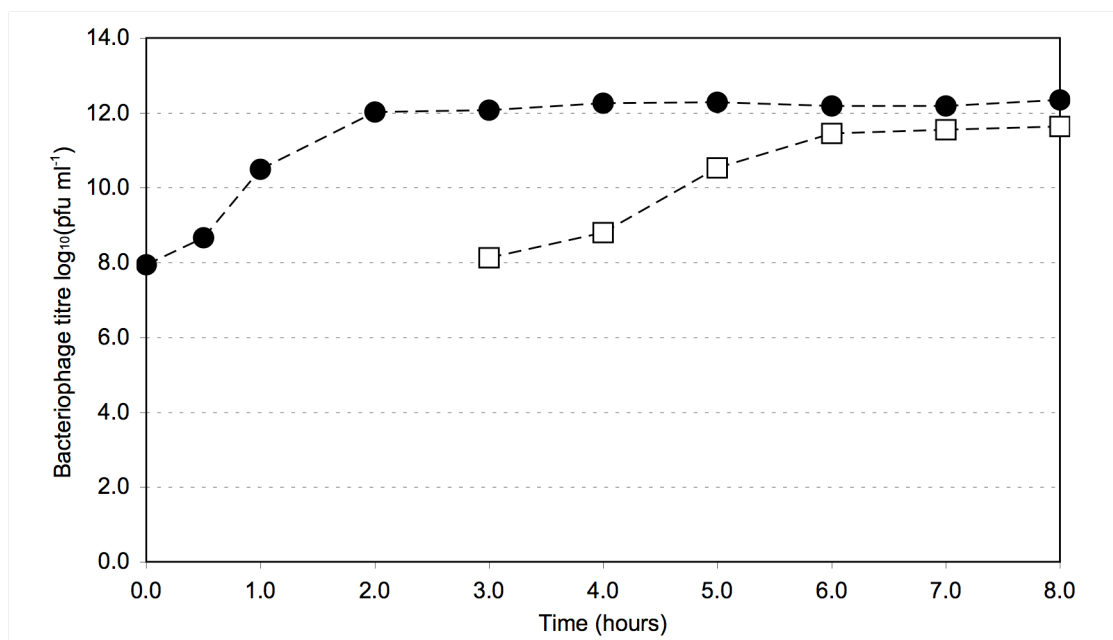
Figure 4.28 Bacteriophage concentration in M13 infected Top10F' at t= 0 hours (●) and M13 infected Top10F' at t= 3 hours (□) cultures as a function of incubation time.

4.5.4   Fermentation of M13 infected Top10F-pMMBompnuncB

Top10F' cells holding the pMMBompnucB plasmid were also fermented in the richer medium at the 1.5 litre scale. The fermentation medium in both the starter culture and bioreactor was supplemented with 20 µg ml^{-1} IPTG to induce nuclease production, 100 µg ml^{-1} ampicillin to select for the pMMBompnucB plasmid and 10 mM Ca^{2+} ions to promote nuclease activity. The fermentation was otherwise conducted as described in Section 2.13.2, with bacteriophage M13 infection at the same time as culture inoculation.

Both bacteriophage concentration and culture optical density began to plateau after 3 hours growth. A maximum bacteriophage concentration of 1.6×10^{12} pfu ml^{-1} was achieved after 8 hours growth (Figure 4.29), and a maximum OD$_{600}$ value of 4.88 was achieved after 8 hours growth also (Figure 4.30). The maximum bacteriophage concentration was similar to that achieved by Top10F' cells (1.8×10^{12} pfu ml^{-1}, Section 4.5.2), albeit four hours later. While the Top10F'-pMMBompnucB culture OD$_{600}$ profile was generally similar to that of Top10F', the viable cell count was substantially different (Figure 4.31). Upon infection with bacteriophage M13 the viable cell count dropped over the first three hours of fermentation (from 5.8×10^{8} cfu ml^{-1} to 7.2×10^{5} cfu ml^{-1}) before stabilising. However, over the same three hour period the culture OD$_{600}$ increased from 1.08 to 4.48. The viable cell count of Top10F' cells showed no such decline (Figure 4.31).
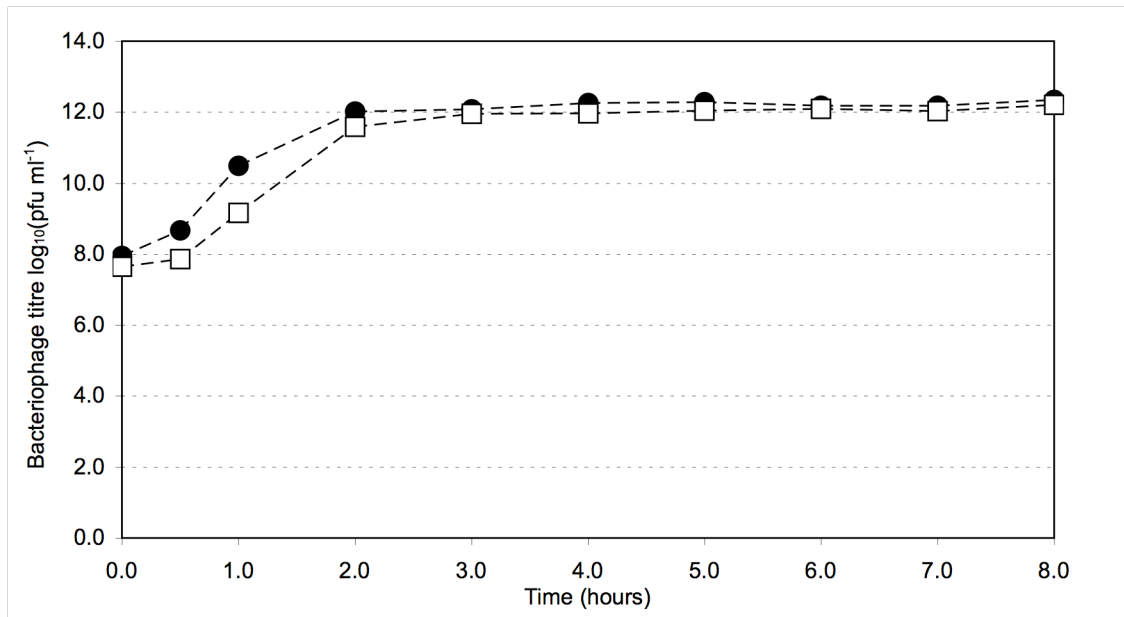
Figure 4.29 Bacteriophage concentration in M13 infected Top10F' (●) and M13 infected Top10F'-pMMBompnucB (□) cultures as a function of incubation time.
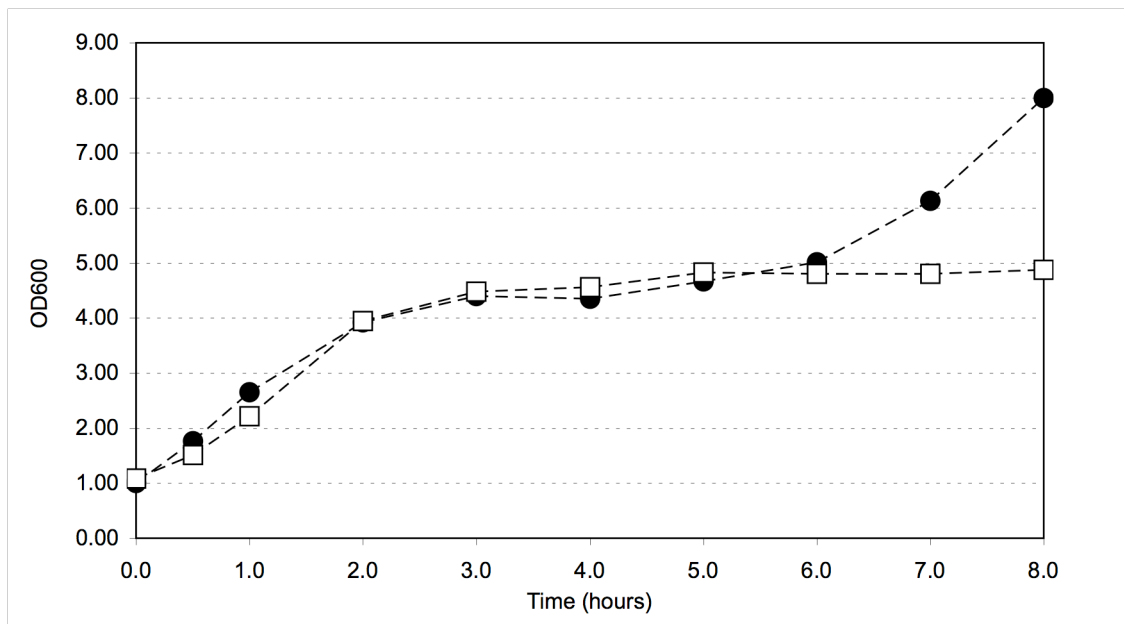
Figure 4.30 OD_{600} value of M13 infected Top10F' (●) and M13 infected Top10F'-pMMBompnucB (□) cultures as a function of incubation time.
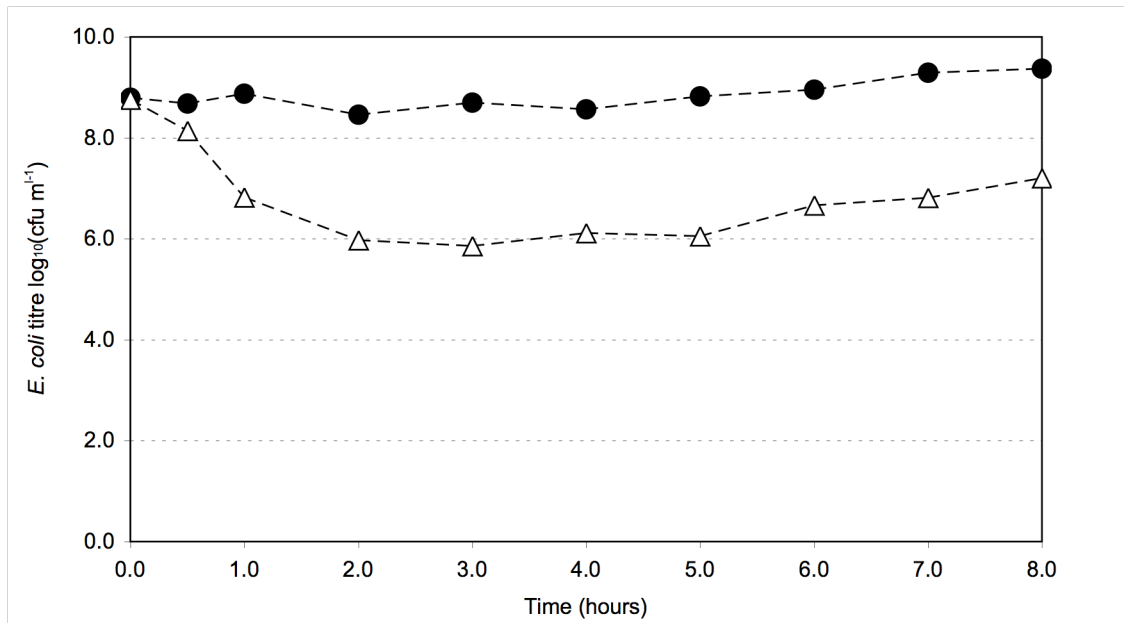
Figure 4.31 Viability counts of M13 infected Top10F' (●) and M13 infected Top10F'-pMMBompnucB (□) cultures as a function of incubation time.

4.5.5　　Quantification of supernatant DNA and protein concentrations

The accumulation of DNA in M13 infected Top10F' and induced Top10F'-pMMBompnucB cultures at the 1.5 litre scale was analysed by agarose gel electrophoresis (Figure 4.32 and Figure 4.33) in a similar fashion to that conducted at the 50 ml scale (Section 4.2.3), although no phenol/chloroform treatment or DNA concentration was performed. The concentration of chromosomal DNA in Top10F' culture increased as growth progressed (Figure 4.32), whereas sufficient nuclease was produced and released in Top10F'-pMMBompnucB culture to degrade all visible chromosomal DNA in untreated supernatant (Figure 4.33).
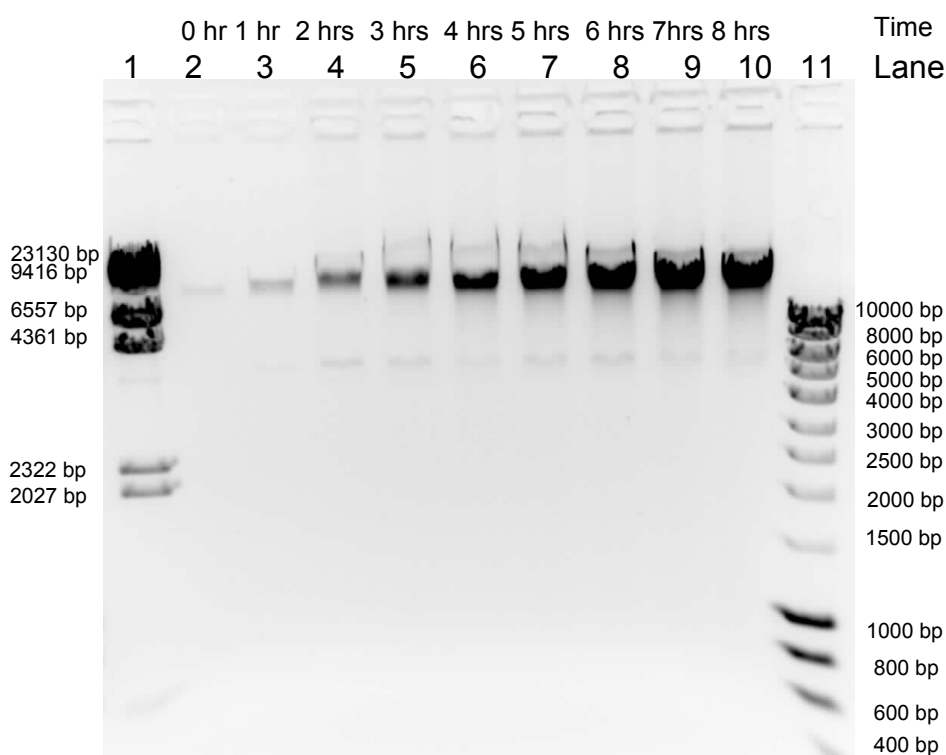
Figure 4.32 Agarose gel indicating the increasing quantity of DNA over time in the Top10F' 1.5 litre fermentation supernatant. Lane 1 is the Fermentas λ/HindIII ladder, Lane 11 is Bioline HyperLadder 1.
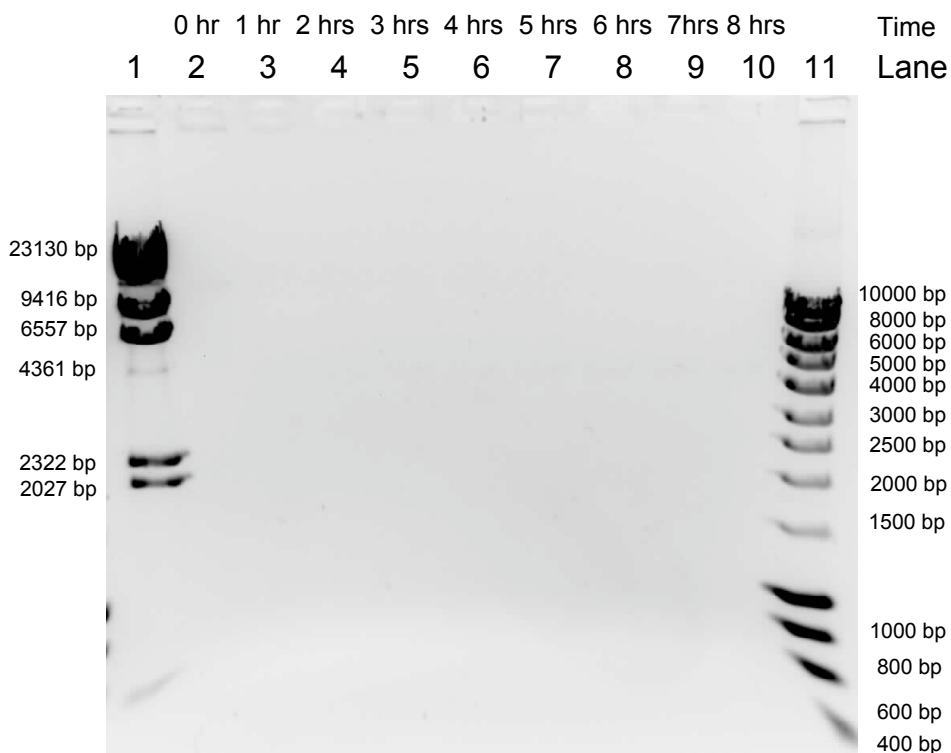
Figure 4.33 Agarose gel indicating the increasing quantity of DNA over time in the induced Top10F'-pMMBompnucB 1.5 litre fermentation supernatant. Lane 1 is the Fermentas λ/HindIII ladder, Lane 11 is Bioline HyperLadder 1.

The concentration of chromosomal DNA in M13 infected Top10F' culture was subsequently quantified at the point of maximum bacteriophage concentration (4 hours). Quantification of triplicate 10 μl samples on agarose gel (Section 4.2.3) gave an average concentration of 7.1 μg ml^{-1}.

At the point of maximum bacteriophage concentration (which was similar between cultures), the total amount of protein in the M13 infected Top10F' and Top10F'-pMMBompnucB cultures was measured by Bradford assay. The concentration of protein in Top10F' culture was 166.7 μg ml^{-1} (4 hours); in Top10F'-pMMBompnucB culture it was 114.0 μg ml^{-1} (8 hours). This was counter to the trend observed on the 50 ml scale (Section 4.4.3).

4.6 Discussion

The purpose of this chapter was to explore aspects of the growth of the non-lytic bacteriophage M13 in *E. coli*. It was hypothesized that bacteriophage yield may be increased by a richer growth medium or by utilising a different *E. coli* strain. The choice of *E. coli* strain was also assessed in terms of the impact upon culture contamination levels, since it was a key aim to examine the composition of the post-fermentation process fluid.

4.6.1 Selection of analyses to track contamination levels

The first part of this chapter was concerned with the identification of contamination levels in 50 ml Top10F' culture and the selection of analyses to identify them. Accumulation of *E. coli* cell debris during normal culture meant that cell components such as DNA, RNA, proteins, lipids, endotoxins and chemical residuals would be present in the milieu (Eastman and Durland, 1998; Prazeres and Ferreira, 2004), albeit at low concentrations since rates of cell death during growth are virtually undetectable (Hewitt *et al.*, 1998; Salivar *et al.*, 1964). Of these components, quantities of released chromosomal DNA and protein were measured. DNA measurement was selected due to the availability of a standard sensitive, robust detection method in the form of agarose gel electrophoresis. Since the second largest proportion of the *E. coli* cell (after water) is protein (Atkinson and Mavituna, 1991), it was considered an important quantity to measure. It was identified by Bradford assay and SDS-PAGE with silver staining.

It was shown (Section 4.2.2) that the analyses chosen were able to detect both protein and chromosomal DNA in 50 ml Top10F' culture supernatant. Quantitative data was obtained from agarose gels and the Bradford assay respectively. Quantification of silver-stained protein in acrylamide gels was not performed: silver staining performance is known to be particularly protein-specific and the linear dynamic range relatively limited (Gromova and Celis, 2006; Yan *et al.*, 2000)

4.6.2 Comparison of M13 infected and non-infected Top10F' cultures

In both non-infected and M13 infected Top10F' cultures, chromosomal DNA and protein was observed to accumulate as culture growth progressed and cell density increased, as predicted. (Figure 4.4 and Figure 4.7). Assuming a 4.6 Mbp *E. coli* genome has a mass of 4.9×10^{-15} g (Lawrence and Ochman, 1998), and an average of 4 genomes exist per cell (Akerlund *et al.*, 1995), then approximately 5×10^7 cells needed to be lysed to produce 1 µg of DNA. After 5 hours growth, the concentration of chromosomal DNA in the supernatant of non-infected culture was measured to be 0.24 µg ml^{-1}. In infected culture the concentration was 0.63 µg ml^{-1}. Therefore, in non-infected Top10F' culture the measured quantity of DNA represented less than 1 % of the final viable cell count, and in the equivalent M13 infected culture this represented 20

% of the final viable cell count. The proportion is greater for infected Top10F' cells because the culture density (OD_{600}) and viable cell counts were substantially lower than non-infected and the chromosomal DNA concentration was higher. The lower infected culture density was expected, since reduced *E. coli* growth rates upon infection by bacteriophage M13 has been reported (Bradley and Dewar, 1967; Salivar *et al.*, 1964). However it was shown that when normalised for optical density, the viability of infected *E. coli* cells was lower than non-infected cells after incubation times greater than two hours. It is apparent that M13 infection, while not generally lethal to *E. coli*, reduced the proportion of viable Top10F' cells and increased the release of chromosomal DNA (implying greater cell lysis). It has been reported that the infection of *E. coli* cells with filamentous bacteriophage causes damage to the cell membrane (Chen *et al.*, 2009). Defined increases in cell sensitivity to several chemical and physical stresses, such as exposure to SDS, osmotic shock and freeze-thawing have also been noted as a result of M13 infection (Roy and Mitra, 1970). Such cell membrane damage may explain the increased rate of cell lysis during normal culture growth.

In a similar pattern to that observed for DNA, after 5 hours of growth the total concentration of protein measured by Bradford assay was significantly higher in infected Top10F' culture (30.5 μg ml^{-1}) than non-infected Top10F' (20.6 μg ml^{-1}) (Figure 4.8). However, unlike the measured chromosomal DNA concentration, this pattern may not only be a result of M13 infection causing increased cell lysis: it must be taken into account that the Bradford assay also detected medium components. The lower OD_{600} value of the infected culture could have meant a higher concentration of medium components remained. The unused NB2 medium was measured to contain an average of 24 μg ml^{-1}. Since the change in concentration of medium components over time could not be determined alone (and thereby subtracted from the total protein reading) the Bradford assay was found to be suitable only for total protein comparison at the end of growth, not for tracking protein contaminant accumulation over time.

4.6.3   Comparison between *E. coli* Top10F', JM107 and W1485 culture

At the 50 ml scale, the optical density (OD_{600}) of M13 infected JM107 cells was 19 % lower than that of infected Top10F' cells at the cessation of growth. Conversely, the viable cell count of JM107 was 63 % higher than Top10F' (Figure 4.9 and Figure 4.10). This discrepancy in OD_{600} and cell count between strains is likely due to Top10F' being *recA*$^-$: the proportion of viable cells in a *recA*$^-$ culture is typically half that of a *recA*$^+$ one (Capaldo-Kimball and Barbour, 1971). In terms of cumulative contaminant release by the end of growth, the concentration of chromosomal DNA and protein in JM107 culture were found to be significantly less than the values in Top10F' culture. In Top10F' culture, the lower proportional viability of M13 infected cells relative to non-infected coincided with greater levels of DNA

and protein. It therefore followed that the lower viability levels of M13 infected Top10F' cells relative to JM107 also translated to a greater concentration of contaminants.

The growth of *E. coli* strain W1485 resulted in similar levels of protein contamination after 5 hours growth as Top10F', but from a culture with a 20 % greater OD_{600} value and only a 13% higher viable cell count. This suggested that on a unit OD_{600} basis, the proportion of viable cells in W1485 culture was lower than Top10F', although as a near wild-type strain, it may have been expected to be the most resilient. The growth dynamics of strain W1485 were noteworthy for other reasons too. Firstly, upon infection with bacteriophage M13 at the start of culture, the viable cell count decreased over the following two hours (Figure 4.10) even though OD_{600} value increased rapidly (Figure 4.9). It is unlikely that considerable cell death occurred here, since the quantity of free chromosomal DNA and protein did not spike by two hours growth (Figure 4.13 and Figure 4.16). Rather, they were consistent with Top10F' and JM107 accumulation profiles. OD_{600} increase due to greater average cell size can also be discounted: it has been reported that M13 infection does not change average cell size (Brown and Dowell, 1968). However, a similar pattern of viability decrease upon M13 infection coupled with a lack of measurable cell death has been previously noted (Salivar *et al.*, 1964). Here, it was surmised that the effect was a reaction of cells to the transfer from liquid culture to agar plate. W1485 may have been more susceptible to this effect than JM107 and Top10F', perhaps due to a different cell stress response. Alternatively, some form of extra-cellular component may have particularly contributed to the OD_{600} increase in W1485 culture.

A further W1485 growth characteristic of note was a possible second phase of growth between 7 and 9 hours incubation. The concentration of bacteriophage plateaued after five hours growth, in a fashion similar to Top10F' and JM107 cultures (Figure 4.11). However, unlike these two strains the concentration of bacteriophage subsequently increased such that after nine hours the titre was significantly higher. Over this period the concentration of viable W1485 cells and the OD_{600} value also increased. In practice, Top10F' and JM107 strains may also have exhibited this "biphasic" growth on the 50 ml scale but with the second phase sufficiently delayed such that hourly monitoring was already halted. It can be seen in Table 4.2 that all three cultures exhibited an increase in OD_{600} and viable cell count between the last timepoint of the growth curve and the 24 hour sample. However, no culture experienced a statistically significant rise in bacteriophage concentration over this time. Therefore, from the perspective of maximising bacteriophage yield it would still be appropriate to cease fermentation of Top10F' and JM107 culture at this scale after five hours. For W1485 culture, harvesting at 5 hours would return the same bacteriophage concentration as Top10F' and JM107 (4-4.5 x 10^{11} pfu ml^{-1}) whereas four further hours of culture would return 7.8 x 10^{11} pfu ml^{-1} (Section 4.3.1). A more marked biphasic growth pattern was later observed in the 2 L fermentation of Top10F' cells, cultured in

the richer fermentation medium (Figure 4.26), although this was not accompanied by an increase in bacteriophage titre and formed a single replicate. In theory, the growth of cells without the F-plasmid could explain this biphasic pattern, although it is unlikely since tetracycline selection was employed in the seed culture and the F-plasmid is known for its stability (Zielenkiewicz and Ceglowski, 2001).

Each *E. coli* strain provided benefits and weaknesses. Despite being *recA⁻* (and therefore actively dividing cells made up only 49 % of all cells (Capaldo *et al.*, 1974)), M13 infected Top10F' culture gave the same bacteriophage yield as JM107 after 5 hours. However, JM107 culture resulted in lower free chromosomal DNA and protein. W1485 culture resulted in the greatest bacteriophage yield after 9 hours incubation, but at the cost of the highest DNA and protein concentrations (Sections 4.3.2 and 4.3.4). The yield of bacteriophage must also be balanced with the quality of the product. Mutations to the *recA* (Top10F') gene are known to reduce recombination effects, which could offer an improvement in stability for M13 derivatives holding longer sequences of insert DNA (Yanisch-Perron *et al.*, 1985). Therefore, in product quality terms the strain Top10F' may be preferable, particularly since the effect of the *recA* mutation on the viability of the cultures appeared not to compromise the bacteriophage yield.

The nature of the F-plasmid within each strain must also be considered. The use of a conjugation-proficient F episome of the kind within W1485 has long been discouraged by NIH guidelines (Yanisch-Perron *et al.*, 1985). The F-plasmids within strains JM107 and Top10F' hold a mutation to the *tra* operon, thereby preventing conjugation whilst allowing for M13 infection (Achtman *et al.*, 1971; Yanisch-Perron *et al.*, 1985). An alternative to W1485 could be to transform the closely-related (F-) daughter strain MG1655 with a conjugation-deficient version of the F-plasmid.

4.6.4   Culture of an M13 infected Top10F' strain producing a recombinant nuclease

The *S. aureus* nuclease-producing pMMBompnucB vector was previously developed in our laboratory in response to the need for a cost-effective, non-bovine derived nuclease for the degradation of contaminating *E. coli* DNA in recombinant protein production (Cooke, 2003). This solution was applied to the issue of contaminating chromosomal DNA in M13-infected Top10F' culture (Section 4.4). Since the nuclease was targeted to the periplasmic space, interference with M13 assembly was therefore of concern: extrusion of bacteriophage particles from the *E. coli* cell occurs through gated channels traversing the inner and outer cell membranes (Russel, 1995). Culture was therefore conducted with and without nuclease production induced by IPTG. When nuclease production was not induced it was found that the growth characteristics of M13 infected Top10F'-pMMBompnucB cells closely matched those of

infected Top10F' cells without the plasmid (Figure 4.18). When induced, maximum bacteriophage titre was achieved an hour later, but was not significantly less than that achieved by non-induced culture. However, both culture OD_{600} and cell viability were consistently lower throughout growth (Figure 4.18 and Figure 4.19). The burden of nuclease production has been shown to reduce *E. coli* culture OD_{600} by up to 20 % in early-to-mid stage exponential growth (Cooke, 2003), although this discrepancy closed as growth progressed. Even so, it was thought that the burden of nuclease production coupled with M13 infection probably caused the relative decline in culture OD_{600} and cell viability. The one hour delay in achieving maximum bacteriophage concentration could be explained by either membrane-area interference or metabolic burden effects. Nevertheless, whether induced or not, sufficient nuclease was produced and released into the milieu to degrade free chromosomal DNA such that it was not visible by agarose gel electrophoresis. It has been reported that some basal level transcription from the *tac* operon, which controls nuclease production, occurs (Cooke *et al.*, 2003). This explains why degradation of supernatant chromosomal DNA occurred in non-induced Top10F' cultures too. In terms of protein concentration, the cost of induced nuclease production was a near 25 % rise in supernatant protein relative to Top10F' culture without the nuclease plasmid (Table 4.5).

4.6.5   Fermentation at the 2 L bioreactor scale

Fermentation of M13 infected Top10F' in a richer fermentation medium gave a four-fold greater bacteriophage yield than that obtained in NB2 (Section 4.5.2). At the end of growth, the OD_{600} of Top10F' culture in fermentation medium was double that in NB2. Therefore in this study the richer medium was not only associated with greater cell density but also bacteriophage concentration. These findings agree with those of Reddy and McKenney (1996), where shakeflask growth in a richer medium resulted in up to 60 % higher bacteriophage yields, but are counter to those of Grieco *et al.* (2009), where fermentation in a richer medium doubled cell mass but produced only one third of the filamentous bacteriophage. These seemingly conflicting results may be reconciled by the knowledge that production of bacteriophage from *E. coli* is a more complicated function than just quantity of carbon source. For example bacteriophage yield has been negatively correlated with cell growth rate during culture (Salivar *et al.*, 1964). Since the fermentation medium used in this study was of different composition to NB2, it is possible that several factors were favourably altered.

An attempt was made to increase overall fermentation bacteriophage yield by delaying bacteriophage infection to 3 hours post *E. coli* inoculation (Section 4.5.3). It was postulated that this action would allow the growth of Top10F' to a higher density, which upon infection would result in a greater bacteriophage yield. However, this was not the case in this study (Figure 4.28). This could have been due to bacteriophage infection occurring too late in the culture

growth cycle, where a proportion of the culture population may have reached stationary phase before being infected. Furthermore, identical quantities of M13 were added to infect cultures at 0 and 3 hours post *E. coli* inoculation, resulting in a lower effective MOI when infection occurred at the latter time. As will be demonstrated, a lower MOI requires a longer culture time to achieve maximum bacteriophage yield (Section 5.3.1). Further work to repeat this experiment, and to investigate earlier infection times would be of great interest.

In terms of contamination levels, the increased cell and bacteriophage growth in the fermentation medium resulted in elevated DNA and protein concentrations. The concentration of supernatant DNA measured at the point of harvest was 11-fold greater than that at the 50 ml scale, for a 4.4-fold increase in bacteriophage titre and 4.1-fold rise in OD_{600} (Sections 4.2 and 4.5). Similarly, the concentration of supernatant protein at the point of harvest was 5.5-fold greater at the 1.5 litre scale than at the 50 ml scale. However, the 1.5 litre fermentation of Top10F' cells producing the nuclease enzyme resulted in a DNA-free culture (Figure 4.33) of maximum bacteriophage concentration (1.6×10^{12} pfu ml^{-1}) virtually identical to that of nuclease-free cells (Section 4.5.4). Further, at this scale the concentration of supernatant protein was not increased and was indeed measured to be lower than Top10F' culture without the nuclease plasmid (Section 4.5.5). However, in this study it took twice as long to reach the maximum bacteriophage concentration, thereby requiring a total fermentation time of eight hours. It is noteworthy at this scale that whilst OD_{600} values were similar, the viability of M13 infected Top10F' cells expressing the nuclease enzyme was substantially decreased (up to 100-fold) relative to Top10F' cells which did not (Figures 4.30 and 4.31). The poor correlation between cell count and OD_{600} value has been noted repeatedly throughout this chapter (Figures 4.1 and 4.2, Figures 4.9 and 4.10, Figures 4.18 and 4.19) and commented on earlier in this discussion. Further fermentations are necessary to confirm the findings at this scale, and to examine the effects of nuclease expression on bacteriophage yield in depth.

Overall, the utilization of an *E. coli* strain producing a nuclease enzyme may provide a useful and potentially cost effective option to remove contaminating chromosomal DNA. More generally, purification would be achieved by the exploitation of physicochemical differences between the bacteriophage and contaminants. Methods such as the selective adsorption of chromosomal DNA to nitrocellulose membranes (Levy *et al.*, 2000a), selective precipitation processes (Juckes, 1971; Lander *et al.*, 2002; Wenzig *et al.*, 1993) or chromatographic steps (Atkinson *et al.*, 1987) each employ different bases of separation to achieve the desired purification.

When *E. coli* cells were infected at the start of fermentation, the resulting analytical profiles showed distinct features coinciding with the cessation of bacteriophage production (Figure

4.26). From a bioprocessing standpoint, these would provide useful indicators that harvesting could proceed since bacteriophage concentration cannot be measured in an on-line fashion. In particular, the end of bacteriophage production usefully correlated with a plateau in OD_{600} value and a levelling in the OUR and CER. All three of these measurements can be made on-line or at-line to the bioreactor. Since similar trends between cell growth and bacteriophage production were observed throughout this chapter and in the literature (Brown and Dowell, 1968; Grieco *et al.*, 2009; Salivar *et al.*, 1964), it seems certain that these methods provide a reproducible way to track *filamentous* bacteriophage production. In the literature a similar approach has been taken to explicitly track the completion of *lytic* bacteriophage production. Here, CER or OD_{600} have been used as a guide to bacterial cell density which substantially decreases upon bacteriophage release (and therefore cell lysis) at the end of production (Sargeant, 1970; Sargeant *et al.*, 1968).

4.6.6   Concluding remarks

In summary, this chapter investigated aspects of the fermentation production of bacteriophage M13. The composition of the post-fermentation process fluid was explored and it was found that significant levels of chromosomal DNA and protein were released into the fermentation medium during growth. Contaminant concentration was found to be a function of bacteriophage infection, *E. coli* strain and culture time. A novel method for the removal of supernatant DNA was successfully tested by the culture of *E. coli* harbouring a nuclease-producing expression cassette. Small-scale experimentation (50 ml) showed that the yield of bacteriophage M13 was not significantly compromised by growth in $recA^-$ cells (Top10F') relative to a $recA^+$ strain (JM107). However, bacteriophage yield was 4-fold improved by host cell growth in a richer fermentation medium. Therefore in light of the results of this chapter, bacteriophage M13 growth in strain Top10F' harbouring the nuclease-producing plasmid in fermentation medium offered the best combination of bacteriophage yield, quality and purity.

5 The Effect of Hydrodynamic Shear on *E. coli* Cell Integrity

5.1 Introduction

The multiplicity of infection (MOI) is defined as the inoculating ratio of infective bacteriophage particles to viable *E. coli* cells at the start of propagation. A previous small-scale bacteriophage propagation study suggested that the final yield of bacteriophage M13 was independent of MOIs in the range of 10^{-6} to 10^{-4} (Reddy and McKenney, 1996). However, no detail was given concerning the overall fermentation time required to achieve maximum bacteriophage yield. It was hypothesised that lower MOIs would require a longer fermentation time, since further bacteriophage replication would be required to achieve total *E. coli* infection. As will be demonstrated, this was shown to be the case (Section 5.2).

It was shown in Chapter 4 that the level of cellular debris in the culture supernatant increased concomitantly with *E. coli* growth. It might therefore be expected that the longer growth times and greater cell counts associated with lower MOI cultures would result in higher levels of cellular debris in the supernatant. If this translated to the large-scale, this could have a detrimental effect on further downstream processing. One aim of this chapter, therefore, was to examine the level of supernatant contamination at the harvest point as a function of culture MOI.

Since bacteriophage M13 is an extracellular product it would be useful to process the cells without disruption and thereby avoid unnecessary contamination of the supernatant with cellular debris. The handling of cells in the early stages of a purification sequence therefore requires consideration to prevent this. To meet this goal, understanding of the effect of shear stresses on *E. coli* cells is important. In bacteriophage M13 processing, the cells are likely to experience shear stresses of varying levels and times, principally in the fermentation, pumping and centrifugation stages. Existing literature in the area has demonstrated the disruption of *E. coli* cells by homogenisation (Keshavarz-Moore *et al.*, 1990), capillary shear (Lange *et al.*, 2001) and jets (Chan *et al.*, 2006). However, it has been shown by Hewitt *et al.* (1998) that under typical fermentation conditions (where shear forces are less) the shear effects on *E. coli* strain W3110 were minimal.

The primary aim of this study, therefore, was to determine the response of *E. coli* cultures to high energy turbulent shear conditions. A USD rotating disk shear device was again used, and it was hypothesised that an older, more dense culture resulting from a low MOI would respond differently to a high MOI culture (which would be harvested sooner). For example, if similar fractions of cells are damaged in both low and high MOI cultures, it may be expected that the culture with a higher cell density would therefore result in greater supernatant contamination

with cellular debris. The implications for the large-scale processing of host *E. coli* cells were subsequently assessed.

It was also shown in Chapter 4 that the level of supernatant DNA and protein contamination in an M13 infected culture was higher than that in a non-infected culture of equivalent age, even though the optical density (OD_{600}) was lower. This suggested that M13 infection had a detrimental effect on *E. coli* viability. Moreover, it is known that the infection of *E. coli* cells with filamentous bacteriophage causes damage to the cell membrane (Chen *et al.*, 2009) resulting in a defined increase in sensitivity to several chemical and physical stresses, such as exposure to SDS, osmotic shock and freeze-thawing (Roy and Mitra, 1970). A secondary aim of this chapter, therefore, was to investigate whether this translated into a greater cell susceptibility to turbulent shear, relative to non-infected cells. Of course, in a bacteriophage M13 bioprocess the *E. coli* cells will be infected with M13, but it was considered important to run a parallel series of non-infected *E. coli* cultures to assist in interpreting the infected cell data. Furthermore, if infected cells are proven to be less shear resistant than infected, it lends further proof to the findings of Chapter 4 and elsewhere.

5.2   The Effect of MOI on Bacteriophage M13 Propagation in *E. coli*

A detailed bacteriophage M13 growth study was conducted in our laboratory under the guidance of Dr. Emma Stanley (publication in preparation). As part of this work, MOIs of 1×10^{-5}, 1×10^{-2} and 1×10^{1} were investigated for their effect on bacteriophage M13 growth characteristics at the two-litre shakeflask scale.

Starter 400 ml NB2 cultures of *E. coli* Top10F' were prepared as described in the Materials and Methods (Section 2.3.2), and grown overnight in two-litre baffled shakeflasks at 37 °C with 5 μg ml^{-1} tetracycline antibiotic selection. *E. coli* cells were previously enumerated from identically prepared overnight culture as described in Section 2.5.1, to allow for the subsequent calculation of MOI. Triplicate 400 ml NB2 filled two-litre baffled shake flask were pre-warmed to 37 °C and inoculated with 40 ml of overnight starter culture (measured to contain 4×10^{11} cfu). Cultures were then inoculated with 2 ml of appropriately diluted (by 10 mM Tris, pH 7.5 at 25 °C) caesium chloride purified bacteriophage M13 to give the desired MOI (Table 5.1). Cultures were then incubated at 37 °C (with shaking at 200 rpm). Growth was monitored by absorbance readings at 600 nm at hourly intervals (OD_{600}), plus an extra sample at 30 minutes. Samples were suitably diluted with fresh media and absorbances measured in triplicate. Bacteriophage were enumerated as described in Section 2.5.2. The experiment was conducted for each of the MOIs listed in Table 5.1.

Table 5.1 The tested multiplicities of infections (MOIs) together with the corresponding concentrations of two millilitre M13 inocula.

Multiplicity of infection (MOI)	Concentration of M13 inoculum required
5×10^1	1×10^{12} pfu ml^{-1}
5×10^{-2}	1×10^9 pfu ml^{-1}
5×10^{-5}	1×10^6 pfu ml^{-1}

As was hypothesised, it was shown that the lower the MOI, the longer it took to reach the maximum bacteriophage titre (Figure 5.1). At an MOI of 1×10^1, the maximum bacteriophage yield was reached after two hours growth. At an MOI of 1×10^{-2} it took three hours to reach the maximum bacteriophage yield, and at an MOI 1×10^{-5} it took five hours. Correspondingly, it was found that lower MOIs resulted in cultures of a greater OD$_{600}$ value at the point maximum bacteriophage yield (Figure 5.2).
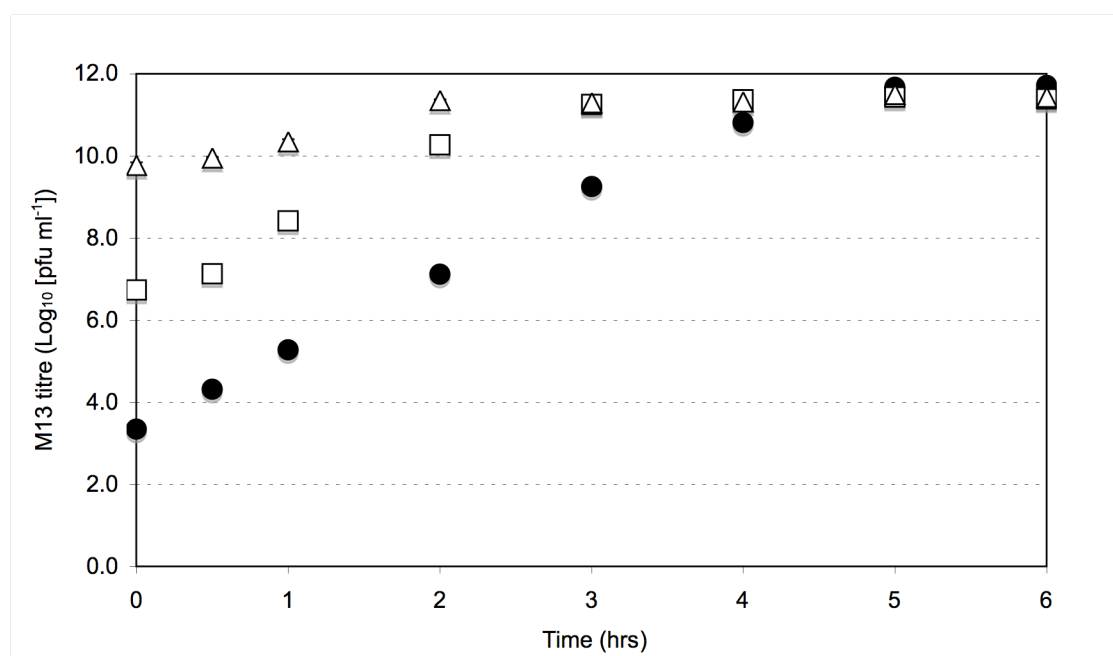
Figure 5.1 Increase of bacteriophage M13 titre in cultures with initial multiplicity of infections (MOIs) of 5×10^1 ($\triangle$), 5×10^{-2} ($\square$) and 5×10^{-5} ($\bullet$) as a function of time. The maximum yields of bacteriophage M13 were achieved after 2 hours (5×10^1), 3 hours (5×10^{-2}) and 5 hours (5×10^{-5}). Error bars represent the standard error, N=3.
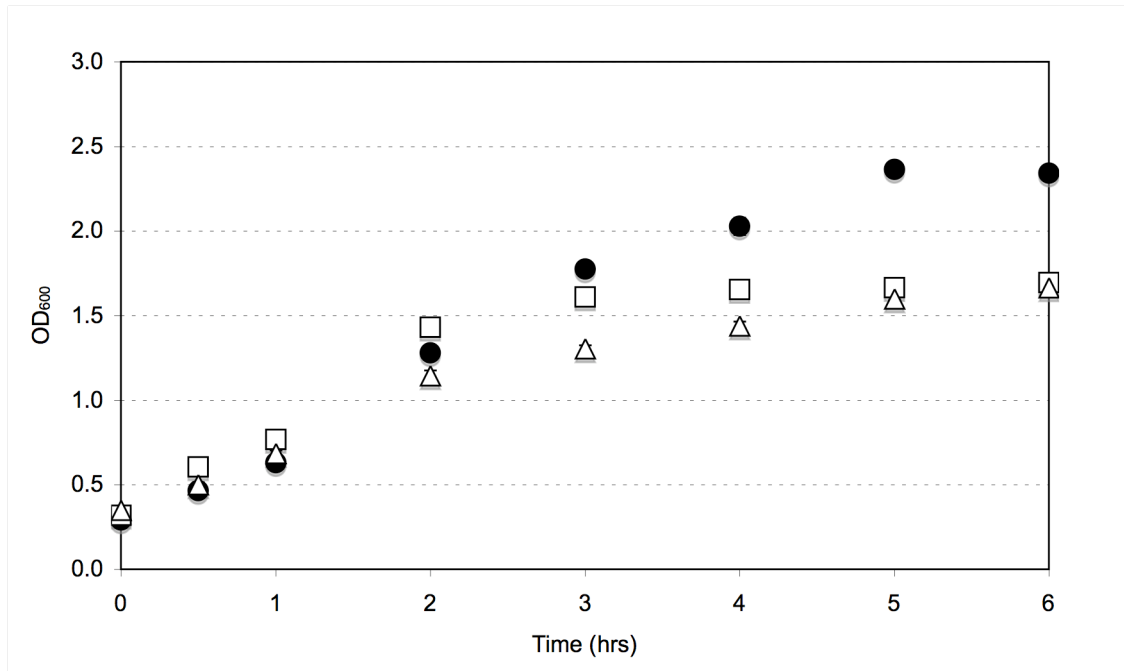
Figure 5.2 Increase of OD_{600} in cultures with initial multiplicity of infections (MOIs) of 5×10^1 ($\triangle$), 5×10^{-2} ($\square$) and 5×10^{-5} ($\bullet$) as a function of time. The maximum yields of bacteriophage M13 were achieved after 2 hours (5×10^1), 3 hours (5×10^{-2}) and 5 hours (5×10^{-5}). Error bars represent the standard error, N=3.

5.3   Studying The Effect of Hydrodynamic Shear on *E. coli*

5.3.1   M13 infected and non-infected *E. coli* culture

As described in the Introduction to this chapter, the primary aim of this study was to determine the response of *E. coli* cultures to high energy turbulent shear conditions. The reasoning for this experimentation was two-fold. Firstly, since M13 infection is known to cause damage to the cell membrane (Chen *et al.,* 2009), it was of interest whether this would translate to a greater susceptibility to turbulent shear. Secondly, it was noted in Section 5.2 that a lower MOI resulted in an older and more dense culture at harvest. Would this result in an altered susceptibility to turbulent shear? If differences are observed, then consideration would need to be given as to whether contamination of the supernatant by cellular debris could be reduced. The potential implications for large-scale processing would then be discussed.

The growth data gained in Section 5.2 was used to prepare *E. coli* cultures of three different ages for investigation with shear forces. Fresh triplicate two-litre shakeflasks were prepared and inoculated exactly as described in Section 5.2. Cultures inoculated with an MOI of 5×10^{1} were therefore harvested for shear studies after 2 hours growth. Cultures inoculated with an MOI of 5×10^{-2} were harvested after 3 hours growth, and cultures with an MOI of 5×10^{-5} after 5 hours. The initial (0 hr) OD_{600} of every culture was measured to be in the range OD_{600} 0.48- 0.62.

Triplicate non-infected *E. coli* Top10F' cultures were also prepared identically to that described in Section 5.2, except that no bacteriophage were added. These comparison cultures were harvested at the same times as the M13 infected ones. Therefore cultures were grown for 2, 3 and 5 hour durations.

In Table 5.2 the average culture OD_{600} readings and bacteriophage titres at the harvest points in this study are tabulated. The OD_{600} values measured for non-infected cultures were higher at the harvest times as compared with M13 infected cultures. This is expected since *E. coli* cells infected with bacteriophage M13 display a reduced rate of growth (Salivar *et al.*, 1964).

Table 5.2 The OD_{600} and M13 titres achieved in infected and non-infected cultures by the harvest points in this study.

| MOI | Harvest time (hrs) | M13 infected cultures | | Non-infected cultures |
		OD_{600}	M13 titre x 10^{11} (pfu ml^{-1})	OD_{600}
5×10^1	2	1.2	2.2	1.5
5×10^{-2}	3	1.7	2.7	1.9
5×10^{-5}	5	2.3	2.2	2.8

5.3.2   USD rotating disk shear device operation

At the appropriate harvest time, cultures were immediately removed from the 37 °C incubator and placed in an ice bath to arrest growth for at least 10 minutes. A 20 ml sample from each culture was taken for shearing within the rotating disk shear device. Shearing was conducted as described in the Material and Methods (Section 2.12.2) with a disk rotation speed of 533 rps. This was to mimic the feed-zone conditions of a production-scale multi-chamber bowl continuous centrifuge, identified as a production-scale step imposing one of the greatest energy dissipation rates on the process fluid (Boychyn *et al.*, 2004). A 20 ml non-sheared control was incubated at room temperature (25 °C) and run concurrently. Samples (500 μl) were taken from both sheared and non-sheared runs at 0, 2, 5 and 10 minutes and incubated on ice until needed. Additional triplicate non-sheared controls were sampled at the zero timepoint. Cell and bacteriophage counts in each sample were determined by the surface droplet technique (Section 2.5.2). The remainder of every sample was then centrifuged at 17 000 x g for 3 minutes to pellet the cells. Supernatants were carefully decanted and stored at -20 °C. Each MOI was tested three times. The level of supernatant contamination was assessed in terms of the quantity of chromosomal DNA present (Chapter 4); agarose gels were prepared and quantified as described in the Material and Methods (Sections 2.7.2 and 2.7.4). The shearing experimentation was then repeated for the non-infected cultures harvested at the same 2, 3 and 5 hour timepoints indicated in Table 5.2.

5.3.3 The effect of shear on *E. coli* cell viability

The viability of cells in all non-sheared runs remained stable over time, whether infected with M13 or not (Figure 5.3). Indeed, there were no significant drops in viability over the course of the experiments ($P>0.05$, Dunnett). This gave confidence that observed drops in viability in sheared samples would be due to the effects of shear.
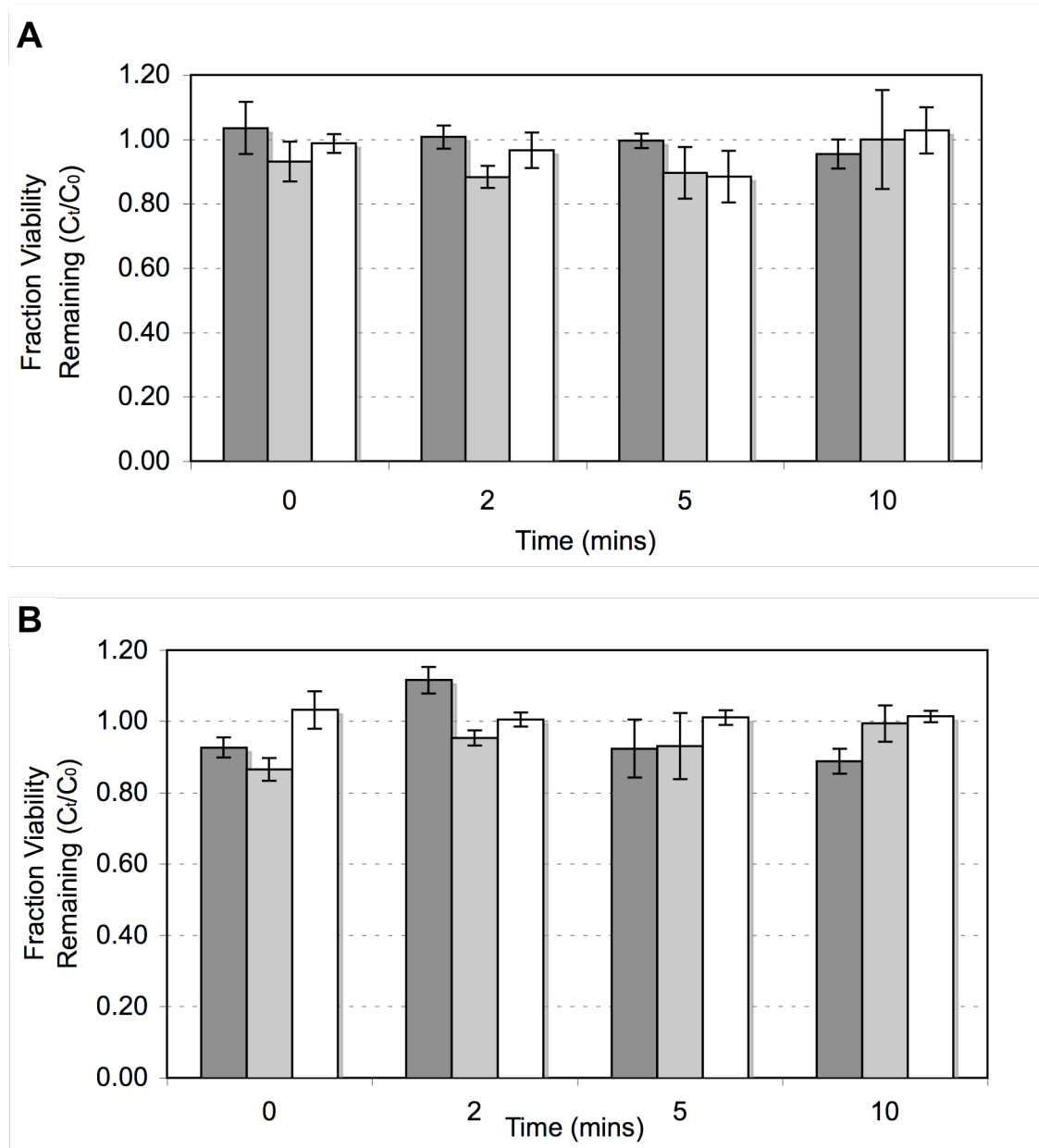
Figure 5.3 Fraction of viable *E. coli* Top10F' remaining in non-sheared controls as a function of time. Graph (A): M13 infected cells, MOI 5×10^{1} (■), 5×10^{-2} (■) and 5×10^{-5} (□). Graph (B): non-infected cells, 2 hours (■), 3 hours (■) and 5 hours (□) growth. Viability was determined by the surface-droplet technique (see Materials and Methods). Error bars represent the standard error of the mean fractions, N=3.

Prior to shearing, the average viable cell counts in M13-infected cultures were 9.2×10^7 pfu ml^{-1}, 7.3×10^8 pfu ml^{-1} and 1.1×10^9 pfu ml^{-1} for the MOIs of 5×10^1, 5×10^{-2} and 5×10^{-5} respectively. The resulting decay profiles are shown in Figure 5.4, where remaining viability was expressed as a fraction of the viability of the triplicate non-sheared controls. The subjection to shear at 533 rps within the shear device resulted in fractional viability drops in all three cultures, to 0.60 (MOI 5×10^1), 0.71 (MOI 5×10^{-2}) and 0.77 (MOI 5×10^{-5}) after 10 minutes. These drops were all significantly different from their respective non- sheared controls ($P=0.001$, 0.010 and 0.032 respectively, t-test), but as fractional drops were not significantly different from one another ($P>0.05$, Tukey). It could not therefore be concluded that MOI had an effect on the overall viability decline.
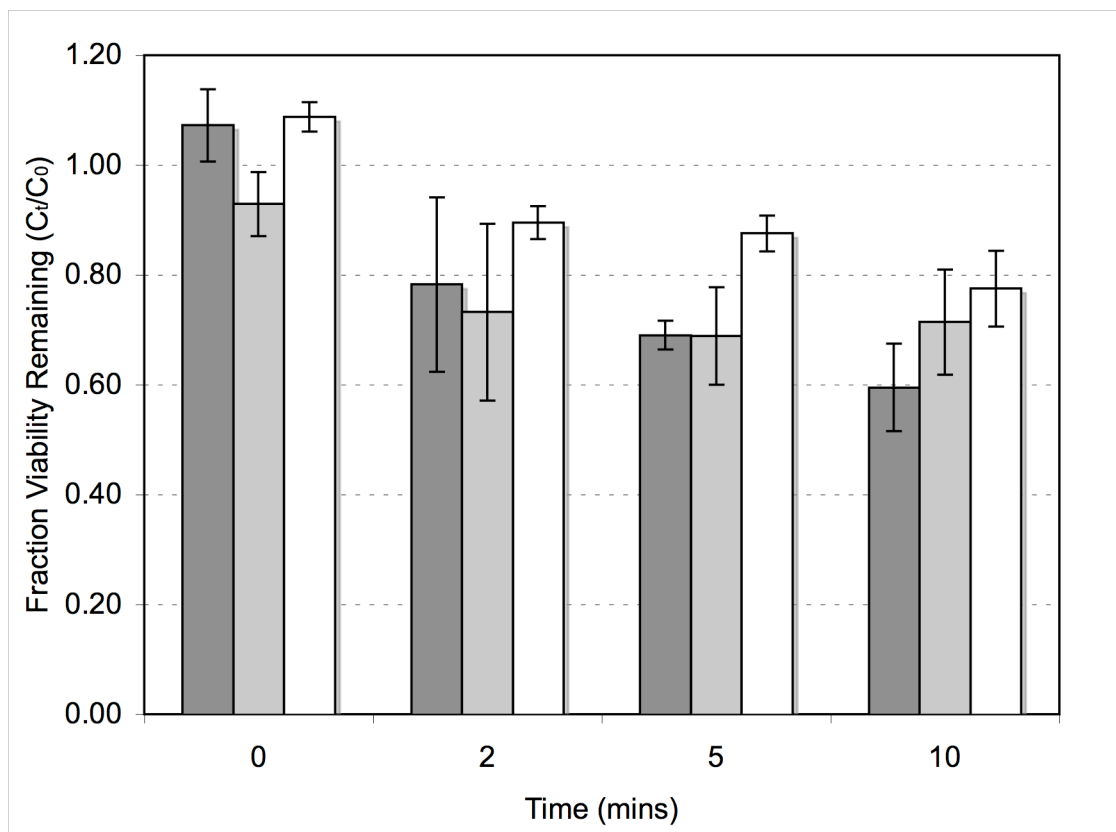
Figure 5.4 Fraction of viable *E. coli* Top10F' remaining at disk speed 533 rps for culture infected with MOI 5×10^1 (■), 5×10^{-2} (▨) and 5×10^{-5} (□) as a function of time. Viability was determined by the surface-droplet technique (see Materials and Methods). Error bars represent the standard error of the mean fractions, N=3.

The decay profiles of non-infected *E. coli* cultures are shown in Figure 5.5, also expressed as fractional viabilities relative to the triplicate non-sheared controls. Prior to shearing, the viable cell counts were 9.6×10^8 pfu ml^{-1} (2 hours incubation), 1.9×10^9 pfu ml^{-1} (3 hours incubation) and 2.7×10^9 pfu ml^{-1} (5 hours incubation). The subjection to shear at 533 rps within the shear

device resulted in smaller fractional viability drops in all three cultures relative to the infected cultures. After 10 minutes, the viability of the 2 hour culture (equivalent to MOI 5×10^{1}) had declined to 0.69, that of the 3 hour culture (equivalent to MOI 5×10^{-2}) to 0.93 but the viability of the 5 hour culture (equivalent to MOI 5×10^{-5}) remained at 1.02. The drop in viability in the 2 hour culture alone was significantly different from its non- sheared controls over this time ($P=0.004$, t-test). This was also significantly different from the 3 hour and 5 hour culture cell viabilities at the same 10 minute timepoint ($P<0.01$ and $P<0.001$, Tukey), which were not significantly different from one another ($P>0.05$, Tukey).
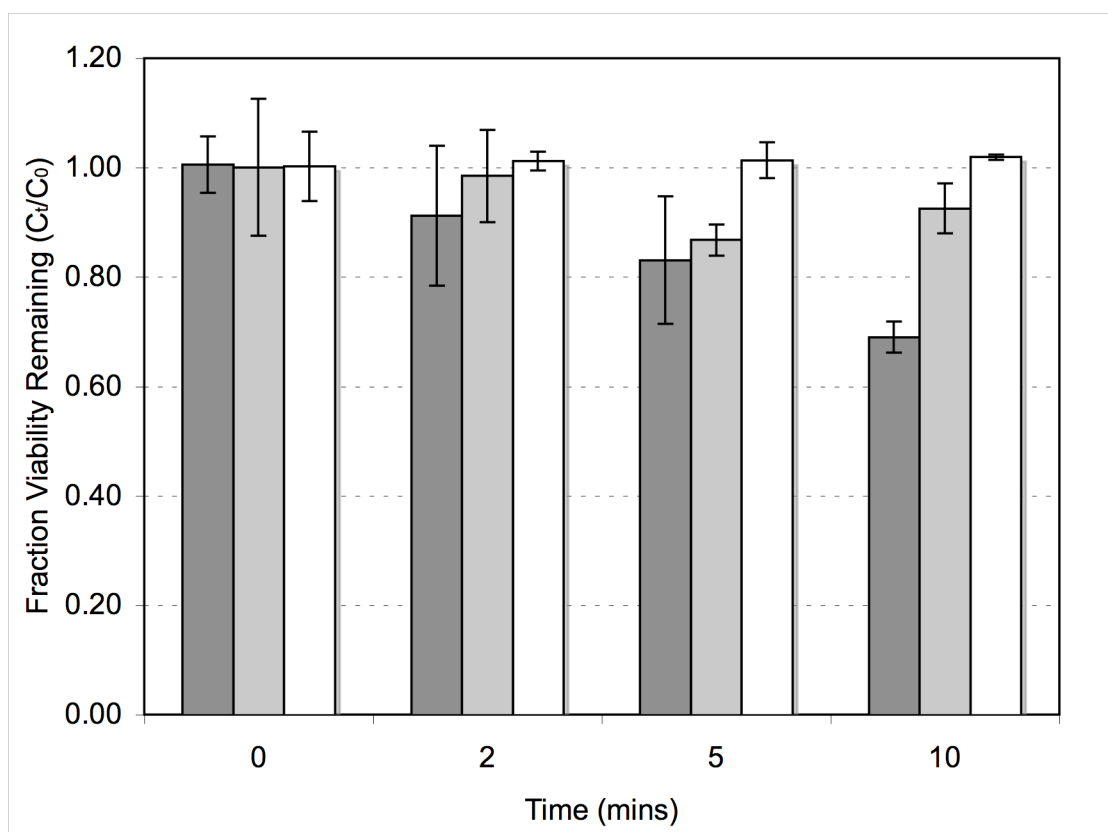
Figure 5.5 Fraction of viable *E. coli* Top10F' remaining at disk speed 533 rps for culture of age 2 hours (■), 3 hours (▨) and 5 hours (□) as a function of time. Viability was determined by the surface-droplet technique (see Materials and Methods). Error bars represent the standard error of the mean fractions, N=3.

Since the OD_{600} of infected and non-infected cultures of the same age differed, it was thought that a plot of fractional cell viability after 10 minutes shearing versus OD_{600} may help delineate the potential effects of M13 infection and culture density (Figure 5.6). For infected cell cultures, regression analysis indicated that the linear relationship between OD_{600} and cell viability was not significantly different from zero ($R^2=0.94$, $P=0.15$). Therefore OD_{600} did not affect shear resistance, which was expected since the cell viabilities had been shown to not be significantly

different from one another after 10 minutes shearing (Figure 5.4). For non-infected cells the increase in fractional viability with OD_{600} was not well described by a linear relationship (R^2=0.81, P=0.28). Instead, the trend appeared more of a "step-change" increase in fractional viability, where the viability of the more optically dense 3 and 5 hour cultures appeared virtually unchanged by shearing, whereas the 2 hour culture showed a 30 % fractional loss of viability.
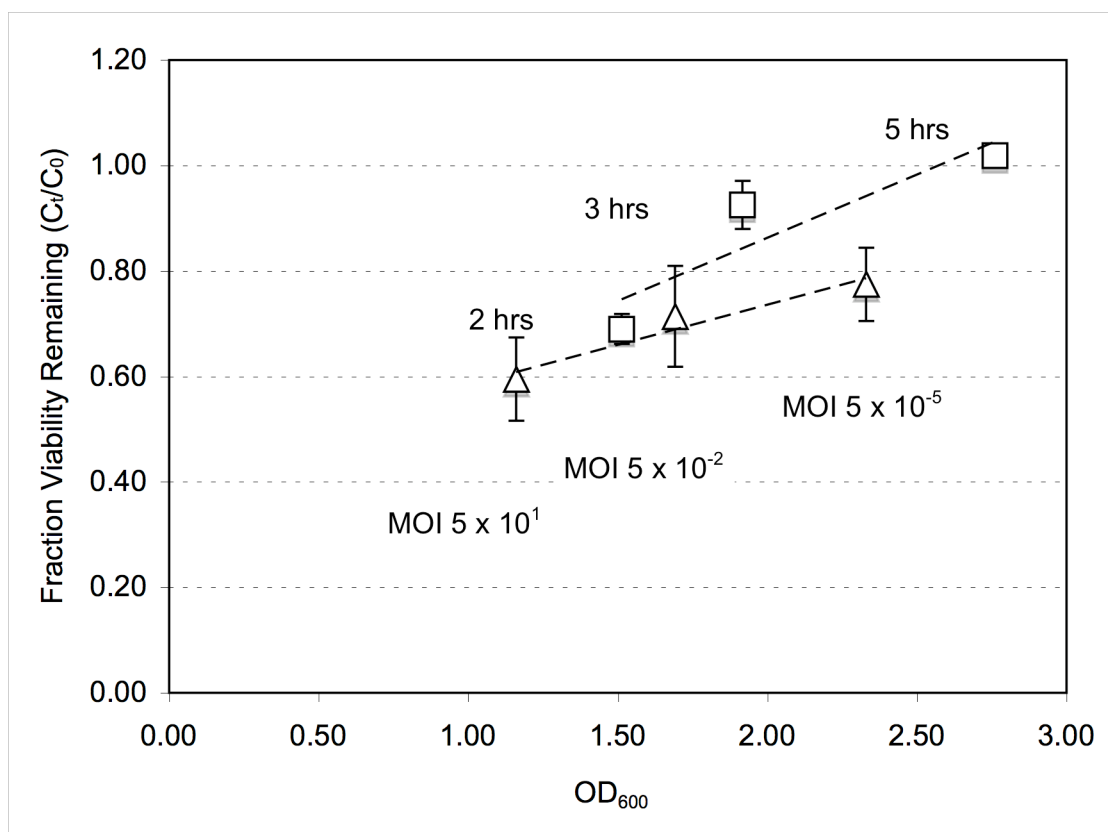
Figure 5.6 Fraction of viable *E. coli* Top10F' remaining after 10 minutes at disk speed 533 rps when infected ($\triangle$) and non-infected ($\square$) as a function of culture OD_{600}. Viability was determined by the surface-droplet technique (see Materials and Methods). R^2 values for linear trends are 0.94 (infected) and 0.81 (non-infected). Error bars represent the standard error of the mean fractions, N=3.

Since OD_{600} did not have an effect on the fractional viability of infected cells, it was therefore considered appropriate to compare the fractional viabilities of infected and non-infected cultures at the same harvest time, even though their OD_{600} values differed slightly. After 10 minutes shearing time, the difference in fractional viability between infected (MOI 5×10^1) and non-infected cultures harvested at 2 hours was not significant (P=0.32, t-test), nor at 3 hours/ MOI 5×10^{-2} (P=0.12, t-test). However, the differences were significant at 5 hours/ MOI 5×10^{-5} (P=0.025, t-test).

5.3.4   Quantification of DNA release as a measure of cell breakage

Sheared, non-sheared and control culture supernatants were loaded onto agarose gels to observe the levels of released chromosomal DNA. Figure 5.7, Figure 5.8 and Figure 5.9 show gels run for the experiments with MOIs 5 x 10^1, 5 x 10^{-2} and 5 x 10^{-5} respectively. For non-infected cultures, Figure 5.10, Figure 5.11 and Figure 5.12 show the gels run for the experiments harvested at 2, 3 and 5 hours respectively. A gel was run for each experimental repeat, that is, three gels for each MOI/ harvest time.

In all cases it was found that the subjection of culture to shear reduced the size of the chromosomal DNA in the supernatant from approximately 20 kb to a smear between 1 and 6 kb (Figure 5.7- Figure 5.12). The quantity of DNA in the supernatant increased as shearing progressed, suggesting that release of DNA from cells was occurring. As might be expected, the amount of smaller DNA fragments also increased as shearing progressed. Meanwhile, the quantity of DNA in the non-sheared samples remained stable over time.
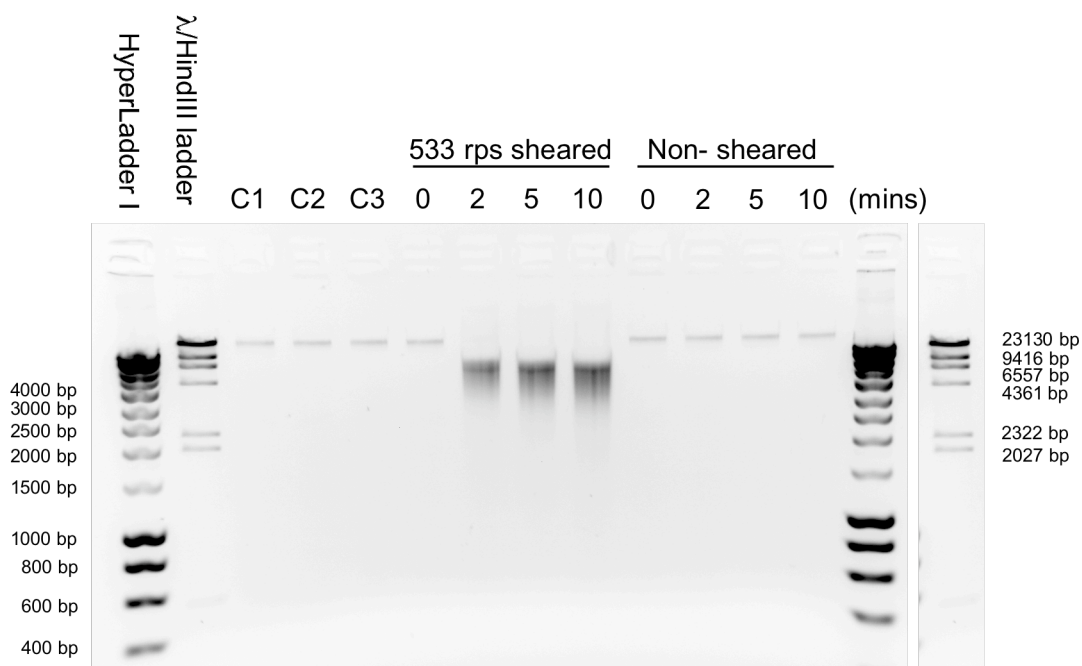
Figure 5.7 Agarose gel indicating the quantity of DNA in the culture supernatant. This culture was inoculated with bacteriophage M13 to an MOI of 5 x 10^1. The triplicate non-sheared controls are labelled C1, C2 and C3. Shearing at 533 rps caused an increase in the amount of DNA in the supernatant.
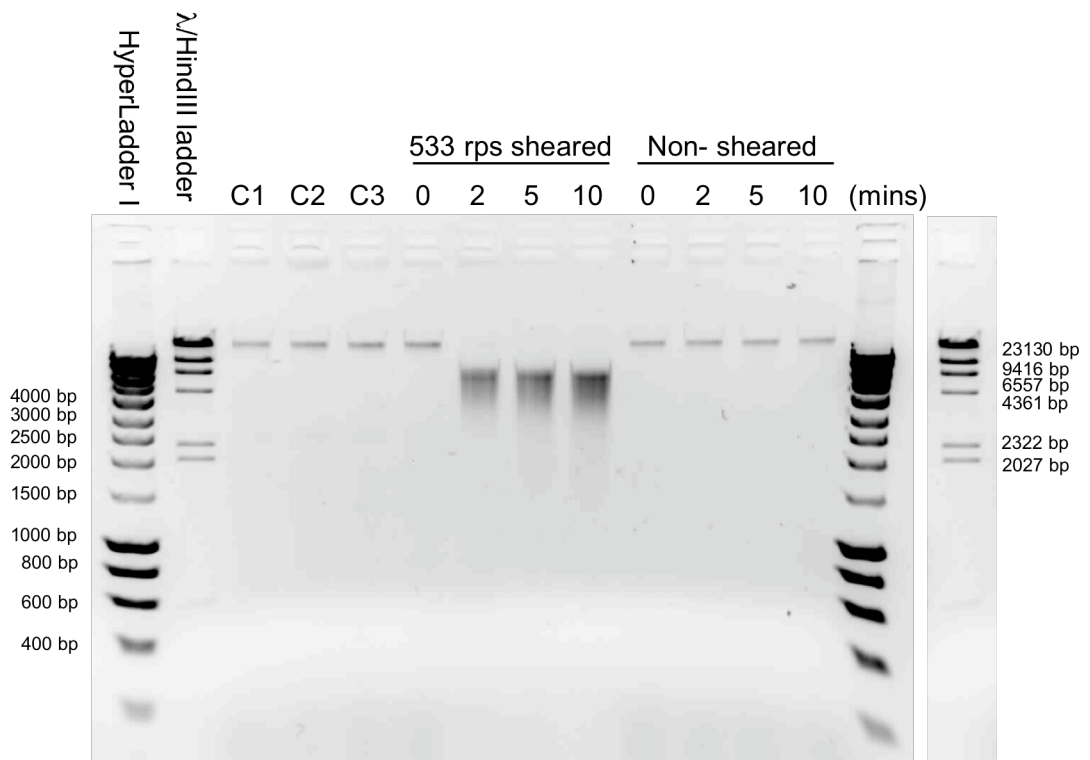
Figure 5.8 Agarose gel indicating the quantity of DNA in the culture supernatant, similar to Figure 5.7. This culture was inoculated with bacteriophage M13 to an MOI of 5×10^{-2}.
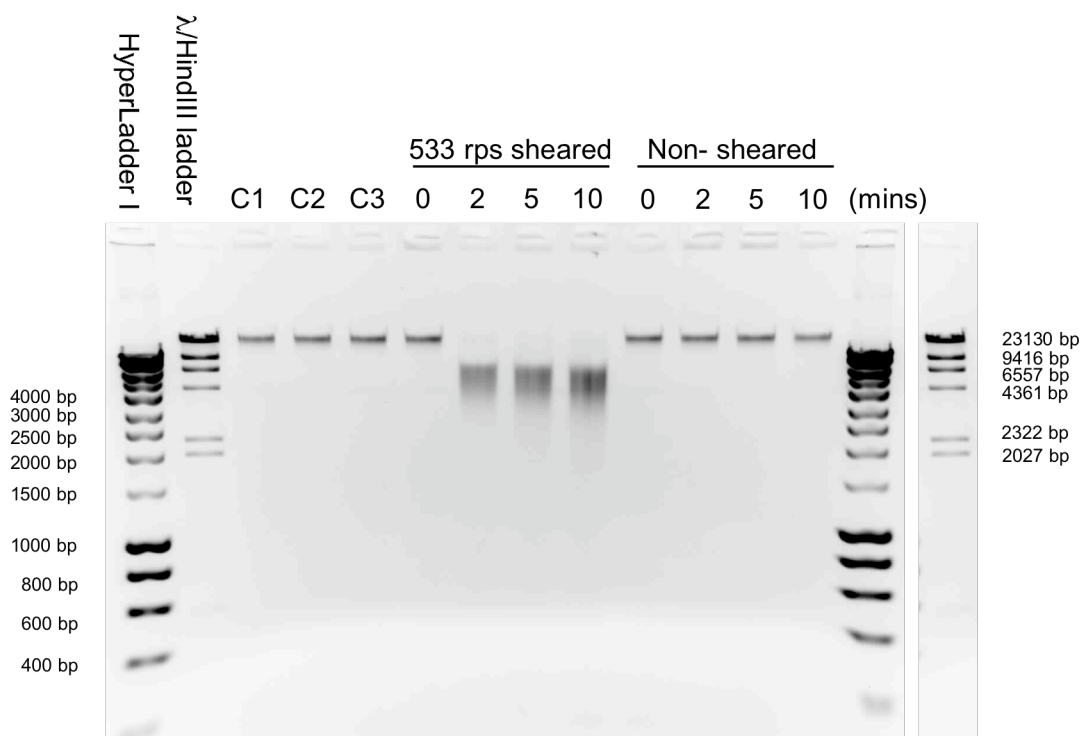
Figure 5.9 Agarose gel indicating the quantity of DNA in the culture supernatant, similar to Figure 5.7. This culture was inoculated with bacteriophage M13 to an MOI of 5×10^{-5}.
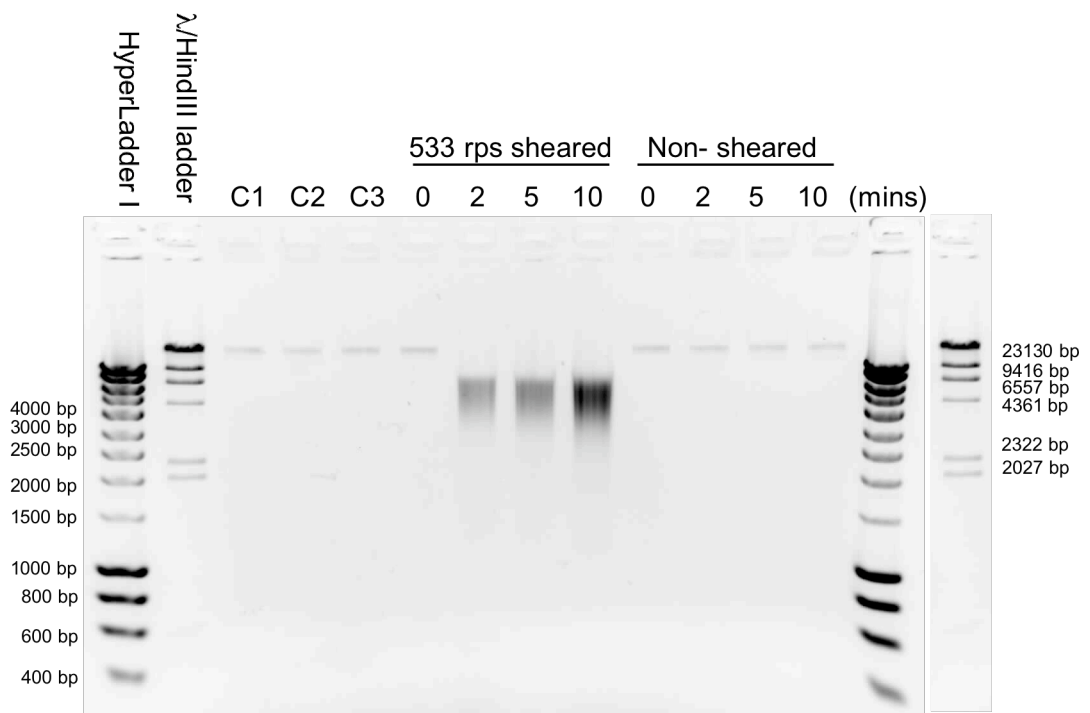
Figure 5.10 Agarose gel indicating the quantity of DNA in the culture supernatant. This non-infected culture was harvested after 2 hours. The triplicate non-sheared controls are labelled C1, C2 and C3. Shearing at 533 rps caused an increase in the amount of DNA in the supernatant.
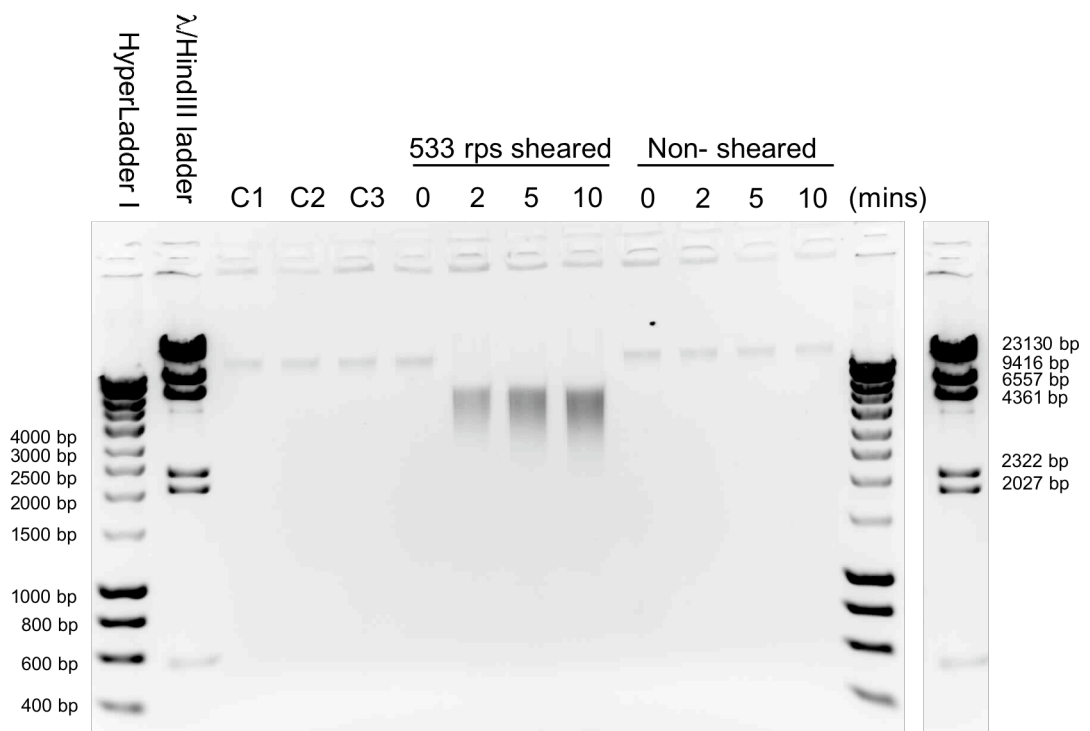
Figure 5.11 Agarose gel indicating the quantity of DNA in the culture supernatant, similar to Figure 5.10. This non-infected culture was harvested after 3 hours.
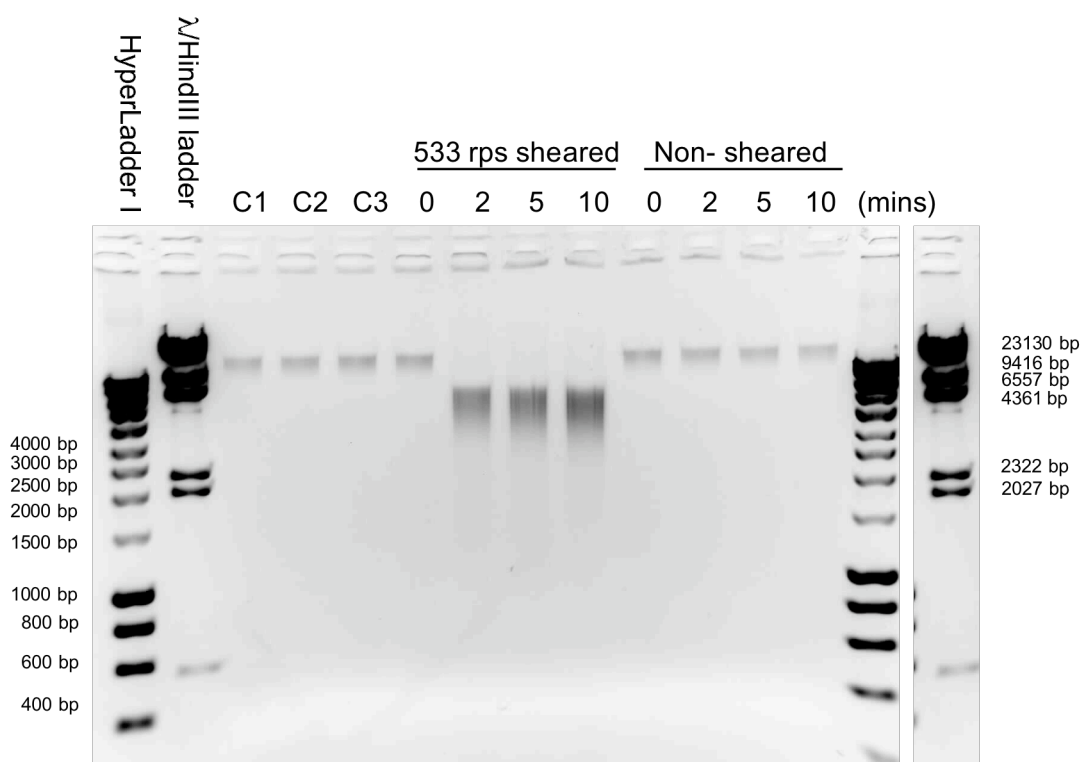
Figure 5.12 Agarose gel indicating the quantity of DNA in the culture supernatant, similar to Figure 5.10. This non-infected culture was harvested after 5 hours.

The absolute amount of DNA in the supernatants was determined by the densitometric quantification of band intensities in the agarose gels (Section 2.7.4) relative to the Bioline HyperLadder 1. The standard curves generated by the HyperLadders displayed strong linear relationships between intensities and DNA quantities ($R^2 > 0.96$ in all cases, data not shown).

Prior to shearing, the quantity of DNA in the supernatants of infected and non-infected cultures was similar after 2 hours growth (MOI 5×10^1), but diverged as growth continued. At the 3 hour (MOI 5×10^{-2}) and 5 hour (MOI 5×10^{-5}) harvest times the quantity of DNA in non-infected cultures was significantly less ($P<0.001$, t-test). (Table 5.3 and Table 5.4). However, on a per OD_{600} unit basis, the amount of DNA in non-infected cultures was substantially less in all cases (Table 5.5). This trend was consistent with the findings of Chapter 4, where it was noted that relative to the culture OD_{600}, M13-infected cultures result in more heavily contaminated supernatants at the same timepoints than those that are not.

In M13 infected cultures, it was observed that the quantity of DNA in the supernatant appeared dependent on the MOI used (Table 5.3). That is, the smaller the MOI the greater the concentration of DNA. This pattern corresponded with the greater optical density readings for

cultures grown with a lower MOI in Table 5.2. Moreover, the measured quantities of DNA were all found to be significantly different from one another (P<0.01, Tukey).

Table 5.3 DNA quantity in M13 infected culture supernatants, measured from agarose gels. The Control sample represented an average of the triplicate non-sheared controls. Culture was sheared at 533 rps and samples taken at 0, 2, 5 and 10 minutes. Uncertainties represent the standard error, N=3.

Sample	Quantity of DNA ($\mu g\ ml^{-1}$)		
	MOI 5×10^{1}	MOI 5×10^{-2}	MOI 5×10^{-5}
Control	0.41 ± 0.02	0.65 ± 0.03	1.40 ± 0.16
0 mins	0.42 ± 0.02	0.69 ± 0.02	1.48 ± 0.25
2 mins	5.39 ± 0.70	3.95 ± 0.41	5.23± 0.95
5 mins	7.25 ± 1.01	4.94 ± 0.49	6.15± 0.96
10 mins	8.15 ± 1.19	6.23 ± 0.56	7.41± 1.69

Table 5.4 DNA quantity in non-infected culture supernatants, measured from agarose gels. The Control sample represented an average of the triplicate non-sheared controls. Culture was sheared at 533 rps and samples taken at 0, 2, 5 and 10 minutes. Uncertainties represent the standard error, N=3.

Sample	Quantity of DNA ($\mu g\ ml^{-1}$)		
	2 hours	3 hours	5 hours
Control	0.48 ± 0.08	0.34 ± 0.03	0.83 ± 0.09
0 mins	0.54 ± 0.10	0.32 ± 0.05	0.65 ± 0.13
2 mins	5.87 ± 1.47	3.24 ± 0.63	4.47 ± 0.65
5 mins	8.48 ± 2.34	4.37 ± 1.10	5.49 ± 0.83
10 mins	14.5 ± 3.37	5.74 ± 1.17	6.92 ± 1.21

Table 5.5 Supernatant DNA quantities per OD_{600} unit at the point of harvesting. Uncertainties represent the standard error, N=3.

M13 infected *E. coli* supernatant $\mu g\ ml^{-1}$ DNA per OD_{600} unit			Non-infected *E. coli* supernatant $\mu g\ ml^{-1}$ DNA per OD_{600} unit		
MOI 5 x 10^1	MOI 5 x 10^{-2}	MOI 5 x 10^{-5}	2 hours	3 hours	5 hours
0.35 ± 0.02	0.38 ± 0.01	0.60 ± 0.07	0.32 ± 0.05	0.18 ± 0.02	0.30± 0.03

The quantity of DNA in all supernatants from infected cultures was confirmed to increase strongly with shearing at 533 rps. After 10 minutes there was a 20-fold increase in DNA concentration in cultures infected with an MOI 5 x 10^1; a 10-fold increase in cultures infected with an MOI of 5 x 10^{-2}; and a 5-fold increase in cultures infected with a MOI of 5 x 10^{-5} (Table 5.3). Therefore, while the absolute DNA concentrations were not significantly different after 10 minutes shearing between all three MOIs (P>0.05, Tukey), the relative increases in DNA were dependent on the MOI. The data also showed that the greatest factor increase in DNA concentration was within the first two minutes of shearing. Between two and six minutes exposure time, the factor increase in DNA concentration in all three MOIs was only in the range 1.4- 1.6.

Similarly, the quantity of DNA in all non-infected culture supernatants was confirmed to increase strongly with shearing at 533 rps. After 10 minutes there was a 30-fold increase in DNA concentration in cultures harvested at 2 hours; a 17-fold increase in cultures harvested at 3 hours; and an 8-fold increase in cultures harvested at 5 hours (Table 5.4). Therefore, the relative increases in DNA were dependent on the harvest time. Again, the data also shows that the greatest factor increase in DNA concentration was within the first two minutes of shearing.

5.3.5 Relationship between cell viability and supernatant contamination

It may have been expected that upon exposure to 533 rps within the shear device, the absolute number of *E. coli* cells losing viability over 10 minutes would have correlated with the increase in DNA in the supernatant over the same time period (Figure 5.13). However this was not the case. Regression analysis confirmed that the linear relationship was not significantly different from zero (R^2=0.18, P=0.42). Where the enumerated quantity of viable cells after 10 minutes of shear was greater than the control value, the quantity of cells "losing viability" was therefore calculated as a negative value.
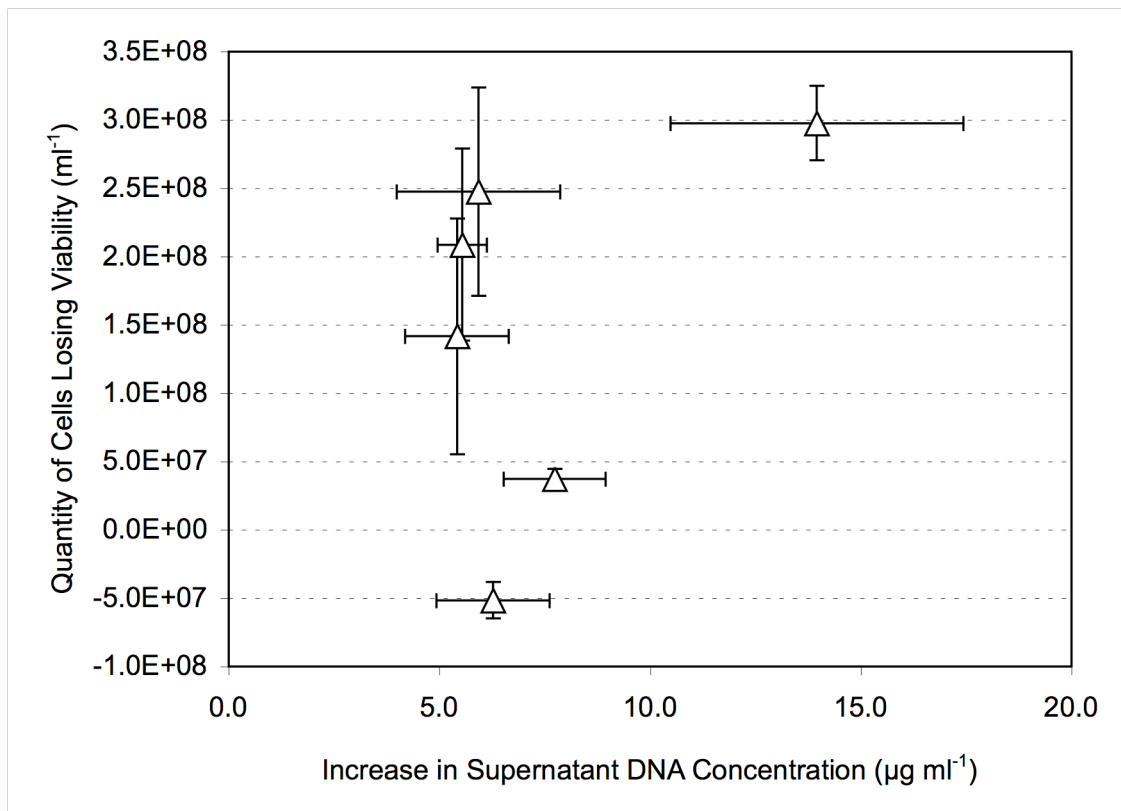
Figure 5.13 Quantity of *E. coli* Top10F' cells losing viability after 10 minutes at disk speed 533 rps ($\triangle$) as a function of increased supernatant DNA concentration. The R^2 value for the linear trend was 0.18. Error bars represent the standard error, N=3.

5.4   Discussion

The primary aim of this chapter was to identify the response of *E. coli* culture to turbulent shear forces and to investigate the effect of bacteriophage M13 infection. Specifically, the initial multiplicity of infection (MOI) of infected cultures was explored to determine if there were consequences for remaining cell viability and supernatant DNA levels. If so, it needed to be assessed whether this would alter the choice of MOI.

5.4.1   The effect of shear on *E. coli* cell viability

Both infected and non-infected *E. coli* cultures were exposed to shear at 533 rps for 10 minutes. In Chapter 3 (Section 3.3.3) 533 rps was modelled to impart a maximum energy dissipation rate of 3.1×10^5 W kg^{-1}. Furthermore, this rotation speed has been predicted in the literature to mimic the high shear conditions within the feed-zone of a production scale multichamber bowl centrifuge, the most damaging from a selection of designs studied (Boychyn *et al.*, 2004). It was therefore chosen as a "worst case" scenario. For M13 infected cells the viability drops were independent of the MOI, and therefore culture age and culture optical density (OD$_{600}$) (Figure

5.4). However, for non-infected cells, the viability drops in the older cultures (3 and 5 hours) were significantly less than for the 2 hour culture (Figure 5.5). These trends may be explained as an interaction of two effects. Firstly, cell damage occurs once a threshold shear stress is breached (Lange *et al.*, 2001), and evidence suggests that the cell membrane damage caused by M13 infection will reduce this threshold (Chen *et al.*, 2009). This would explain the generally greater susceptibility of infected cells to shear. Secondly, it is important to note that the *non-infected* cultures were in different stages of growth when subject to shear, unlike M13 infected cultures. All M13 infected cultures were in early stationary phase at the time of shearing, which correlated with the end of M13 production (and therefore harvesting) (Figure 5.1). However, for non-infected cultures, after two and three hours growth cells were still undergoing active cell division, since the OD_{600} value continued to increase up to 5 hours growth (Table 5.2). Furthermore, in Chapter 4 (Section 4.5.1), Top10F' culture in NB2 at the 2 L bioreactor scale (with the same 10 % (v/v) inoculum size as used in this study) had reached stationary phase by 5 hours. This is important, since the physiological state of *E. coli* cells changes as growth progresses, particularly once cells reach stationary phase (Diaz-Acosta *et al.*, 2006). Here, cells exhibit a distinct rounded morphology of reduced volume (Lange and Hengge-Aronis, 1991; Loewen and Hengge-Aronis, 1994), and a generalised resistance to extremes of temperatures, sodium chloride and oxidizing agents such as hydrogen peroxide (Kolter *et al.*, 1993). It is possible that these effects contributed towards the greater shear-resistance observed in the non-infected *E. coli* cultures harvested at the later times in this study. Since all M13 infected cultures were in stationary phase upon exposure to shear, this could explain why such an effect would not cause a differentiation between them.

5.4.2 The effects of MOI and shear on supernatant DNA concentration

The level of contaminating DNA in the non-sheared culture supernatant was found to decrease with increased MOI (Table 5.3). This pattern was consistent with the trends outlined in Chapter 4, where the levels of DNA and protein contamination in the culture supernatant were found to increase concomitantly with *E. coli* growth. There is a trade-off: increased MOI results in a shorter fermentation time (and a less contaminated supernatant), but at the cost of needing a larger bacteriophage inoculum for no overall gain in yield. When normalised on a per OD_{600} unit basis, it was also confirmed that the level of supernatant DNA was lower in non-infected cultures of equivalent age to infected cultures (Table 5.5).

However, it was subsequently demonstrated that the level of supernatant DNA in all cultures increased sharply upon exposure to shear (Table 5.3, Table 5.4). After a 10 minute exposure time, the quantities of DNA in infected culture supernatants were no longer significantly different from one another. Therefore, MOI did not affect the *overall* quantity of supernatant DNA. For non-infected cells, cultures harvested after 2 hours growth released double the

quantity of DNA after 10 minutes of shear, relative to the 3 hour and 5 hour cultures. This result mirrored the viability data: the 2 hour culture experienced the greatest proportional decrease in viability.

In downstream processing the exposure time to the highest-energy dissipation conditions (for example, within continuous centrifuge designs) is of the order of a fraction of a second, not 10 minutes (Byrne *et al.*, 2002). Nevertheless, if the threshold shear stress resistance is exceeded, *E. coli* breakage can occur within such timeframes (Chan *et al.*, 2006; Lange *et al.*, 2001). The potential for an increase in contaminating supernatant chromosomal DNA therefore remains. Verification studies would need to be conducted to confirm this prediction for large-scale processing. From a bioprocessing perspective, the extra release of chromosomal DNA is generally undesirable, since it is known to be particularly susceptible to scission by the action of shear. This trend was observed in Figure 5.7- Figure 5.12, where the supernatant chromosomal DNA was noted to be reduced from >20 kbp to a 1 to 6 kbp smear. Particularly for plasmid DNA processing, fragmentation makes the removal of the chemically identical chromosomal DNA significantly more difficult, depending on the choice of downstream unit operation (Meacle *et al.*, 2004). In bacteriophage downstream processing, however, since bacteriophage product and DNA contaminant are chemically and physically different, several purification options are available, as discussed in the Introduction to this thesis (Section 1.6.2.).

It was not possible to accurately model the release of DNA into the supernatant as a function of shearing time since the majority of the DNA was generally released by the first two minute sample point. Similar degradation profiles have been reported for other biological materials subject to high shear conditions, where an initial high rate of damage occurs to a point beyond which little further loss is observed (Oliva *et al.*, 2003; Thomas *et al.*, 1979). However, putting this into perspective, even after a full 10 minutes of shearing at 533 rps, the quantity of supernatant DNA was relatively low (at an average of approximately 7 μg ml^{-1}). Revisiting an estimation for the quantity of chromosomal DNA in a single *E. coli* cell (Chapter 4, Section 4.6), lysis of a typical 2×10^9 cfu ml^{-1} culture would release approximately 40 μg ml^{-1} of chromosomal DNA. Such a scenario could be expected at the end of lytic bacteriophage culture.

5.4.3   Relationship between cell viability and supernatant contamination

The overall lack of correlation between the quantity of cells losing viability and the increase in supernatant DNA concentration (Figure 5.13) indicates that, in practical terms, measurement of the loss of viability was a poor indicator of contaminant release. Firstly, this may have been because viability loss did not necessarily result in lysis. Secondly, this pattern may be explained by the strain used in this study, Top10F, being *recA⁻*. As noted in Chapter 4, in *recA⁻ E. coli* culture, cells which actively grow and divide (and are therefore countable on an agar plate)

typically represent only a 49 % fraction of the total population (Capaldo *et al.*, 1974). It was also noted in Chapter 4 that M13 infection further reduced the cell count per OD_{600} unit. Therefore, large subpopulations of residually and non-diving cells existed to contribute towards the quantity of supernatant DNA measured. It is likely that these subpopulations behaved differently upon high shear exposure than viable cells (for example, by having a lower breakage threshold), or were susceptible to smaller differences in culture conditions (e.g. culture cell density) that did not affect cell viability (Figure 5.6). Such effects could mask a viability loss/DNA release relationship.

5.4.4 Concluding remarks

This chapter goes some way towards understanding the effect of shear upon *E. coli* culture. M13 infection reduced the resistance of *E. coli* to shear forces after five hours of growth: it therefore appears that cell integrity is marginally compromised by bacteriophage infection. Exposure to high shear conditions increased the concentration of supernatant DNA in culture, although this correlated poorly with cell viability losses. This was thought to be due to contributions from large subpopulations of residually and non-dividing cells. Post-exposure to 10 minutes of high shear conditions, it was found that there was no correlation between MOI and the concentration of supernatant DNA. Therefore, from a practical perspective, the data obtained does not alter the main trade-off identified. That is, increasing the MOI decreases the fermentation time, but at the cost of a larger bacteriophage inoculum. This work suggests that cell removal by centrifugation could result in a supernatant DNA concentration significantly higher than the quantity recorded by the end of fermentation, although further experimentation would be needed to confirm this at scale. However, several straightforward options exist to separate DNA contamination from bacteriophage, from treatment with DNAse to precipitation and chromatography steps. In particular, it will be shown in the next chapter that DNA and bacteriophage M13 can be separated by precipitation.

6 The Primary Purification of Bacteriophage M13

6.1 Introduction

In the Introduction to this thesis, an outline of the steps for bacteriophage M13 processing was given (Section 1.6). The subsequent chapters have addressed aspects of this process. Essentially, once fermentation is complete (studied in Chapter 4), the resulting process fluid will contain bacteriophage M13 of concentration 10^{11} to 10^{12} pfu ml^{-1}, intact *E. coli* cells, cell debris and medium components. A clarification step (often centrifugation) is then required to remove host cells and debris from the process stream. The effect of the hydrodynamic shear conditions imparted by large-scale equipment such as continuous centrifuges was addressed in Chapter 3 (for bacteriophage M13) and Chapter 5 (for *E. coli*). The next stage is typically a concentration step, reducing the volume of the process stream and making further downstream process stages more manageable. This is the primary purification stage, and forms the focus of this study. More than one competitive option exists at the large-scale (Chapter 1, Section 1.6.2), but this chapter shall focus on precipitation as a method for the primary purification of bacteriophage M13.

In processing terms, bacteriophage M13 can be considered as a large (16 MDa) protein in solution, since the surface of the bacteriophage is protein coat. The precipitation characteristics of proteins are dependent on several factors including temperature; pH; precipitant type and concentration; precipitation time; and protein charge, size, shape and concentration (Wenzig *et al.*, 1993). Therefore it is important to not only carefully control the factors being examined, but also those needing to be held constant.

At the laboratory-scale, the precipitation of bacteriophage from solution is typically achieved by 2- 10 % (w/v) polyethylene glycol (PEG) and up to 500 mM sodium chloride (Vajda, 1978; Yamamoto *et al.*, 1970). Indeed, PEG-salt precipitation was used in this thesis to prepare working stocks of bacteriophage M13 (Section 2.3.3), although it was unknown whether the concentrations used were optimal. Therefore, the first aim of this chapter was to investigate the PEG precipitation characteristics of bacteriophage M13 in detail. Initial studies were conducted in systems containing only purified bacteriophage M13, to allow for the effect of each individual precipitation component to be assessed.

However, many other precipitation techniques are available for the precipitation of protein, which exploit several underlying principles. The second aim of this study was to therefore identify other effective precipitants of bacteriophage M13. Isoelectric precipitation was first investigated, based on the method of Bachrach and Friedmann (1971) for several T-odd and T-even type bacteriophage. Five further precipitants (CTAB, manganese sulphate, calcium

chloride, spermidine and ammonium sulphate) were also studied in a qualitative screening experiment, of which effective precipitants were taken forward for further analysis.

In reality, bacteriophage M13 will be precipitated from clarified process fluid. The third aim of this study was to examine the ability of candidate precipitants to precipitate bacteriophage M13 from a broth system. Effective precipitants from this screening experiment were subsequently analysed in detail. An early primary purification step that achieves substantial concentration and purification simultaneously can reduce the overall cost of the bioprocess (Tsoka *et al.*, 2000) either by reducing the number of processing stages required (Wenzig *et al.*, 1993) or lessening the burden on subsequent chromatography stages (Thommes and Etzel, 2007). Therefore, the final aim of this chapter was to identify the precipitants that offered the greatest improvement in bacteriophage M13 purity.

6.2   PEG Precipitation of Bacteriophage M13

6.2.1   Introduction to PEG Precipitation

PEG is a well known protein precipitation agent (Atha and Ingham, 1981; Sharma and Kalonia, 2004; Vajda, 1978; Yamamoto *et al.*, 1970). From an industrial perspective, its advantages include effecting protein precipitation without denaturation and requiring relatively small quantities to do so (generally 5- 20 % (w/v)). Experimental evidence of the action of PEG points to a volume exclusion mechanism: that is, proteins are sterically excluded from the regions of solvent that are occupied by the PEG chains (Atha and Ingham, 1981). Proteins are consequently concentrated and finally precipitated when their solubility is exceeded. However, the mechanism of precipitation must also include an electrostatic component, since the quantity of PEG required to precipitate a protein is affected by the system pH and ionic strength (Mahadevan and Hall, 1990; 1992). Protein-protein repulsion can be reduced by more favourable pH or ionic strength conditions, thereby making PEG precipitation occur more readily. Overall, PEG precipitation is poorly understood on the fundamental level (Ingham, 1990) thus hampering efforts to fully explain or predict precipitation behaviour. Partial explanations of the theory of PEG precipitation are numerous, however, and are generally based on the volume exclusion mechanism (Atha and Ingham, 1981; Mahadevan and Hall, 1990; Shulgin and Ruckenstein, 2006).

As noted in Section 6.1, the precipitation of bacteriophage by PEG and salt is itself a longstanding and common technique. Since larger proteins tend to precipitate at lower PEG concentrations (Atha and Ingham, 1981), bacteriophage precipitation typically requires the addition of only up to 10 % (w/v) PEG, usually of average molecular weight 6 or 8 000. Several

hundred millimolars of salt, usually sodium chloride (NaCl), is also added to the bacteriophage solution (Vajda, 1978; Yamamoto *et al.*, 1970).

In this thesis, working stocks of bacteriophage M13 were produced using PEG and NaCl for the primary purification of M13 from clarified NB2 (Section 2.3.3). Precipitation was performed using a final concentration of 3.33 % (w/v) PEG 6 000, 330 mM NaCl, and incubated on ice for 1 hour without pH monitoring (Bahri, 1990). The precipitant concentrations and conditions were not optimised. Therefore, the starting point of this study was to assess the recovery of M13 by this method and to scale-down to a system containing only purified bacteriophage for detailed investigation.

6.2.2   Method development: calculation of bacteriophage M13 recoveries and scale-down of precipitation

Bacteriophage M13 was propagated at the two-litre shakeflask scale and precipitated from NB2 as described in Section 2.3.3. Samples (50 µl) were taken from each processing stage: culture, supernatant (*E. coli* cells removed), resuspended bacteriophage precipitate and post-precipitation supernatant (bacteriophage M13 removed). Each sample was titred for bacteriophage by the surface droplet method (Section 2.5.2). The experiment was repeated three times.

The concentration of bacteriophage M13 in both culture and culture supernatant was 3.5×10^{11} pfu ml^{-1}: as expected, no bacteriophage losses arose from *E. coli* removal. It was then checked whether bacteriophage losses had occurred by precipitation. A bacteriophage concentration of 4×10^{11} pfu ml^{-1} was recovered post-precipitation (and resuspended in the same volume), which was not significantly different to the concentration in culture supernatant (P=0.43, t-test). It was therefore assumed for future experimentation that PEG precipitation did not result in bacteriophage losses. Bacteriophage M13 separation into precipitate and supernatant was subsequently expressed as a percentage of the total recovered bacteriophage (Table 6.1), a standard method used in the literature (Yamamoto *et al.*, 1970). It was found that the employed precipitation step was efficient: 98 % of recovered bacteriophage were in the precipitate.

Table 6.1 The PEG-salt precipitation of bacteriophage M13 from NB2, using 3.3 % (w/v) PEG 6 000, 330 mM NaCl. Recoveries are expressed as a percentage of the total. Uncertainties represent the standard error, N=3.

	Condition	
	Bacteriophage precipitate	Precipitation supernatant
Recovered bacteriophage (%)	98.2 ± 0.9	1.8 ± 0.9

Precipitation was then scaled down. Since successful, reproducible partitioning of bacteriophage T7 at 2 ml and 10 ml scales had been demonstrated (Negrete *et al.*, 2007), precipitation of M13 was initially trialled at these scales (in 2 ml and 15 ml polypropylene tubes) in duplicate. Precipitations were conducted as described in the Materials and Methods (Section 2.14.2) for 10 ml scale precipitations, and at one-fifth scale for 2 ml precipitations. The concentration of purified bacteriophage examined, at about 4×10^{11} pfu ml^{-1}, was chosen to represent the typical concentration of bacteriophage found in the post-fermentation broth. This variable was then held constant throughout this chapter, since it is known that bacteriophage concentration can affect precipitation performance (Yamamoto *et al.*, 1970). The adjustment of each stock to pH 7 with dilute sodium hydroxide (and sulphuric acid) was estimated to only add a maximum of 5 mM of sodium ions to each precipitation reaction. The precipitation conditions were based upon previously reported methods (Yamamoto *et al.*, 1970). As was used in broth, precipitation was performed using a final concentration of 3.3 % (w/v) PEG 6 000, 330 mM NaCl.

Early experimentation found that white bacteriophage precipitates were visible post-centrifugation, observed along the outermost wall of the polypropylene tube. These precipitates were unstable at the 2 ml scale; some of the precipitate was noted to come away as supernatants were decanted. Better precipitate stability was observed at the 10 ml scale, which was used for all further experimentation. Upon enumeration, bacteriophage recovery in the precipitate averaged 94 %. All further experimentations proved that successful precipitation resulted in recoveries typically in the range 90- 96 % in the precipitate.

Several factors affecting precipitation efficiency were subsequently assessed at the 10 ml scale. These were PEG molecular weight (chain length) and concentration; precipitation temperature and time; salt type and concentration. Whilst one factor was being varied, all others were kept constant.

6.2.3 The effect of PEG molecular weight on bacteriophage M13 precipitation

The degree of polymerisation increases the average molecular weight of PEG. It has been shown that using PEG of increased average molecular weight reduces the amount required for bacteriophage λ precipitation from broth (Yamamoto *et al.*, 1970). Similarly, all other factors being constant, the solubility of lysozyme is reduced as PEG molecular weight is increased (Boncina *et al.*, 2008). It was therefore expected that PEG molecular weight would have an effect on M13 precipitation. Experiments were conducted as described in the Materials and Methods, Section 2.14.2, using purified bacteriophage. PEG of average molecular weight 600, 2 000, 6 000, 8 000, 12 000 and 20 000 were tested. The concentration of NaCl remained at 330 mM throughout. The concentration of PEG was altered in 1 % (w/v) increments, reduced to 0.5 % (w/v) increments in the region of bacteriophage precipitation. Experiments were conducted three times in total.

The effect of increasing PEG molecular weight was greatest at the lowest average molecular weights (Figure 6.1). That is, a 3.3-fold increase in molecular weight from PEG 600 to PEG 2 000 reduced the concentration required for total (>90 %) bacteriophage recovery from 10 % (w/v) to only 4 % (w/v). In comparison, a 3.3-fold increase in molecular weight from PEG 6 000 to PEG 20 000 reduced the concentration required for total bacteriophage recovery from 2 % (w/v) to 1.5 % (w/v).

It was also noted that the amount of PEG 6 000 required to recover >90 % of the bacteriophage particles (2 % (w/v)) was substantially less than the non-optimised amount used previously (3.3 % (w/v)).
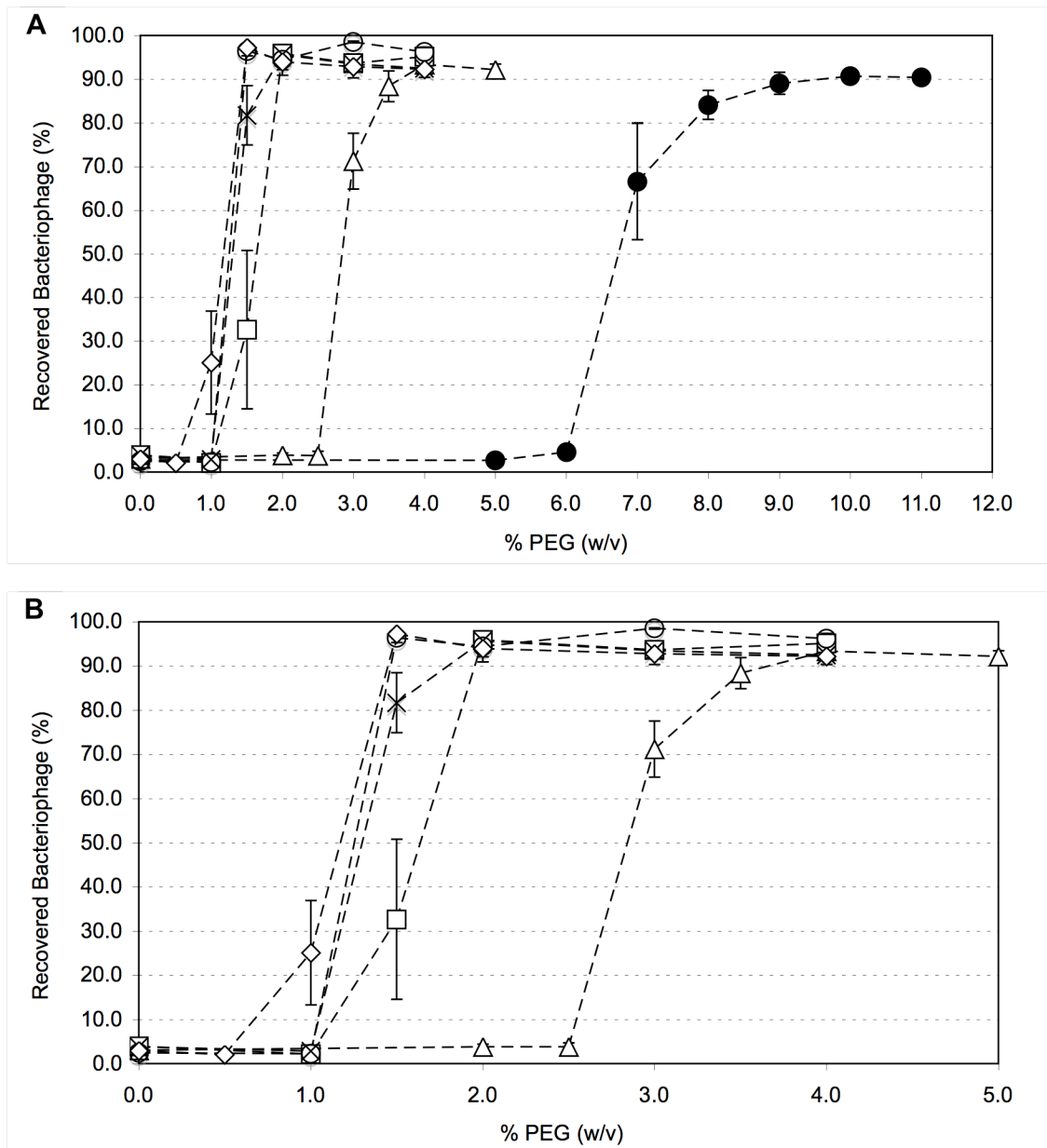
Figure 6.1 The effect of PEG molecular weight on the concentration required to induce precipitation of bacteriophage M13 with 330 mM NaCl. The percentage of recovered bacteriophage was calculated from the quantity of bacteriophage recovered in the precipitate as a proportion of the total. Symbols: PEG 600 (●), PEG 2 000 (△), PEG 6 000 (□), PEG 8 000 (×), PEG 12 000 (○) and PEG 20 000 (◇). Graph (A) shows all PEG molecular weights. Graph (B) shows PEG 2 000 to 20 000 only. Errors bars represent the standard error, N=3.

When precipitated by PEG 600, it was noted that the percentage recovery of bacteriophage M13 in the precipitate appeared consistently lower (2- 5 %) than for higher molecular weights. To check that this was not a result of insufficient centrifugal force, eight identical 10 ml precipitation reactions were prepared with 11 % (w/v) PEG 600. Following incubation on ice for 1 hour, four were centrifuged at 8 000 x g for 10 minutes, and four at 15 000 x g for the

same period. It was found there was no significant difference between the M13 recoveries achieved (P=0.15, t-test). The reduced recovery was therefore considered to be either due to an inherent inability of PEG 600 to precipitate M13 as completely, or as a result of the precipitate being less stable under these conditions when subject to supernatant removal.

6.2.4   Relationship between PEG molecular weight and solution viscosity

On a quantity basis, it was shown that the effect of PEG molecular weight above 6 000 was small (Figure 6.1). However, the viscosity of the solution will rise as molecular weight, and therefore chain length, increases (Gonzalez-Tello et $al.$, 1994). To investigate the effect of PEG molecular weight in this system, the viscosity of 10 ml precipitation reactions was measured. All reactions contained 3.3 % (w/v) PEG and 330 mM NaCl, as well as the purified bacteriophage, and were incubated on ice for one hour. The viscosity of each was measured as described in the Materials and Methods (Section 2.11) using a cone and plate viscometer. Chilled (4 °C) water was circulated around the viscometer chamber to keep the sample cool.

A linear relationship existed between shear stress and shear rate (Figure 6.2). Thus every solution was Newtonian and the viscosity (μ, Pa s) could be measured as the gradient of the line. The measured viscosity of the water control (μ= 1.0 mPa s) was lower than expected: the viscosity of pure water at 4 °C is approximately 1.5 mPa s (Perry et $al.$, 1998). This most likely suggested that the temperature of the sample was higher than 4 °C (and therefore less viscous). Nevertheless, as the average molecular weight of the PEG increased, the viscosity of the solution significantly rose (Figure 6.2). For example, the measured viscosity of the PEG 20 000 solution was 2.9 mPa s, which was 70 % greater than the viscosity of PEG 6 000 solution of the same concentration (1.7 mPa s).
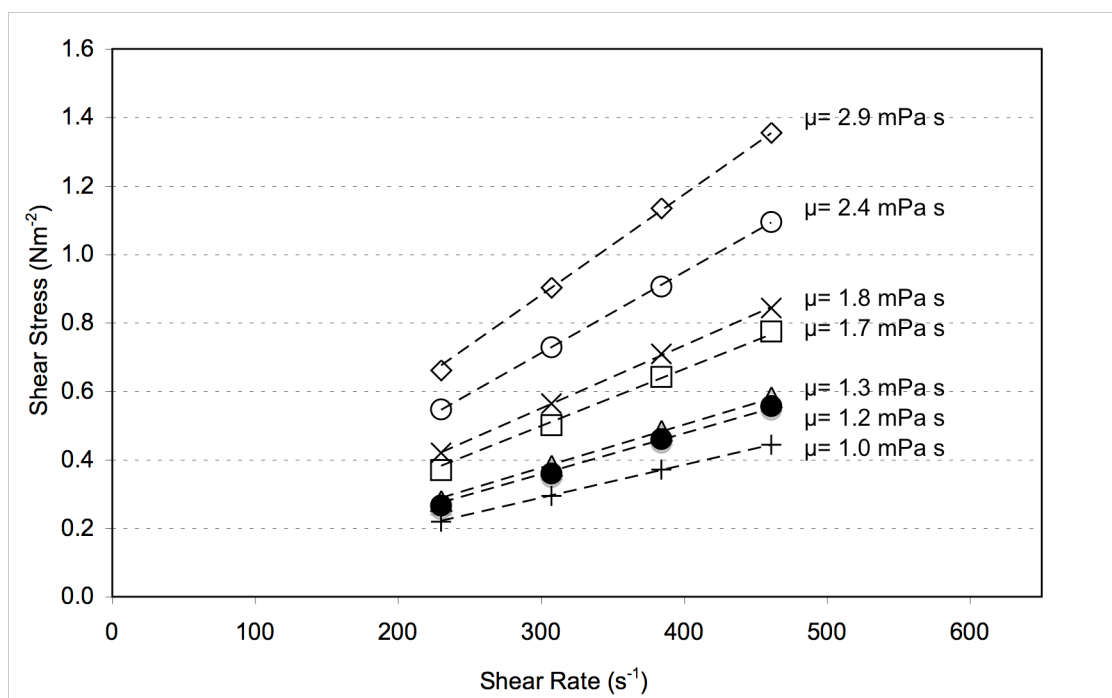
Figure 6.2 Viscosity measurement of several solutions of 3.3 % (w/v) PEG, 330 mM NaCl, 4 x 10^{11} pfu ml^{-1} bacteriophage M13. A linear relationship existed between shear stress and shear rate: every solution was Newtonian in behaviour. Viscosity (μ) was therefore calculated from the gradient of each line. Symbols: PEG 600 (●), PEG 2 000 (△), PEG 6 000 (□), PEG 8 000 (×), PEG 12 000 (○) and PEG 20 000 (◇). N=2.

6.2.5   The effect of PEG and NaCl concentration on bacteriophage M13 precipitation

In Section 6.2.3, the concentration of NaCl was held at 330 mM while the concentration and molecular weight of PEG was altered. However, it was also of interest to determine the minimum concentration of NaCl required to induce precipitation at a particular concentration of PEG 6 000. The salt concentration (or ionic strength) of solution is known to affect protein solubility (Atha and Ingham, 1981; Boncina *et al.*, 2008; Mahadevan and Hall, 1992). Therefore, from a processing perspective, investigation of ionic strength gives the option of precipitating under high salt/ low % (w/v) PEG or low salt/ high % (w/v) PEG conditions. Experiments were again conducted as described in the Materials and Methods, Section 2.14.2. The concentration of NaCl was altered in 100 mM increments, reduced to 35 mM increments in the region of bacteriophage precipitation. Experiments were conducted three times in total. Figure 6.3 shows the relationship between bacteriophage M13 recovery and the concentration of NaCl at a range of PEG 6 000 concentrations. It was found that a 1 % (w/v) PEG 6 000 solution was not sufficient to precipitate M13 at NaCl concentrations up to 1 M. When precipitation did occur, it was observed that a higher percentage PEG solution reduced the minimum required salt concentration for bacteriophage precipitation. In the range examined, a 2-fold increase in PEG

173

concentration (2 % (w/v) to 4 % (w/v)) was found to approximately reduce the concentration of NaCl required 2-fold (265 mM to 135 mM).

In this system the addition of 3.3 % (w/v) PEG 6 000 and 330 mM NaCl to precipitate M13 was sub-optimal. It can be seen in Figure 6.3 that a PEG 6 000 concentration of 3.3 % (w/v) required only 165 mM NaCl for 93 % of precipitated bacteriophage particles to be recovered in the precipitate. Alternatively, 330 mM NaCl resulted in the successful precipitation of bacteriophage M13 with only 2 % (w/v) PEG 6 000 (Figure 6.1).
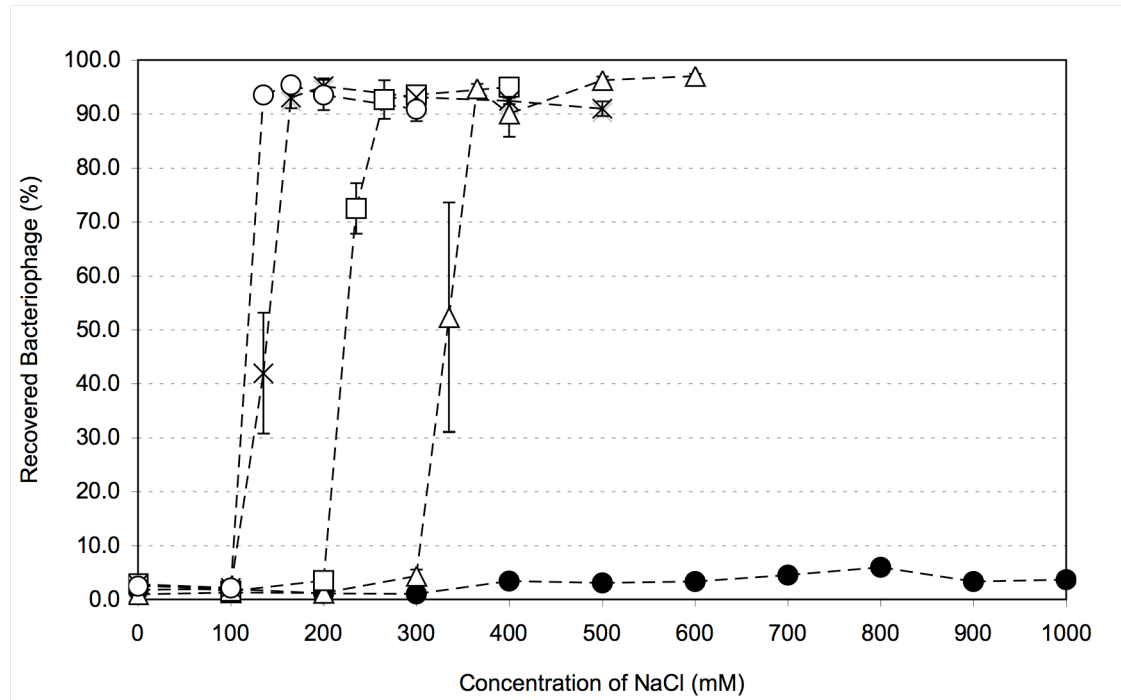
Figure 6.3 The recovery of bacteriophage M13 in the precipitate as a function of NaCl concentration for five concentrations of PEG 6 000. The percentage of recovered bacteriophage was calculated from the quantity of bacteriophage recovered in the precipitate as a proportion of the total. Symbols: 1 % (w/v) PEG 6 000 (●), 1.5 % (w/v) PEG 6 000 (△), 2 % (w/v) PEG 6 000 (□), 3.3 % (w/v) PEG 6 000 (×), 4 % (w/v) PEG 6 000 (○). Errors bars represent the standard error, N=3.

Similarly to the trend observed in Figure 6.1, it was expected that at a fixed concentration of PEG in solution, increasing the average molecular weight would reduce the minimum quantity of NaCl required for successful bacteriophage precipitation. This was found to be the case when 4 % (w/v) concentrations of PEG 2 000, 6 000 and 20 000 were compared (Figure 6.4). Again, the relative advantage of a PEG molecular weight significantly greater than 6 000 was small: PEG 20 000 reduced the minimum quantity of NaCl over PEG 6 000 by only 35- 70 mM. In

comparison, increasing the PEG molecular weight from 2 000 to 6 000 reduced the required concentration of NaCl by at least 130 mM.
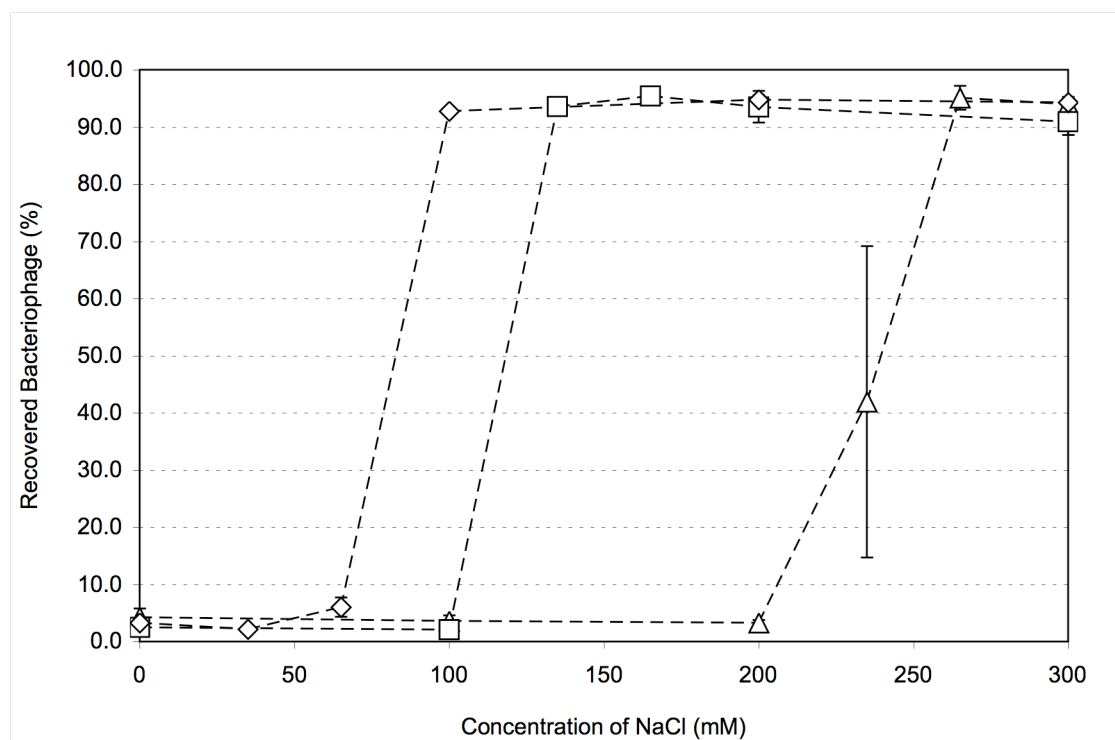
Figure 6.4 The recovery of bacteriophage M13 in the precipitate as a function of NaCl concentration with 4 % (w/v) PEG of molecular weights 2 000 ($\triangle$), 6 000 ($\square$), and 20 000 ($\diamond$). The percentage of recovered bacteriophage was calculated from the quantity of bacteriophage recovered in the precipitate as a proportion of the total. Errors bars represent the standard error, N=3.

6.2.6 The effect of incubation time and temperature

After the addition of precipitants to a solution, it is important that sufficient time is allowed for the complete precipitation of the bacteriophage particles. The incubation temperature (on ice) and time (1 hour) used in this study were derived from existing laboratory protocols for M13 processing, based upon the methods of Bahri (1990) and Yamamoto *et al.* (1970). Sambrook *et al.* (2001) proposed similar conditions, albeit employing higher PEG 6 000 (4 % (w/v)) and NaCl (500 mM) concentrations, whereas Messing and Vieira (1982) incubated for only 30 minutes at room temperature (3.6 % (w/v) PEG 6 000, 440 mM NaCl). It is obvious that some flexibility of incubation conditions exists. While the exact precipitation time for any protein (or bacteriophage) is a function of the many input factors affecting the precipitation reaction, it was considered useful to assess the temperature dependence and timescale of the reaction for a set of precipitant concentrations.

Six 10 ml precipitation reactions were prepared as described in the Materials and Methods (Section 2.14.2), except that tubes were pre-cooled on ice for 20 minutes prior to bacteriophage addition. Following bacteriophage addition, tubes were re-incubated on ice (3.3 % (w/v) PEG 6 000 and 330 mM NaCl in each) and one tube was removed and centrifuged for 10 minutes, 8 000 x g at 4 °C at each of the following times: 0, 12, 24, 36, 48 and 60 minutes. Post centrifugation treatment was identical to that described in Section 2.14.2. The experiment was repeated for incubation at room temperature (25 °C), where centrifugation was also at 25 °C. All experiments were repeated three times.

Data was plotted as the proportional difference in bacteriophage recovery in the precipitate from the standard incubation conditions of 1 hour, on ice (Figure 6.5). Only the 0 minute incubation on ice was significantly lower than the standard conditions (P=0.009, t-test). No recoveries from incubation at room temperature were significantly lower than the 1 hour, on ice standard. Indeed, recoveries after 12 and 36 minute incubations were significantly higher (P=0.043 and P=0.044 respectively, t-test).
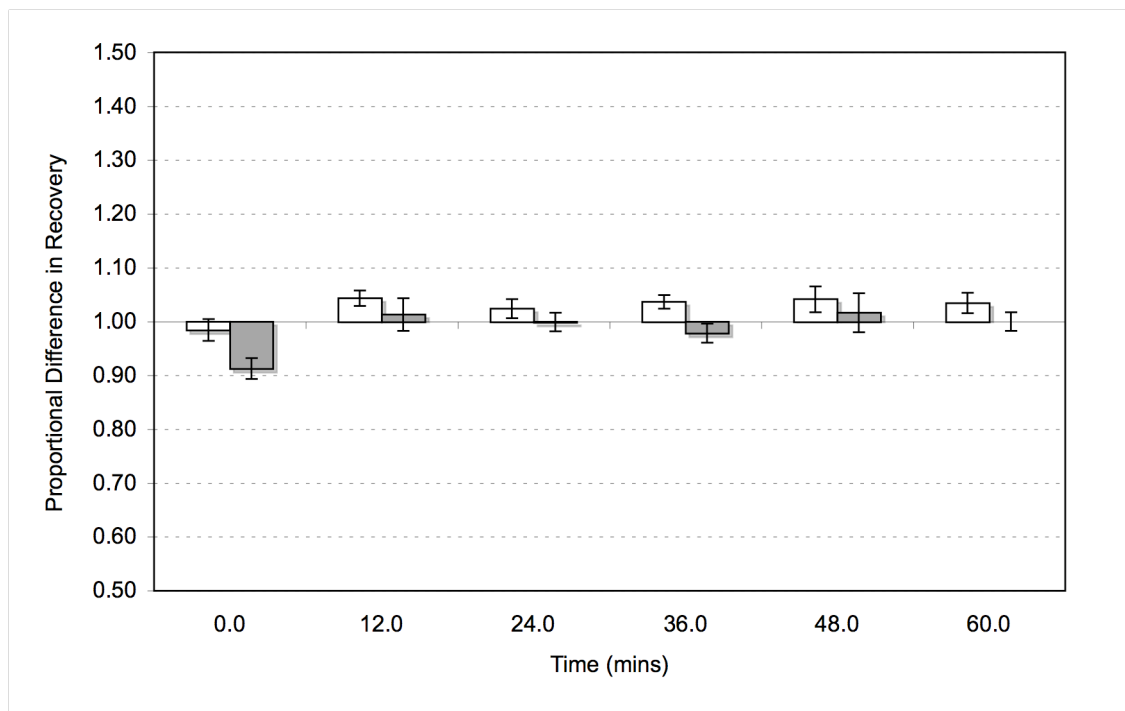
Figure 6.5 The effect of reducing the incubation time from 1 hour for incubations at room temperature (□) and on ice (▪). Bacteriophage recoveries in the precipitate were plotted as the proportional difference from the standard incubation conditions of 1 hour, on ice. Only a 0 minute incubation on ice gave a bacteriophage recovery that was significantly lower than the standard (P=0.009, t-test). Error bars represent the standard error, N=3.

6.2.7 The effect of salt type on bacteriophage M13 precipitation

It was noted in Section 6.2.5 that PEG precipitation was assisted by an increase in solution ionic strength. This was achieved experimentally by increasing the concentration of NaCl. However, ionic strength is also a function of the charge of the ions in solution. Further, even ions of the same charge and concentration can perform differently (Boncina *et al.*, 2008; Collins, 1997).

Therefore, PEG precipitation of bacteriophage M13 was conducted with two additional salts. Magnesium sulphate ($MgSO_4$) and sodium sulphate (Na_2SO_4) were compared with NaCl for effectiveness at concentrations of 0, 2, 3.3 and 4 % (w/v) PEG 6 000. Experiments were conducted as described in Section 2.14.2. The concentration of each salt was altered in 100 mM increments, reduced to 35 mM increments in the region of bacteriophage precipitation. Where precipitation was successful at less than 35 mM, 5, 15 and 25 mM intervals were tested. Experiments were conducted three times in total.

Significant differences in the solubility of bacteriophage M13 were observed as a result of changing salt. At concentrations of 2, 3.3 and 4 % (w/v) PEG 6 000, $MgSO_4$ was found to consistently induce precipitation at the lowest salt concentrations (Figure 6.6). At a concentration of 4 % (w/v) PEG 6 000, precipitation was induced with 15 mM $MgSO_4$, less than one sixth the quantity of the next most efficient salt. Na_2SO_4 was a more effective precipitant than NaCl at higher concentrations of PEG (3.3 and 4 % (w/v), but was marginally less efficient at 2 % (w/v) PEG. The precipitation curves at 0 % PEG 6 000 confirmed that precipitation was a result of the presence of PEG and salt, not the salt alone. Overall, the reduced solubility of bacteriophage M13 in $MgSO_4$, particularly compared to Na_2SO_4 (both having the same anion), clearly indicated the effectiveness of the Mg^{2+} ion relative to Na^+.
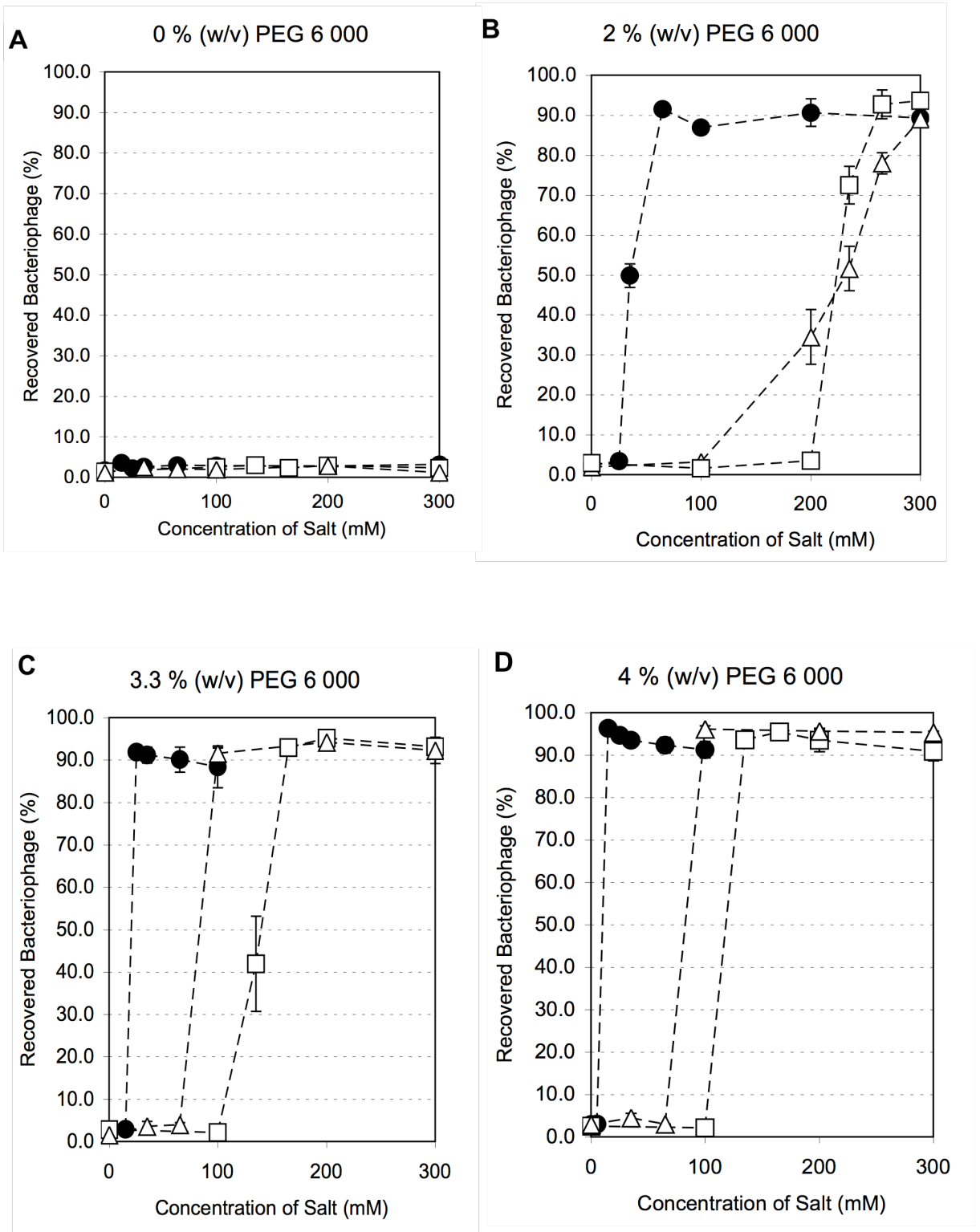
Figure 6.6 The minimum concentrations of magnesium chloride (●), sodium sulphate (△) and sodium chloride (□) required to induce precipitation of bacteriophage M13 at (A) 0 % (w/v) PEG 6 000, (B) 2 % (w/v) PEG 6 000, (C) 3.3 % (w/v) PEG 6 000 and (D) 4 % (w/v) PEG 6 000. Error bars represent the standard error, N=3.

6.3 The Isoelectric Precipitation of Bacteriophage M13

6.3.1 Introduction to isoelectric precipitation

Proteins usually posses a net positive or negative charge which alters according to the pH of the solution. For most proteins there is a pH at which the net charge is neutralised: this is known as having reached the *isoelectric point*. It is here that protein-protein mutual repulsion is reduced to a minimum, and therefore precipitation may occur (Atkinson *et al.*, 1987). Compared to other precipitation methods, such as PEG, the chief advantage of isoelectric precipitation is that no precipitant is added which will subsequently require removal (Wenzig *et al.*, 1993).

The precipitation of several bacteriophage by isoelectric precipitation has been demonstrated by the addition of hydrochloric acid to clarified lysate (Bachrach and Friedmann, 1971), although none were filamentous bacteriophage. The recoveries achieved were variable, ranging from nil to 53 %. The authors surmised that some bacteriophage were more susceptible to inactivation by low pH values: indeed, protein denaturation is the main drawback of this method (Wenzig *et al.*, 1993). However, the chosen pH (3.9 for all bacteriophage studied) did not appear to have been optimised either. Since limited literature exists on isoelectric bacteriophage precipitation, the feasibility of the isoelectric precipitation of bacteriophage M13 was investigated. The theoretical isoelectric point of the particle was first calculated to determine the pH region to focus on for experimentation (Section 6.3.2, below).

6.3.2 Calculation of the isoelectric point of bacteriophage M13

Generally, a theoretical estimation of the net charge of a protein must be calculated with caution. Despite being a fundamental parameter, the net charge of a protein not only depends on the number of ionisable residues, but also the amino acid sequence and the solution ionic strength (Winzor, 2003). However, agreement between theory and experimentation has been achieved for bacteriophage fd (which is closely related to M13) in low ionic strength conditions (Zimmermann *et al.*, 1986). The isoelectric point of bacteriophage M13 was therefore calculated by a similar method. Essentially, the charge of the particle was modelled as a function of pH, where the number of negatively charged amino acid residues was subtracted from the positive. The Henderson-Hasselbalch equation was used to calculate the degree of ionisation of each ionisable amino acid (Stryer, 1995). Only the charge of the major coat protein (pVIII) was considered, since at 2700 copies per bacteriophage, it is the dominating molecule. Importantly, agreement with experimentation was found only when the charges on the exposed, hydrophilic outer portion of the pVIII molecule were considered (Zimmermann *et al.*, 1986). Therefore, for bacteriophage fd the ionisable residues were (with position from the N-terminal end) the NH_2 terminus, Glu (2), Asp (4), Asp (5), Lys (8), Asp (12) and Glu (20) (Zimmermann *et al.*, 1986). Due to a point mutation, the aspartic acid (Asp) residue of bacteriophage fd at position 12 is

asparagine (Asn) for M13 (Model and Russel, 1988). M13 consequently carries approximately 30 % less charge per particle than fd (Tang *et al.*, 2002).

For clarity, a derivation of the total charge of a protein is included in Appendix A. The total charge, Z, of a protein is given by:

$$Z = \sum_{j=1}^{n} \frac{1}{1 + 10^{pH - pK_a}} - \sum_{i=1}^{m} \frac{1}{1 + 10^{pK_a - pH}} \qquad (1)$$

where *j* is each of *n* positively charged residues and *i* is each of *m* negatively charged residues. At the isoelectric point the total charge is equal to zero. For comparison purposes, the taken pK_a values of the amino acid residues were those used for the calculation of the charge of bacteriophage fd at 25 °C (Zimmermann *et al.*, 1986). For bacteriophage fd the isoelectric point was calculated to occur at pH 4.32, for bacteriophage M13, pH 4.50. The estimated value for fd was close to an experimental value of 4.2 measured by titration by Zimmerman *et al.* (1986), but greater than the value of 3.9 measured by isoelectric focusing (Berkowitz and Day, 1976). It was therefore assumed that the estimated isoelectric point of bacteriophage M13 was broadly correct.

6.3.3 Experimental isoelectric precipitation of bacteriophage M13

The precipitation of purified bacteriophage M13 was conducted at a range of pH values (3.7, 3.9, 4.1, 4.3, 4.5, 4.7, 4.9 and 7.0) about the theoretical isoelectric point of pH 4.5. Experiments were conducted at the 10 ml scale as described in the Materials and Methods (Section 2.14.3), using purified bacteriophage M13. Precipitation was conducted at two temperatures: on ice and at room temperature. The incubation time (24 hours) and centrifugation speed (equivalent to 30 minutes at 4 000 x g) were based on the method of Bachrach and Friedmann (1971). Bacteriophage precipitates were resuspended in 10 mM Tris (pH 7.5 at 25 °C). Post-precipitation, in addition to the usual percentage calculation of bacteriophage recovery in the precipitate, the recovered bacteriophage were investigated for viability decline from the acidic conditions (Section 6.3.4). Any temperature-induced alteration of optimal pH was also of interest, since amino acid pK_a values (and therefore bacteriophage isoelectric point) show a weak dependence on temperature (Stryer, 1995). All experimentation was conducted three times.

The recovery of bacteriophage M13 in the precipitate as a function of pH is shown in Figure 6.7. At the end of incubation, pH values were re-measured immediately prior to centrifugation. In this unbuffered system, it was found that pH values had often varied from the initial target.

Therefore, every data point was plotted in Figure 6.7 instead of average recoveries at each target pH.

Recoveries of bacteriophage M13 >90 % in the precipitate occurred in range pH 3.9- 4.5 (Figure 6.7). The incubation temperature made little observable difference to this range. Therefore it may be assumed that the isoelectric point of the bacteriophage did not vary with temperature (Zimmermann *et al.*, 1986). Bacteriophage recovery in the precipitate decreased to below 50 % at pH values below 3.9 and decreased to less than 10 % by pH 5.0 and above. Experimental reproducibility diminished at the limits of successful precipitation, particularly at pH 4.5 and above. This was most likely due to the critical dependence on pH at these borderline conditions.
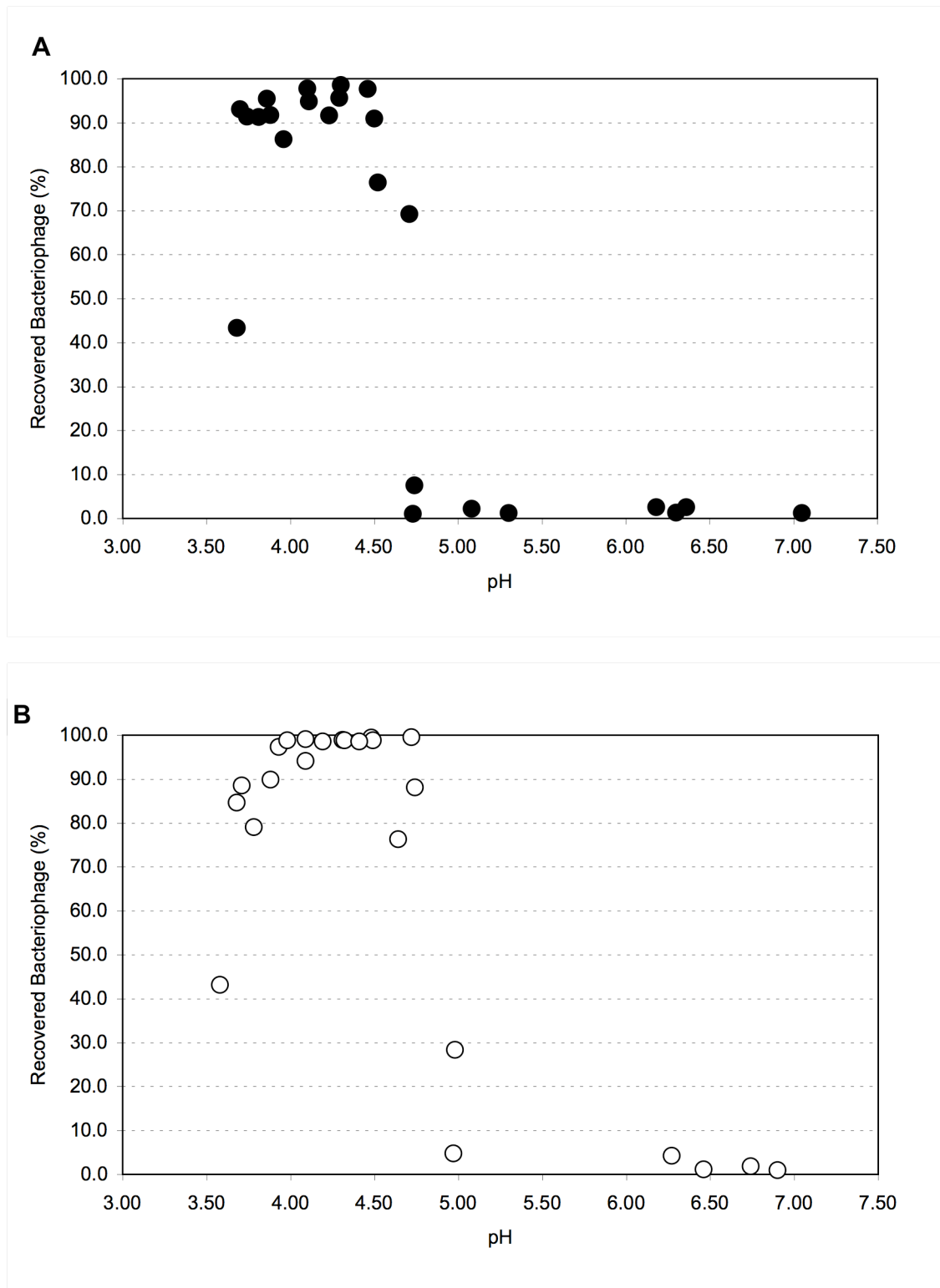
Figure 6.7 The recovery of bacteriophage M13 in the precipitate as a function of pH. (A) Incubation on ice for 24 hours (●). (B) Incubation at room temperature for 24 hours (○)."Recovered Bacteriophage (%)" refers to the quantity of bacteriophage in the precipitate as a proportion of the total recovered from the precipitate and supernatant fractions. Each data point represents an individual recovery, not an average of three recoveries. The experiment was conducted three times.

6.3.4 Assessment of bacteriophage degradation from acidic conditions

The total quantity of bacteriophage recovered (i.e. a summation of precipitate and supernatant counts) was calculated for each data point to allow for an assessment of bacteriophage degradation from the acidic conditions. The recoveries in the target pH ranges 3.7- 4.1, 4.1- 4.5 and 4.5- 4.9 were compared with the pooled recoveries at pH 7 for the experiments conducted on ice and at room temperature.

Table 6.2 shows that when incubated on ice for 24 hours the average bacteriophage titres at pH 7 and at pHs in the ranges 3.7- 4.1, 4.1- 4.5 and 4.5- 4.9 were not significantly different. When incubation was conducted at room temperature for 24 hours, the average bacteriophage titres at pH 7 and at pHs in the range 4.5- 4.9 were not significantly different, but were between titres at pH 7 and at pHs in the ranges 3.7- 4.1 and 4.1- 4.5. The data therefore suggest that conducting the experiment at a lower temperature may reduce the drop in titre. The "loss" of bacteriophage may be due to degradation by the acidic conditions, or perhaps aggregation, but since precipitation occurred on ice and viability losses were not significant it suggests that viability losses at room temperature were due to bacteriophage degradation.

Table 6.2 Total bacteriophage M13 recoveries (precipitate plus supernatant) expressed as pfu, post-isoelectric precipitation. Recoveries were averaged within the pH ranges of 3.7- 4.1, 4.1- 4.5 and 4.5- 4.9, and compared with the average recovery at pH 7. Statistical tests (t-test) were conducted on $\log_{10}$-transformed data. Uncertainties represent the standard error.

	pH condition			
	pH 3.7- 4.1	pH 4.1- 4.5	pH 4.5- 4.9	pH 7
Average titre after incubation on ice (pfu)	$3.23 \times 10^{12} \pm$ 7.8×10^{11}	$3.88 \times 10^{12} \pm$ 8.4×10^{11}	$4.29 \times 10^{12} \pm$ 7.1×10^{11}	$4.34 \times 10^{12} \pm$ 6.2×10^{11}
P value (t-test)	0.10	0.44	0.88	-
Average titre after incubation at room temperature (pfu)	2.5×10^{12} $\pm 3.6 \times 10^{11}$	$3.16 \times 10^{12} \pm$ 5.5×10^{11}	$3.42 \times 10^{12} \pm$ 6.8×10^{11}	$4.34 \times 10^{12} \pm$ 6.2×10^{11}
P value (t-test)	0.002	0.04	0.12	-

6.3.5 Reduction of the isoelectric precipitation incubation time

Since isoelectric precipitation of bacteriophage M13 was found to be possible, it was considered that the next appropriate step was to deviate from the conditions outlined by Bachrach and Friedmann (1971). In particular, the 24 hour incubation time was considered impractical. It was therefore investigated whether the incubation time could be reduced to zero, one or two hours without a reduction in bacteriophage recovery. The experiment was conducted as described in the Materials and Methods (Section 2.14.3). As a result of the data collected in Section 6.3.3, all precipitations were conducted at pH 4.3 and incubated on ice.

It was found that a 24 hour incubation time was unnecessary: an average 96.7 % of bacteriophage M13 were recovered in the precipitate even after no incubation on ice (Figure 6.8), increasing to 99.0 % after 1 hour. It was decided that one hour's incubation on ice would be prudent since the exact starting point of precipitation was subject to variation of several seconds depending on the speed of titration to pH 4.3. This variation may be reflected in the larger standard error of the zero hour incubation time relative to the 1 hour, 2 hour and 24 hour incubations (Figure 6.8).
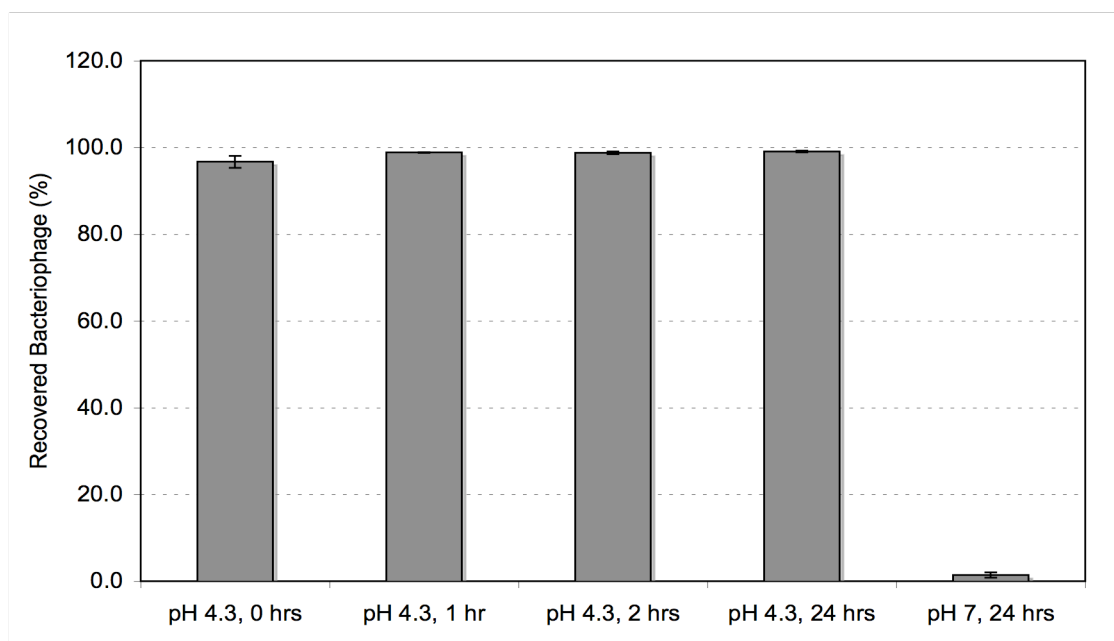
Figure 6.8 The percentage recovery of bacteriophage M13 in the precipitate as a function of incubation time on ice at pH 4.3 and pH 7. The percentage of recovered bacteriophage was calculated from the quantity of bacteriophage recovered in the precipitate as a proportion of the total. Errors bars represent the standard error, N=3.

6.4   Screening Experimentation of Several Precipitants

6.4.1   Introduction

Five further precipitants were investigated for the ability to precipitate bacteriophage M13 in a qualitative screening experiment. It was recognised in the previous work (Sections 6.2 and 6.3) that successful precipitation resulted in obvious white precipitates of bacteriophage at the tube wall after centrifugation. Using this knowledge to aid the speed of screening in this experiment, precipitation was solely judged on the appearance of the white bacteriophage precipitate. Precipitants CTAB, manganese sulphate, calcium chloride, spermidine and ammonium sulphate were selected for their diversity of action.

6.4.2   Reasoning for precipitant selection

The cationic precipitant CTAB has been demonstrated to selectively precipitate plasmid DNA from RNA, protein and LPS in clarified lysate (Lander *et al.*, 2001; Lander *et al.*, 2002; Tomanee *et al.*, 2004) at a concentration of less than 1 % (w/v). The dependence of protein solubility on CTAB concentration in clarified alkaline lysate has also been demonstrated (Tomanee *et al.*, 2004). The logic in investigating CTAB was that like DNA, bacteriophage M13 is a large biological polyanion which may therefore be readily precipitated.

The divalent cations Mn^{2+} (as manganese sulphate) and Ca^{2+} (as calcium chloride) have been shown to precipitate bacteriophage fd and M13 in a low ionic strength system (Tang *et al.*, 2002). In particular, bacteriophage M13 was shown to aggregate at concentrations as low as 15 mM (Mn^{2+}) and 60 mM (Ca^{2+}) and displayed resolubilisation as the concentration of calcium ions increased. Since these chemicals may afford effective low-cost bacteriophage precipitation, it was considered important to include them in this study.

Similarly to CTAB, the polycation spermidine has been demonstrated to selectively precipitate DNA from smaller oligonucleotides (Murphy *et al.*, 1999; Pelta *et al.*, 1996) at very low concentrations, typically of the order 1 mM in a low ionic strength system. However, in common with divalent cations, the action of spermidine is very sensitive to the concentration of monovalent cations, such as Na^+. It is thought that the monovalent cations reduce the bundling efficiency by a competitive mechanism (Murphy *et al.*, 1999; Tang *et al.*, 2002). The extent of this sensitivity was explored since the process fluid will contain several tens of millimoles of monovalent salts (such as sodium chloride).

Finally, the precipitation of bacteriophage M13 by 50 % (w/v) ammonium sulphate was assessed, based on the method of Rossomando and Zinder (1968). Although precipitation by inorganic salts lacks selectivity, ammonium sulphate precipitation was included for comparison because it has been employed on the large scale for many years (Atkinson *et al.*, 1987).

6.4.3   Experimentation

Screening experiments were conducted at the 1 ml scale, as described in the Materials and Methods (Section 2.14.1). The precipitation reactions were incubated for 15 minutes at room temperature, the most conservative conditions found in the literature (Pelta *et al.*, 1996). The exception was ammonium sulphate precipitation, which required a 24 hour incubation at room temperature (Rossomando and Zinder, 1968). Centrifugation speeds and times also varied between methods, so 10 minutes at 8 000 x g was chosen, which reflected the PEG precipitation conditions. The ranges of precipitant concentrations examined were based upon the existing literature (cited above). To investigate the effect of monovalent cations upon polyvalent cation precipitation, calcium chloride precipitation was conducted at 0, 50 and 100 mM NaCl, and spermidine precipitation was conducted at 0, 25 and 50 mM NaCl. All experiments were conducted twice.

6.4.4   Results

It was observed that, as expected, successful precipitation resulted in a white bacteriophage precipitate after centrifugation (first noted in Section 6.2.2). Again, the exception was ammonium sulphate precipitation where the bacteriophage formed a white float on the liquid surface. The measurement of pH of the reactions at the extremes of precipitant concentration showed that the pH remained between 6 and 7 in all cases, except for CTAB where the pH was 5.5 at 10 % (w/v). Successful precipitation was not observed from the addition of CTAB in the range 0.2- 10 % (w/v) (Table 6.3).

Table 6.3 Precipitation of bacteriophage M13 by CTAB of concentration 0- 10 % (w/v). Symbols: white bacteriophage precipitate observed (✓), no precipitate observed (✗).

	Concentration of CTAB, % (w/v)										
	0	0.2	0.4	0.6	0.8	1.0	2.0	4.0	6.0	8.0	10
M13 precipitate?	✗	✗	✗	✗	✗	✗	✗	✗	✗	✗	✗

Precipitation was observed from a concentration of 40 mM Mn^{2+} (Table 6.4) and 50 mM Ca^{2+} (Table 6.5). These values were similar to that reported by Tang *et al.* (2002) for Ca^{2+} ions, but was somewhat higher than the 15 mM reported for Mn^{2+}.

In low ionic strength conditions, spermidine was an effective precipitant of bacteriophage M13: precipitation was induced by 1.5 mM (Table 6.6). However, precipitation by both spermidine and Ca^{2+} ions was strongly dependent on the monovalent cation concentration (Table 6.5 and Table 6.6). The minimum concentration of Ca^{2+} ions to induce precipitation increased to 80 mM with the addition of 50 mM NaCl, and was prevented by the addition of 100 mM NaCl. Spermidine proved even more susceptible to Na^+ ions since precipitation was prevented by only 50 mM NaCl.

Table 6.4 Precipitation of bacteriophage M13 by Mn^{2+} ions of concentration 0- 50 mM. Symbols: white bacteriophage precipitate observed (✓), no precipitate observed (✗).

	Concentration of Mn^{2+} (mM)					
	0	15	20	30	40	50
M13 precipitate?	✗	✗	✗	✗	✓	✓

Table 6.5 Precipitation of bacteriophage M13 by Ca^{2+}ions of concentration 0- 20 mM (0 or 50 mM NaCl present) and 0- 800 mM (100 mM NaCl present). Symbols: white bacteriophage precipitate observed (✓), no precipitate observed (✗).

	Concentration of Ca^{2+} (mM)							
	0	20	40	50	60	80	100	120
0 mM NaCl M13 precipitate?	✗	✗	✗	✓	✓	✓	✓	✓
50 mM NaCl M13 precipitate?	✗	✗	✗	✗	✓	✓	✓	✓

	Concentration of Ca^{2+} (mM)							
	0	50	100	200	300	400	600	800
100 mM NaCl M13 precipitate?	✗	✗	✗	✗	✗	✗	✗	✗

Table 6.6 Precipitation of bacteriophage M13 by spermidine of concentration 0- 4 mM (0 mM NaCl present) and 0- 50 mM (25 or 50 mM NaCl present). Symbols: white bacteriophage precipitate observed (✓), no precipitate observed (✗).

	Concentration of spermidine (mM)					
	0	1	1.5	2	3	4
0 mM NaCl M13 precipitate?	✗	✗	✓	✓	✓	✓

	Concentration of spermidine (mM)						
Spermidine mM	0	4	10	20	30	40	50
25 mM NaCl M13 precipitate?	✗	✗	✗	✓	✓	✓	✓
50 mM NaCl M13 precipitate?	✗	✗	✗	✗	✗	✗	✗

Precipitation of bacteriophage M13 by the traditional "salting out" method occurred at concentrations above 40 % (w/v) ammonium sulphate (Table 6.7). The resulting bacteriophage "float" on the liquid surface could be removed by filtration (Rossmando and Zinder 1968).

Table 6.7 Precipitation of bacteriophage M13 by ammonium sulphate of concentration 0- 50 % (w/v). Symbols: white bacteriophage float observed (✓), no precipitation observed (✗).

	Concentration of ammonium sulphate (%, w/v)					
	0	15	20	30	40	50
M13 precipitate?	✗	✗	✗	✗	✓	✓

6.5 Divalent and Polyvalent Cation Precipitation of Bacteriophage M13

Of the five methods tested in Section 6.4, spermidine and Ca^{2+} ion precipitations were taken forward for investigation at the 10 ml scale and titred for bacteriophage recovery. It was considered that these offered the greatest potential benefits in terms of cost (little is needed for precipitation), biocompatibility (less likely to denature protein) and potential selectivity

(demonstrated in the literature). Precipitation experiments were conducted as described in the Materials and Methods (Section 2.14.4), and were repeated three times. Spermidine and Ca^{2+} ions were examined under low ionic strength conditions and at the NaCl concentrations found in Section 6.4 to prevent the formation of visible bacteriophage precipitates. The concentration ranges were increased beyond those examined in Section 6.4 to observe the resolubilisation phenomenon reported elsewhere for Ca^{2+} ions (Tang *et al.*, 2002) and spermidine (Pelta *et al.*, 1996). If carefully controlled, such a phenomenon could be exploited to assist bacteriophage purification.

Post-centrifugation, it was confirmed that the visibility of a white precipitate in Ca^{2+} and spermidine precipitations in Section 6.4 correlated with a >70 % recovery of bacteriophage in the precipitate (Figure 6.9 and Figure 6.10). In Ca^{2+} ion precipitations (Figure 6.9) with 0 mM NaCl present, bacteriophage recovery above 94 % in the precipitate was observed in the range 60- 100 mM Ca^{2+}, but dropped in the range 100- 200 mM to 73 %. Precipitation was prevented once the concentration of Ca^{2+} ions exceeded 300 mM. No precipitation of bacteriophage occurred in the presence of 100 mM NaCl up to a concentration of 400 mM Ca^{2+} ions.
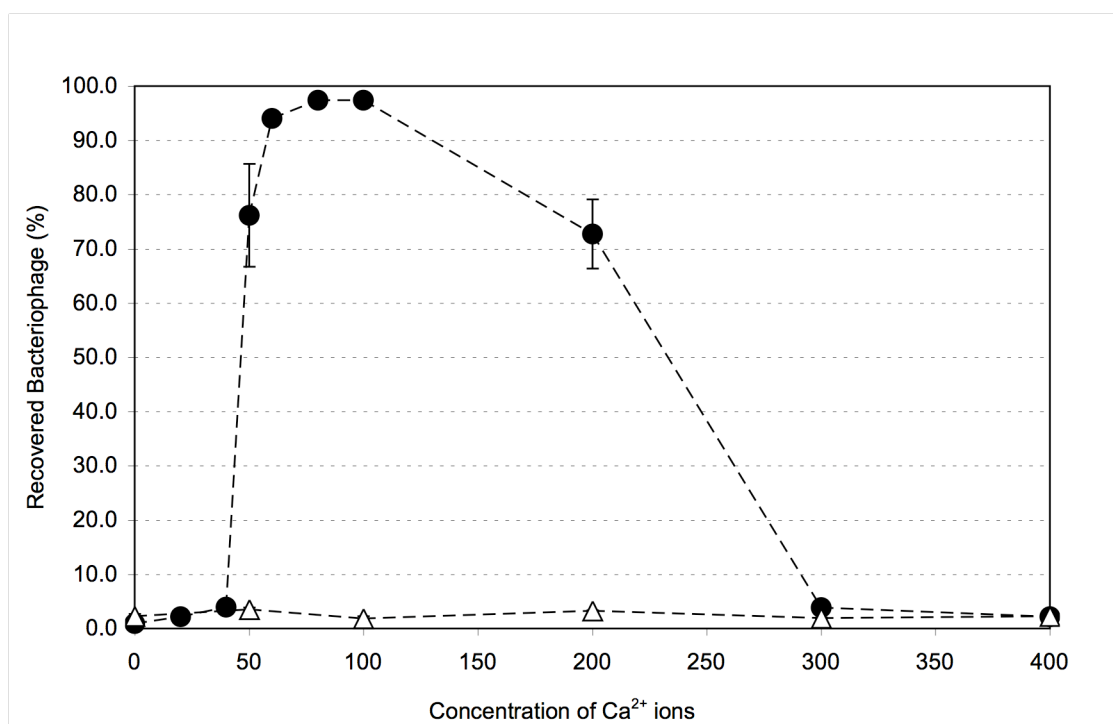
Figure 6.9 The recovery of bacteriophage M13 in the precipitate as a function of Ca^{2+} ion concentration at 0 mM (●) and 100 mM (△) NaCl. The percentage of recovered bacteriophage was calculated from the quantity of bacteriophage recovered in the precipitate as a proportion of the total. When no NaCl was present, it can be seen that >90 % recovery of bacteriophage M13 in the precipitate was achieved between Ca^{2+} ion concentrations of 60 mM and 100 mM. Errors bars represent the standard error, N=3.

For spermidine precipitation in the absence of NaCl, bacteriophage recovery above 95 % in the precipitate was observed above a spermidine concentration of 1.5 mM (Figure 6.10). No failure to precipitate was observed at the higher spermidine concentrations tested in this experiment. However, a resolubilisation phenomenon may still be possible at concentrations of spermidine greater than those tested here. No precipitation of bacteriophage occurred in the presence of 50 mM NaCl up to a concentration of 50 mM spermidine.
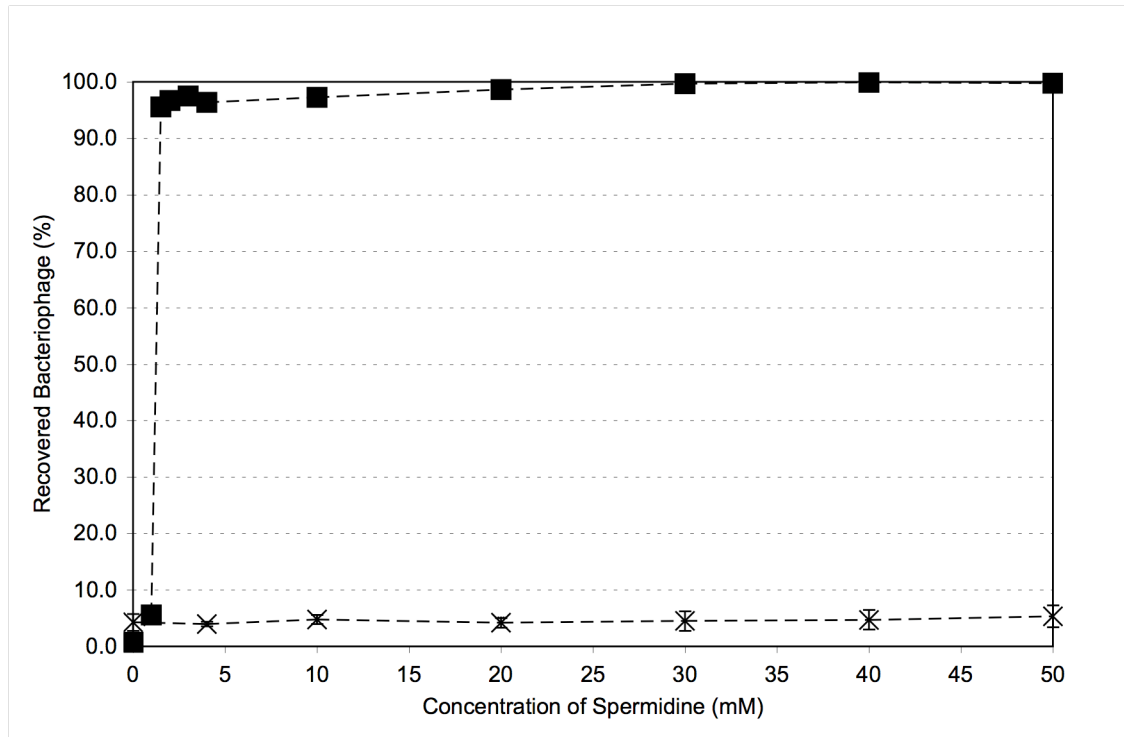
Figure 6.10 The recovery of bacteriophage M13 in the precipitate as a function of spermidine concentration at 0 mM (■) and 50 mM (×) NaCl. The percentage of recovered bacteriophage was calculated from the quantity of bacteriophage recovered in the precipitate as a proportion of the total. Error bars represent the standard error, N=3.

6.6 Precipitation of Bacteriophage M13 from Broth

6.6.1 Determination of the major NB2 ion components

In reality, bacteriophage M13 will be precipitated out of a culture medium. Since the components present will depend on the media used, precipitant performance needs to be examined prior to use in a new medium. Of particular importance will be the ion concentration. The medium used in this study was NB2 (see Section 2.1.6). Chemical analysis of NB2 shows it should contain approximately 92 mM of NaCl at 1x concentration (data supplied by the manufacturer), which suggests that it will alter precipitation behaviour. This value was confirmed experimentally by the testing of three 1 ml samples of sterile unused NB2 in a Nova BioProfile 400 chemical analysis device (Table 6.8). For comparison, three 1 ml samples of used NB2 were also tested (three 50 ml M13 infected *E. coli* Top10F' cultures grown for 5 hours, cells pelleted at 13 000 x g for 3 minutes. See Chapter 4, Section 4.2.2). It can be seen that in addition to the 95 mM of Na^+ ions in fresh NB2, several millimolars of ammonium (NH_4^+) and potassium (K^+) ions were present, both of which are monovalent cations and therefore may also affect precipitation behaviour. It can also be seen that ion levels were broadly unchanged by culture growth.

Table 6.8 Chemical analysis of fresh and used NB2 by Nova BioProfile 400. Figures are an average of three readings. In addition to these components the BioProfile also outputs readings for glucose and lactose, neither of which were detected.

Component	Concentration in broth (mM)		
	Fresh sterile NB2	Post culture NB2	P value (t-test)
Glutamine	0.61	0.22	5.5×10^{-6}
Glutamic acid	2.05	1.5	7.7×10^{-5}
NH_4^+	1.42	5.45	1.3×10^{-7}
Na^+	95	97	0.24
K^+	4.9	5.0	0.25

6.6.2 Screening experimentation of precipitants in broth

Seven precipitants were tested for their ability to precipitate bacteriophage M13 from clarified culture medium in a qualitative screening experiment at the 10 ml scale (Materials and Methods, Section 2.14.5). These were: 2 % (w/v) PEG 6 000 with $MgSO_4$ or NaCl; 4 % (w/v) PEG 6 000 with $MgSO_4$ or NaCl; isoelectric precipitation (pH 4.3); spermidine; Ca^{2+} ions. The PEG

concentrations were selected to represent the higher PEG/ low salt and lower PEG/ higher salt options (Section 6.2.5). As was conducted in Section 6.4, successful precipitation was primarily determined by the appearance of a bacteriophage precipitate post-centrifugation. However, reactions giving successful precipitation (at the lowest precipitant quantities) were investigated for bacteriophage recovery in the precipitate. All experiments were conducted twice.

For PEG-salt precipitation reactions, successful precipitation occurred by the addition of 135 mM NaCl to 2 % (w/v) PEG 6 000 (Table 6.9), which was over 100 mM less than the concentration of NaCl required to induce precipitation in the pure system (Section 6.2.5). In Table 6.10 it can be seen that precipitation occurred by the addition of 25 mM $MgSO_4$ to 2 % (w/v) PEG 6 000, which was 40 mM less than the concentration required to induce precipitation in the pure system (Section 6.2.7).

Table 6.9 Precipitation of bacteriophage M13 in NB2 by 2 % (w/v) PEG 6 000 and NaCl of concentration 0- 500 mM. The percentage of recovered bacteriophage was calculated from the quantity of bacteriophage recovered in the precipitate as a proportion of the total. Symbols: white bacteriophage precipitate observed (✓), no precipitate observed (✗).

	Concentration of NaCl (mM)									
	0	35	65	100	135	165	200	300	400	500
M13 precipitate?	✗	✗	✗	✓	✓	✓	✓	✓	✓	✓
Recovered Bacteriophage (%)				75.0	97.0	97.3				

Table 6.10 Precipitation of bacteriophage M13 in NB2 by 2 % (w/v) PEG 6 000 and $MgSO_4$ of concentration 0- 200 mM. The percentage of recovered bacteriophage was calculated from the quantity of bacteriophage recovered in the precipitate as a proportion of the total. Symbols: white bacteriophage precipitate observed (✓), no precipitate observed (✗).

	Concentration of $MgSO_4$ (mM)						
	0	15	25	35	65	100	200
M13 precipitate?	✗	✗	✓	✓	✓	✓	✓
Recovered Bacteriophage (%)			97.4				

Under pure conditions, the precipitation of bacteriophage M13 by 4 % (w/v) PEG 6 000 required the addition of 135 mM NaCl or 15 mM $MgSO_4$. In NB2, it was found that precipitation occurred due to the addition of 4 % (w/v) PEG 6 000 alone (Table 6.11 and Table 6.12). The ionic strength of NB2 was therefore sufficiently high already. It was of subsequent interest to determine the minimum concentration of PEG 6 000 in NB2 that would induce precipitation of M13. It was found that 4 % (w/v) PEG 6 000 was the minimum required (Table 6.13).

Table 6.11 Precipitation of bacteriophage M13 in NB2 by 4 % (w/v) PEG 6 000 and NaCl of concentration 0- 300 mM. The percentage of recovered bacteriophage was calculated from the quantity of bacteriophage recovered in the precipitate as a proportion of the total. Symbols: white bacteriophage precipitate observed (✓), no precipitate observed (✗).

NaCl mM	Concentration of NaCl (mM)							
	0	15	25	35	65	100	200	300
M13 precipitate?	✓	✓	✓	✓	✓	✓	✓	✓
Recovered Bacteriophage (%)	95.3							

Table 6.12 Precipitation of bacteriophage M13 in NB2 by 4 % (w/v) PEG 6 000 and $MgSO_4$ of concentration 0- 200 mM. The percentage of recovered bacteriophage was calculated from the quantity of bacteriophage recovered in the precipitate as a proportion of the total. Symbols: white bacteriophage precipitate observed (✓), no precipitate observed (✗).

	Concentration of $MgSO_4$ (mM)						
	0	15	25	35	65	100	200
M13 precipitate?	✓	✓	✓	✓	✓	✓	✓
Recovered Bacteriophage (%)	90.2						

Table 6.13 Precipitation of bacteriophage M13 in NB2 by PEG 6 000 of concentration 2- 4 % (w/v). Symbols: white bacteriophage precipitate observed (✓), no precipitate observed (✗).

	Concentration of PEG 6 000, % (w/v)					
	2.0	2.5	3.0	3.3	3.5	4.0
M13 precipitate?	✗	✗	✗	✗	✗	✓

Isoelectric precipitation of bacteriophage M13 in NB2 was successful at pH 4.3 with an average of 99.7 % of recovered bacteriophage in the precipitate.

As a result of experimentation with purified bacteriophage M13 (Section 6.5) it was hypothesized that since spermidine and Ca^{2+} ions failed to precipitate M13 in the presence of up to 100 mM NaCl, precipitation would not be successful in NB2. This indeed proved to be so (Table 6.14 and Table 6.15). No white bacteriophage precipitates were observed at any concentration of spermidine. No white bacteriophage precipitates were observed at any concentration of Ca^{2+} ions either, but a heavy brown sediment was observed in every tube to which Ca^{2+} ions had been added. To check that this sediment did not include M13, precipitates and supernatants were titred for bacteriophage (Table 6.15). As a further check a control run was conducted, essentially repeating the experiment in fresh sterile NB2 (no bacteriophage present). Identical brown sedimentation was observed. The 1 M $CaCl_2$ stock (made up in sterile NB2) was noted to be turbid from which brown sediment could also be pelleted. It was concluded that irreversible precipitation of NB2 components may have occurred in the 1 M $CaCl_2$ stock. Enumeration of bacteriophage M13 showed that no bacteriophage precipitation had occurred.

Table 6.14 Precipitation of bacteriophage M13 in NB2 by spermidine of concentration 0- 50 mM. Symbols: white bacteriophage precipitate observed (✓), no precipitate observed (✗).

	Concentration of spermidine (mM)						
	0	4	10	20	30	40	50
M13 precipitate?	✗	✗	✗	✗	✗	✗	✗

Table 6.15 Precipitation of bacteriophage M13 in NB2 by Ca^{2+} ions of concentration 0- 400 mM. The percentage of recovered bacteriophage is the proportion within the precipitate. Symbols: white bacteriophage precipitate observed (✓), no precipitate observed (✗).

	Concentration of Ca^{2+} (mM)					
	0	50	100	200	300	400
M13 precipitate?	✗	✗	✗	✗	✗	✗
Recovered Bacteriophage (%)	2.4	1.7	1.8	2.0	2.6	2.0

6.7 Precipitant Comparison in Terms of Bacteriophage M13 Purification

6.7.1 Introduction

The aim of the final stage of this chapter was to take candidate precipitants of bacteriophage M13 and compare them in terms of the purification factor achieved. In this study, purification factor (P.F.) is defined as:

$$P.F. = \frac{pfu/X}{pfu_0/X_0} \qquad (2)$$

where *pfu* is the concentration of bacteriophage, *X* the concentration of contaminant and subscript *0* denotes an initial concentration. Purification is important, since application of the most selective primary purification step possible could reduce the number of further downstream processing stages, thereby reducing production costs. Since every one of the successful precipitants identified in Section 6.6 achieved greater than 90 % bacteriophage recovery, differentiation instead must focus on their relative purification abilities, costs and removal.

On the large-scale, precipitation ingredients are typically added as a dry powder, rather than as concentrated liquid stocks (Belter *et al.*, 1988). To reflect this, precipitants were added as dry ingredients to clarified, filtered culture. Since at the 10 ml scale the quantities of precipitants added would be very small, precipitation reactions were scaled to 40 ml in 50 ml polypropylene tubes. As a result of the findings of Section 6.6, the precipitants examined were:

- 2 % (w/v) PEG 6 000 with 135 mM NaCl
- 2 % (w/v) PEG 6 000 with 25 mM $MgSO_4$
- 4 % (w/v) PEG 6 000 alone
- isoelectric precipitation at pH 4.3

Experiments were conducted as described in the Materials and Methods (Section 2.14.6). Each precipitate was resuspended in 800 μl 20 mM Tris to give a 50-fold increase in bacteriophage concentration: this represented a realistic concentration factor (Asenjo and Patrick, 1990). A portion of each resuspended precipitate (5 μl) was 50-fold diluted back to the same bacteriophage concentration found in untreated culture, which allowed for a like-for-like comparison of the purification achieved. All experiments were conducted three times.

Following the methods described in Chapter 4, the quantities of chromosomal DNA (Section 4.2.3) and protein (Section 4.2.5) were measured in each resuspended precipitate, 50-fold diluted precipitate, supernatant and untreated culture. Therefore, DNA was measured by agarose gel electrophoresis and protein by Bradford assay (for total protein) and SDS-PAGE (for larger polypeptides).

6.7.2 Comparison of bacteriophage M13 recovery

The recoveries of bacteriophage M13 by each precipitation method are shown in Table 6.16. As usual, the percentages of recovered bacteriophage from precipitation are presented, calculated from the quantity of bacteriophage enumerated in the precipitate (or supernatant) as a proportion of the total. In addition, absolute bacteriophage numbers are given (in pfu) in the untreated culture, precipitate and supernatant environments. Finally, the bacteriophage recoveries are expressed as fractional quantities relative to the average amount of bacteriophage in all untreated cultures.

It can be seen that recoveries of bacteriophage M13 were in excess of 90 % in the precipitate from precipitation methods 2 % (w/v) PEG 6 000 with 135 mM NaCl (93 %), 4 % (w/v) PEG 6 000 alone (92 %) and isoelectric precipitation (96 %). The exception was 2 % (w/v) PEG 6 000 with 25 mM MgSO$_4$, which yielded a recovery of 89 %. Here, it was noted that some precipitate loss occurred on supernatant decantation.

When compared on a fractional basis – that is, bacteriophage recovery expressed as a fraction of the average quantity enumerated in untreated cultures – all precipitants performed similarly (Table 6.16). A >0.9 fraction of the input bacteriophage were recovered in the precipitate in every case.

In terms of the percentage bacteriophage recovery in the precipitate, the recoveries achieved by isoelectric precipitation in this chapter were consistently higher than those achieved by PEG precipitation methods. Since PEG precipitation methods generally produced maximum recoveries in the range 90- 96 % by this assay (Section 6.2.2), it was assumed that isoelectric

precipitation either led to more firmly attached precipitates or that the lower solution viscosity resulted in less precipitate disturbance on supernatant decantation.

Table 6.16 Precipitation of bacteriophage M13 in NB2 by four precipitation methods. The percentage of recovered bacteriophage was calculated as a proportion of the total recovered. Bacteriophage quantities (in pfu) represent the total population in each environment. Each fractional quantity was calculated relative to the average quantity of bacteriophage in untreated cultures.

Precipitants	Recovered Bacteriophage (%)		
	Untreated culture	Precipitate	Supernatant
2 % (w/v) PEG 6 000, 135 mM NaCl	-	93.0 ± 0.8	6.9 ± 0.8
2 % (w/v) PEG 6 000, 25 mM MgSO$_4$	-	89.1 ± 1.3	10.9 ± 1.3
4 % (w/v) PEG 6 000	-	92.2 ± 0.1	7.8 ± 0.1
Isoelectric precipitation, pH 4.3	-	95.5 ± 0.2	4.5 ± 0.2

Precipitants	Bacteriophage quantity (pfu)		
	Untreated culture	Precipitate	Supernatant
2 % (w/v) PEG 6 000, 135 mM NaCl	2.2×10^{13} ± 1.2×10^{12}	2.2×10^{13} ± 1.9×10^{12}	1.6×10^{12} ± 2.9×10^{11}
2 % (w/v) PEG 6 000, 25 mM MgSO$_4$	2.2×10^{13} ± 1.6×10^{12}	2.0×10^{13} ± 8.6×10^{11}	2.5×10^{12} ± 3.6×10^{11}
4 % (w/v) PEG 6 000	2.1×10^{13} ± 2.2×10^{12}	2.0×10^{13} ± 2.6×10^{12}	1.7×10^{12} ± 1.9×10^{11}
Isoelectric precipitation, pH 4.3	1.9×10^{13} ± 5.5×10^{11}	1.9×10^{13} ± 1.4×10^{12}	9.2×10^{11} ± 3.1×10^{10}

Precipitants	Fractional value		
	Untreated culture	Precipitate	Supernatant
2 % (w/v) PEG 6 000. 135 mM NaCl	1.04 ± 0.06	0.98 ± 0.06	0.12 ± 0.01
2 % (w/v) PEG 6 000, 25 mM MgSO$_4$	1.00 ± 0.07	0.98 ± 0.08	0.08 ± 0.01
4 % (w/v) PEG 6 000	1.06 ± 0.03	1.07 ± 0.06	0.08 ± 0.01
Isoelectric precipitation, pH 4.3	0.92 ± 0.06	0.93 ± 0.06	0.04 ± 0.00

6.7.3   Quantification of DNA

All three PEG-based precipitation methods resulted in a marked separation of bacteriophage M13 from contaminating DNA (Figure 6.11). DNA remained in the supernatant as bacteriophage M13 was pelleted. Quantification of the chromosomal DNA bands by densitometry showed that there was no significant difference in the precipitate DNA concentration between the three PEG-based methods ($P>0.05$ in all comparisons, Tukey).

In the three PEG-based methods the average reduction in DNA was from 4.7 μg ml^{-1} in untreated culture to only 0.7 μg ml^{-1} in the resuspended precipitates, even though the bacteriophage concentration was fifty-fold greater (Figure 6.12). On an equal bacteriophage concentration basis, this represented an average purification factor in excess of 300.

The purification performance of isoelectric precipitation was different. The quantity of DNA in the precipitate was high such that it could not be enumerated by densitometry (Figure 6.12). However, the amount of DNA quantified in the fifty-fold diluted precipitate, at 4.1 μg ml^{-1}, nearly matched that of the untreated culture (5.0 μg ml^{-1}). This represented an average purification factor of only 1.2.
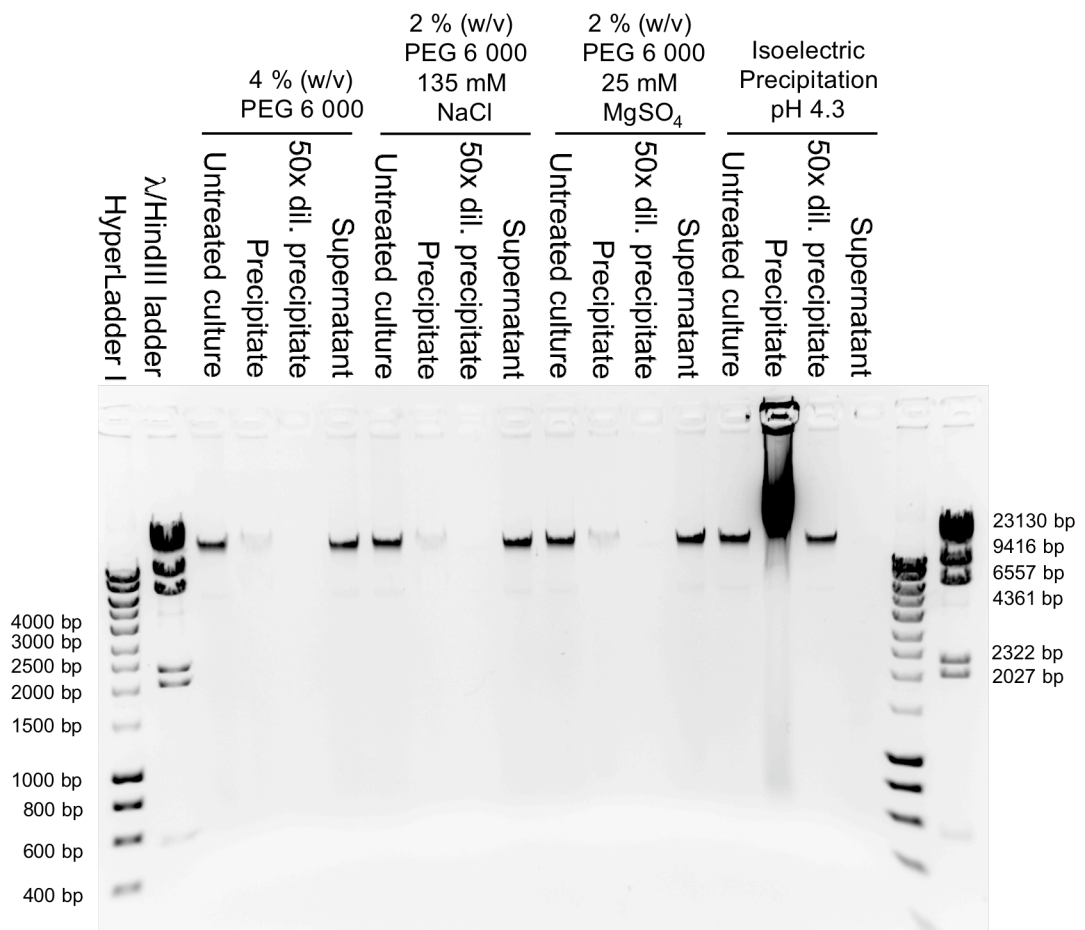
Figure 6.11 Agarose gel showing the fate of chromosomal DNA in each of the four tested precipitations. Bacteriophage M13 DNA is not visible due to the encapsulating protein coat (Section 4.2.3). An equivalent of 10 µl of sample was loaded in each well. The three PEG-based precipitation methods performed similarly, in that DNA remained in the supernatant fractions. Of particular note was the large quantity of DNA that was sedimented by isoelectric precipitation, and was therefore identified in the precipitate. An agarose gel was prepared for each of the three experimental repeats. Band intensities were subsequently quantified by densitometry as described in the Materials and Methods (Section 2.7.4).
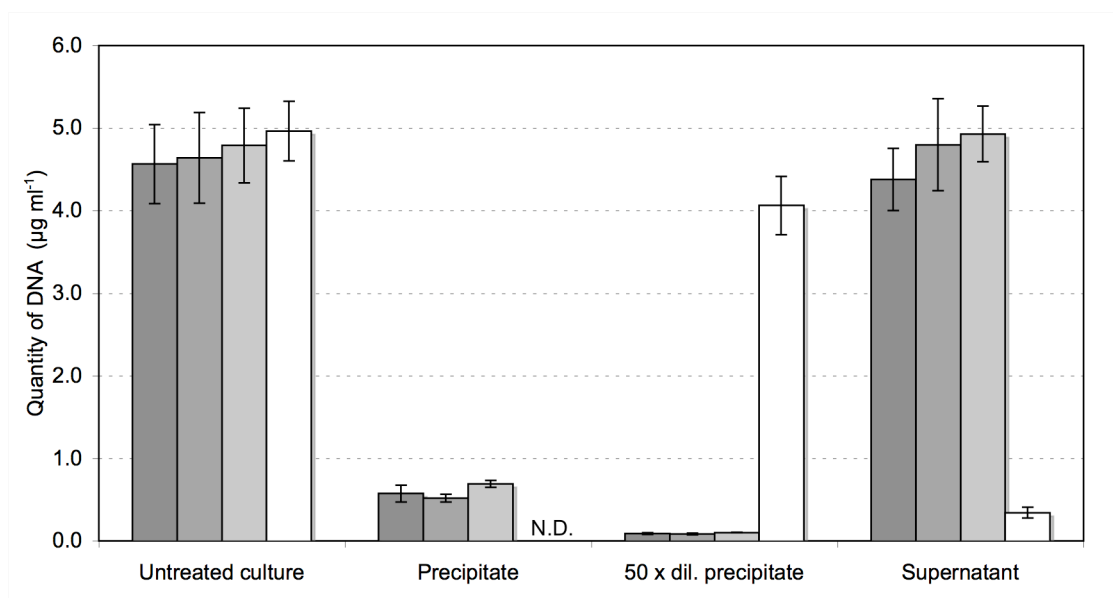
Figure 6.12 Quantification of the DNA band intensities shown in Figure 6.11. The quantity of DNA in the undiluted isoelectric precipitation precipitate was not measured due to its high concentration ("N.D."). Symbols: 4 % (w/v) PEG 6 000 alone (■), 2 % (w/v) PEG 6 000 with 135 mM NaCl (■), 2 % (w/v) PEG 6 000 with 25 mM MgSO$_4$ (■), isoelectric precipitation (□). Error bars represent the standard error, N=3.

6.7.4   Controls for the quantification of protein by Bradford assay

The Bradford assay was performed as described in the Materials and Methods (Section 2.7.5) with a 0.66-fold serially diluted 1 mg ml^{-1} BSA standard. Absorbance at 595 nm was linear in the range 13- 225 µg ml^{-1} BSA. To ensure that readings were not due to chemical interference from the precipitants used, control samples were first analysed. These consisted of each of the candidate precipitants made up in sterile RO water with 4 x 10^{11} pfu ml^{-1} caesium chloride purified bacteriophage M13, as well as unused NB2 and sterile RO water alone. The theoretical concentration of BSA corresponding to each of the absorbances of these precipitants is shown in Table 6.17. It can be seen that the measured effect of each of the precipitants was minimal, giving confidence that absorbances observed were indeed due to protein. As shown previously in Chapter 4 (Section 4.2.5), the peptide content of NB2 is detected by the Bradford assay.

Table 6.17 Bradford assay control samples. Precipitants were made up in sterile RO water (rather than NB2) and the absorbance at 595 nm measured. The equivalent concentration of BSA giving the same absorbance is shown.

Control Sample	Equivalent BSA Concentration μg ml^{-1}
Sterile RO water	0.0 ± 2.7
NB2	24.3 ± 3.5
2 % (w/v) PEG 6 000, 135 mM NaCl	3.3 ± 2.3
2 % (w/v) PEG 6 000, 25 mM MgSO$_4$	1.7 ± 1.6
4 % (w/v) PEG 6 000	1.8 ± 1.9
Isoelectric precipitation, pH 4.3	0.4 ± 2.2

It was also necessary to control for the measurement of protein as a consequence of the bacteriophage present, particularly important after concentration into the precipitate. A 500 μl aliquot of caesium chloride purified bacteriophage M13 of concentration 6.3×10^{13} pfu ml^{-1} was three-fold serially diluted down to a concentration of 2.9×10^{10} pfu ml^{-1}. Samples were then subject to the Bradford assay and the (measured) concentration of protein determined as a function of pfu ml^{-1} (Figure 6.13).

For comparison, the concentration of protein theoretically present (also as a function of pfu ml^{-1}) was calculated by summation of the total quantity of coat protein per bacteriophage (see Chapter 1, Section 1.2.2, for a description of the bacteriophage coat proteins and their corresponding molecular weights). This value was expected to be greater than the measured quantity, since a significant proportion of the amino acids of the bacteriophage coat are not exposed to the surroundings.

The detected concentration of protein was very low up to a bacteriophage count of mid- 10^{12} pfu ml^{-1}, and increased rapidly above this point (Figure 6.13). The concentration of protein correlating to the bacteriophage count in every precipitate was therefore subtracted, since bacteriophage concentrations of the order 10^{13} pfu ml^{-1} were present in these samples.
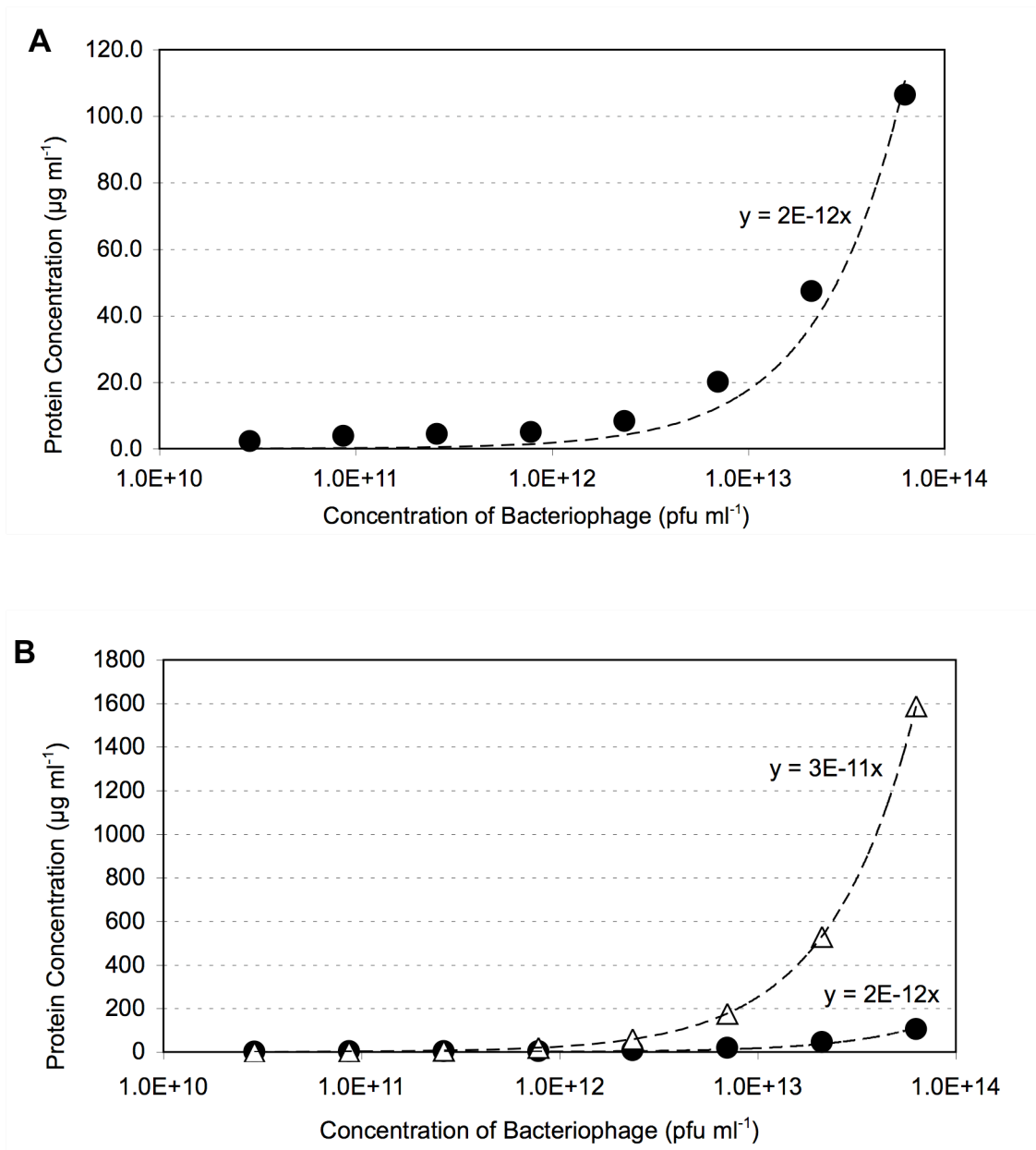
Figure 6.13 The concentration of protein measured by Bradford assay as a function of (A) bacteriophage concentration (●). (B) Comparison between the theoretical quantity of protein as a function of bacteriophage concentration (△) and the measured quantity by Bradford assay (●).

6.7.5 Quantification of protein by Bradford assay

On the basis of measured protein concentration, all three PEG-based precipitation methods again resulted in separation of bacteriophage M13 from contaminants (Figure 6.14). All performed similarly, that is, there was no significant difference in the precipitate protein concentrations (P>0.05 in all comparisons, Tukey). On average, a reduction of protein from approximately 92 µg ml^{-1} in untreated culture to 9 µg ml^{-1} in the resuspended precipitates was observed, even though the bacteriophage concentration was fifty-fold greater. On an equal bacteriophage concentration basis, this represented a minimum purification factor in excess of 250, similar to that observed for DNA. The purification performance of isoelectric precipitation was again different to the PEG-based methods: precipitation of soluble culture protein occurred. The quantity of protein in the fifty-fold diluted precipitate, at 24.2 µg ml^{-1}, was high compared to the virtually undetectable levels of protein in the fifty-fold diluted precipitates of the PEG-based precipitation methods (Figure 6.14). Isoelectric precipitation achieved an average purification factor of 3.8.
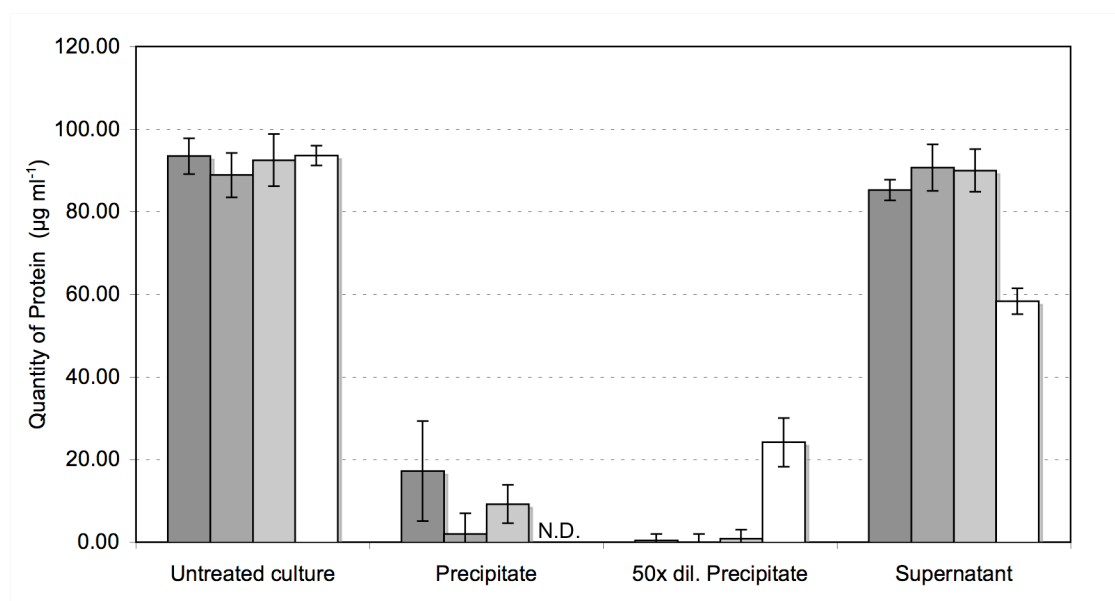
Figure 6.14 The quantity of total protein measured in each sample by the Bradford assay. The protein contribution from bacteriophage M13 was subtracted from all reading (Section 6.7.4). Symbols: 4 % (w/v) PEG 6 000 alone (■), 2 % (w/v) PEG 6 000 with 135 mM NaCl (■), 2 % (w/v) PEG 6 000 with 25 mM MgSO$_4$ (■), isoelectric precipitation (□). Error bars represent the standard error, N=3.

6.7.6 Quantification of protein by SDS-PAGE densitometry

The purification ability of each precipitation method was also visualised by SDS-PAGE (see Materials and Methods, Section 2.7.3, SYPRO Ruby stain). The quantity of protein in the range 20- 212 kDa in each lane was measured relative to the untreated culture sample (Section 2.7.4.). Therefore, protein quantity in each sample was calculated as a fraction of that in untreated culture.

The three PEG-based precipitation methods resulted in lower levels of protein in the precipitate than isoelectric precipitation (Figure 6.15). Compared with the protein concentration in untreated culture, the relative concentrations of protein in each precipitate were 1.4 (4 % (w/v) PEG 6 000 alone), 1.0 (2 % (w/v) PEG 6 000 with 135 mM NaCl), 1.3 (2 % (w/v) PEG 6 000 with 25 mM $MgSO_4$) and 13.4 (isoelectric precipitation). Furthermore, on an equal bacteriophage concentration basis (50-fold diluted precipitate) the PEG-based methods represented an average purification factor of approximately 50, which was substantially less than the purification factors in excess of 250 calculated on the basis of total protein by the Bradford assay. As before, isoelectric precipitation achieved a substantially lower average purification factor, which remained at 3.8.

Top gel:

4 % (w/v) PEG 6 000

2 % (w/v) PEG 6 000 135 mM NaCl

Untreated culture | Precipitate | 50x dil. precipitate | Supernatant | Precipitate | 50x dil. precipitate | Supernatant | Unused NB2 | Purified M13 | Ladder

M13 pIII

212 kDa
158 kDa
97.2 kDa
66.4 kDa
42.7 kDa
34.6 kDa
27.0 kDa
20.0 kDa

Relative intensity: 1.0 1.4 0.1 1.0 1.0 0.1 1.0 0.0 0.0

Bottom gel:

2 % (w/v) PEG 6 000 25 mM MgSO$_4$

Isoelectric Precipitation pH 4.3

Untreated culture | Precipitate | 50x dil. precipitate | Supernatant | Precipitate | 50x dil. precipitate | Supernatant | Unused NB2 | Purified M13 | Ladder

M13 pIII

212 kDa
158 kDa
97.2 kDa
66.4 kDa
42.7 kDa
34.6 kDa
27.0 kDa
20.0 kDa

Relative intensity: 1.0 1.3 0.0 1.1 13.4 0.5 0.7 0.0 0.0

Figure 6.15 SDS-PAGE gels showing the relative quantities of protein in each precipitation sample. An equivalent of 10 µl of sample was loaded in each well. An SDS gel was prepared for each of three experimental repeats. Relative intensities were determined by densitometry as described in the Materials and Methods (Section 2.7.4).

6.8 Discussion

The aim of this chapter was to identify precipitants of bacteriophage M13 which would have potential in an effective primary purification step at the large-scale. Therefore, all precipitations were conducted at a bacteriophage concentration of approximately 10^{11} pfu ml^{-1}, similar to that found in the post-fermentation broth (see Chapter 4). Precipitants were initially investigated with purified bacteriophage to determine fundamental characteristics, before experimentation was conducted in a broth system. Finally, four precipitation candidates were taken forward and compared on the basis of purification ability.

6.8.1 PEG precipitation of M13: the effect of increasing PEG molecular weight

Several precipitants were investigated in this chapter, beginning with the PEG-salt system. Increasing the degree of polymerisation of the PEG (and thereby increasing chain length and average molecular weight) improved its ability to precipitate protein. The effect was found to be most significant at lower average molecular weights, and became increasingly marginal at average molecular weights above 6 000. Such a pattern was consistent with reported experimentation for other proteins (Atha and Ingham, 1981; Boncina et al., 2007; Boncina et al., 2008; Mahadevan and Hall, 1992). This trend suggested that an optimum PEG molecular weight existed. Although increasing the molecular weight from 6 000 to 20 000 only reduced the required PEG concentration by 0.5 % (w/v), solution viscosity was shown to increase by 70 % (Section 6.2.5). Therefore in processing terms there appeared to be little benefit in increasing the PEG molecular weight above 6 000. Similar conclusions have been drawn by reporters investigating the precipitation behaviour of other proteins (Mahadevan and Hall, 1992; Yamamoto et al., 1970).

6.8.2 PEG precipitation of M13: the effect of incubation time and temperature

The volume exclusion mechanism is primarily an entropic rather than enthalpic process (Atha and Ingham, 1981; Boncina et al., 2008), which explains why temperature had only a marginal effect on the precipitation of bacteriophage M13 (Section 6.2.6). The effective precipitation by PEG over a broad temperature range confers certain processing advantages: dispensing with process stream cooling saves on operating expenses, and its robustness means the precipitation temperature can also be less tightly controlled. However, its flexibility means that if lower temperatures were required – for example, to protect a particularly fragile display protein – precipitation would not be compromised. Nevertheless, it has also been extensively noted in the literature that PEG is generally a non-denaturing precipitation agent (Ingham, 1990; Sharma and Kalonia, 2004; Tsoka et al., 2000). That PEG precipitation was observed to occur rapidly (Section 6.2.6) means that such a stage need not be time-intensive.

6.8.3 PEG precipitation of M13: the effect of increasing solution ionic strength

It was noted that PEG precipitation was assisted (that is, required less PEG) by an increase in the ionic strength of the solution. Solution ionic strength is a function of ion type, charge and concentration. Hence, increasing the concentration of NaCl reduced the quantity of PEG required to induce precipitation (Section 6.2.5), and at a fixed PEG concentration different salts could induce precipitation at very different concentrations (Section 6.2.7). Ions in solution augment the volume exclusion mechanism of PEG precipitation by reducing the net repulsive force between like-charged proteins. It is proposed this occurs by a form of *electrostatic screening*, which essentially means the ions allow proteins to aggregate more easily (Mahadevan and Hall, 1990; 1992). Since bacteriophage M13 is a net negatively charged molecule at neutral pH (Graf *et al.*, 1993; Tang *et al.*, 2002), the ions of most importance in electrostatic screening were positively charged (cations), although negatively charged ions (anions) would have had a small effect also.

It is therefore straightforward to explain why solution ionic strength was important: increasing the concentration or charge of cations in solution increased electrostatic screening and thereby reduced protein-protein repulsion. However, the potency difference between cations which are otherwise of identical charge and concentration is less well understood. Many theories exist, but it is generally believed to be function of ion size and charge density, and a resulting altered interaction with water (Boncina *et al.*, 2008; Collins, 1997). These competing effects explain the trends observed in Section 6.2.7 where $MgSO_4$ was found to be far more effective than either Na_2SO_4 or NaCl. The higher valency (charge) and ion-specific abilities of Mg^{2+} must have outweighed the effect of adding two moles of Na^+ ions per mole of Na_2SO_4. This also explains why Na_2SO_4 proved a more effective precipitant than NaCl. Although Cl^- anions reduce protein solubility more than SO_4^{2-} (Zhang and Cremer, 2006), the effect of adding two moles of Na^+ ions per mole of salt in Na_2SO_4 more than compensated (Boncina *et al.*, 2008). The difference in effectiveness between salts was shown to reduce as the concentration of PEG reduced. This was consistent with findings elsewhere (Boncina *et al.*, 2008; Mahadevan and Hall, 1990), and is probably a function of the reduction in the dominance of the volume exclusion mechanism.

From a practical perspective, the choice between high PEG/low salt or low PEG/high salt concentrations will be determined by the relative chemical costs and the tolerable limit of solution viscosity for the bioprocess. Choice between salts also depends on the supplier costs versus the quantity required. A further consideration is the corrosive nature of salt chlorides (such as NaCl) relative to non-halide salts (such as sulphates) with regard to the usually stainless steel downstream processing equipment (Korb, 1987; Shreir *et al.*, 1994). While the

process decision will necessarily be a function of the individual circumstances, it is clear that flexibility of PEG precipitation allows for some tailoring to suit the conditions.

6.8.4 Isoelectric precipitation of M13

Similarly to the effect of ions in solution, judicious alteration of pH reduces mutual protein-protein repulsion, even to a point where precipitation occurs alone (Atkinson *et al.*, 1987). It was shown that bacteriophage M13 could be precipitated by so-called isoelectric precipitation, and exhibited a >90 % recovery in the precipitate in the range pH 3.9- 4.5 (Section 6.3.3). Such a broad pH range may be advantageous since it can be difficult to control pH on the large scale due to imperfect mixing (Hofland *et al.*, 2003). Bacteriophage M13 also exhibited reasonable resistance to the acidic conditions imposed, particularly when incubated on ice (eliminating significant drops in titre) but especially when compared to the T-odd and T-even bacteriophage types (T2, T3, T4, T5 and T7) investigated by Bachrach and Friedmann (1971). Severe bacteriophage denaturation by the acidic environment was described, which appeared to have been a factor in the poor recoveries (< 55 %) obtained.

It was shown in this chapter that the isoelectric precipitation of bacteriophage M13 needed only one hour of incubation rather than 24, which could save time and resources if translation to the large-scale was similarly effective. However, the large scale isoelectric precipitation of other proteins, such as casein, is known to depend on dynamic factors such as acid mixing, particle aggregation/break-up and mass transport phenomena into and out of the precipitate particles (Hofland *et al.*, 2003).

6.8.5 Divalent and polyvalent cation precipitation of M13

The cations spermidine and Ca^{2+} were shown to be effective facilitators of bacteriophage M13 precipitation, requiring only 1.5 and 50 mM respectively in the low ionic strength systems (Sections 6.4 and 6.5). However, as expected, their action was shown to be very dependent on the monovalent cation concentration (Murphy *et al.*, 1999; Tang *et al.*, 2002). Indeed, precipitation by spermidine was prevented by only 50 mM NaCl and Ca^{2+} ions by 100 mM NaCl. As a result it was hypothesized, then proven, that due to the monovalent cation content of NB2 neither spermidine nor Ca^{2+} would precipitate bacteriophage M13 from clarified shakeflask fermentation broth (Section 6.6).

The effect of monovalent cation addition on the spermidine precipitation of bacteriophage M13 appeared greater than that reported for plasmid DNA. It has been demonstrated that 5- 10 mM of spermidine would still precipitate a 6 kb plasmid in the presence of 100 mM NaCl (Murphy *et al.*, 1999), in contrast to the present study where only 50 mM of NaCl prevented bacteriophage precipitation by up to 50 mM spermidine. This may be because bacteriophage

M13 exhibited a higher solubility than DNA in the presence of spermidine, thereby making precipitation more susceptible to competitive interference. Existing literature studying the selective precipitation of DNA by CTAB supports this theory, since it was shown that DNA precipitated at lower CTAB concentrations than protein (Lander *et al.*, 2002; Tomanee *et al.*, 2004). This may also explain why bacteriophage M13 was not precipitable by CTAB under the conditions studied.

Work to model the net attractive forces between filamentous bacteriophage molecules as a result of divalent cation action has shown that these are reduced in a competitive manner by the presence of monovalent cations (Tang *et al.*, 2002). Therefore, with regards to bacteriophage M13 processing, precipitation by spermidine and Ca^{2+} may be useful further downstream under lower ionic strength conditions, particularly if the bacteriophage resolubilisation phenomenon observed by Ca^{2+} ions could be carefully exploited. Alternatively, the filamentous bacteriophage could be modified to become a more highly-charged molecule. The naturally occurring variant of bacteriophage M13, fd, possesses a net 30 % greater negative charge at neutral pH and has been shown to be precipitable by Ca^{2+} ions in the presence of 100 mM of monovalent salt (Tang *et al.*, 2002). Therefore, the deliberate creation of even more highly charged filamentous bacteriophage molecules may augment divalent and polyvalent cation precipitation further. It would then be of interest if selective precipitation of bacteriophage from DNA and protein contaminants could be achieved.

6.8.6   Evaluation of screening experimentation

Overall, the screening experiments under pure conditions provided useful insight into the effectiveness of several precipitants. They rapidly highlighted the effective concentration of precipitant, and, by analysing the ion concentration of the growth mediums of interest, could allow for the revised prediction of precipitation behaviour. In particular, the failure of spermidine and Ca^{2+} ions to precipitate bacteriophage M13 from NB2 would have meant two potentially useful precipitants would have been missed if the screening under pure conditions had not come first. In industry, where optimisation of conditions is important, the use of factorial design in conjunction with this screen could provide a rapid robust method to achieve this aim.

6.8.7   PEG and isoelectric precipitation purification performance

Bacteriophage M13 is in effect a very large, highly asymmetric 16 MDa protein. For PEG precipitation this resulted in very sharp precipitation curves, like those reported for the similarly rod-like tobacco mosaic virus (TMV) (Juckes, 1971). That is, bacteriophage recovery in the precipitate increased from near zero to >90 % within a narrow range of precipitant concentration. Furthermore (although the trend is less defined) large proteins such as M13 tend

to display a lower solubility than smaller ones (Atha and Ingham, 1981; Honig and Kula, 1976; Mahadevan and Hall, 1992). Firstly, this explains why the minimum concentration of PEG 6 000 shown in this study to precipitate bacteriophage M13 – at 1.5 % (w/v) – is five- to ten-fold lower than values published in the literature for smaller proteins, and indeed other bacteriophage (Atha and Ingham, 1981; Juckes, 1971; Sharma and Kalonia, 2004; Tsoka *et al.*, 2000; Yamamoto *et al.*, 1970) (Section 6.2.5). Secondly, this explains why high purification factors (approximately 250) were achieved from total protein by the three PEG-based precipitation methods analysed in Section 6.7, and why purification factors were lower (at approximately 50) from larger proteins. Since the total protein measurement by the Bradford assay included the many small polypeptide media components, it is perhaps of no surprise that almost all of these smaller components were not precipitated. Meanwhile, isoelectric precipitation appeared to perform consistently by both protein measures (Bradford Assay and SDS-PAGE densitometry), which is consistent with bacteriophage precipitation being by a different mechanism.

Although PEG-based precipitation of DNA is also possible, it typically requires 5- 15 % (w/v) of at least PEG 6 000 to induce precipitation of even the larger fragments (e.g. 10 kbp) (Field, 1993; Paithankar and Prasad, 1991; Sambrook and Russell, 2001). Hence at the PEG 6 000 concentrations used in this study, DNA remained in solution (Section 6.7). The fact that all three PEG-based precipitation methods performed similarly in terms of bacteriophage M13 purification is probably due to the dominant volume exclusion mechanism of precipitation, which is common to all. Although careful control of pH should in theory have meant that only proteins of similar isoelectric point to bacteriophage M13 would co-precipitate, it was clear from Section 6.7 that many contaminating proteins (and DNA) were precipitable around pH 4.3. Hence the purification factors achieved by isoelectric precipitation were substantially lower than those by PEG-precipitation. That said, the average purification factor achieved by isoelectric precipitation for protein removal (at 3.8) was not necessarily poor in absolute terms, since similar purification factors have been reported for the PEG precipitation of VLPs from total protein (Tsoka *et al.*, 2000). Furthermore, in Chapter 4 (Section 4.4) it was shown that alternative methods of DNA removal exist, such as nuclease addition.

That isoelectric precipitation requires essentially no precipitant addition is a benefit relative to PEG precipitation (Wenzig *et al.*, 1993). However, the low quantities of PEG required in this study somewhat assuages the drawbacks of precipitant cost and solution viscosity (Rodrigues *et al.*, 2007). Reduced precipitant cost is especially important since PEG polymer recycling can be difficult (Mahadevan and Hall, 1990; Nagaraj *et al.*, 2005). Although it has been shown that there is little co-precipitation of PEG with protein (Sharma and Kalonia, 2004; Yamamoto *et al.*, 1970), options on the large-scale to remove PEG from the concentrated bacteriophage

include ultrafiltration (Busby and Ingham, 1980; Papamichael and Kula, 1987) or standard chromatographic steps to which PEG has no tendency to absorb (Ingham, 1990). Therefore, the negative impact on subsequent high-resolution purification steps is likely to be minimal, although the performance of some size-exclusion columns may be altered due to osmotic effects of the polymer (Ingham, 1990). Overall, the processing benefits of a highly selective primary purification step, such as the PEG-precipitation options outlined in this chapter, are clear: subsequent high resolution purification steps will be less susceptible to fouling if the feed stream is less heavily contaminated (Thommes and Etzel, 2007) and fewer steps may be needed thereby improving the overall yield (Wenzig *et al.*, 1993).

6.8.8   Concluding remarks

In summary, millilitre-scale screening methods were used to identity several potentially useful precipitants of bacteriophage M13 for large-scale processing. Understanding the effect of monovalent salt concentration on precipitation allowed for the prediction of precipitant behaviour in culture medium. PEG-based precipitation methods showed selective precipitation of bacteriophage M13 particles from protein and DNA contaminants. Isoelectric precipitation was shown to be an efficient method to precipitate bacteriophage M13, but gave a lower improvement in purity. It was noted that the novel precipitation agents spermidine and Ca^{2+} ions could potentially offer an alternative precipitation option for more highly charged bacteriophage molecules. However, for bacteriophage M13, PEG-based precipitation appeared to offer the best combination of reproducibility, robustness and selectivity. The choice between the three PEG-based precipitation techniques (4 % (w/v) PEG 6 000 or 2 % (w/v) PEG 6 000 with 135 mM NaCl or 25 mM $MgSO_4$) remains a function of the relative costs of the precipitants and the ease of handling.

7 Consideration of the Issues Concerning the Introduction of Bacteriophage M13 to a Mixed-Use Production Facility

7.1 Introduction

Bacteriophage attack has always been a key issue in industrial fermentations, especially in the dairy industry (Brussow *et al.*, 1994). Here, contamination of the fermenter or starter culture by virulent bacteriophage can result (at best) in reduced product yield but total culture and product loss can commonly be expected. The costs can be considerable and so consequently, extensive effort has been devoted to controlling bacteriophage contamination (Jones *et al.*, 2000; Moineau, 1999)

In contrast, the deliberate culture of bacteriophage has been a cornerstone of this thesis. However, the introduction of a bacteriophage to a production facility that also requires the routine (successful) culture of permissive bacteria raises several important issues concerning their co-experimentation. Indeed, successful bacteriophage production itself requires the ability to grow non-infected starter cultures. These issues are especially relevant for small bioscience firms and academic institutions operating areas of mixed-use. Prior to bacteriophage introduction it is essential to consider not only the implications of accidental release but also the risk of such an event occurring and how it could be minimised. Further, in the event of release occurring, remedial actions would need to be predefined.

The precise level of precaution required depends on several factors. Ideally, the host range of the bacteriophage of interest would not encompass bacterial strains routinely (or intended to be) cultured in unrelated experimentation. However, if this were unavoidable, then extra measures would need to be exercised to prevent unplanned bacteriophage propagation. It would also be important to assess the potential environmental persistence of the bacteriophage of interest, since bacteriophage vary enormously in their resistance to the challenges of desiccation, temperature and pH (Jepson and March, 2004; Pollard and Solosko, 1971; Rahn, 1945) For example, a bacteriophage displaying a strong desiccation resistance would warrant more concern that one showing acute sensitivity. Such information would allow an informed judgement to be made on the long-term implications of accidental bacteriophage release.

While the bacteriophage studied in this thesis (M13) infects the common microbiological tool *E. coli*, it can only infect cells harbouring the F-plasmid, an episome which is not essential for recombinant protein production. However, because bacteriophage M13 infection is not lethal to the host cell, which continues to grow whilst extruding progeny bacteriophage particles, the infected cells themselves must be treated with the same caution as free bacteriophage.

It was considered that the determination of an effective decontamination regime was essential; several commercial disinfectant agents were therefore tested for effectiveness against bacteriophage M13 and subsequently *E. coli* cells. The resistance of bacteriophage M13 to several challenges was then examined, relevant for the assessment of its safe fermentation in a mixed-use facility. This included exposure to extremes of temperature, pH and to desiccated conditions. Additionally, the effect of desiccation on *E. coli* cells was also investigated. In light of these data the consequences of accidental bacteriophage M13 release was discussed. This experimentation gave context to the derivation of a method for the contained propagation of bacteriophage M13 at the 20 litre scale in the UCL Department of Biochemical Engineering fermentation suite. Several Standard Operating Procedures (SOPs) were derived, and their more general application discussed.

7.2   Determination of an Effective Decontamination Agent

7.2.1   Effect of Tego on bacteriophage M13 viability

Tego 2001 is liquid amphoteric surfactant typically used at a working concentration of 2 % (v/v) at room temperature. It is of proprietary composition, but is based on 1-alkyl-1,5-diazapetane in aqueous solution. Experimentation was conducted as described in the Materials and Methods (Section 2.15.1). Briefly, caesium chloride purified bacteriophage M13 (Section 2.4) were diluted to a final concentration of 1×10^{12} pfu ml^{-1} in 0, 1, 2 and 10 % (v/v) Tego solutions. Samples were taken for bacteriophage enumeration (Section 2.5.2) after 10 second, 1 minute, 5 minute, 10 minute and 20 minute incubations with Tego at room temperature. Upon sampling, bacteriophage were immediately ten-fold serially diluted to 10^{-2} of their original concentration to remove the detergent; further serial dilution to enumerate the bacteriophage was conducted once all sampling was complete. A control of 10 % Tego solution alone (no bacteriophage) was also serially diluted and plated onto Top10F' overlay agar plates to test for bacterial lawn inhibition. Each treatment was repeated three times.

It was found that the concentration of viable bacteriophage decreased as the concentration of Tego increased (Figure 7.1). The greatest reduction in bacteriophage titre therefore occurred at a 10 % (v/v) Tego after 20 minutes. The concentration of viable bacteriophage at this point was 1.4×10^{11} pfu ml^{-1}, which was a 0.14 fraction of the 0 % (v/v) Tego control value. Statistical analysis showed that the drop in viability at this timepoint was the only one which was significantly lower than the 0 % (v/v) Tego control ($P<0.05$, Dunnett).

A serially diluted control of 10 % (v/v) Tego alone resulted in zones of clearing on the Top10F' overlay plates at the 10^{-1} dilution, and poorer growth at the 10^{-2} and 10^{-3} dilutions. No alteration to bacterial lawn growth was observed at greater dilutions.
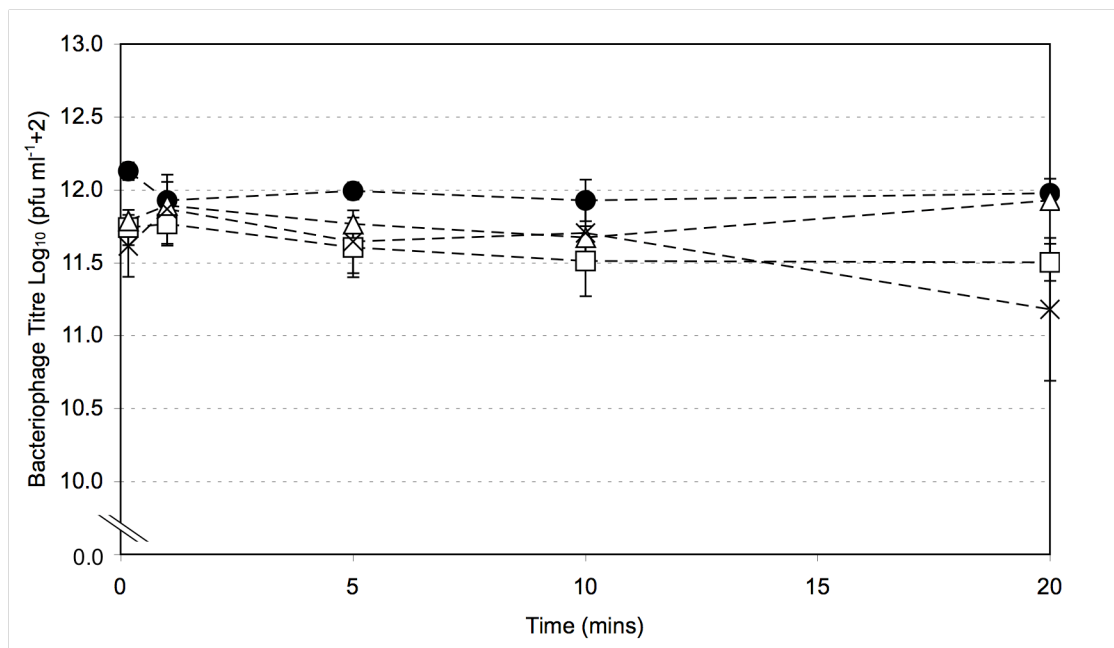
Figure 7.1 The change in concentration of viable bacteriophage M13 as a function of time, when incubated at room temperature in 0 % (v/v) Tego (●), 1 % (v/v) Tego (△), 2 % (v/v) Tego (□) and 10 % (v/v) Tego (×). Bacteriophage titre was expressed as the $\log_{10}$ value of the pfu ml^{-1} concentration. A value of 2 was added to every bacteriophage concentration, since $\log_{10}(0)$ is undefined. Error bars represent the standard error, N=3.

7.2.2   Effect of Solquest on bacteriophage M13 viability

Solquest is a liquid surfactant typically used at a working concentration of 1 % (v/v), described for use in hot water. Like Tego, it is also of proprietary composition, but is based on 10- 30 % (w/v) tetrasodium EDTA, 5- 10 % (v/v) amino-tri(methylene phosphonic acid) and 5- 10 % (w/v) sodium hydroxide. Experimentation was conducted as described in the Materials and Methods (Section 2.15.1) at two temperatures (50 and 70 °C) to determine the temperature dependence of the detergent effectiveness. Caesium chloride purified bacteriophage M13 (Section 2.4) were diluted to a final concentration of 1 x 10^{12} pfu ml^{-1} in 0, 0.5, 1 and 5 % (v/v) Solquest solutions, pre-warmed to the required temperature. Samples were taken for bacteriophage enumeration as described for Tego experimentation (Section 7.2.1). A control of 5 % Solquest solution alone (no bacteriophage) was also serially diluted and plated onto Top10F' overlay agar plates to test for bacterial lawn inhibition. The experiment was repeated three times.

At 50 °C, the concentration of viable bacteriophage in the 0.5 and 1 % (v/v) Solquest samples only diverged significantly from the 0 % (v/v) control after the full 20 minute exposure time

(P<0.01, Dunnett). However, at a concentration of 5 % (v/v) Solquest the concentration of viable bacteriophage was very low by the first 10 second timepoint (5.0 x 10³ pfu ml⁻¹) and did not significantly decrease further over the following 20 minutes (Figure 7.2).
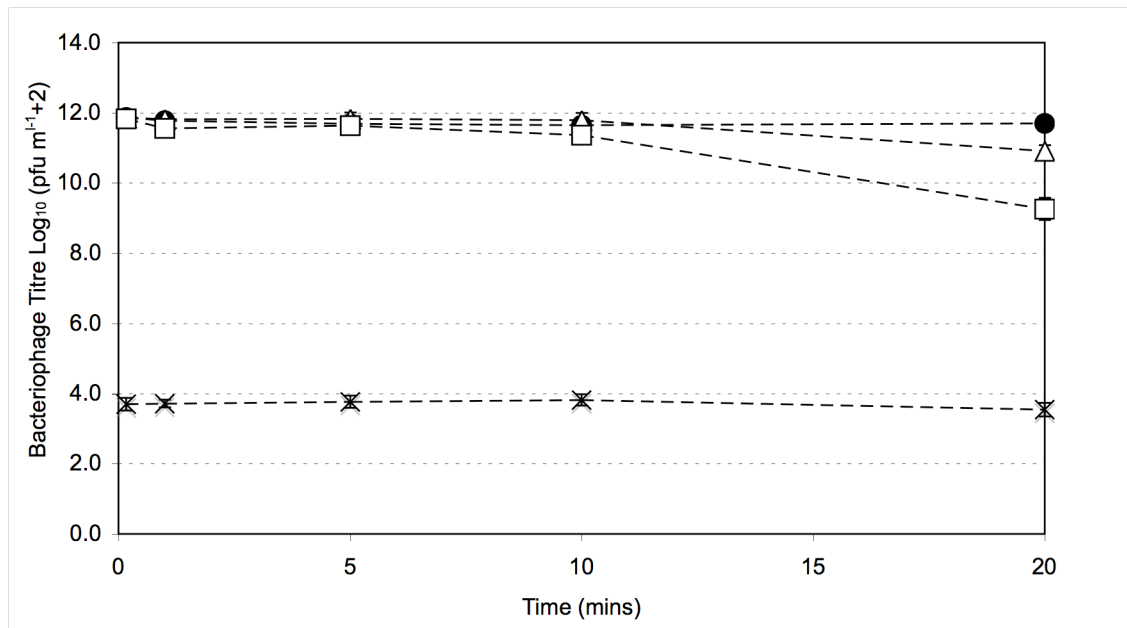
Figure 7.2 The change in concentration of viable bacteriophage M13 as a function of time, when incubated at 50 °C in 0 % (v/v) Solquest (●), 0.5 % (v/v) Solquest (△), 2 % (v/v) Solquest (□) and 5 % (v/v) Solquest (×). A value of 2 was added to every bacteriophage concentration, since $\log_{10}(0)$ is undefined. Error bars represent the standard error, N=3.

The effect on bacteriophage viability was stronger upon incubation with Solquest at 70 °C. A ten second contact time was sufficient for the concentration of viable bacteriophage in the 1 % (v/v) Solquest samples to significantly diverge from the 0 % (v/v) control (P<0.01, Dunnett), whilst a five minute contact time was required for the 0.5 % (v/v) samples to diverge significantly (P<0.01, Dunnett) (Figure 7.3). At a concentration of 5 % (v/v) Solquest, no viable bacteriophage were detected in any sample taken after 10 minutes incubation.

The serially diluted control of 5 % (v/v) Solquest alone did not result in any alteration to bacterial lawn growth at any dilution.
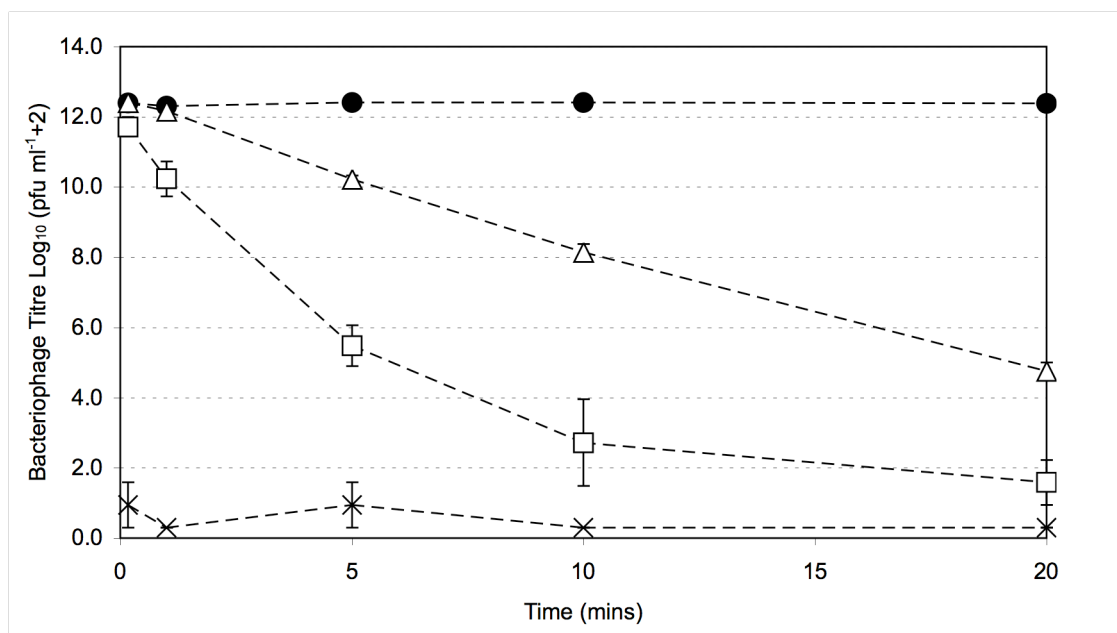
Figure 7.3 The change in concentration of viable bacteriophage M13 as a function of time, when incubated at 70 °C in 0 % (v/v) Solquest (●), 0.5 % (v/v) Solquest (△), 1 % (v/v) Solquest (□) and 5 % (v/v) Solquest (×). A value of 2 was added to every bacteriophage concentration, since $\log_{10}(0)$ is undefined. Error bars represent the standard error, N=3.

7.2.3   The effect of Virkon on bacteriophage M13 viability

Virkon is an oxidising disinfectant powder typically used at a working concentration of 1 % (w/w) in water. Like Tego and Solquest it is of proprietary composition, but is based on < 50 % (w/w) pentasodium bis(peroxymonosulphate) bis(sulphate), 5- 10 % (w/w) sulphamidic acid, 5-15 % (w/w) sodium dodecylbenzenesulfonate, <2 % (w/w) dipotassium peroxdisulphate. Experimentation was conducted as described in the Materials and Methods (Section 2.15.1). Caesium chloride purified bacteriophage M13 (Section 2.4) were diluted to a final concentration of 1×10^{12} pfu ml^{-1} into Virkon solutions of final concentrations 0, 0.01, 0.1 and 1 % (w/v) Virkon at room temperature. Samples were taken for bacteriophage enumeration as described for Tego experimentation (Section 7.2.1). A control of 1 % Virkon solution alone (no bacteriophage) was also serially diluted and plated onto Top10F' overlay agar plates to rest for bacterial lawn inhibition. The experiment was repeated three times.

It was found that the concentration of viable bacteriophage substantially decreased upon incubation with 0.1 and 1 % (w/v) Virkon solutions. No viable bacteriophage were detected in 1 % (w/v) Virkon after a contact time greater than 1 minute (Figure 7.4). Incubation with 0.01 % (w/v) Virkon solution did not result in a significant drop in the concentration of viable bacteriophage over 20 minutes.

The serially diluted control of 1 % (w/v) Virkon alone did not result in any alteration to bacterial lawn growth at any dilution.
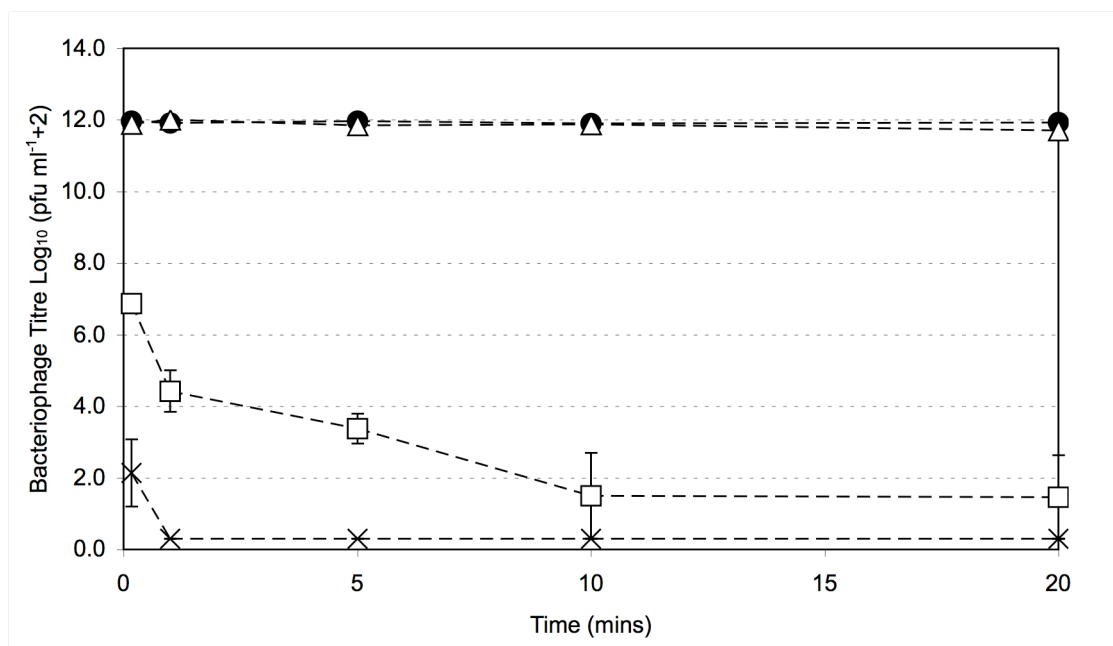
Figure 7.4 The change in concentration of viable bacteriophage M13 as a function of time, when incubated at room temperature in 0 % (w/v) Virkon (●), 0.01 % (w/v) Virkon (△), 0.1 % (w/v) Virkon (□) and 1 % (w/v) Virkon (×). A value of 2 was added to every bacteriophage concentration, since $\log_{10}(0)$ is undefined. Error bars represent the standard error, N=3.

7.2.4   The effect of Virkon on *E. coli* viability

Experimentation to study the effect of Virkon on *E. coli* cells was conducted as described in the Materials and Methods (Section 2.15.1). Virkon was added to overnight W1485 culture to give final concentrations of 0, 0.1, 0.5 and 1 % (w/v). Experiments were conducted at room temperature. Samples were taken for bacterial enumeration as described in the Materials and Methods (Section 2.5.1).

Over the course of the twenty minute experiment the concentration of viable *E. coli* cells was significantly reduced by incubation at all three Virkon concentrations (Figure 7.5). At the lowest Virkon concentration– 0.1 % (w/v)– the concentration of viable cells decreased significantly after 5 minutes incubation (P=<0.01, Dunnett). After 20 minutes, it had decreased to a 0.24 fraction of that of the 0 % (w/v) Virkon control. The effect of greater Virkon concentrations on cell viability was more pronounced. At Virkon concentration of 0.5 and 1 % (w/v), no viable cells were detected after 5 minutes or more incubation.
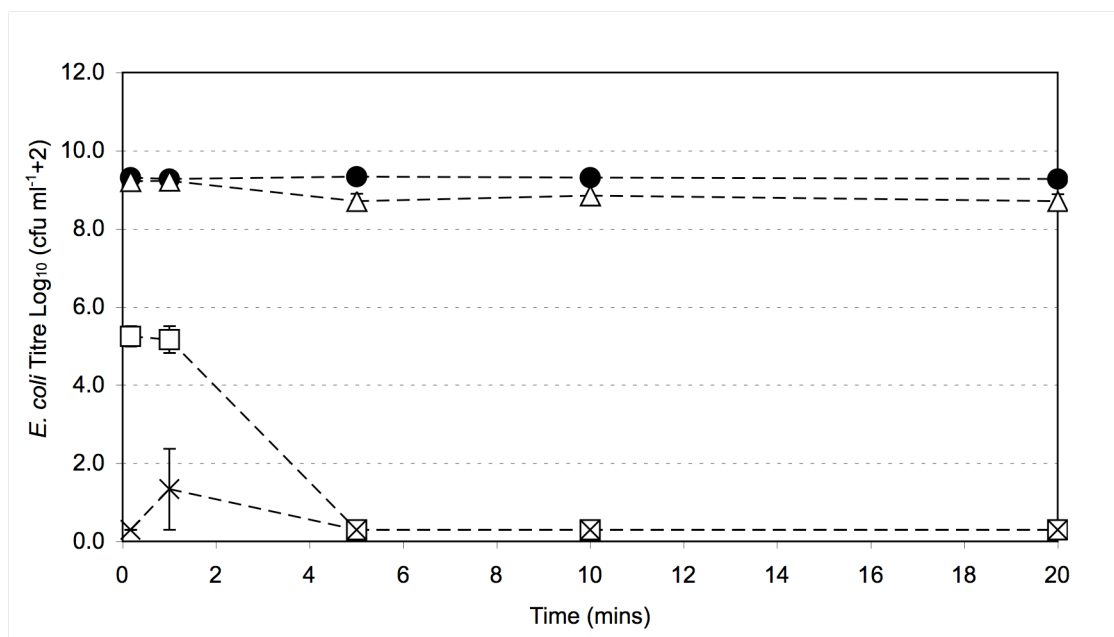
Figure 7.5 The change in concentration of viable *E. coli* as a function of time, when incubated at room temperature in 0 % (w/v) Virkon (●), 0.1 % (w/v) Virkon (△), 0.5 % (w/v) Virkon (□) and 1 % (w/v) Virkon (×). A value of 2 was added to every *E. coli* concentration, since $\log_{10}(0)$ is undefined. Error bars represent the standard error, N=3.

7.3 The Effect of Desiccation on Bacteriophage M13 and *E. coli*

The effect of desiccation on bacteriophage M13 and *E. coli* Top10F' was studied as described in the Materials and Methods (Section 2.15.2). In summary, caesium chloride purified bacteriophage M13 solutions of concentration 10^{13}, 10^{10}, 10^7 and 10^4 pfu ml^{-1} in NB2 were desiccated, as were 50 ml overnight cultures of M13 infected and non-infected *E. coli* cells in NB2. Desiccation was conducted in polystyrene round-bottomed 96-well plates loaded with 200 μl of each sample. All loaded plates to be desiccated were first dried in a fume hood, necessary to rapidly remove the 200 μl of fluid in each well. Non-desiccated control plates were also prepared, sealed with a self-adhesive impermeable membrane and stored alongside the drying plates in the fume hood.

Immediately after drying in the fume hood, half the plates were subsequently desiccated under dry (silica gel desiccator) conditions and half under standard (laboratory) conditions. Non-desiccated control plates were stored alongside the dried plates. Desiccated plates were stored with their corresponding plate lids supported above the wells, allowing for air circulation beneath. At the desired timepoints, dried samples were rehydrated and resuspended with 200 μl 20 mM Tris (pH 7.5 at 25 °C) per well. Non-desiccated control samples were simply

resuspended. Bacteriophage and *E. coli* were enumerated by the surface droplet technique (Section 2.5.2). Triplicate cultures and bacteriophage dilutions were prepared and desiccated concurrently.

The effect of the initial desiccation on *E. coli* and bacteriophage in the fume hood was investigated. It was noted that there was a significant drop in *E. coli* titre on drying, though not of bacteriophage M13. The drop in M13 infected *E. coli* titre was insignificant (Table 7.1).

Table 7.1 The effect of the initial desiccation on the viability of *E. coli* Top10F' and bacteriophage M13 in a fume hood. Statistical analysis was conducted on $\log_{10}$ transformed data.

Sample		Pre-desiccation titre pfu/ cfu ml^{-1}	Post-desiccation titre pfu/ cfu ml^{-1}	P value (t-test)
Caesium	M13 10^{13} pfu ml^{-1}	1.2×10^{13}	1.2×10^{13}	0.84
chloride purified	M13 10^{10} pfu ml^{-1}	1.3×10^{10}	9.8×10^{9}	0.15
bacteriophage M13	M13 10^{7} pfu ml^{-1}	1.3×10^{7}	9.8×10^{6}	0.18
in NB2	M13 10^{4} pfu ml^{-1}	1.3×10^{4}	1.1×10^{4}	0.34
	M13 in Top10F' culture	8.1×10^{11}	6.9×10^{11}	0.28
	E. coli Top10F'	1.0×10^{9}	4.9×10^{8}	0.0002
	M13 infected *E. coli* Top10F'	2.5×10^{8}	3.6×10^{7}	0.09

Over the course of the subsequent 47 day experiment the mean average relative humidity in the laboratory was 43.5 %, the median 43.9 %. Relative humidity ranged from 35.4 to 49.2 %. The mean average relative humidity in the desiccator was 5.6 % and ranged from 5.4 to 5.7 %. The relative humidity in the desiccator was measured to drop below 10 % within four hours and reached 5.5 % within 48 hours. The mean temperature was 22 °C.

7.3.1 The effect of desiccation on bacteriophage M13

Figure 7.6 shows the change in measured bacteriophage concentration over the course of the experiment for all four starting concentrations of 10^{13}, 10^{10}, 10^7 and 10^4 pfu ml^{-1}. Table 7.2 summarises the average count data at days zero and 47. It was observed that after 47 days the measured concentration of bacteriophage had significantly decreased in all cases from the zero timepoints under each of the desiccated dry, laboratory and non-desiccated conditions (Table 7.3).

Compared to the non-desiccated control the drops in titre from a bacteriophage concentration of 10^{13} pfu ml^{-1} after 47 days were significantly greater when desiccated under laboratory (P<0.001, Tukey) and dry conditions (P<0.001, Tukey). Between these, the decrease in titre from desiccation under laboratory conditions was significantly greater than that from dry conditions (P<0.001, Tukey). However, at bacteriophage concentrations of 10^{10}, 10^7 and 10^4 pfu ml^{-1}, the drops in titre were not significantly different between all three conditions after 47 days.
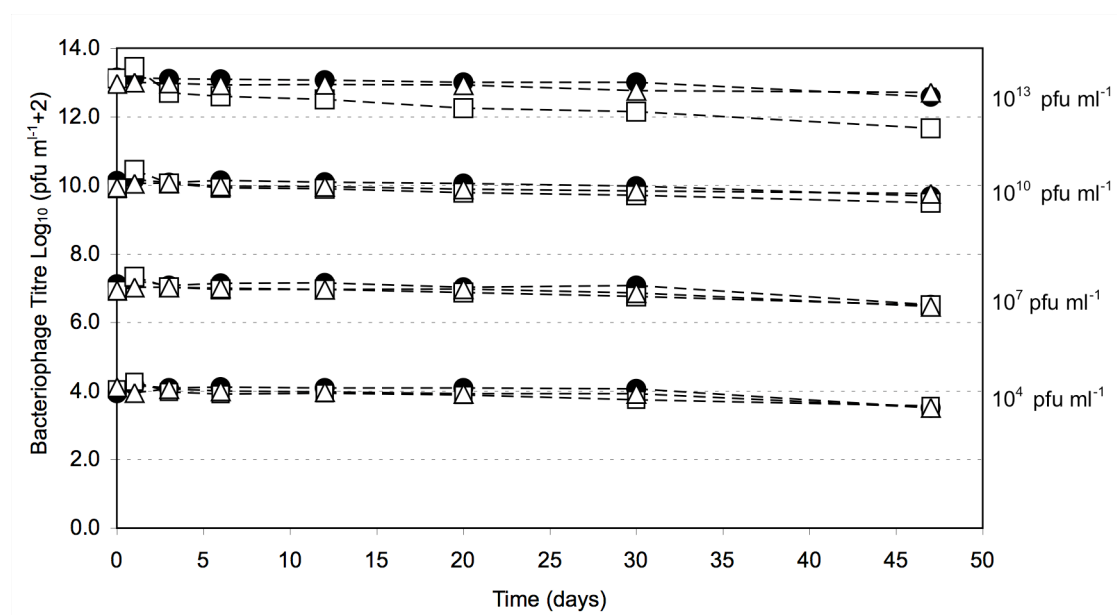
Figure 7.6 The change in concentration of viable caesium chloride purified M13 bacteriophage in NB2 as a function of time, when stored at room temperature under non-desiccated conditions (●), desiccated dry conditions (△), and desiccated laboratory conditions (□). The four starting bacteriophage concentrations were 10^{13}, 10^{10}, 10^7 and 10^4 pfu ml^{-1}. A value of 2 was added to every bacteriophage concentration, since $\log_{10}(0)$ is undefined. Error bars represent the standard error, N=3.

Table 7.2 Average count data comparing the viable bacteriophage M13 concentrations at desiccation days zero and 47 under non-desiccated, desiccated dry and desiccated laboratory conditions. N=3.

Initial bacteriophage concentration (pfu ml^{-1})	Bacteriophage concentration (pfu ml^{-1})		
	Non-desiccated	Desiccated, dry conditions	Desiccated, laboratory conditions
1.2×10^{13}	3.8×10^{12}	5.2×10^{12}	4.5×10^{11}
9.8×10^{9}	4.8×10^{9}	5.7×10^{9}	3.1×10^{9}
9.8×10^{6}	3.3×10^{6}	2.9×10^{6}	3.2×10^{6}
1.1×10^{4}	3.2×10^{3}	3.3×10^{3}	3.6×10^{3}

Table 7.3 Significance data comparing the viable bacteriophage M13 concentrations at desiccation days zero and 47 under non-desiccated, desiccated dry and desiccated laboratory conditions. Statistical analysis was conducted on $\log_{10}$ transformed data, N=3.

Initial bacteriophage concentration (pfu ml^{-1})	P value (t-test)		
	Non-desiccated	Desiccated, dry conditions	Desiccated, laboratory conditions
1.2×10^{13}	0.0001	0.037	0.0001
9.8×10^{9}	0.001	0.003	0.006
9.8×10^{6}	0.001	0.001	0.022
1.1×10^{4}	0.001	0.0003	0.003

Assuming an exponential decay trend, the half-life of purified bacteriophage M13 at each concentration under each desiccation condition was calculated using Equation 1:

$$T_{0.5} = \frac{\ln(2)}{m} \qquad (1)$$

where $T_{0.5}$ is the half-life, and m the gradient of the fitted trend line (linear on the plot of Figure 7.6). The resulting half-lives are shown in Table 7.4. The shortest calculated half-life was 22 days, corresponding with bacteriophage of initial concentration 10^{13} pfu, desiccated under

laboratory conditions. The longest half-lives were in excess of 100 days, achieved by desiccation under dry conditions.

Table 7.4 Summary of the half-life data of purified bacteriophage M13 in NB2 desiccated under laboratory and dry conditions, together with non-desiccated control. Half-lives were calculated using Equation (1), applied to the data in Figure 7.6.

Initial bacteriophage concentration (pfu ml^{-1})	Half-life of bacteriophage M13 under each condition (days)		
	Non-desiccated	Desiccated, dry conditions	Desiccated, laboratory conditions
1.2 x 10^{13}	68	115	22
9.8 x 10^9	79	120	50
9.8 x 10^6	61	71	57
1.1 x 10^4	75	70	62

7.3.2   Effect of desiccation on bacteriophage M13 in culture

The desiccation conditions affected the rate of decay of bacteriophage M13 titre in Top10F' culture (Figure 7.7). Here, the bacteriophage titre decreased most when desiccated under laboratory conditions and least when non-desiccated. After 47 days the bacteriophage titres had significantly decreased relative to the corresponding zero timepoints when desiccated under dry (P=0.005, t-test) and laboratory (P=0.00004, t-test) conditions. Conversely, there was no significant decrease in bacteriophage titre when stored under non-desiccated conditions. After 47 days the bacteriophage titre was not significantly different between desiccated laboratory and dry conditions. However, the bacteriophage titre under each of these treatments was significantly lower than under non-desiccated conditions after 47 days (P<0.001 in each case, Tukey).

Using Equation (1), the half-life of bacteriophage M13 was calculated for each of the trends in Figure 7.7. It was calculated that under non-desiccated conditions, the half-life was 182 days, under desiccated dry conditions it was 74 days, and under desiccated laboratory conditions 38 days.
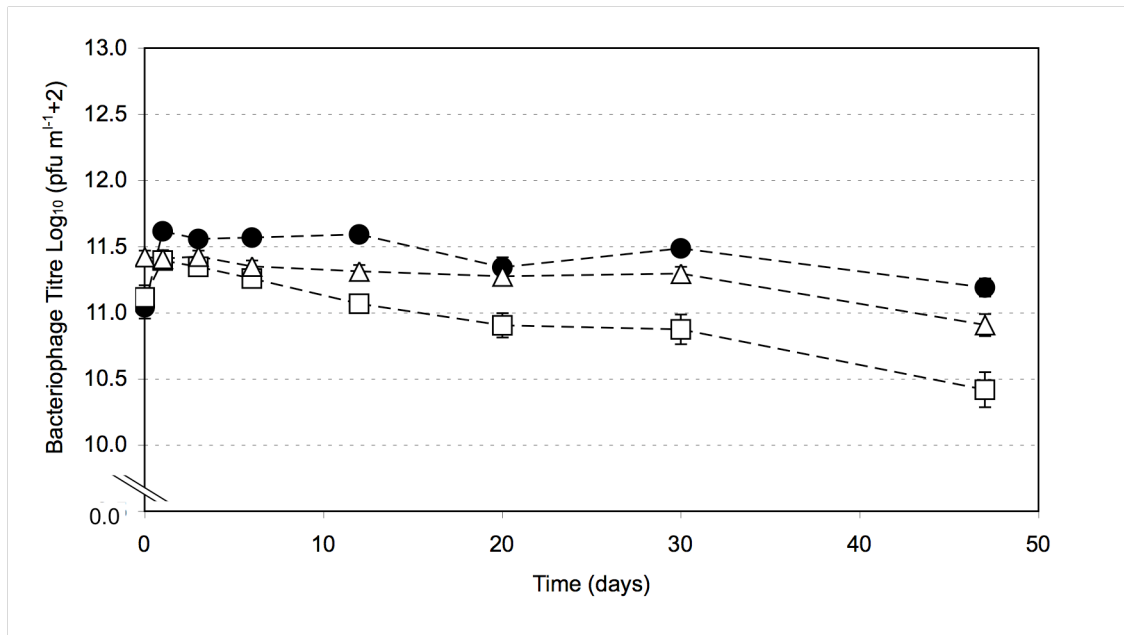
Figure 7.7 The change in concentration of viable M13 bacteriophage in *E. coli* Top10F' culture as a function of time, when stored at room temperature under non-desiccated conditions (●), desiccated dry conditions (△), and desiccated laboratory conditions (□). A value of 2 was added to every bacteriophage concentration, since $\log_{10}(0)$ is undefined. Error bars represent the standard error, N=3.

7.3.3 The effect of desiccation on *E. coli*

It was observed that there was a marked effect of desiccation on the titre of *E. coli* strain Top10F'. The titre of non-infected cells dropped considerably over the 47 day experiment (Figure 7.8): the viable cell count dropped from 5.2×10^8 cfu ml^{-1} at the zero timepoint to 4.8×10^2 cfu ml^{-1} after desiccation under laboratory conditions. Under dry conditions, it dropped from 4.4×10^8 cfu ml^{-1} at the zero timepoint to 1.2×10^5 cfu ml^{-1}. However, under non-desiccated conditions the drop in titre was only from 5.1×10^8 cfu ml^{-1} at the zero timepoint to 9.4×10^7 cfu ml^{-1} after 47 days

Over 47 days the decline in viability of M13 infected cells was similarly large (Figure 7.9). The greatest decline in titre was again observed for cells desiccated under laboratory humidity conditions, where the cell titre declined from 2.7×10^7 cfu ml^{-1} at the zero timepoint to 6.2×10^2 cfu ml^{-1} over 47 days. Over the same time span the viability decline under dry conditions was from 9.5×10^6 cfu ml^{-1} at the zero timepoint to 2.8×10^3 cfu ml^{-1}. When stored under non-desiccated conditions, the drop in titre was only from 1.9×10^8 cfu ml^{-1} at the zero timepoint to 8.6×10^7 cfu ml^{-1}.
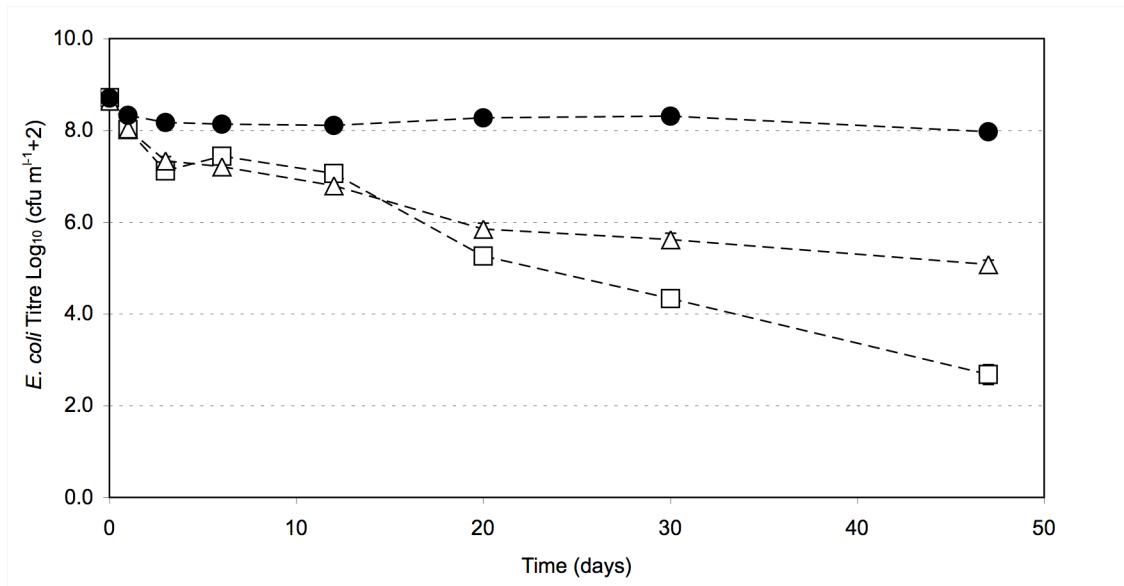
Figure 7.8 The change in concentration of viable *E. coli* Top10F' cells as a function of time, when stored at room temperature under non-desiccated conditions (●), desiccated dry conditions (△), and desiccated laboratory conditions (□). A value of 2 was added to every *E. coli* concentration, since $\log_{10}(0)$ is undefined. Error bars represent the standard error, N=3.
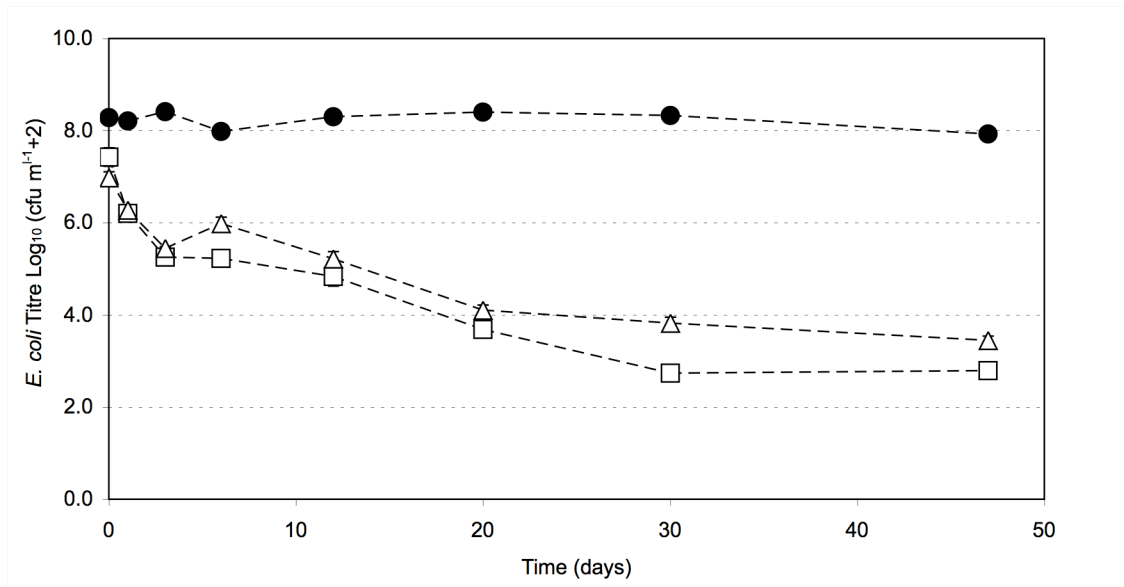
Figure 7.9 The change in concentration of viable M13 infected *E. coli* Top10F' cells as a function of time, when stored at room temperature under non-desiccated conditions (●), desiccated dry conditions (△), and desiccated laboratory conditions (□). A value of 2 was added to every *E. coli* concentration, since $\log_{10}(0)$ is undefined. Error bars represent the standard error, N=3.

Again using Equation (1), the half-life of *E. coli* Top10F' was calculated for each of the trends in Figure 7.8 and Figure 7.9. It was calculated that under non-desiccated conditions, the half-life was *E. coli* Top10F' was above 100 days, i.e. the decline in viability over the 47 day treatment was small (Table 7.5). Upon desiccation, there was little observed difference between the half-lives of infected and non-infected *E. coli* cells under each desiccation condition: 8 days and 6 days respectively under laboratory conditions, 10 days each under dry conditions.

Table 7.5 Summary of the half-life data of *E. coli* Top10F' desiccated under laboratory and dry conditions, together with non-desiccated control. Half-lives were calculated using Equation (1), applied to the data in Figure 7.8 and Figure 7.9.

E. coli culture type	Half-life of *E. coli* under each condition (days)		
	Non-desiccated	Desiccated, dry conditions	Desiccated, laboratory condition
Non-infected	100	10	6
M13 infected	173	10	8

7.4 The Effect of Extremes of pH on Bacteriophage M13

Caesium chloride purified bacteriophage M13 was subject to a range of pH values as described in the Materials and Methods (Section 2.15.3). In summary, 100 µl of bacteriophage M13 of concentration 1×10^{13} pfu ml^{-1} in NB2 was added to 9.9 ml of acid or alkali solution at room temperature. Samples were taken after 1, 5, 10 and 20 minute incubations, neutralised (Section 2.15.3) and enumerated by the surface droplet technique. Experiments were repeated three times.

Two experiments were conducted. In the first experiment, bacteriophage M13 was subject to incubation at pH 1.0, 3.0, 7.0, 11.0 and 13.0. It was found that exposure to pH 3.0, 7.0 or 11.0 did not result in a significant reduction in infective titre over the course of 20 minutes (Figure 7.10). Upon incubation at pH 1.0, the titre had decreased significantly from the pH 7.0 control by 5 minutes incubation ($P<0.01$, Dunnett). After 20 minutes, the titre has decreased 300-fold to 4.7×10^8 pfu ml^{-1}. At pH 13.0, however, the titre decreased by seven orders of magnitude by the first 1 minute timepoint, and continued to decrease as time progressed.
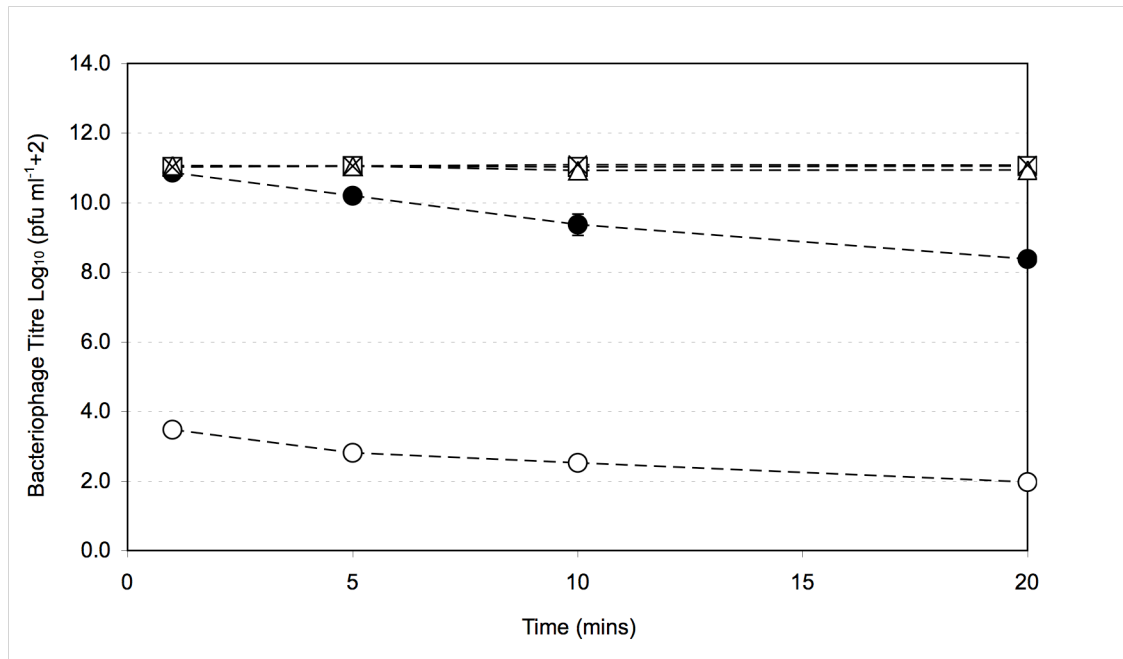
Figure 7.10 The change in concentration of viable bacteriophage M13 as a function of time, when incubated at room temperature at pH 1.0 (●), 3.0 (△), 7.0 (□), 11.0 (×) and 13.0 (○). A value of 2 was added to every bacteriophage concentration, since $\log_{10}(0)$ is undefined. Error bars represent the standard error, N=3.

In the second experiment, bacteriophage M13 was subject to incubation under acidic and alkaline conditions representative of those used for the pH control of pilot-scale fermentations. Here, concentrated acid and alkaline solutions are typically connected directly to the fermenter by flexible hoses and fed in as required under computer control. As such, during the course of a fermentation bacteriophage may be expected to be in contact with the acid and base lines. Bacteriophage M13 was therefore incubated with 10 % (v/v) sulphuric acid (pH 0.0) solution and 4 M sodium hydroxide (pH 14.0) solutions to investigate the ability of the bacteriophage to survive these conditions. It was found that by the 5 minute timepoint there were no detected bacteriophage in either the 10 % (v/v) sulphuric acid or 4 M sodium hydroxide solutions (Figure 7.11). Indeed, no bacteriophage were detected in the 4 M sodium hydroxide solution by the first 1 minute sample.
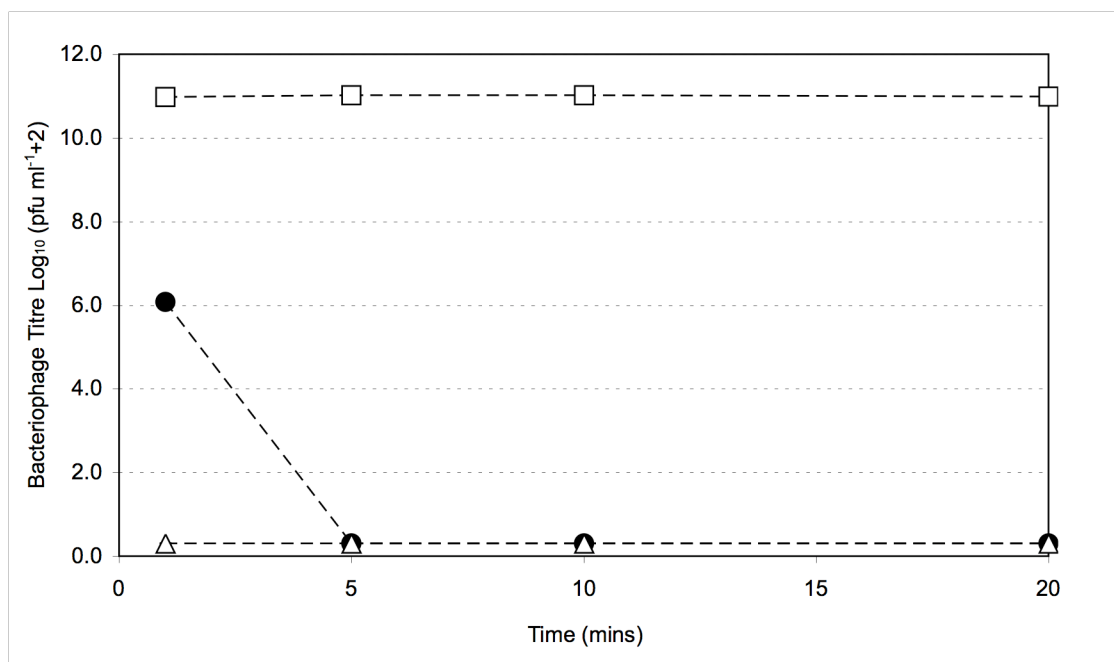
Figure 7.11 The change in concentration of viable bacteriophage M13 as a function of time, when incubated at room temperature with 10 % (v/v) sulphuric acid ($\bullet$), at pH 7.0 ($\square$) and with 4 M sodium hydroxide ($\triangle$). A value of 2 was added to every bacteriophage concentration, since $\log_{10}(0)$ is undefined. Error bars represent the standard error, N=3.

7.5 The Effect of Temperature on Bacteriophage M13

Caesium chloride purified bacteriophage M13 of concentration 1×10^{12} pfu ml^{-1} in NB2 was incubated at a range of temperatures in a PCR block as described in the Materials and Methods (Section 2.15.4). In summary, 50 µl aliquots of bacteriophage solution were incubated at 99, 95, 90, 80, 70, 60, 50, 40, and 25 °C, together with a room temperature control not incubated within the device. Single aliquots were removed after 1, 5, 10, 20, 30, 40, 50 and 60 minute incubations, cooled and enumerated by the surface droplet technique. Experiments were repeated three times.

It was found that decreases in bacteriophage M13 titre of several orders of magnitude occurred upon incubation at temperatures above 80 °C (Figure 7.12). There were no detected bacteriophage after 20 minutes incubation at 99 °C and 50 minutes at 95 °C. At 90 °C there was an eight order of magnitude drop in titre over 60 minutes. However, a 60 minute incubation at 80 °C only decreased the titre from 6.0×10^{11} pfu ml^{-1} to 1.5×10^{11} pfu ml^{-1}. Incubation at progressively lower temperatures resulted in correspondingly smaller decreases in titre relative to the room temperature control (Figure 7.13). Indeed, even after incubation at 70 °C the bacteriophage viability did not diverge significantly from the room temperature control over the entire 60 minute experiment.
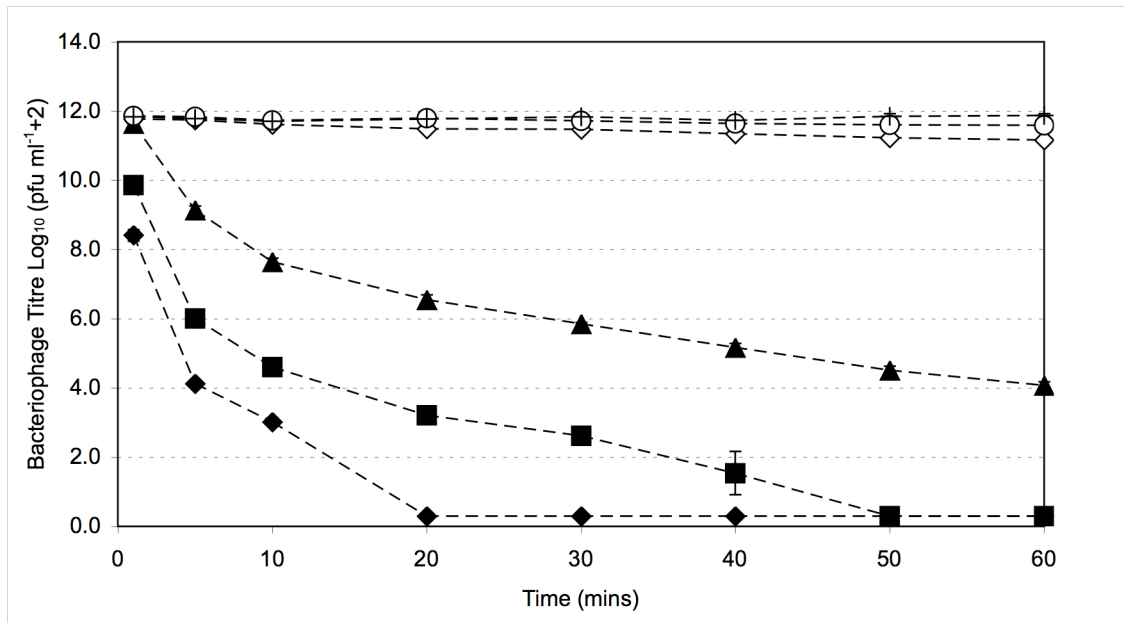
Figure 7.12 The change in concentration of viable bacteriophage M13 as a function of time, when incubated at temperatures 99 °C (◆), 95 °C (■), 90 °C (▲), 80 °C (◇), 70 °C (○) and room temperature (+). A value of 2 was added to every bacteriophage concentration, since $\log_{10}(0)$ is undefined. Error bars represent the standard error, N=3.
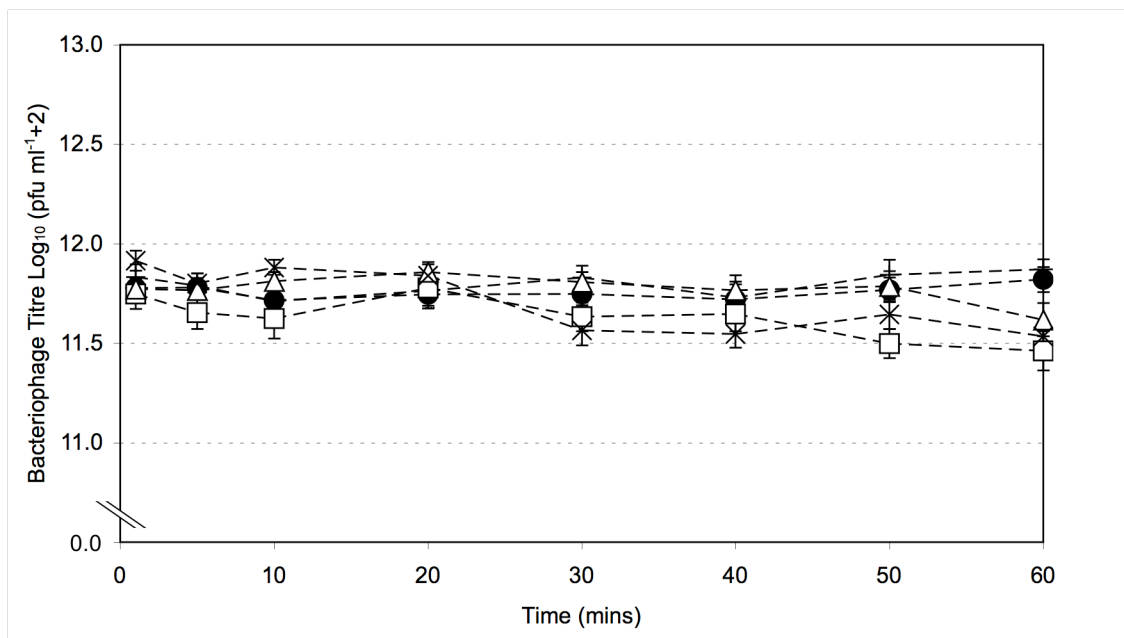
Figure 7.13 The change in concentration of viable bacteriophage M13 as a function of time, when incubated at temperatures 60 °C (×), 50 °C (□), 40 °C (△), 25 °C (●) and room temperature (+). A value of 2 was added to every bacteriophage concentration, since $\log_{10}(0)$ is undefined. Error bars represent the standard error, N=3.

7.6 Derivation of Modified Standard Operating Procedures to Minimise Bacteriophage Release at the 20 L Fermentation Scale.

The UCL Department of Biochemical Engineering hosts extensive fermentation and downstream processing facilities, enabling study at scales close to those used in industry. These facilities are necessarily mixed-use; the bioprocessing of various strains of *E. coli* and *S. cerevisiae* are routine. The purpose of this section is to derive a practical method for the fermentation of bacteriophage M13 in such a facility whilst minimising the risk of release.

7.6.1 Applikon 20 litre fermenter

This study investigates the fermentation of bacteriophage using an existing piece of plant equipment: the Applikon 20 litre capacity stirred tank reactor. This particular fermenter is sterilisable *in situ*, and as such requires connection to a steam supply. Connection to a cooling water supply is also necessary for normal fermentation temperature regulation and off-gas condenser functionality. Sterilisation and operation of the fermenter is assisted by computer control, and is therefore semi-automatic. In the sterilisation cycle the fermenter will automatically heat to 121 °C, but user action is required to steam sterilise the associated pipework, such as the sample, harvest and addition lines. During normal operation, automatic control of pH and temperature is routine, whilst air flow-rate and stirrer speed are manually controlled as standard. Proprietary "BioXpert" software is loaded onto an attached PC, and allows for variable control and data logging during operation. A photograph and schematic drawing of the fermenter is shown in Figure 7.14. It can be seen that the air supply to the fermenter is filtered (typically 0.22 μm) to prevent contamination of the fermenter contents, and the air exit supply is similarly filtered to prevent escape of micro-organisms. The pH of the fermenter is controlled by automatic addition of acid and base through two lines at the top of the fermenter. Typically, 10 % (v/v) sulphuric acid and 4 M sodium hydroxide are used. A third connection allows for the manual addition of antifoam to the fermenter (polypropylene glycol of average molecular weight 2 000). The addition port lies above the fluid level in the fermenter and allows for the introduction of inocula or other additions (such as broth, carbon source or inducer) at any point during the fermentation *via* a steam-sterilisable connection. Small fluid samples can be taken from the sample port during the course of the fermentation, and the larger harvest port allows for the drainage of the vessel.
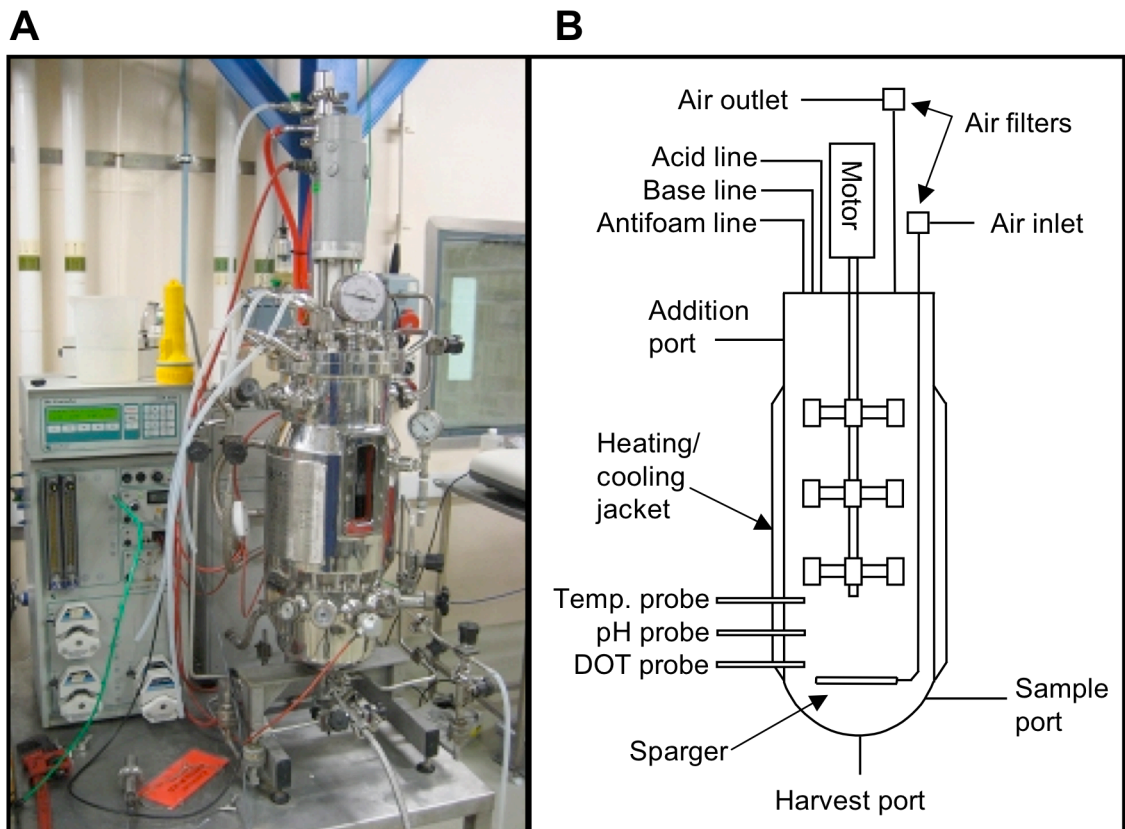
Figure 7.14 The 20 litre Applikon fermenter. **(**A) shows a photograph of the equipment, (B) a schematic diagram. The working volume is 15 litres.

7.6.2 Update of Standard Operating Procedures

A Standard Operating Procedure (SOP) is a set of written instructions that documents a routine or repetitive activity followed within an organisation (Sherwood, 1996). As such, an SOP exists for the routine sterilisation and operation of the Applikon 20 litre fermenter, as does every fermenter within the facility. The development and use of SOPs is an essential part of the successful operation of plant equipment, since they provide users with the information needed to perform each task correctly and consistently. Therefore, within manufacturing organisations SOPs form an important component of achieving Good Manufacturing Practice (GMP) (Sherwood, 1996).

The existing SOP for the Applikon 20 litre fermenter was studied with a view to adapting it for the particular needs of a bacteriophage fermentation (SOP 45, see Appendix B). Four key points were noted from data gained in Sections 7.2- 7.5 to highlight areas within the existing SOP which may require modification. These points were:

1. Virkon (1 % (w/v) solution) is an effective bacteriophage M13 and *E. coli* decontamination agent (Section 7.2). TEGO and Solquest are inadequate for bacteriophage M13 inactivation.

2. Bacteriophage M13 and *E. coli* are relatively desiccation resistant, therefore release (particularly by means of aerosolisation) should be avoided (Section 7.3).

3. The acid and alkali lines to the fermenter should be self-sterilising, due to the demonstration that bacteriophage M13 can be inactivated by exposure to such conditions (Section 7.4).

4. Bacteriophage M13 is sensitive to elevated temperatures, particularly above 99 °C (Section 7.5). Therefore, steam-based sterilisation of the fermenter should be effective provided that it is verified (by temperature mapping) that all contaminated parts will reach in excess of 100 °C for at least 20 minutes.

The assumption was made that the fermentation area would continue to be used for unrelated experimentation on permissive bacterial strains. Therefore, in conjunction with the plant manager, several modifications were made to the existing SOP for the operation of the Applikon 20 litre fermenter (Table 7.6). The chief alterations concerned the avoidance of actions that may result in the aerosolisation of fermentation fluid. Further, areas such as inoculation, sampling and harvesting were described in greater depth, such that separate SOPs were defined for each. Finally, an SOP was written to describe the remedial actions required if accidental spillage of bacteriophage-containing fermentation fluid occurred. The practicality of each of the new methods was verified by a "blank" fermentation run, filled with RO water.

Table 7.6 Details of the major changes made to the standard operating procedure (SOP) for the sterilisation and operation of the 20 L Applikon fermenter. The SOP references given in the Document Reference column refer to the new SOP document. SOP documents can be found in Appendix C.

Action	Standard method	Revised Method	Document Reference
Fermenter inoculation	Inoculum transfer (shake-flask culture to fermenter addition flask) occurs in the fermentation suite.	Inoculum transfer is conduced in a separate laboratory. Flask surfaces are 1 % (w/v) Virkon treated before introduction to facility.	SOP 45/P2
Fermentation sampling method	Samples of fermentation fluid are collected from sample port into open 25 ml polypropylene tubes.	Sterile silicone tubing is attached to sample port with Robertsite^{TM} needleless valve. Samples are drawn through the valve into a sterile polypropylene syringe. The junction is surrounded by paper towel dampened with 1 % (w/v) Virkon.	SOP 45/P3
Fermentation harvesting method	Fermentation fluid is harvested into a connected 20 litre capacity Nalgene container without air exit filters. The harvest line end is exposed upon Nalgene disconnection.	0.22 μm filter is attached to the Nalgene container. To disconnect, silicone harvest line is double clamped under 1 % (w/v) Virkon solution and cut between clamps. Incubated for 10 minutes to sterilise.	SOP 45/P4

<div align="right">(cont.)</div>

Action	Standard method	Revised Method	Document Reference
Fermentation post-culture sterilisation procedure	Acid, base and antifoam lines are disconnected, and steam is vented directly from fermenter chamber into the plant area.	Acid, base and antifoam lines are closed but not disconnected due to contamination in fermenter chamber. No direct venting from fermenter chamber to surroundings occurs.	SOP 45/P1
Fermentation post-culture sterilisation procedure	In the event of an emergency shutdown during sterilisation, pressure is released by venting from the fermentation chamber into the plant area via one of the acid/base/antifoam ports.	A 1 litre Nalgene container with 0.22 μm air exit filter is connected to fermenter addition port prior to the fermentation sterilisation procedure. If emergency venting is required, it will be into this container.	SOP 45/P1
Fermentation post-culture sterilisation procedure	Steam is vented directly from sample port into plant area to sterilise.	A 1 litre Nalgene container with 0.22 μm air exit filter is connected to sample port during fermentation sterilisation procedure.	SOP 45/P1
Fermentation post-culture sterilisation procedure	Steam is vented directly from harvest port into plant area to sterilise.	A 20 litre Nalgene container with 0.22 μm air exit filter is connected to harvest port during fermentation sterilisation procedure.	SOP 45/P1

The SOP document describing the remedial actions required if accidental spillage of bacteriophage-containing fermentation fluid occurred (SOP 45/P5, see Appendix C) was written for spillages of three scales. Spillages of the few millilitre scale should be treated with 1 % (w/v) Virkon solution and left for 10 minutes. Spillages of the tens of millilitre scale should be treated with Virkon power directly, following the manufacturer's instructions. Spillages of the litre scale should also be treated with Virkon power directly, but the area subsequently requires monitoring at regular intervals for confirmation of bacteriophage control. If persistent infection

of subsequent cultures in the facility occurs in the following months, then hydrogen peroxide or formaldehyde fumigation of the facility may need to be considered.

7.6.3   Evaluation of risk

With the modified SOPs in place, an overall evaluation of the risk of bacteriophage release from the fermenter was conducted. This was considered to be a useful further step in the risk management process, and as such was conducted in the style of a Risk Assessment. Therefore, the potential hazards were identified and an assessment made of the likelihood of occurrence together with the potential severity of the outcome. Finally, the control measures taken were described to minimise the risk of bacteriophage release.

Principally, it was identified that the remaining areas of potential culture release stemmed from silicone line leaks (inoculation, sample or harvest lines) or inoculum flask or harvest container failure (Appendix D). It was concluded that careful checking and renewal of silicone lines prior to inoculation would mitigate the risk of line leak. It was also concluded that release of bacteriophage from the inoculum flask remained one of the most likely release points. Mitigating actions included flask transport in a secure manner, and the use of plastic (rather than glass) flasks. The 20 litre capacity Nalgene harvest container was identified as presenting the greatest consequences in the event of bacteriophage release, due to the large post-fermentation volumes being handled, although the likelihood of this occurring was considered small. The mitigating action was identified as proper adherence to SOP 45/P4, which was updated to stipulate the checking of the plastic container and silicone line for damage before use.

7.7   Discussion

The purpose of this chapter was to investigate several physical and chemical challenges to bacteriophage M13 and *E. coli* to assist in their safe introduction to a mixed-use facility. This experimentation gave context to the derivation of a method for the contained propagation of bacteriophage at the 20 litre scale in the UCL Department of Biochemical Engineering fermentation suite. Several SOPs incorporating additional measures preventing bacteriophage release were then derived.

7.7.1   Determination of an effective decontamination agent

That bacteriophage are small, infectious particles makes the determination of efficient control methods important. Therefore, an investigation into effective decontamination agents against bacteriophage M13 (and *E. coli*) was conducted. The results showed the importance of experimentation (Section 7.2): the performance of the three agents tested was found to vary considerably. The least effective agent was Tego. After a twenty minute exposure time the

maximum bacteriophage inactivation was only 85 %, at a Tego concentration five-fold more concentrated than that used as standard in the department. Solquest proved more effective, albeit also at concentrations five-fold greater than that used as standard. Total bacteriophage inactivation was only achieved for 5 % (v/v) Solquest at 70 °C. From a practical standpoint the performance was not sufficiently effective. Specifically, the concentration of Solquest was relatively high and performance was very dependent on temperature: it was found that 5 % (v/v) Solquest at 50 °C was not measured to inactivate all the bacteriophage over the twenty minute experiment. The use of a surface disinfectant agent that is only effective at 70 °C is not realistic. In contrast, Virkon proved effective at inactivating all bacteriophage within one minute at the standard working concentration– 1 % (w/v)– at room temperature. Furthermore, no viable *E. coli* cells were detected within five minutes incubation with Virkon of the same concentration. The effectiveness of Virkon was perhaps to be expected: Virkon is widely marketed as a "broad spectrum" bactericidal, fungicidal and virucidal agent with use in the veterinary, agriculture, hospital and laboratory arenas (Dunowska *et al.*, 2005; Moreton and Delves, 1999). Specifically, Virkon effectiveness against several other bacteriophage has been demonstrated in the literature (Barrow *et al.*, 1998; Halfhide *et al.*, 2008). In conclusion, Virkon was considered to be the disinfectant of choice for all bacteriophage M13 experimentation, and was specifically included in the SOP written for clean-up of bacteriophage spillages.

7.7.2 The effect of desiccation on bacteriophage M13 and *E. coli*

Bacteriophage M13 was shown to be remarkably resistant to desiccation: the shortest half-life observed out of all treatments was 22 days, although half-lives in excess of 50 days were typical. The longevity of M13 was found to depend on the conditions of desiccation. In all treatments desiccation under laboratory conditions (45 % relative humidity) resulted in shorter half-lives than dry conditions (6 % relative humidity). These results are consistent with reports linking bacteriophage survival to desiccation to the relative humidity: generally, survival at moderate humidity (30- 50 %) is poorer than either high or low humidity environments (Abad *et al.*, 1994; Songer, 1967). Whilst desiccation studies on bacteriophage vary considerably in the methods of drying and the conditions imposed, it has been found that several other bacteriophage similarly display a strong resistance to desiccation (Iriarte *et al.*, 2007; Jepson and March, 2004; Prouty, 1953; Schade and Caroline, 1944). In the context of the long-term storage of a bacteriophage-based product, such stability is beneficial. However, from the standpoint of bacteriophage persistence in the laboratory space, such resistance indicates that it is indeed important to take steps to prevent their release, particularly on the large-scale. That said, the desiccation experimentation conducted in this study is likely to *overestimate* the survivability of bacteriophage M13; desiccation was conducted under dark stagnant conditions. Under less controlled conditions, other sources such as low-level UV irradiation (to which

bacteriophage M13 is sensitive) are likely to contribute towards its degradation (Kurosaki *et al.*, 2003).

In comparison to bacteriophage M13, the desiccation survival of *E. coli* Top10F' was relatively poor. The half-life under laboratory conditions was only six days. The rate of inactivation of dried cells is known to depend on many factors, including the cell growth phase, cell concentration, drying method and storage conditions (Lievense and van't Riet, 1993). Overall however, in terms of concern for bacteriophage M13 persistence in the laboratory, these results suggest that the bacteriophage is itself more of a contamination concern than the infected host.

7.7.3   The effect of extremes of pH on bacteriophage M13

In this study, bacteriophage M13 was found to be completely stable when incubated for twenty minutes in solutions of pH 3.0 to 11.0, a result in close agreement with existing literature (Marvin and Hohn, 1969). Stability over such a broad pH range is not confined to bacteriophage M13, however. Studies on the pH stability of bacteriophage λ suggest that it is a similarly robust particle (Jepson and March, 2004). Nevertheless, the key purpose of this study was to provide experimental support for the procedures necessary for the contained fermentation of bacteriophage M13. Since bacteriophage M13 was completely inactivated within five minutes exposure to 4 M sodium hydroxide or 10 % (v/v) sulphuric acid, it could be subsequently determined that the acid and base lines to a 20 litre fermentation of bacteriophage M13 should be "self sterilising" with regards to the bacteriophage. With regards to the *E. coli* host, existing literature states that the range of survival lies approximately between pH 2 and pH 10.5 (Lin *et al.*, 1995; Small *et al.*, 1994). Therefore, providing the lines were completely "primed" (that is, filled with acid or base from the reservoir to the fermenter) before disconnection, no special measures needed be taken for the decontamination of bacteriophage or *E. coli*.

7.7.4   The effect of temperature on bacteriophage M13

The assessment of the thermal resistance of bacteriophage M13 also aimed to support procedures for the prevention of bacteriophage release during fermentation in the 20 litre Applikon fermenter. In particular, the air exit filter from the fermenter has the potential to become blocked from excess moisture during normal operation, thereby preventing the subsequent passage of steam through the condenser and filter assembly. The result is that instead of the normal sterilising temperature of 121 °C, temperatures only of the order 100 to 110 °C can be achieved (confirmed by temperature mapping) (Orsborn, 2007, UCL Department of Biochemical Engineering, pers. comm.). Since it was found that bacteriophage M13 was inactivated within 20 minutes of heating to 99 °C, and *E. coli* thermal death above 70 °C is of the order of seconds (Mazzotta, 2001), it is likely that such a scenario would still allow for component sterilisation.

7.7.5 Evaluation of challenge experimentation

The challenge experiments conducted in this study were of the "time kill" variety, where bacteriophage M13 or *E. coli* were exposed to challenges for a certain period before neutralisation. Following this, survivors within the test solutions were directly enumerated. For desiccation, pH and elevated temperature treatments, the neutralisation of the challenge was trivial: rehydration, pH neutralisation or cooling. But neutralisation of chemical antimicrobial agents presented more of a challenge. For bacterial studies, there is the option of cell capture by filtration, but no similarly straightforward capture of bacteriophage was possible. Instead, "neutralisation" of detergent was achieved by 100-fold dilution of the test solution, which was found to be appropriate since no detergent was effective when diluted by this amount. An alternative strategy could have been to employ a version of "fraction-negative" determination, where small samples of the bacteriophage test solution are diluted into growth media, inoculated with cells and allowed to propagate (McDonnell, 2007). The fraction of cultures that avoid bacteriophage infection thus allows the concentration of the original bacteriophage solution to be deduced. Versions of each of the tests outlined here are embodied in guidelines established by the (U.S. based) Association of Official Analytical Chemists (AOAC) (Sarli, 2007).

7.7.6 Derivation of modified standard operating procedures

Overall, the experiments challenging bacteriophage M13 to detergents, desiccation, pH and temperature provided useful evidence for the modifications required to the standard Applikon fermenter SOP. The five resulting SOPs covering inoculation, operation and sterilisation, sampling, harvesting and remedial action against spillages were aimed to minimise bacteriophage release from the fermenter and reduce the likelihood of affecting any unrelated work in the plant. Any new SOP will require rounds of modification and improvement, and the SOPs written for bacteriophage fermentation were no exception. Each was subject to two rounds of review. The first followed a blank fermentation, principally allowing for the practicality of the prescribed alterations to be tested. The second followed the Risk Assessment document, where each fermentation action was analysed for its effectiveness in controlling the potential for bacteriophage release. Further rounds of review and modification are to be expected. Nevertheless, the process of risk evaluation was an extremely useful tool. The process of assessing of the likelihood of a release occurring together with the potential severity of the outcome highlighted some hazards (such as harvest vessel failure) which may otherwise have been overlooked.

The containment of a large-scale bacteriophage process would be assisted by the careful consideration of plant design (e.g. air flow, layout, non-shared facilities) and the equipment used (minimisation of aerosol generation, contained design). However, the ability to control all

these design aspects is not always possible, particularly regarding budgetary, building or time constraints (Litman, 1997). Instead, sensible utilisation of selected existing equipment, modification of operating procedures, and adherence to high standards of facility hygiene, equipment sterilisation and good microbial practice may prevent unwanted bacteriophage release, cross-contamination and propagation.

7.7.7 Concluding remarks

The work presented in this chapter goes some way towards the contained propagation of bacteriophage M13 in the Department of Biochemical Engineering pilot-scale facility. The process of experimentation, SOP derivation and risk evaluation followed here was conducted with bacteriophage M13 in mind. However the process itself is general and is therefore applicable for the fermentation of most bacteriophage.

8   Overall Discussion

Some of the most pressing health issues of our time demand the development of new and stable antibiotics and vaccines. Globally, malaria causes up to three million deaths per year (Breman, 2001) and 30 million people are living with HIV-AIDS (Merson, 2006). Meanwhile, the cost of antibiotic resistance is estimated at $7.7 billion in the USA alone (Reed *et al.*, 2002). Recent reports on the use of bacteriophage-based tools and therapies to tackle these important diseases are extremely encouraging, although many investigations are at an early stage (Demangel *et al.*, 1998; Sathaliyawala *et al.*, 2006; Wright *et al.*, 2009). It is clear, however, that there is a large potential demand for successful therapies. It is perhaps timely that public and commercial awareness of bacteriophage is gaining momentum in light of the latest scientific advances in the field and as the first bacteriophage products come to market. As such, there is now a clear and growing need for the establishment of strong biochemical engineering foundations to serve as a guide for future bioprocessing. It has been the purpose of this study to contribute towards this knowledge base.

Five aspects of large-scale filamentous bacteriophage production were investigated in this study, each with a corresponding thesis objective. The knowledge gained in fulfilling these objectives will now be discussed.

8.1   Objective 1: Evaluate the Effect of Hydrodynamic Shear on the Filamentous Bacteriophage Particle

The intensity of fluid flow over critical structures within large-scale process equipment has often been characterised in terms of the associated maximum energy dissipation rate ($W\ kg^{-1}$) (Hutchinson *et al.*, 2006; Mollet *et al.*, 2004). This has allowed for the identification of the types of process equipment that are likely to be the most damaging to the processed biologics within. This is important because considerable variation in fluid stress can occur even between types of process equipment that otherwise serve the same function (Boychyn *et al.*, 2004). For common pieces of process equipment the magnitude of the energy dissipation rate increases in order from stirred fermentation vessels ($10^2\ W\ kg^{-1}$) to pumps ($10^4 - 10^5\ W\ kg^{-1}$), continuous centrifuges ($10^5\ W\ kg^{-1}$) and finally homogenisers ($10^7 - 10^8\ W\ kg^{-1}$) (Yim and Shamlou, 2000). It is perhaps of no surprise that homogenisers, frequently used to disintegrate micro-organisms, are associated with imparting the greatest energy dissipation rate on the process fluid.

Extensive literature exists demonstrating the sensitivity of many biological products to the hydrodynamic shear forces within process equipment, USD devices, or both. For example, entities such as fungal hyphae and filamentous bacteria have been demonstrated to be directly damaged within stirred fermentation vessels (Heydarian *et al.*, 2000; Li *et al.*, 2000).

Meanwhile, plasmid DNA of size 20 kb and above has been shown to be sensitive to the action of pumps and continuous centrifuges (Zhang *et al.*, 2007), and by a rotating disk USD device imparting a similar energy dissipation rate (Levy *et al.*, 1999b). Furthermore, hydrodynamic shear damage to mammalian cells (Hutchinson *et al.*, 2006) and protein precipitates (Boychyn *et al.*, 2001) have been demonstrated at the USD scale and verified by experimentation with pilot scale process equipment. Finally, whole antibodies have been shown to be shear sensitive from experimentation at the USD scale (Biddlecombe *et al.*, 2007).

However, until now no such data has existed for bacteriophage. It was therefore of concern that bacteriophage M13 may also prove extensively shear sensitive, since each virus is in effect a large protein rod 200- 400 times that of the average globular protein (Schmidt *et al.*, 2000) and of contour length approaching the characteristic dimensions of a supercoiled 20 kb plasmid (Arulmuthu *et al.*, 2007). If so, this would have important implications for the processability of filamentous bacteriophage-based products; severe susceptibility to hydrodynamic shear forces could in theory constrain the choice of unit operations, and hamper the purification of the product.

This study has provided the first evidence of the response of bacteriophage M13 to hydrodynamic shear forces. Using the USD shear device, it was found that exposure to a maximum energy dissipation rate of 1.8×10^5 W kg^{-1} did not reduce bacteriophage viability over 25 minutes. This suggests that unit operations such as pumps and stirred fermentation vessels may not cause any damage to bacteriophage M13, since the maximum energy dissipation rates associated with these unit operations are lower than this threshold level. At higher energy dissipation rates (up to 3.1×10^5 W kg^{-1}) bacteriophage damage was found to occur. However, the loss of 60- 90 % of viability occurred over 25 minutes, which is a considerable period. In comparison, the exposure time to the similarly shear-intensive feed-zone of a continuous centrifuge is only of the order of a fraction of a second (Byrne *et al.*, 2002). Therefore, even repeated exposure to continuous centrifugation (or even high-shear ancillary pumps) over the course of a bioprocess is probably unlikely to approach the 25 minute treatment time studied. Large-scale verification of these predications would be the next logical step to take. Furthermore, USD and large-scale experimentation could examine the effect of exiting a continuous centrifuge; impaction effects can occur on both the exiting clarified process fluid and (depending on the design) the dewatered sediment (Chan *et al.*, 2006; Tustian, 2008). A study on *E. coli*, at least, showed impaction damage linearly increasing with discharge velocity up to a maximum of 85 ms^{-1} with 6 % cell breakage (Chan *et al.*, 2006). The actual discharge velocity will depend critically on the design of the centrifuge, making prediction of the likely response of M13 difficult. However, since bacteriophage M13 is of smaller size and mass than an *E. coli* cell, it may be feasible that impaction damage could be correspondingly less.

Of further use to process design was the testing of bacteriophage M13 in several process fluid environments, including post-fermentation process fluid (with and without *E. coli* cells), post-precipitation (with polyethylene glycol) and post-purification (in buffer). This work demonstrated a dependence of the hydrodynamic shear resistance of bacteriophage M13 on the state of the process fluid. After a 25 minute treatment to 3.1×10^5 W kg^{-1} (the maximum studied), the remaining bacteriophage viability was found to increase in the order of culture supernatant (0.12) < post-precipitation (0.25) < post-purification (0.38)< culture medium with cells (0.39). It was also determined that shear-related damage to bacteriophage M13 could be halved by the prevention of air-liquid interfaces. That is, over 25 minutes, the viability loss of purified bacteriophage M13 was reduced from 60 % loss to only 20 %, providing useful bioprocessing knowledge for bacteriophage M13 that already existed for plasmid constructs. Here, it has been demonstrated that under conditions resulting in a maximum energy dissipation rate of 1.4×10^5 W kg^{-1} (less than that in this study), air-liquid interfaces decreased 20 kb plasmid supercoiling by as much as a factor of 10 within 5 seconds exposure (Levy *et al.*, 1999b).

The hydrodynamic shear data has two important implications for the large-scale bioprocessing of bacteriophage M13. Firstly, it indicates that a decision to use fermentation, pumping or continuous centrifugation steps can be mainly made on the basis of cost and/or effectiveness, rather than particle fragility. In contrast, selection of continuous centrifugation conditions for fragile molecules (such as >20 kb supercoiled plasmids) can involve a trade-off between clarification achieved and product damage (Levy *et al.*, 2000b). Secondly, it is important to note that the extent of damage caused to (otherwise similar) particles by hydrodynamic shear is often closely related to its size (Levy *et al.*, 1999b). In this study, wild-type bacteriophage M13 of contour length 900 nm was examined for shear-resistance, but the results have implications for the processability of M13 derivatives, namely phagemids. Since the genetic material within a phagemid does not encode for the entire bacteriophage particle (the necessary genes are provided by helper phage superinfection, see Chapter 1, Section 1.3.3), phagemids are typically of half the contour length of wild-type viruses (Khalil *et al.*, 2007). Therefore it is highly likely that phagemids will be equally resistant to, if not more than, hydrodynamic shear in the bioprocess.

The benefits of the ultra scale-down approach to this study are apparent. This technique tested several process fluids at many energy dissipation rates, allowing for a fuller characterisation of the bacteriophage whilst using only small amounts of material. The rotating-disk shear device has potential as a decisional tool in bacteriophage bioprocess design, in a similar fashion to that found for other complex macromolecules (Boychyn *et al.*, 2001; Zhang *et al.*, 2007).

8.2 Objective 2: Investigate the Fermentation and Harvesting of Bacteriophage M13

The fermentation step is unique in the bioprocess since it presents the only opportunity for the biochemical engineer to increase product yield, rather than just minimise losses. As noted in the Introduction (Section 1.6.1), the primary purpose of the fermentation stage is to maximise productivity: that is, the quantity of product produced per litre of fermentation fluid per unit time. At the time of harvest, the fermentation medium will primarily consist of the bacteriophage M13 product, intact cells, cell debris and medium components (chiefly ions, short chain soluble polypeptides and nucleotides). Some low level accumulation of cell debris was expected as a result of usual *E. coli* culture (Salivar *et al.*, 1964), which will include host chromosomal DNA, RNA, proteins, lipids, endotoxins and chemical residuals (Eastman and Durland, 1998; Prazeres and Ferreira, 2004). In this chapter the quantities of chromosomal DNA and protein were measured to represent the level of culture contamination. If contamination of the process stream with these components could be reduced, then subsequent downstream processing would be assisted.

Generally, it is known that there is no substitute for experimentation when selecting an *E. coli* strain to maximise recombinant protein or plasmid DNA production. It is generally impossible to predict the outcome from cell genotype alone (Harrison and Keshavarz-Moore, 1996; Yau *et al.*, 2008). An examination of three *E. coli* strains was made at the 50 ml shakeflask scale, and the results of this small study suggested it may be similarly difficult to predict bacteriophage quantity (and purity) on the basis of *E. coli* genotype. Strains Top10F', JM107 and W1485 were selected for comparison. JM107 and Top10F' are laboratory strains, and of these two Top10F' is *recA*. W1485, in contrast, is near wild-type in genotype. A *recA* strain was deliberately chosen because of the far-reaching effects of this genotype: a benefit is the potential protection of M13 derivatives holding repeater sequences from recombination effects (Yanisch-Perron *et al.*, 1985), whilst it was hypothesized that the known detrimental effect on cell viability (Capaldo *et al.*, 1974) may compromise bacteriophage yield.

It was found that the concentrations of supernatant chromosomal DNA or protein varied considerably between the three strains. The highest levels of supernatant DNA and protein accumulated in *E. coli* W1485 culture (5.7 and 38 μg ml^{-1} respectively), the lowest in JM107 (0.38 and 22 μg ml^{-1} respectively). Bacteriophage M13 production in Top10F' and JM107 strains ceased by 5 hours growth (at an average M13 concentration of 4×10^{11} pfu ml^{-1}) and was not significantly different between all three strains at this time. However, in W1485 culture, the concentration of M13 continued to increase such that by 9 hours growth the titre of M13 was significantly higher at 7.8×10^{11} pfu ml^{-1}. Therefore, despite the detrimental effects on cell

viability, the *recA⁻* mutation did not result in Top10F' culture having the highest chromosomal and protein concentrations, and neither was the final bacteriophage yield compromised in comparison to a *recA⁺* strain (JM107).

In a complementary approach to this study, a novel biological route was utilised to eliminate the chromosomal DNA from the process stream (Cooke, 2003). It was shown that propagation of bacteriophage M13 in *E. coli* Top10F' concurrently expressing a recombinant nuclease was a feasible method of early DNA removal. For an unaffected yield of bacteriophage M13, all DNA contamination was degraded to below measurable levels by 0.8 % (w/v) agarose gel electrophoresis. However, at the 2 L bioreactor scale, concurrent nuclease expression doubled the time to achieve maximum bacteriophage yield. Nevertheless this was the first time that such an approach had been examined for bacteriophage M13 production. It offers a successful, low-cost alternative to commercial exogenous nucleases such as Benzonase (Cooke *et al.*, 2003). This technique is applicable to the production of other bacteriophage therapeutics, particularly those requiring lytic bacteriophage propagation in *E. coli*. Here, wholesale lysis of host cells can be expected to result in a process stream heavily contaminated with chromosomal DNA.

Use of two different complex media at the 2 L bioreactor scale resulted in a 4-fold difference in bacteriophage yield, which highlighted the potential importance of this variable when designing a fermentation process. Using Top10F', the overall maximum titre of bacteriophage achieved in this study was 2×10^{12} pfu ml^{-1}. As a result of its non-lytic replication strategy, the concentrations of contaminating *E. coli* Top10F' chromosomal DNA in the post-fermentation process fluid was quantified to be only 7 μg ml^{-1}. The concentration of protein was quantified to be 170 μg ml^{-1}, a figure which included both intracellular and medium components.

Since bacteriophage concentration in fermentation culture cannot be measured in an on-line fashion, the use of indirect measurements will be necessary in the fermentation process to determine the cessation of bacteriophage production. The completion of lytic bacteriophage growth is characterised by a spike in dissolved oxygen tension (DOT) and a sharp reduction in carbon dioxide evolution rate (CER) as bacteria cease to respire prior to lysis (and therefore bacteriophage release) occurring (Sargeant *et al.*, 1968). Hence the end of production can be easily noted. Although less stark, it was noted in this study that the end of bacteriophage M13 production usefully correlated with a plateau in the culture OD$_{600}$ value and a levelling in the oxygen uptake rate (OUR) and CER. That is, bacteriophage M13 production ended as *E. coli* growth ceased. From a bioprocessing standpoint, these measurements could provide indicators for when harvesting can proceed.

8.3 Objective 3: Evaluate the Effect of Hydrodynamic Shear on *E. coli* Cell Integrity

It was shown in Chapter 5 that *E. coli* damage could result from exposure to high-energy turbulent shear conditions. The quantity of chromosomal DNA in the post-fermentation process fluid increased 5 to 10-fold within two minutes exposure to a maximum energy dissipation of 3.1×10^5 W kg^{-1}. However, the increase in supernatant DNA did not correlate against the measured number of cells losing viability. This may have been due to further DNA release from existing subpopulations of non-viable Top10F' cells, a known effect of the *recA*$^-$ genotype (Capaldo *et al.*, 1974). Furthermore, the relationship between culture OD_{600} and supernatant DNA release on shearing was not linear. That is, an increase in culture OD_{600} did not translate into greater supernatant DNA upon shearing. In practical terms, this meant that the multiplicity of infection (MOI) of M13 infected culture could be selected without concern for chromosomal DNA release from shearing.

A high MOI (5×10^1) culture was found to require only a two hour fermentation time to reach maximum bacteriophage yield, and resulted in a lower cell density at harvest than lower MOI cultures. In comparison, a culture with MOI of 5×10^{-5} took nearly three times longer to produce the same bacteriophage yield. A trade-off exists in weighting the cost of a greater bacteriophage inoculum against the cost of an increased fermentation time. The final choice would depend on the overall costing of the bioprocess.

Post-fermentation, a solids separation stage is needed remove the *E. coli* cells from the process stream. Future experimentation using pilot-scale centrifugation equipment could determine whether the clarified process fluid will indeed be significantly higher in chromosomal DNA than the post-fermentation fluid. Since the cumulative exposure time *E. coli* would experience in the feed-zone of a continuous centrifuge would be considerably shorter than two minutes (Byrne *et al.*, 2002), it may well be that the increase in chromosomal DNA is lower than that observed in this USD study. Although from a bioprocessing perspective the extra release of chromosomal DNA is generally undesirable, the primary purification study of Chapter 6 suggested that DNA and bacteriophage M13 can be separated by precipitation.

Finally, although not studied as part of this thesis, microfiltration remains a less shear intensive step for *E. coli* removal from the process stream. The viability of this option should be considered in the assembly of a large-scale bacteriophage production process.

8.4   Objective 4: Investigate the Primary Purification of Bacteriophage M13

Once biomass has been separated from the process stream, it is certain that a concentration stage is required since the bacteriophage product is relatively dilute. A reduction in process stream volume makes further downstream process stages more manageable. The feasibility of bacteriophage precipitation as a volume reduction step was investigated in Chapter 6, with encouraging results.

An effective large-scale precipitant of bacteriophage is one which would inexpensively offer a high bacteriophage yield, display robust precipitation characteristics and ideally offer some selectivity early on in the downstream process. Several precipitation methods were tested in this thesis against these criteria, including PEG-salt (volume exclusion), sulphuric acid (isoelectric), ammonium sulphate (salting out), calcium chloride (divalent cation) and spermidine (polyvalent cation).

In this chapter the fundamental actions of each precipitant on M13 was analysed in pure system work, and, depending on precipitant effectiveness, the effect of broth components on precipitation behaviour was subsequently studied.

It was identified that the monovalent ion concentration in broth was an important factor affecting many of the precipitation characteristics observed: for example, bacteriophage M13 precipitation by calcium ions and spermidine did not occur at the 100 mM monovalent salt concentration in NB2. In particular, the potential of spermidine as a precipitant of bacteriophage M13 would have been missed if experimentation was conducted purely in broth. Overall, isoelectric and PEG-salt precipitations were found to be effective precipitants of bacteriophage M13 in NB2.

For PEG-salt precipitation, consideration of the existing ion concentration in broth meant that – depending on the PEG concentration – added salt would not always be necessary, thereby reducing processing costs. Furthermore, it was demonstrated in this study that when salt addition is required, there exists much flexibility in the choice of salt type. Sodium chloride is traditionally used with PEG to precipitate bacteriophage at the laboratory scale (Vajda, 1978; Yamamoto *et al.*, 1970), but magnesium sulphate in particular was demonstrated to be much more effective, the concentration required to induce precipitation was up to 80 % lower. For the biochemical engineer, a further consideration is the corrosive nature of salt chlorides (such as sodium chloride) relative to non-halide salts (such as sulphates) with regards to the usually stainless steel downstream processing equipment (Korb, 1987; Shreir *et al.*, 1994).

There are many variables in PEG-salt precipitation. In this study, PEG of average molecular weight 6 000 was selected as a balance between effectiveness and solution viscosity. Precipitation appeared equally effective at room temperature or on ice. In NB2 systems, PEG 6 000 of concentration 4 % (w/v) was sufficient to induce bacteriophage precipitation alone. Reducing the amount of PEG to 2 % (w/v) therefore required salt addition, of which either 135 mM sodium chloride or 25 mM magnesium sulphate was necessary. It is noteworthy that the minimum effective concentration of PEG in this study (at 1.5 % (w/v) PEG 6 000) was five- to ten-fold lower than values published in the literature for smaller proteins, and indeed other bacteriophage (Atha and Ingham, 1981; Juckes, 1971; Sharma and Kalonia, 2004; Tsoka *et al.*, 2000; Yamamoto *et al.*, 1970). From a practical perspective, the choice of PEG and salt concentrations and types will be a function of the relative chemical costs, corrosion considerations and the tolerable limits of solution viscosity.

Isoelectric precipitation of bacteriophage M13 from NB2 was also found to be feasible: reducing solution pH into the range 3.9- 4.5 resulted in near 100 % bacteriophage recovery. Bacteriophage losses to the acidic conditions were not significant if the precipitation temperature was kept at 4 °C, which was in contrast to the severe effects reported for several T-odd and T-even type bacteriophage precipitated by the same method (Bachrach and Friedmann, 1971). It also determined that the incubation time could be reduced by 95 % (to one hour) without affecting recovery.

Cost-effectiveness and robustness are important hallmarks of an efficient precipitation step. Furthermore, if high purification of the bacteriophage molecule can simultaneously be achieved, the overall cost of the downstream process could be reduced (Tsoka *et al.*, 2000; Wenzig *et al.*, 1993). It has been shown in this thesis that bacteriophage M13 can be selectively precipitated from the post-fermentation process fluid. Particularly effective were the PEG-salt systems tested, where the ratios of DNA and protein contaminants to bacteriophage M13 were reduced to less than 1 % of their previous values. The corresponding purification factors (>100) were far in excess of those achieved in the literature for smaller, more spherical particles such as VLPs (Tsoka *et al.*, 2000). Such an improvement in bacteriophage purity from a relatively low-cost step is important. Firstly, it increases flexibility of the upstream process, meaning decisions can be made to increase bacteriophage yield or reduce processing costs without penalty in terms of increasing process stream contamination. Secondly, for high-purity applications requiring high resolution purification, the burden on subsequent chromatography or monolith stages is therefore reduced (Thommes and Etzel, 2007).

The precipitation behaviour of systems such as PEG-salt depend on the protein (or bacteriophage) of study (Ingham, 1990; Juckes, 1971). Therefore, the optimal precipitation

concentration will vary between bacteriophage species. The precipitation techniques used in this thesis are rapid and were conducted at the laboratory bench scale. Therefore, their application to derivatives of M13 or indeed other bacteriophage would allow for the straightforward identification of optimal conditions for any bacteriophage of interest.

8.5 Objective 5: Consider the Issues Concerning the Introduction of Bacteriophage M13 to a Mixed-Use Production Facility

The principles determined for the contained fermentation of bacteriophage M13 are also applicable to all bacteriophage (Chapter 7). If a bacteriophage product is biologically infective, then the bioprocessing of such a therapeutic raises important issues regarding containment; bacteriophage (including M13) can effectively propagate from very low infecting numbers (Reddy and McKenney, 1996). It was shown in this chapter that it is important to test for an effective decontamination agent against the bacteriophage of interest *prior* to commencing large-scale work: standard disinfection agents in use may not be effective. Experimentation to determine the fundamental resistance of the target bacteriophage to various physical and chemical challenges have been shown to assist in the modification of the fermentation Standard Operating Procedures (SOPs). In the case of bacteriophage M13, it was found that the particle was indeed remarkably desiccation resistant. However, it proved sensitive to temperatures above 99 °C and was completely inactivated by strongly acidic and alkaline conditions.

The implications for bioprocessing were that firstly, the generation of bacteriophage M13 aerosols should be avoided, and that decontamination procedures must be defined prior to experimentation. However, fermenter acid and base pH control lines should be self sterilising, and that steam-based sterilisation should be effective if all fermenter parts are verified to exceed 100 °C. The fermentation SOPs were updated to reflect these findings.

Modern published guidance on the specific containment needs of large-scale bacteriophage production is limited. Specific strategies cited in early literature have included continuous centrifugation within an enclosed cabinet with exhaust air filter (Sargeant and Yeo, 1966), preparation of seed cultures in remote laboratories (Sargeant, 1970) and the storage of host stock ampoules prior to bacteriophage work (Sargeant and Yeo, 1966). Most obviously, aspects of existing literature regarding the issues of bacteriophage infection of industrially important cultures – such as in the dairy industry (McGrath *et al.*, 2007; Moineau, 1999) – may be applicable. This uncertainty may explain anecdotal evidence of difficulty in securing contract manufacture of bacteriophage-based therapies (Anonymous, 2009). Overall, the work presented in this chapter contributes practical knowledge towards the containment needs of bacteriophage M13, although the principles are applicable to all bacteriophage-based therapeutics.

9 Conclusions and Future Work

9.1 Conclusions

In summary, the insights gained are drawn together in Figure 9.1, where a prospective production scheme has been assembled for the large-scale manufacture of bacteriophage M13. In addition, the knowledge gained in relation to each unit operation has been tabulated. In essence it has been found that the resistance of bacteriophage M13 to high-energy shear forces may mean it can be manufactured on the large-scale using existing designs of fermentation, pumping or continuous centrifugation equipment. It was found that the *E. coli* strain used can affect the composition of the post-fermentation process fluid. The choice of strain will depend on the application: for genetically modified bacteriophage containing repeated sequences in their genome, growth in a *recA⁻ E. coli* strain such as Top10F' may be preferable. Bacteriophage growth in a recombinant nuclease-producing *E. coli* strain can provide a cost-effective improvement in purity if further downstream processing is to be limited. The growth medium was confirmed to play an important role in the bacteriophage yield. That is, a four-fold increase in bacteriophage titre was achieved by changing the growth medium for one which supported denser *E. coli* growth. Post-fermentation, hydrodynamic shear was found to reduce M13 infected *E. coli* cell integrity, and the concentration of DNA in the clarified process fluid was found to increase. However, the subsequently identified selective precipitation options suggest that less shear-intensive biomass separations may not be necessary. PEG-salt precipitation was found to result in a >100-fold improvement in bacteriophage M13 purity, with regards to contaminating DNA and protein. Precipitation typically required relatively low PEG concentrations in the range 2- 4 % (v/w), depending on the salt concentration desired. It was found to be effective at both chilled and room temperatures, giving operative flexibility. In conclusion, this work has contributed towards the processing knowledge of bacteriophage M13 by investigating the fundamental properties of this unusual entity. Moreover, the methods used have a broader applicability to M13-derivatives and beyond to other bacteriophage.
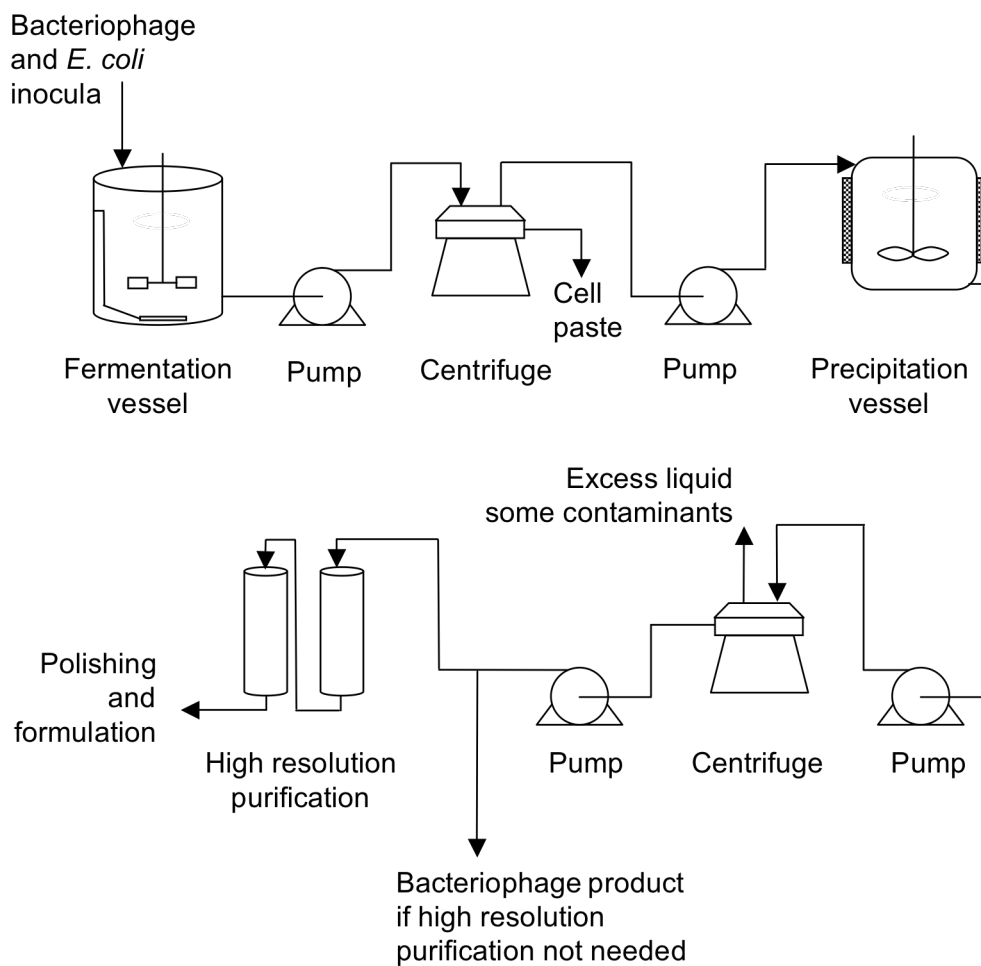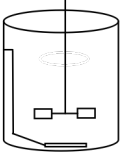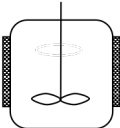
Stage		Summary of knowledge gained
	Fermentation	Hydrodynamic shear damage unlikely. Fermentation medium influences bacteriophage yield. Greater bacteriophage inoculum reduces fermentation time. *E. coli* strain affects contamination accrual. M13 growth in nuclease-producing *E. coli* strain effective.
	Pump	Hydrodynamic shear damage unlikely.
	Centrifuge	Hydrodynamic shear damage to M13 and *E. coli* may not be severe in feed-zone of continuous types.
	Precipitation	Several effective precipitants identified. PEG-salt precipitation offers concurrent purification of M13. Isoelectric precipitation is a potential alternative.

Figure 9.1. A scheme outlining the essential production stages in the large-scale manufacture of bacteriophage M13.

9.2 Future Work

Since the bioprocessing of bacteriophage is a relatively new area, there is much to understand about the response of these novel therapeutics to large-scale manufacture. This thesis goes some way to understanding the fundamentals of bacteriophage M13 bioprocessing, and as may be expected it has opened up several interesting future lines of enquiry.

9.2.1 Extending Objective 1: Evaluate the Effect of Hydrodynamic Shear on the Filamentous Bacteriophage Particle

This work has shown that bacteriophage M13 demonstrates considerable resistance to hydrodynamic shear conditions imposed by the USD rotating disk device. Moreover, contributions were made towards understanding the causes of damage, including assaying for cavitation, and demonstrating damage enhancement by air-liquid interfaces. That said, the physical mechanisms behind the loss of bacteriophage viability still remain largely unknown.

From a practical perspective, work to further assess the effects of air-liquid interfaces could utilise a shear device with an optically clear top plate. This would allow for verification of the elimination of all air from the chamber. Alternatively, in air-liquid systems, such a "viewing window" could help determine the distribution of air within the chamber whilst the disk is spinning. In addition, a study of bacteriophage M13 exposure to shear in degassed fluids would allow for an extended assessment of the effects of air-liquid interfaces.

A further area of interest concerns the extent to which shear-related damage has depended on the type of shear device disk. That is, how the nature of the *solid-liquid* interface affects shear stability. In this study, a 316 stainless steel disk was used for all shear experiments. However, recent work has shown that the severity of shear damage to antibodies is a function of not only disk surface roughness, but also the material of construction (Biddlecombe, 2009). It would therefore be of considerable interest to investigate solid-liquid interface effects on the shear resistance of bacteriophage M13. Further work could not only attempt to understand the fundamental nature of the bacteriophage-surface interaction, but to quantify the effect of solution properties (such as ionic strength and pH) on this system. Such work would relate back to the findings of this thesis, where various solutions of suspension were found to alter the pattern of bacteriophage decay.

The physical changes to the bacteriophage particle that result in viability loss also remain to be examined. Further work to tackle this area could help elucidate the specific mechanisms of bacteriophage damage. For example, an EM study could highlight whether wholesale bacteriophage fragmentation has occurred in tandem with viability loss.

This thesis focused on wild-type M13 as a model filamentous bacteriophage, but the effects of hydrodynamic shear on M13 derivatives (namely phagemids) would be of considerable interest for two reasons. Firstly, phagemids are typically of shorter contour length than the wild-type, suggesting that a study to correlate shear damage against bacteriophage length would be extremely useful. Secondly, phagemids typically display a foreign protein on their surface. The shear resistance of these surface proteins remains unknown, as does whether attachment to the bacteriophage capsid alters their inherent resistance to hydrodynamic shear. There is much to understand about the potential processability of these entities.

Extending shear work beyond the rotating disk device, further endeavour could explore the effect of other fluid physical challenges on the bacteriophage particle, such as extensional shear forces and impaction damage. Investigations of this type have been conducted at the USD scale for *E. coli* cells (Chan *et al.*, 2006) and plasmid DNA (Meacle *et al.*, 2004).

An obvious next step is to verify the USD predictions of bacteriophage shear stability at the pilot scale. The subjection of bacteriophage M13 suspensions to hydrodynamic shear within pumps and continuous centrifuges would then provide comparable data to that for biological macromolecules such as plasmids (Zhang *et al.*, 2007).

9.2.2 Extending Objective 2: Investigate the Fermentation and Harvesting of Bacteriophage M13

In this thesis the yield of bacteriophage M13 was increased by growth in a medium which supported increased cell density. A logical extension could be to translate this work from batch to fed batch fermentation, to further increase cell density and therefore bacteriophage titre. At the same time, a detailed investigation of delayed bacteriophage infection could be conducted to extend the experiment conducted here. The observed biphasic growth at the fermentation scale could also be revisited, primarily to determine the reproducibility of this phenomenon in Top10F', but also to determine whether it occurs for other *E. coli* strains cultured in the same medium. The results of producing bacteriophage by fermentation in defined or semi-defined media would certainly be of enduring use.

Three *E. coli* strains were investigated for their ability to produce M13. Further work could involve the wide-ranging screening of many more *E. coli* strains to obtain a more detailed picture of which provide the highest bacteriophage yields.

This chapter looked at the growth of M13 as a model filamentous bacteriophage. A new study to examine the fermentation of phagemids would be useful. This work could complement

existing literature in the area (Grieco *et al.*, 2009) by extending to fed-batch growth or by comparing the growth characteristics of several different phagemids in parallel.

A plasmid was transformed into Top10F' to allow recombinant nuclease production (Cooke *et al.*, 2003), and several experiments were conducted to study the success of degrading supernatant DNA whilst producing bacteriophage M13. This work could be usefully extended by further growth studies at the fermenter scale. For example, it could be confirmed that the achievement of maximum bacteriophage yield is markedly delayed by concomitant nuclease production.

9.2.3 Extending Objective 3: Evaluate the Effect of Hydrodynamic Shear on *E. coli* Cell Integrity

Several extensions to the bacteriophage M13 shear work in Objective 1 also apply to the study of *E. coli*. Of particular interest would be the determination of the physical effects of *E. coli* viability loss upon exposure to shear. One way to achieve this could be to study cells by transmission electron microscopy.

Future experimentation could attempt to determine differences in the shear resistance of several *E. coli* strains. It would be of particular interest to compare the DNA release from a $recA^+$ *E. coli* culture to the $recA^-$ Top10F' studied here. It was postulated in this thesis that the dominant source of supernatant DNA in Top10F' culture was the characteristic $recA^-$ subpopulations of residually and non-dividing cells.

Finally, the subjection of M13 infected *E. coli* cultures to pilot plant scale processing equipment would provide a valuable verification of the USD hydrodynamic shear work conducted thus far.

9.2.4 Extending Objective 4: Investigate the Primary Purification of Bacteriophage M13

The net surface charge of a protein molecule strongly affects its precipitation characteristics. For example, bacteriophage M13 and its close relation fd do not possess the same net charge and therefore exhibit differences in precipitation (Tang *et al.*, 2002). A future investigation could involve the design, by mutagenesis, of bacteriophage M13 particles with a specified net charge to optimise precipitation.

The precipitation behaviour of proteins can also depend on molecular size (Juckes, 1971), where larger molecules generally precipitate more easily. Because the length of a filamentous bacteriophage depends only on the size of its encapsulated genome, it is straightforward to manipulate this parameter. The value of this is twofold. Firstly, from an academic perspective,

the generation of such molecules would allow for a controlled study of the effects of particle size on precipitation behaviour. Secondly, such data could be used to predict the optimal precipitation conditions for novel phagemids.

Since phagemids also typically display a foreign protein on their capsid, a new study could also be performed to examine whether such modifications have a strong effect on precipitation behaviour.

Here, the purification performance of several precipitations was measured on the basis of reductions in supernatant DNA and protein. Additional work could analyse reductions in other important process stream contaminants, such as LPS and lipids.

9.2.5   Extending Objective 5: Consider the Issues Concerning the Introduction of Bacteriophage M13 to a Mixed-Use Production Facility

Further studies into the contained bioprocessing of bacteriophage must be welcomed. A continuation of the containment work presented here would lead to trial fermentations of a non-*E. coli* bacteriophage to check for containment, whilst minimising the effect on unrelated experimentation in the facility.

Studies on contained downstream processing would also be timely, since little data currently exists for bacteriophage in this area. A starting point could be to extend related experimentation on the bacterial biocontainment of downstream processing equipment (Tinnes and Hoare, 1992) to bacteriophage. In addition to investigating these physical containment methods, work could also be conducted to explore biological routes to prevent unwanted bacteriophage propagation.

Appendix A

Derivation of an Equation to Estimate the Total Charge of a Protein

Proteins have many different ionisable groups in their structures. Therefore, at a particular pH, some parts take on a negative charge while others take on a positive charge. The net charge of the protein will be the difference between the number of positive and negative charges arising from the deprotonation of acidic groups and the protonation of basic groups. The Henderson-Hasselbalch equation allows for the estimation of the charge of each ionisable species in solution at a particular pH. Finding the pH at which all the charges on a protein sum to zero is the process of finding that protein's isoelectric point, or pI. The resulting equation can be found directly in the literature (Bergfors, 1999), although a derivation has been included here for reference.

For acidic residues, the Henderson-Hasselbalch equation (Stryer, 1995) is:

$$pH = pK_a + \log \frac{\left[A^- \right]}{\left[HA \right]}$$

where the pK_a is the acid dissociation constant, $[A^-]$ the concentration of conjugate base and $[HA]$ the concentration of acid. For basic residues the equivalent equation is:

$$pOH = pK_b + \log \frac{\left[B^+ \right]}{\left[BOH \right]}$$

where pK_b is the base dissociation constant, $[B^+]$ the concentration of conjugate acid and $[BOH]$ the concentration of base.

The concentration (C) of negatively charged elements on the ith acidic residue (a) as a fraction of the total is:

$$C_{a,i} = \frac{\left[A^- \right]}{\left[AH \right] + \left[A^- \right]}$$

Inserting the Henderson-Hasselbalch equation for acidic residues gives:

$$C_{a,i} = \frac{1}{1 + 10^{pK_a - pH}}$$

The corresponding equation for the jth basic residue (b) is thus:

$$C_{b,j} = \frac{1}{1 + 10^{pK_b - pOH}}$$

The following equation (Sutton *et al.*, 2000):

$$pH + pOH = pK_a + pK_b$$

is used to substitute for pK_b and pOH, making the concentration of positively charged elements on a single basic residue as a fraction of the total:

$$C_{b,j} = \frac{1}{1 + 10^{pH - K_a}}$$

The total charge of a protein is a sum of the fractional positive and negative charges from the ionisable residues. Therefore the total charge, Z:

$$Z = \sum_{j=1}^{n} C_{b,j} - \sum_{i=1}^{m} C_{a,i}$$

$$Z = \sum_{j=1}^{n} \frac{1}{1 + 10^{pH - pK_a}} - \sum_{i=1}^{m} \frac{1}{1 + 10^{pK_a - pH}}$$

where j is each of n positively charged residues and i is each of m negatively charged residues. At the isoelectric point, pI, the total charge, Z is equal to zero. Therefore, for given pKa values, one can determine the pI of a protein.

Appendix B

Standard Operating Procedure

SOP No. 45

_____

Title:

Sterilisation and Operation of Applikon 20L Fermenter, located in ACBE

_____

WRITTEN BY	DATE	OPERATING HEAD	DATE	DOC.REF.
I.BUCHANAN	20/08/03	B.DOYLE	20/08/03	SOP.45
Signature		Signature		

1.0   Introduction

1.1   This document outlines the procedure to follow for sterilising and setting up the fermenter vessel prior to inoculation. The Applikon 20L fermenter has an ADI 1030 Bio Controller for process variables, an ADI 1065 Bio Bench console for insitu sterilisation and temperature control and an ADI 1035 Bio Console for gas addition and stirrer speed control. BioXpert PC software is also connected for control and data logging.

1.2   **SAFETY NOTE: In the event of having to leave the building in an emergency (ie fire alarm), whilst vessel is at pressure during sterilisation cycle, the EMERGENCY SHUTDOWN PROCEDURE outlined in steps 3.12 or 3.14 must be followed.**
There is no need to take any action before leaving the area if operation is not part of sterilisation cycle.

2.0   Pre sterilisation Set-Up

2.1   Refer to technician or previous fermenter checklist to ensure that no technical faults encountered with this fermenter from the previous run, and if any faults noted, verify with a member of the technical staff that these have been rectified.

2.2   Ensure the vessel is clean. If vessel is not clean, carry out appropriate cleaning procedure as outlined in SOP No. 32D.

2.3   Check condition of all 'O'-rings and replace any if damaged.

2.4   If the **foam probe** is to be used, ensure that it is in place and at an appropriate height. If at this stage there is any doubt regarding the appropriate height, ensure that the probe is fully down into the headplate so that any later repositioning after sterilisation involves moving the probe up to an appropriate height rather than pushing down which may possibly cause contamination.

2.5   **Check the main air supply PRV is set to 10psi**.

2.6   Check condition of **Domnick Hunter tetpor air** filter cartridges for inlet and exit air housings.

2.7   Prepare fermenter ancillaries for separate sterilisation in autoclave.
          e.g.   Acid addition reservoir, line and conical connector
                    Alkali addition reservoir, line and conical connector
                    Inoculum flask, line and connector
                    Antifoam reservoir, line and conical connector

Media addition flask, line and connector

2.8   Calibrate pH probe - see SOP No. 6. Place probe in fermenter

2.9   Check DOT probe calibration (do not calibrate at this stage) - see SOP No. 7. Place probe in fermenter.

2.10   Ensure agitator is correctly attached to motor drive shaft.

2.11   Ensure harvest port is closed.

2.12   Ensure sample valve is closed.

2.13   Disconnect quick release **water to condenser** line on Bio Bench.
        Disconnect quick release **water from condenser** line on Bio Bench.

2.14   Remove pressure gauge and fill vessel with medium to required level. Replace pressure gauge ensuring seal and tri-clamp are firmly connected.

2.15   Carry out checks on Fermenter Sterilisation Checklist.

3.0   Heating Up – Sterilisation

3.1   **Ensure protective safety gowns and face visors are worn during sterilisation cycle.**

3.2   **NOTE.** Ensure to check previous fermenter checklists/calibration records for last recorded temperature map of vessel to determine temperature reading to use as sterilisation holding temperature.
        Due to non linearity of temperature amplifier over entire range, this holding temperature reading may not correspond to 121°C, likewise Pressure Gauge may not correspond to 1.0 Bar at sterilsation temperature.

3.3   Ensure all valves are closed at this time.

3.4   Open air exit valve **V11.01**.

3.5   Check agitator speed control is wound fully counter-clockwise. Set tumbler switch to **On** and manually increase setpoint to 200rpm.

3.6   Open main condensate return valve at wall.

3.7   Open blue handled ball valve to condensate return.

3.8   Open main steam supply valve at wall.

3.9   On the ADI 1030 change the temperature process setpoint to 126°C

3.10   Change the temperature process control to **Start**

3.11   Set the 'Ferm/Off/Ster' tumbler switch on the ADI 1065 to **'Ster'**(-ilisation)

3.12   Increase the steam PRV to 30psi

3.13   Valve V-11.01 on exit air filter housing is open to evacuate air from the headspace while the vessel heats up. At around 99°C steam will begin to enter the condenser. Carefully feel the top of the condenser until it gets hot, at which point close the valve.

3.14 **EMERGENCY SHUT DOWN:** at this stage when vessel is not yet under pressure.
Close main steam valve at services panel. Close main condensate return at services panel.
Press Emergency Stop button on ADI 1065.

3.15 When the temperature in the fermenter reaches 105°C the Biocontroller is programmed to open valve VY-10.05 to allow steam into the inlet air filter. Listen for an audible click at which point open condensate drain valve **V-10.06** below the inlet air filter.

3.16 **EMERGENCY SHUT DOWN:** at this stage and from now on when vessel is under pressure. **Close main steam valve at services panel. Close main condensate return valve at services panel. Press Emergency Stop button on ADI 1065. Using heat resistant gloves crack open one of the conical connections on the 3 way port, note: this may cause media to boil out.**

3.17 At 110°C open steam valve **V-14.04** and condensate valve **V-14.02**.

3.18 At 122°C slowly open valve **V-11.01** to allow a small amount of steam to vent through the filter for the remainder of the sterilisation period.

3.19 Close valve **V-14.04**. Open side addition valve **V-14.03**.

3.20 On the **3 way port** turn each connector ring slightly counter clockwise and pull the blinded hose barb out in order to create a small bleed of steam.

3.21 Close valve **V-10.06**. Open valve **V-10.08** to sparge line. Open valve **V-10.07** to headspace.

3.22 To sterilise the sample assembly close sample valve **V-17.01**. Open steam supply valve **V-20.02**. Open condensate valve **V-17.02**.

3.23 To sterilise the harvest port assembly close harvest valve **V-12.01**. Open steam supply valve **V-20.03**. Open condensate valve **V-12.02**.

3.24 Maintain sterilisation temperature in the vessel for the desired time (usually 20 minutes).

4.0 Cooling Down After Sterilisation

4.1 Close valves **V-17.02** and **V-20.02** on sample assembly.

4.2 Close valves **V-12.02** and **V 20.03** on harvest port.

4.3 Close connical connectors on the **3 way port**.

4.4 Close valves **V-14.02** and **V14.03**.

4.5 Close valve **V-11.01** on exit air line.

4.6 On BioXpert go to Control Laws and select **Manual Setpoint → sGas**. Check the box next to Manual and enter a value of 10 L/m. **Check for positive air pressure and connect air line to inlet Air filter.**

4.7 Close valves **V10.08** and **V10.07**.

4.8   Set Ferm/Off/Ster tumbler switch to Off.

4.9   **Close blue handled condensate valve at wall**. This is to prevent the Kill Tanks filling up with cooling water returning from the condenser.

4.10   Open Cooling Water Return valve at wall. Open Cooling Water Supply valve at wall.

4.11   Open valve **V-10.09** to inlet air filter.

4.12   On the ADI 1030 change the temperature setpoint to the desired process temperature.

4.13   Set 'ferm/off/ster' tumbler switch to **'ferm'**(entation).
        Water will now begin to enter the jacket and the fermenter will begin to cool down.

4.14   At 0.1Bar open valve **V-10.07** allowing air into the headspace.
        The fermenter will now pressurise to 10psi. and cool safely to the new temperature setpoint.

5.0   <u>Set-Up for Fermentation Running</u>

5.1   The fermenter should now be sterile, pressurised to 10psi., agitator running and temperature at setpoint. The fermenter ancillaries should be sterilised and ready for insertion.

5.2   Connect condenser line labelled **'water from condenser'** to Bio bench.
        Connect condenser line labelled **'water to condenser'** to Bio Bench.

5.3   Open blue handled cooling water return ball valve at wall. Check that the condenser gets cold otherwise adjust the condenser tuning valve inside Biobench.

5.3   Slowly release the pressure in the fermenter by gradually opening valve **V-11.01** on the exit air line.

5.4   Open valve **V-10.08** to sparge line. Close valve **V-10.07** to headspace.
        Check thar air is sparging and there is no head pressure in the vessel

5.5   Change setpoint of **sGas** to running value.

5.6   Take a sample and use it to recheck pH. Refer to SOP No. 6 for adjustment of the pH probe at this stage. A sample can be taken to check sterility.

5.7   With stirrer and air flow at desired settings, check DOT probe is reading 100.0%. Refer to SOP No. 7 for adjustment of DOT probe at this stage. Ensure **mass spec. pump** is connected and switched on. Sparge nitrogen through air inlet filter to check DOT probe response and to check readings on mass spec. Once the probe response has been checked, reconnect fermenter air supply to air inlet filter and ensure air flow is at the correct setting.

5.8   For acid, alkali and PPG additions run the tubing through the appropriate **pumphead** on the ADI 1035. Using aseptic technique remove the blinded conical connectors from the 3 way inlet and replace with connectors from the addition bottles. Check and adjust the pH setpoint if necessary. Prime the lines up to the addition inlets. Switch the **acid and alkali control switches** to the **remote** position to achieve pH control.

5.9   Once any other remaining media additions have been added, the fermenter can now be inoculated. Ensure logging has started on BioXpert computer before inoculating. It

may be necessary to stop or reduce the air flow, to allow the inoculum to run into the fermenter by gravity, or it can pumped in with a peristaltic pump.

6.0   Closing Down The Fermenter

6.1   Switch off automatic control of temperature, pH, *etc*. Stop logging on BioXpert.

6.2   Harvest cells if required through **harvest port,** leaving stirrer running during harvesting. Turn off stirrer when vessel is almost drained. Ensure good containment practices are adhered to.

6.3   Turn off the stirrer by turning control fully counter-clockwise then set tumbler switch to **Off**

6.4   Disconnect and drain acid, alkali and antifoam cylinders.

6.5   If the cells are not to be harvested, then they should be killed off by sterilisation, following the same procedure as for sterilising the media, but exercising more care due to the increased danger of flash boiling. Additional antifoam can be added to counteract any cell lysis which may cause foaming. Do not attempt to vent steam out through air outlet filter if foaming occurs.
        In the event of having to carry out an **emergency shut down** when the vessel is at pressure carry out Step 3.16.
        If this does cause release of any live culture, ensure that the collection vessel used is dosed with 2% Tego solution for a contact time of at least 30 minutes on return to the area.

6.6   If cells are harvested, then refill with RO water up to the working volume and carry out Sterilisation Kill Cycle using the same procedure as for sterilising the media.

6.7   After killing the cells, clean the fermenter referring to SOP No.32D. Ensure that both the DOT and pH probes are removed and properly stored before carrying out the cleaning procedure.
        Remove air inlet and exit filters.

6.8   Ensure that all valves are closed, all control switches are in the off position and no steam or water is left on.

Appendix C

Standard Operating Procedure

SOP No. 45/P1

_____

Title:

Bacteriophage Fermentation: Sterilisation and Operation of Applikon 20L Fermenter

_____

WRITTEN BY DATE   OPERATING HEAD   DATE   DOC.REF.
S. BRANSTON 16/08/07   SOP. 45/P1

1.0   Introduction

1.1   This document outlines the procedure to follow for sterilising and setting up the fermenter vessel prior to inoculation. It is based upon SOP 45 (written by I. Buchanan) with a few modifications, principally regarding closing down the fermenter. The Applikon 20L fermenter has an ADI 1030 Bio Controller for process variables, an ADI 1065 Bio Bench console for insitu sterilisation and temperature control and an ADI 1035 Bio Console for gas addition and stirrer speed control. BioXpert PC software is also connected for control and data logging.

1.2   **SAFETY NOTE: In the event of having to leave the building in an emergency (i.e. fire alarm), whilst vessel is at pressure during sterilisation cycle, the EMERGENCY SHUTDOWN PROCEDURE outlined in steps 3.14 or 3.16 must be followed. There is no need to take any action before leaving the area if operation is not part of sterilisation cycle.**

2.0   Pre sterilisation Set-Up

2.1   Refer to technician or previous fermenter checklist to ensure that no technical faults encountered with this fermenter from the previous run, and if any faults noted, verify with a member of the technical staff that these have been rectified.

2.2   Ensure the vessel is clean. If vessel is not clean, carry out appropriate cleaning procedure as outlined in SOP No. 32D.

2.3   Check condition of all 'O'-rings and replace any if damaged.

2.4   If the **foam probe** is to be used, ensure that it is in place and at an appropriate height. If at this stage there is any doubt regarding the appropriate height, ensure that the probe is fully down into the headplate so that any later repositioning after sterilisation involves moving the probe up to an appropriate height rather than pushing down which may possibly cause contamination.

2.5   **Check the main air supply PRV is set to 10psi.**

2.6   Check condition of **Domnick Hunter tetpor air** filter cartridges for inlet and exit air housings.

2.7   Prepare fermenter ancillaries for separate sterilisation in autoclave.
        _e.g._   Acid addition reservoir with 0.2 μm filter, line and conical connector
                    Alkali addition reservoir with 0.2 μm filter, line and conical connector

Antifoam reservoir 0.2 μm filter, line and conical connector
Two Inoculum flasks, lines with Tee'd connector and side-addition valve tree
1L Nalgene, line with Tee'd connector and side-addition valve tree
20L Nalgene container, line and connector (for harvesting)
(optional: sterilisation of 1L and 20L Nalgenes for the post-harvesting
sterilisation of sample and harvest lines)
All Nalgenes must have a 0.2 μm exit air filter.

2.8   Calibrate pH probe - see SOP No. 6. Place probe in fermenter

2.9   Check DOT probe calibration (do not calibrate at this stage) - see SOP No. 7. Place
        probe in fermenter.

2.10   Ensure agitator is correctly attached to motor drive shaft.

2.11   Ensure harvest port is closed. Attach woven metal mesh harvest line.

2.12   Ensure sample valve is closed. Attach silicone sample line to the sample port.

2.13   Disconnect quick release **water to condenser** line on Bio Bench.
        Disconnect quick release **water from condenser** line on Bio Bench.

2.14   Remove pressure gauge and fill vessel with medium to required level. Replace pressure
        gauge ensuring seal and tri-clamp are firmly connected.

2.15   Carry out checks on Fermenter Sterilisation Checklist.

3.0   Heating Up – Sterilisation

3.1   **Ensure protective safety gowns and face visors are worn during sterilisation cycle.**

3.2   **NOTE.**   Ensure to check previous fermenter checklists/calibration records for last
        recorded temperature map of vessel to determine temperature reading to use as
        sterilisation
        holding temperature.
        Due to non linearity of temperature amplifier over entire range , this holding temperature
        reading may not correspond to 121°C, likewise Pressure Gauge may not correspond to
        1.0 Bar
        at sterilisation temperature.

3.3   Ensure all valves are closed at this time.

3.4   Open air exit valve **V11.01**.

3.5   Check agitator speed control is wound fully counter-clockwise. Set tumbler switch to **On**
        and
        manually increase setpoint to 200rpm.

3.6   Open main condensate return valve at wall.

3.7   Open blue handled ball valve to condensate return.

3.8   Open main steam supply valve at wall.

3.9   On the ADI 1030 change the temperature process setpoint to 126°C

3.10   Change the temperature process control to **Start**

3.11   Set the 'Ferm/Off/Ster' tumbler switch on the ADI 1065 to **'Ster'**(-ilisation)

3.12   Increase the steam PRV to 30psi

3.13   Valve V-11.01 on exit air filter housing is open to evacuate air from the headspace while the vessel heats up. At around 99°C steam will begin to enter the condenser. Carefully feel the top of the condenser until it gets hot, at which point close the valve.

3.14   **EMERGENCY SHUT DOWN:** at this stage when vessel is not yet under pressure. **Close main steam valve at services panel. Close main condensate return at services panel.**
Press Emergency Stop button on ADI 1065.

3.15   When the temperature in the fermenter reaches 105°C the Biocontroller is programmed to open valve VY-10.05 to allow steam into the inlet air filter. Listen for an audible click at which point open condensate drain valve **V-10.06** below the inlet air filter.

3.16   **EMERGENCY SHUT DOWN:** at this stage and from now on when vessel is under pressure. **Close main steam valve at services panel. Close main condensate return valve at services panel. Press Emergency Stop button on ADI 1065. Using heat resistant gloves crack open one of the conical connections on the 3 way port, note: this may cause media to boil out.**

3.17   At 110°C open steam valve **V-14.04** and condensate valve **V-14.02**.

3.18   At 122°C slowly open valve **V-11.01** to allow a small amount of steam to vent through the filter for the remainder of the sterilisation period.

3.19   Close valve **V-14.04**. Open side addition valve **V-14.03**.

3.20   On the **3 way port** turn each connector ring slightly counter clockwise and pull the blinded hose barb out in order to create a small bleed of steam.

3.21   Close valve **V-10.06.** Open valve **V-10.08** to sparge line. Open valve **V-10.07** to headspace.

3.22   To sterilise the sample assembly close sample valve **V-17.01**.   Open steam supply valve **V-20.02**. Open condensate valve **V-17.02**. Crack open sample valve **V-17.01** and allow steam to pass through the tubing into a suitable container.

3.23   To sterilise the harvest port assembly close harvest valve **V-12.01**. Open steam supply valve   **V-20.03**. Open condensate valve **V-12.02**. Crack open harvest valve **V-12.01** and allow steam to pass through the tubing into a suitable container.

3.24   Maintain sterilisation temperature in the vessel for the desired time (usually 20 minutes).

4.0   Cooling Down After Sterilisation

4.1   Close valves **V-17.01, V-17.02** and **V-20.02** on sample assembly.

4.2   Close valves **V-12.01, V-12.02** and **V 20.03** on harvest port.

4.3   Close conical connectors on the **3 way port**.

4.4   Close valves **V-14.02** and **V14.03**.

4.5   Close valve **V-11.01** on exit air line.

4.6   On BioXpert go to Control Laws and select **Manual Setpoint → sGas**. Check the box next to Manual and enter a value of 10 L/m. **Check for positive air pressure and connect air line to inlet Air filter.**

4.7   Close valves **V10.08** and **V10.07**.

4.8   Set Ferm/Off/Ster tumbler switch to Off.

4.9   **Close blue handled condensate valve at wall**. This is to prevent the Kill Tanks filling up with cooling water returning from the condenser.

4.10   Open Cooling Water Return valve at wall. Open Cooling Water Supply valve at wall.

4.11   Open valve **V-10.09** to inlet air filter.

4.12   On the ADI 1030 change the temperature setpoint to the desired process temperature.

4.13   Set 'ferm/off/ster' tumbler switch to **'ferm'**(entation).
        Water will now begin to enter the jacket and the fermenter will begin to cool down.

4.14   At 0.1Bar open valve **V-10.07** allowing air into the headspace.
        The fermenter will now pressurise to 10psi. and cool safely to the new temperature setpoint.

5.0   Set-Up for Fermentation Running

5.1   The fermenter should now be sterile, pressurised to 10psi., agitator running and temperature at setpoint. The fermenter ancillaries should be sterilised and ready for insertion.

5.2   Connect condenser line labelled **'water from condenser'** to Bio bench.
        Connect condenser line labelled **'water to condenser'** to Bio Bench.

5.3   Open blue handled cooling water return ball valve at wall. Check that the condenser gets cold otherwise adjust the condenser tuning valve inside Biobench.

5.3   Slowly release the pressure in the fermenter by gradually opening valve **V-11.01** on the exit air line.

5.4   Open valve **V-10.08** to sparge line. Close valve **V-10.07** to headspace. Check that air is sparging and there is no head pressure in the vessel

5.5   Change setpoint of **sGas** to running value.

5.6   Take a sample and use it to recheck pH. Refer to SOP No. 6 for adjustment of the pH probe at this stage. A sample can be taken to check sterility.

5.7   With stirrer and air flow at desired settings, check DOT probe is reading 100.0%. Refer to SOP No. 7 for adjustment of DOT probe at this stage. Ensure **mass spec. pump** is connected and switched on. Sparge nitrogen through air inlet filter to check DOT probe response and to check readings on mass spec. Once the probe response has been

checked, reconnect fermenter air supply to air inlet filter and ensure air flow is at the correct setting.

5.8   For acid, alkali and PPG additions run the tubing through the appropriate **pumphead** on the ADI 1035. Using aseptic technique remove the blinded conical connectors from the 3 way inlet and replace with connectors from the addition bottles. Check and adjust the pH setpoint if necessary. Prime the lines up to the addition inlets. Switch the **acid and alkali control switches** to the **remote** position to achieve pH control.

5.9   If using foam control, set the probe height to the working height in the fermenter. Note: The probe should **not** be moved outwards during the fermentation (post inoculation) to prevent bacteriophage release.

5.10   Once any other remaining media additions have been added, the fermenter can now be inoculated. Connect the inoculum valve tree to the side addition port. Sterilise side addition port by opening steam valve **V-14.04** and condensate valve **V-14.02** for 20 minutes. Close valves **V-14.04** and **V-14.02** once sterilised. Ensure logging has started on BioXpert computer before inoculating. It may be necessary to stop or reduce the air flow, to allow the inoculum to run into the fermenter by gravity, or it can pumped in with a peristaltic pump. Sterilise the side addition port following inoculation, and disconnect inoculum valve tree once cool.

5.11   Connect the valve tree attached to the 1L Nalgene with Tee'd connector to the side addition port. Sterilise side addition port by opening steam valve **V-14.04** and condensate valve **V-14.02** for 20 minutes. Close valves **V-14.04** and **V-14.02** once sterilised.

5.12   Refer to SOP 45/P3 regarding the sampling procedure once inoculation has occurred.

6.0   <u>Closing Down The Fermenter</u>

6.1   Switch off automatic control of temperature, pH, *etc*. Stop logging on BioXpert.

6.2   Harvest cells if required through **harvest port** as outlined in SOP 45/P4, leaving stirrer running during harvesting. Turn off stirrer when vessel is almost drained. Ensure good containment practices are adhered to.

6.3   Turn off the stirrer by turning control fully counter-clockwise then set tumbler switch to **Off**

6.4   Close the acid, alkali and antifoam connectors on the 3-way port.

6.5   If the cells are not to be harvested, then they should be killed off by sterilisation, following the same procedure as for sterilising the media, but exercising more care due to the increased danger of flash boiling. Additional antifoam can be added to counteract any cell lysis which may cause foaming. Do not attempt to vent steam out through air outlet filter if foaming occurs.
       In the event of having to carry out an **emergency shut down** when the vessel is at pressure carry out Step 6.6, below:

6.6   EMERGENCY SHUT DOWN: when vessel is under pressure and contains live culture. **Close main steam valve at services panel. Close main condensate return valve at services panel. Press Emergency Stop button on ADI 1065. Crack open the side-addition port valve leading to the 1L Nalgene.** If this does cause release of any live culture, ensure that the collection vessel is autoclaved once the valve tree is re-sterilised as in step 5.10 before disconnection.

6.7 If cells are harvested, attach the sterile end of the harvest line to the second 20L Nalgene container. Remove the harvest line clamp. To sterilise the whole harvest line, ensure the **harvest port** is closed. Open steam supply valve **V-20.03** and carefully open the harvest valve **V-12.01.** Ensure steam is passing through into the 20L Nalgene container. Leave for 20 minutes to sterilise the line, then close valves **V-20.03** and **V-12.01.** The harvest line can now be disconnected.

6.8 Similarly, to sterilise the sample line, attach the sterile end of the line to the second 1L Nalgene container. Remove the sample line clamp. To sterilise the whole sample line, ensure the **sample port** is closed. Open steam supply valve **V-20.02** and carefully open the sample valve **V-17.01.** Ensure steam is passing through into the 1L Nalgene container. Leave for 20 minutes to sterilise the line, then close valves **V-20.02** and **V-17.01.** The sample line can now be disconnected.

6.9 Refill the vessel with RO water to the working volume via the side addition port, and carry out a Sterilisation Kill Cycle using the same procedure as for sterilising the media.

6.10 After killing the cells, clean the fermenter referring to SOP 32D. Ensure that both the DOT and pH probes are removed and properly stored before carrying out the cleaning procedure. Disconnect and drain the acid, alkali and antifoam vessels.
Disconnect the side addition valve-tree.
Remove air inlet and exit filters.

6.11 Ensure that all valves are closed, all control switches are in the off position and no steam or water is left on.

Standard Operating Procedure

SOP No. 45/P2

_____

Title:

Bacteriophage Fermentation: Inoculation of the Applikon 20L Fermenter to Minimise Bacteriophage Release

_____

WRITTEN BY DATE   OPERATING HEAD   DATE   DOC.REF.
S. BRANSTON 16/08/07   SOP. 45/P2
Signature   Signature

1.0   Introduction

1.1   This document describes the inoculation of the 20 L Applikon fermenter from a shake flask culture so as to minimise the release of bacteriophage into the facility.

1.2   All culture transfers must be conducted away from the ACBE with thorough cleaning with 1 % Virkon solution after use.

1.3   All fermentations must be carried out in the Advanced Centre fermentation suite where all drains are fed to kill tanks and negative air pressure is maintained so as to contain any release.

1.4   Gloves must be worn during all culture transfer operations.

2.0   Preparation for inoculation

2.1   Take both sterilised inoculum flasks (joined by a T joint to a single addition line) to the biochemistry department laboratory G09 in a suitable sealed container. Ensure that the flasks, tubing and fittings are sound. Ensure gate clamps leading from each inoculum flask are closed.

2.2   Aseptically transfer bacteriophage and _E. coli_ inocula from their respective shake flasks into the inoculum flasks.

2.3   Should any spillage occur refer to cleanup SOP 45/P5.

2.4   Transfer inoculum flasks to the ACBE fermenter in a suitable sealed container.

3.0   Inoculation

3.1   Turn off the air supply to the fermenter to reduce pressure inside the vessel. Wind the silicone tubing through the appropriate **pumphead** on the ADI 1035 if adding inocula by peristaltic pump.

3.2　　Connect the inoculum valve tree to the side addition port. Sterilise side addition port by opening steam valve **V-14.04** and condensate valve **V-14.02** for 20 minutes. Close valves **V-14.04** and **V-14.02** once sterilised. Remove clamps and allow the inocula to siphon into fermenter by gravity, or by peristaltic pump. Close clamps once inoculation is complete. Sterilise the side addition port and disconnect inoculum valve tree once cool.

3.4　　Treat disconnected inocula flasks with 1% Virkon solution for a minimum of 10 minutes, or autoclave to sterilise.

Standard Operating Procedure

SOP No. 45/P3

_____

Title:

Bacteriophage Fermentation: Sampling from the Applikon 20L Fermenter, minimising bacteriophage release.

_____

WRITTEN BY DATE   OPERATING HEAD   DATE   DOC.REF.

S.BRANSTON 16/08/07   SOP. 45/P3

Signature   Signature

1.0   Introduction

1.1   This document describes a sampling procedure from the 20 L Applikon fermenter during normal operation into 5 ml syringes. The procedure is designed to minimise the likelihood of bacteriophage release.

2.0   Preparation of sampling equipment

2.1   Following sterilisation and cooling of the fermenter, aseptically attach the Robersite needle-less valve to the sterilised sample port silicone tubing. Ensure that the sample tubing is sound.

3.0   Sampling

3.1   Swab the needle-less valve with towel dampened with 1% Virkon. Insert a sterile 5 ml syringe into the needle-less valve, and hold the assembly within paper towel dampened with 1 % Virkon solution. Carefully open the sample valve and draw 5 ml into the syringe. Close the sample valve.

3.2   Hold the syringe vertically and disconnect from the needle-less valve within the Virkon-soaked towel. Immediately cap the syringe and discard. Swab the needle-less valve with towel dampened with 1% Virkon.

3.3   Insert a fresh 5 ml syringe and repeat the procedure to take the actual sample. Remove the capped syringe from the fermentation suite in a suitable container. In case of spillage, refer to SOP 45/P5

4.0   Closing down after sampling

4.1   Once the last sample has been taken, immerse the needle-less valve in a container containing 1 % Virkon solution. Clamp the line and detach the needle-valve from the end. Ensure Virkon solution enters the line right up to the clamp seal. Leave in the solution for at least 10 minutes. Then follow the closing down section of SOP 45/P1.

Standard Operating Procedure

SOP No. 45/P4

_____

Title:

Bacteriophage Fermentation: Harvesting from the Applikon 20L Fermenter, minimising bacteriophage release.

_____

WRITTEN BY DATE   OPERATING HEAD   DATE   DOC.REF.
S. BRANSTON   SOP. 45/P4
Signature   Signature

1.0   Introduction

1.1   This document describes the harvesting procedure of the 20 L Applikon fermenter into sterile 20 L Nalgene containers in a manner minimizing the risk of bacteriophage release.

2.0   Preparation of harvesting equipment

2.1   Attach silicone lines with connectors at both ends to entry and exit ports on a 20 L Nalgene container. Ensure the lines are sound. Attach a 0.2 µm filter. Cover exposed line connectors with foil. Autoclave. Post-autoclaving, inspect the container and all lines for sign of damamge. If identified, renew where necessary.

3.0   Harvesting

3.1   Using aseptic technique, attach the harvest line from the 20 L Nalgene to the fermenter **harvest port**.

2.2   Open the harvest port valve and drain cells and bacteriophages into the Nalgene. Turn off the stirrer when vessel is almost drained.

2.3   Once drained, close the **harvest port** and valve **V-12.01.** Clamp the silicone harvest line in two places near the Nalgene. Immerse the line and both gate clamps under 1% Virkon solution and cut the line between the clamps. Ensure Virkon solution enters the line right up to the clamp seal. Leave for 10 minutes. In case of spillage, refer to SOP 45/P5.

2.4   Continue to close down the fermenter as outlined in SOP 45/P1.

Standard Operating Procedure

SOP No. 45/P5

_____

Title:

Procedure for Decontamination following Bacteriophage Spillage

_____

WRITTEN BY DATE	OPERATING HEAD	DATE	DOC.REF.
S. BRANSTON			SOP. 45/P5
Signature	Signature		

1.0   <u>Introduction</u>

1.1   This document describes the procedure to be followed following accidental release of bacteriophage in the ACBE fermentation suite.

1.2   This SOP is based upon experimental data to show the effectiveness of the disinfectant chosen in achieving sterility; in particular the length of time required for contact of the sterilising agent with the spillage.

2.0   <u>Small spills (a few mls)</u>

2.2   In the event of a spillage, the operator should wear latex or nitrile gloves in addition to the usual lab coat and glasses. Small spills of the order of a few millilitres should be treated with 1 % Virkon solution. Liberally spray the Virkon solution around the spillage area and leave for 10 minutes.

2.3   **Wearing gloves**, after 10 minutes any broken glassware can be collected and carefully disposed.

2.4   The spillage can then be safely mopped up and dried with paper towels. All paper towels should be discarded in the contaminated waste bin.

2.5   The building manager or person responsible for safety should be informed of the spillage and the   measures taken to deal with it.

3.0   <u>Large spills (tens of mls)</u>

3.1   In the event of a large spillage, again the operator should wear latex or nitrile gloves in addition to the usual lab coat and glasses. Treat the spill by the addition of Virkon powder **directly**, until all liquid is absorbed. Take care not to inhale the dry powder. Scrape or sweep the damp powder into a container for disposal. Subsequently apply 1 % Virkon solution to the affected area. After 10 minutes contact time, wipe dry with paper towels.

3.2   The building manager or person responsible for safety should be informed of the spillage and the   measures taken to deal with it.

4.0   Wholesale release (litres)

4.1   In the unlikely event of extremely large spillages (such as fermenter or harvest vessel failure) the operator should follow the procedure for large spills.

4.2   The building manager or person responsible for safety should be informed of the spillage and the measures taken to deal with it.

4.3   The area should be monitored in the weeks afters the spillage: take swabs at regular intervals for viable bacteriophage around the hall and keep a record of future culture infections.

4.4   If persistent infection of cultures by the released bacteriophage occurs in the following months, then hydrogen peroxide or formaldehyde fumigation of the facility may need to be considered.

Appendix D

20 Litre Applikon Fermentation Risk Assessment

Growth of E. coli infected with the filamentous bacteriophage M13

Evaluation of risk concerning bacteriophage containment

Project:

An investigation of the properties of bacteriophage M13 and the implications for its large-scale bioprocessing.

Locations:

The Department of Biochemical Engineering, ACBE fermentation hall and downstream processing areas.

Description of work:

The work will involve fermentation of *E. coli* infected with bacteriophage M13 in the 20L Applikon fermenter. The objective is to investigate the yield of bacteriophage on this scale, as well as to gain bacteriophage stocks for further experimentation.

Persons involved:

Steven Branston and Emma Stanley are the investigators. Involved academic staff are Eli Keshavarz-Moore and John Ward. Clive Orsborn and Gareth Mannall are involved with ensuring containment of bacteriophage.

Hazard Identification (i.e. potential release points):

- o Introduction of bacteria and phage inoculum flasks into fermentation hall
- o Normal operation and sampling
- o Harvesting into sealed containers
- o Operation problems

Risk Assessment:

Assessment of the risks involved concerning bacteriophage release.

Inoculation

Risk of bacteriophage release is low but contamination could arise from:
- o Bacteriophage contaminated inoculum flask outer surface- surface contamination risk.
- o Breakage of the bacteriophage inoculum flask- aerosol and surface contamination risk.
- o Inoculum line leak- aerosol and surface contamination risk

Normal operation and sampling

Risk of bacteriophage release should also be low, but during normal operation unexpected bacteriophage release could arise from:

- o Sample line leak- aerosol and surface contamination risk

Harvesting into sealed containers

Risk of bacteriophage release should be low if proper procedures are followed, but could unexpectedly arise from:

- o Harvest line leak- aerosol and surface contamination risk

Operation problems

Risk of bacteriophage release should be low in the event of a fermenter electrical or mechanical fault, since manual shutdown is always available. Blockage of the exit gas filter may pose a release risk if pressure within the fermenter is allowed to build up to a point such that air pushes back into the acid, base and PPG containers.

Control Measures:

The control measures to minimize the probability of bacteriophage release apply to those in charge of the fermentation.

Inoculation

- o Good laboratory practice ensures flask outer surfaces are not contaminated.
- o Inoculum flasks are transported in a secure manner (i.e. not by the flask necks). Consider the use of plastic, not glass inoculum flasks. Spillage from the bacteriophage inoculum flask presents one of the contamination risks most likely to occur.
- o Applikon fermenter SOP 45/P2 is followed regarding inoculation procedure.

Normal operation and sampling

- o As part of the sampling SOP 45/P3, the sample line must be inspected prior to the fermentation and be renewed if necessary.
- o providing that the SOP specifically concerning sampling are adhered to, there should be a low risk of bacteriophage release. The frequency of sampling means the risk of release may be higher than that of inoculation.
- o The fitting and checking of exit and inlet air filters prior to fermenter sterilisation should prevent bacteriophage release from the fermenter off-gas.

Harvesting into sealed containers

- o All harvest lines must be inspected prior to the fermentation and be renewed if necessary. This procedure is outlined in SOP 45/P4.

- o Adherence to the devised harvesting SOP 45/P4 should minimise the risk of bacteriophage release. Spillage from the post-fermentation liquor presents the greatest consequences of bacteriophage release, due to the high phage concentration and largest volumes being handled.

Operation problems

A known potential issue is the blockage of the exit gas filter. A heated jacket is available, which will minimize the likelihood of blockage. Exit air filters on acid, base and PPG containers will prevent phage release in the event of fermenter pressure build up and flow back. The fermenter will be run in the daytime, and therefore not left unmanned for long periods.

In the event of spillage, the operator should turn to SOP 45/P5, detailing how to deal with bacteriophage-contaminated spills. Briefly, small areas can be treated with a 1 % solution of Virkon, whilst larger areas can be treated with Virkon powder directly.

References

Abad F, Pinto R, Bosch A. 1994. Survival of enteric viruses on environmental fomites. Appl Environ Microbiol 60(10):3704-10.

Achtman M, Willetts N, Clark AJ. 1971. Beginning a genetic analysis of conjugational transfer determined by the F factor in *Escherichia coli* by isolation and characterization of transfer-deficient mutants. J Bacteriol 106(2):529-38.

Ackermann HW. 2005. Bacteriophage Classification. In: Kutter E, Sulakvelidze A, editors. Bacteriophages: CRC Press. p 67-90.

Adams C, Brantner V. 2006. Estimating the cost of new drug development: Is it really $802 million? Health Aff 25(2):420-28.

Akerlund T, Nordstrom K, Bernander R. 1995. Analysis of cell size and DNA content in exponentially growing and stationary-phase batch cultures of *Escherichia coli*. J Bacteriol 177(23):6791-7.

Alisky J, Iczkowski K, Rapoport A, Troitsky N. 1998. Bacteriophages show promise as antimicrobial agents. J Infect 36(1):5-15.

Anonymous. 2009. Phage Biotechnology Announces it Will Review Contract Manufacturing Opportunities for Therapeutic Phage Particles. (www.phagebiotech.com/news/news.html).

Arulmuthu ER, Williams DJ, Baldascini H, Versteeg HK, Hoare M. 2007. Studies on aerosol delivery of plasmid DNA using a mesh nebulizer. Biotechnol Bioeng 98(5):939-55.

Asenjo JA, Patrick I. 1990. Large-Scale Protein Purification. In: Harris ELV, Angal S, editors. Protein Purification Applications: A Practical Approach. Oxford: Oxford University Press. p 1-27.

Asheshov I, Wilson J, Topley W. 1937. The effect of an anti-Vi bacteriophage on typhoid infection in mice. Lancet 1:319-20.

Atha DH, Ingham KC. 1981. Mechanism of precipitation of proteins by polyethylene glycols. Analysis in terms of excluded volume. J Biol Chem 256(23):12108-17.

Atkinson A, Scawen M, Hammond P. 1987. Large Scale Industrial Techniques of Enzyme Recovery. In: Rehm HJ, Reed G, editors. Biotechnology. Weinheim: VCH Verlagsgesellschaft. p 279-323.

Atkinson B, Mavituna F. 1991. Biochemical Engineering and Biotechnology Handbook. Basingstoke: Macmillan. 1271 p.

Bachrach U, Friedmann A. 1971. Practical procedures for the purification of bacterial viruses. Applied Microbiology 22(4):706-15.

Baek H, Suk K, Kim Y, Cha S. 2002. An improved helper phage system for efficient isolation of specific antibody molecules in phage display. Nucleic Acids Res 30(5):e18.

Bahri SM. 1990. Cloning and expression of a thermostable alpha-amylase gene from *Streptomyces thermoviolaceus* CUB74. London: University of London. 180 p.

Balakrishnan PG, Ramesh R, Prem Kumar T. 2006. Safety mechanisms in lithium-ion batteries. J Power Sources 155(2):401-14.

Balogh B, Jones J, Momol M, Olson S, Obradovic A, King P, Jackson L. 2003. Improved efficacy of newly formulated bacteriophages for management of bacterial spot on tomato. Plant Dis 87(8):949-54.

Baneyx F. 1999. Recombinant protein expression in *Escherichia coli*. Curr Opin Biotechnol 10(5):411-21.

Barrow P, Lovell M, Berchieri A. 1998. Use of lytic bacteriophage for control of experimental *Escherichia coli* septicemia and meningitis in chickens and calves. Clin Vaccine Immunol 5(3):294-98.

Barrow PA. 2001. The use of bacteriophages for treatment and prevention of bacterial disease in animals and animal models of human infection. J Chem Technol Biotechnol 76(7):677-82.

Belter PA, Cussler EL, Hu WS. 1988. Bioseparations: Downstream Processing for Biotechnology. New York: Wiley. 368 p.

Bergfors T. 1999. Protein Crystallization: Techniques, Strategies, and Tips. A Laboratory Manual: International University Line. 306 p.

Berkowitz SA, Day LA. 1976. Mass, length, composition and structure of the filamentous bacterial virus fd. J Mol Biol 102(3):531-47.

Biddlecombe JG. 2009. Antibody Stability in Bioprocessing Focusing on Shear Effects at Solid-Liquid Interfaces. London: University College London. 180 p.

Biddlecombe JG, Craig AV, Zhang H, Uddin S, Mulot S, Fish BC, Bracewell DG. 2007. Determining antibody stability: creation of solid-liquid interfacial effects within a high shear environment. Biotechnol Prog 23(5):1218-22.

Birge EA. 2000. Bacterial and Bacteriophage Genetics: Springer. 577 p.

Birnboim HC, Doly J. 1979. A rapid alkaline extraction procedure for screening recombinant plasmid DNA. Nucleic Acids Res 7(6):1513-23.

Boncina M, Rescic J, Kalyuzhnyi YV, Vlachy V. 2007. Computer simulations and theoretical aspects of the depletion interaction in protein-oligomer mixtures. J Chem Phys 127(3):035103.

Boncina M, Rescic J, Vlachy V. 2008. Solubility of lysozyme in polyethylene glycol-electrolyte mixtures: the depletion interaction and ion-specific effects. Biophys J 95(3):1285-94.

Boulding N, Yim SSS, Keshavarz-Moore E, Ayazi Shamlou P, Berry M. 2002. Ultra scaledown to predict filtering centrifugation of secreted antibody fragments from fungal broth. Biotechnol Bioeng 79(4):381-88.

Boychyn M. 2000. Scale-down principles for the accelerated design of protein purification processes. London: University College London. 220 p.

Boychyn M, Doyle W, Bulmer M, More J, Hoare M. 2000. Laboratory scaledown of protein purification processes involving fractional precipitation and centrifugal recovery. Biotechnol Bioeng 69(1):1-10.

Boychyn M, Yim SSS, Ayazi-Shamlou P, Bulmer M, More J, Hoare M. 2001. Characterization of flow intensity in continuous centrifuges for the development of laboratory mimics. Chem Eng Sci 56(16):4759-70.

Boychyn M, Yim SSS, Bulmer M, More J, Bracewell DG, Hoare M. 2004. Performance prediction of industrial centrifuges using scale-down models. Bioprocess Biosystems Eng 26(6):385-91.

Bradley DE, Dewar CA. 1967. Intracellular changes in cells of Escherichia coli infected with a filamentous bacteriophage. J Gen Virol 1(2):179-88.

Breman J. 2001. The ears of the hippopotamus: manifestations, determinants, and estimates of the malaria burden. Am J Trop Med Hyg 64(1, 2 Supp.):1-11.

Bristow AF. 1990. Purification of Proteins for Therapeutic Use. In: Harris ELV, Angal S, editors. Protein Purification Applications: A Practical Approach. Oxford: Oxford University Press. p 29-44.

Brocklebank M. 1986. Large Scale Separation and Isolation of Proteins. In: King R, Cheetham P, editors. Food Biotechnol. London: Elsevier Applied Science. p 139-92.

Brown LR, Dowell CE. 1968. Replication of coliphage M-13. I. Effects on host cells after synchronized infection. J Virol 2(11):1290-5.

Brussow H, Fremont M, Bruttin A, Sidoti J, Constable A, Fryder V. 1994. Detection and classification of *Streptococcus thermophilus* bacteriophages isolated from industrial milk fermentation. Appl Environ Microbiol 60(12):4537-43.

Bruttin A, Brussow H. 2005. Human volunteers receiving *Escherichia coli* phage T4 orally: a safety test of phage therapy. Antimicrob Agents Chemother 49(7):2874-78.

Bujanover S; 2004. Production of bacteriophage compositions for use in phage therapy. Patent WO/2004/052274.

Burg MA, Jensen-Pergakes K, Gonzalez AM, Ravey P, Baird A, Larocca D. 2002. Enhanced phagemid particle gene transfer in camptothecin-treated carcinoma cells. Cancer Res 62(4):977-81.

Burnett J, McKie M, Wood I. 1930. Investigations of bacillary dysentry in infants with special reference to the bacteriophage phenomena. Med J Aust:271-78.

Busby TF, Ingham KC. 1980. Separation of macromolecules by ultrafiltration: removal of poly (ethylene glycol) from human albumin. J Biochem Biophys Methods 2(4):191.

Byrne B, Fitzpatrick J, Pampel L, Titchener-Hooker N. 2002. Infuence of shear on particle size and fractal dimension of whey protein precipitates: implications for scale-up and centrifugal clarification efficiency. Chem Eng Sci 57:3767-79.

Calendar R, Inman R. 2005. Phage Biology. In: Waldor M, Friedman D, Adhya S, editors. Phages: Their Role in Bacterial Pathogenesis and Biotechnology. Washington, DC: ASM Press. p 18-36.

Campbell A. 2006. General Aspects of Lysogeny. In: Calendar R, Abedon S, editors. The Bacteriophages. 2nd ed. Oxford: Oxford University Press. p 66-74.

Capaldo FN, Barbour SD. 1973. Isolation of the nonviable cells produced during normal growth of recombination-deficient strains of *Escherichia coli* K-12. J Bacteriol 115(3):928-36.

Capaldo FN, Ramsey G, Barbour SD. 1974. Analysis of the growth of recombination-deficient strains of *Escherichia coli* K-12. J Bacteriol 118(1):242-49.

Capaldo-Kimball F, Barbour SD. 1971. Involvement of recombination genes in growth and viability of *Escherichia coli* K-12. J Bacteriol 106(1):204-12.

Carlton R. 1999. Phage therapy: past history and future prospects. Arch Immunol Ther Ex 47:267-74.

Carlton RM, Noordman WH, Biswas B, de Meester ED, Loessner MJ. 2005. Bacteriophage P100 for control of Listeria monocytogenes in foods: genome sequence, bioinformatic analyses, oral toxicity study, and application. Regul Toxicol Pharmacol 43(3):301-12.

Chan G, Booth AJ, Mannweiler K, Hoare M. 2006. Ultra scale-down studies of the effect of flow and impact conditions during *E. coli* cell processing. Biotechnol Bioeng 95(4):671-83.

Chanishvili N, Chanishvili T, Tediashvili M, Barrow PA. 2001. Phages and their application against drug-resistant bacteria. J Chem Technol Biotechnol 76(7):689-99.

Chen YY, Wu CC, Hsu JL, Peng HL, Chang HY, Yew TR. 2009. Surface Rigidity Change of *Escherichia coli* after Filamentous Bacteriophage Infection. Langmuir 25(8):4607-14.

Cicchini C, Ansuini H, Amicone L, Alonzi T, Nicosia A, Cortese R, Tripodi M, Luzzago A. 2002. Searching for DNA-protein interactions by lambda phage display. J Mol Biol 322(4):697-706.

Clark J, March J. 2004a. Bacteriophage-mediated nucleic acid immunisation. FEMS Immunol Med Microbiol 40(1):21-26.

Clark JR, March JB. 2004b. Bacterial viruses as human vaccines? Expert Rev Vaccines 3(4):463-76.

Clark JR, March JB. 2006. Bacteriophages and biotechnology: vaccines, gene therapy and antibacterials. Trends Biotechnol 24(5):212-8.

Collins KD. 1997. Charge density-dependent strength of hydration and biological structure. Biophys J 72(1):65-76.

Cooke GD. 2003. Modified *Eschericia coli* nuclease expressing strains for the production of recombinant biotherapeutics London: University of London. 227 p.

Cooke GD, Cranenburgh RM, Hanak JA, Ward JM. 2003. A modified *Escherichia coli* protein production strain expressing staphylococcal nuclease, capable of auto-hydrolysing host nucleic acid. J Biotechnol 101(3):229-39.

Corey D, Shiau A, Yang Q, Janowski B, Craik C. 1993. Trypsin display on the surface of bacteriophage. Gene 128(1):129-34.

d'Herelle F. 1917. An invisible microbe that is antagonistic to the dysentery bacillus. C R Acad Sci Paris 165:373-75.

Danner S, Belasco J. 2001. T7 phage display: a novel genetic selection system for cloning RNA-binding proteins from cDNA libraries. Proc Natl Acad Sci USA 98(23):12954-59.

Davison W. 1922. The bacteriolysant therapy of bacillary dysentery in children: therapeutic application of bacteriolysants; d'herelle's phenomenon. Am J Dis Children 26(6):531-34.

Demangel C, Rouyre S, Alzari P, Nato F, Longacre S, Lafaye P, Mazie J. 1998. Phage-displayed mimotopes elicit monoclonal antibodies specific for a malaria vaccine candidate. Biol Chem 379(1):65.

Diaz-Acosta A, Sandoval M, Delgado-Olivares L, Membrillo-Hernndez J. 2006. Effect of anaerobic and stationary phase growth conditions on the heat shock and oxidative stress responses in *Escherichia coli* K-12. Arch Microbiol 185(6):429-38.

Didenko Y, McNamara III W, Suslick K. 1999. Hot spot conditions during cavitation in water. J Am Chem Soc 121(24):5817-18.

Doblhoff-Dier O, Bliem R. 1999. Quality control and assurance from the development to the production of biopharmaceuticals. Trends Biotechnol 17(7):266-70.

Doermann A. 1952. The intracellular growth of bacteriophages I. Liberation of intracellular bacteriophage T4 by premature lysis with another phage or with cyanide. J Gen Physiol 35(4):645-56.

Dogic Z, Fraden S. 2006. Ordered phases of filamentous viruses. Curr Opin Colloid In 11(1):47-55.

Doig SD, O'Sullivan LM, Patel S, Ward JM, Woodley JM. 2001. Large scale production of cyclohexanone monooxygenase from *Escherichia coli* TOP10 pQR239. Enzyme Microb Technol 28(2-3):265-74.

Doig SD, Simpson H, Alphand V, Furstoss R, Woodley JM. 2003. Characterization of a recombinant *Escherichia coli* TOP10 [pQR239] whole-cell biocatalyst for stereoselective Baeyer–Villiger oxidations. Enzyme Microb Technol 32(3-4):347-55.

Doran PM. 1999. Bioprocess Engineering Principles: Academic Press. 156 p.

Dunowska M, Morley PS, Hyatt DR. 2005. The effect of Virkon S fogging on survival of *Salmonella enterica* and *Staphylococcus aureus* on surfaces in a veterinary teaching hospital. Vet Microbiol 105(3-4):281-89.

Eastman EM, Durland RH. 1998. Manufacturing and quality control of plasmid-based gene expression systems. Adv Drug Del Rev 30(1-3):33-48.

Eckman B. 1997. Validation. In: Goldberg E, editor. Handbook of Downstream Processing. London: Blackie. p 569-98.

Edelstein M, Abedi MR, Wixon J. 2009. Gene Therapy Clinical Trials Worldwide. www.wiley.co.uk/genmed/clinical/.

Ellis E, Delbruck M. 1939. The growth of bacteriophage. J Gen Physiol 22(3):365-84.

Endemann H, Model P. 1995. Location of filamentous phage minor coat proteins in phage and in infected cells. J Mol Biol 250(4):496-506.

Entenza J, Loeffler J, Grandgirard D, Fischetti V, Moreillon P. 2005. Therapeutic effects of bacteriophage Cpl-1 lysin against *Streptococcus pneumoniae* endocarditis in rats. Antimicrob Agents Chemother 49(11):4789-92.

EPA. 2005. "AgriPhage" EPA Registration Number 67986-1.

Etzel M, Riordan W. 2009. Viral clearance using monoliths. J Chromatogr 1216(13):2621-24.

Eykamp W. 1997. Membrane separations in downstream processing. In: Goldberg E, editor. Handbook of Downstream Processing. London: Blackie. p 90-137.

Fairhead H. 2009. SASP gene delivery: a novel antibacterial approach. Drug News Perspect 22(4):197.

Fairhead H, Wilkinson A, Holme S, Pitts K, Jackson A; 2009. Modified bacteriophage including an alpha/beta small acid-soluble spore protein (SASP) gene. Patent WO/2009/019293.

FDA. 1991. Guideline on the preparation of investigational new drug products (human and animal). FDA Center for Drug Evaluation and Research.

FDA. 2006a. Bacteriophage P100 preparation from *Listeria innocua*. GRAS Notice 218.

FDA. 2006b. Food Additives Permitted for Direct Addition to Food for Human Consumption; Bacteriophage Preparation. In: Federal Register. 71. p.47729–32.

Feng JN, Model P, Russel M. 1999. A trans-envelope protein complex needed for filamentous phage assembly and export. Mol Microbiol 34(4):745-55.

Field SJ. 1993. Optimised PEG method for rapid plasmid DNA purification: high yield from "Midi-Prep". BioTechniques 14(4):532-36.

Fiorentin L, Vieira N, Barioni W. 2005. Oral treatment with bacteriophages reduces the concentration of *Salmonella enteritidis* PT4 in caecal contents of broilers. Avian Pathol 34(3):258-63.

Frenkel D, Balass M, Solomon B. 1998. N-terminal EFRH sequence of Alzheimer's beta-amyloid peptide represents the epitope of its anti-aggregating antibodies. J Neuroimmunol 88(1-2):85-90.

Frenkel D, Dewachter I, Van Leuven F, Solomon B. 2003. Reduction of [beta]-amyloid plaques in brain of transgenic mouse model of Alzheimer's disease by EFRH-phage immunization. Vaccine 21(11-12):1060-65.

Gailus V, Rasched I. 1994. The adsorption protein of bacteriophage fd and its neighbour minor coat protein build a structural entity. Eur J Biochem 222(3):927-31.

Garcia-Arrazola R, Siu S, Chan G, Buchanan I, Doyle B, Titchener-Hooker N, Baganz F. 2005. Evaluation of a pH-stat feeding strategy on the production and recovery of Fab fragments from *E. coli*. Biochem Eng J 23(3):221-30.

Gonzalez-Tello P, Camacho F, Blazquez G. 1994. Density and viscosity of concentrated aqueous solutions of polyethylene glycol. J Chem Eng Data 39:611-14.

Gorbet MB, Sefton MV. 2005. Endotoxin: The uninvited guest. Biomaterials 26(34):6811-17.

Graf C, Kramer H, Deggelmann M, Hagenbüchle M, Johner C, Martin C, Weber R. 1993. Rheological properties of suspensions of interacting rodlike FD-virus particles. J Chem Phys 98(6):4920-28.

Grieco SH, Lee S, Dunbar WS, Macgillivray RT, Curtis SB. 2009. Maximizing filamentous phage yield during computer-controlled fermentation. Bioprocess Biosyst Eng.

Gromova I, Celis JE. 2006. Protein detection in gels by silver staining: a procedure compatible with mass-spectrometry. In: Celis JE, editor. Cell Biology A Laboratory Handbook. 3rd ed. Burlington, Mass.: Elsevier. p 2400.

Guttman B, Raya R, Kutter E. 2005. Basic Phage Biology. In: Kutter E, Sulakvelidze A, editors. Bacteriophages: CRC Press. p 29-66.

Hagens S, Blasi U. 2003. Genetically modified filamentous phage as bactericidal agents: a pilot study. Lett Appl Microbiol 37(4):318-23.

Hagens S, Habel A, Blasi U. 2006. Augmentation of the antimicrobial efficacy of antibiotics by filamentous phage. Microb Drug Resist 12(3):164-68.

Hagens S, Habel A, von Ahsen U, von Gabain A, Blasi U. 2004. Therapy of experimental *pseudomonas* infections with a nonreplicating genetically modified phage. Antimicrob Agents Chemother 48(10):3817-22.

Halfhide D, Gannon B, Hayes C, Roe J. 2008. Wide variation in effectiveness of laboratory disinfectants against bacteriophages. Lett Appl Microbiol 47(6):608-12.

Harrison J, Keshavarz-Moore E. 1996. Production of antibody fragments in *Escherichia coli*. Ann N Y Acad Sci 782:143-58.

Harrison JS, Gill A, Hoare M. 1998. Stability of a single-chain Fv antibody fragment when exposed to a high shear environment combined with air-liquid interfaces. Biotechnol Bioeng 59(4):517-19.

Hart SL, Knight AM, Harbottle RP, Mistry A, Hunger HD, Cutler DF, Williamson R, Coutelle C. 1994. Cell binding and internalization by filamentous phage displaying a cyclic Arg-Gly-Asp-containing peptide. J Biol Chem 269(17):12468-74.

Harvey R. 1997. Microorganisms as tracers in groundwater injection and recovery experiments: a review. FEMS Microbiol Rev 20(3-4):461-72.

Hawkes C, McLaurin J. 2007. Immunotherapy as treatment for Alzheimer's disease. Expert Rev Neurotherapeutics 7(11):1535-48.

Heal K, Hill H, Stockley P, Hollingdale M, Taylor-Robinson A. 1999. Expression and immunogenicity of a liver stage malaria epitope presented as a foreign peptide on the surface of RNA-free MS2 bacteriophage capsids. Vaccine 18(3-4):251-58.

Hewitt CJ, Boon LA, McFarlane CM, Nienow AW. 1998. The use of flow cytometry to study the impact of fluid mechanical stress on *Escherichia coli* W3110 during continuous cultivation in an agitated bioreactor. Biotechnol Bioeng 59(5).

Heydarian SM, Ison AP, Lilly MD, Shamlou PA. 2000. Turbulent breakage of filamentous bacteria in mechanically agitated batch culture. Chem Eng Sci 55:1775-84.

Hofland GW, Berkhoff MR, Witkamp GJ, van der Wielen LAM. 2003. Dynamics of isoelectric precipitation of casein using sulfuric acid. AICHE J 49(8).

Hofschneider PH. 1963. Untersuchungun uder "kleine" *E. coli* K-12 Bacteriophagen M12, M13 und M20. Z Naturforsch, C: Biosci 18:203-05.

Honig W, Kula MR. 1976. Selectivity of protein precipitation with polyethylene glycol fractions of various molecular weights. Anal Biochem 72(1-2):502-12.

Housby J, Mann N. 2009. Phage therapy. Drug Discov Today 14(11-12):536-40.

Huang Y, Chiang CY, Lee SK, Gao Y, Hu EL, De Yoreo J, Belcher AM. 2005. Programmable assembly of nanoarchitectures using genetically engineered viruses. Nano Lett 5(7):1429-34.

Husimi Y, Keweloh HC. 1987. Continuous culture of bacteriophage Q-beta using a cellstat with a bubble wall-growth scraper. Rev Sci Instrum 58(6):1109-11.

Hutchinson N, Bingham N, Murrell N, Farid S, Hoare M. 2006. Shear stress analysis of mammalian cell suspensions for prediction of industrial centrifugation and its verification. Biotechnol Bioeng 95(3):483-91.

Iannolo G, Minenkova O, Petruzzelli R, Cesareni G. 1995. Modifying filamentous phage capsid: limits in the size of the major capsid protein. J Mol Biol 248(4):835-44.

ICH. 1999. Specifications: Test procedures and acceptance criteria for biotechnological/ biological products. ICH Tripartite Guideline Q6B.

Ingham KC. 1990. Precipitation of proteins with polyethylene glycol. Methods Enzymol 182:301.

Inman R. 2005. Bacteriophage Lambda. (http://www.biochem.wisc.edu/faculty/inman/empics/virus.htm).

Intasai N, Arooncharus P, Kasinrerk W, Tayapiwatana C. 2003. Construction of high-density display of CD147 ectodomain on VCSM13 phage via gpVIII: effects of temperature, IPTG, and helper phage infection-period. Protein Expression Purif 32(2):323-31.

Iriarte F, Balogh B, Momol M, Smith L, Wilson M, Jones J. 2007. Factors affecting survival of bacteriophage on tomato leaf surfaces. Appl Environ Microbiol 73(6):1704.

Jensen KF. 1993. The *Escherichia coli* K-12 "wild types" W3110 and MG1655 have an rph frameshift mutation that leads to pyrimidine starvation due to low pyrE expression levels. J Bacteriol 175(11):3401-7.

Jepson C, March J. 2004. Bacteriophage lambda is a highly stable DNA vaccine delivery vehicle. Vaccine 22(19):2413-19.

Jones D, Shirley M, Wu X, Keis S. 2000. Bacteriophage infections in the industrial acetone butanol (AB) fermentation process. J Mol Microbiol Biotechnol 2(1):21-26.

Juckes IR. 1971. Fractionation of proteins and viruses with polyethylene glycol. Biochim Biophys Acta 229(3):535.

Jungbauer A, Hahn R. 2008. Polymethacrylate monoliths for preparative and industrial separation of biomolecular assemblies. J Chromatogr 1184(1-2):62-79.

Karlsson F, Malmborg-Hager AC, Borrebaeck CAK. 2005. Genome-wide comparison of phage M13-infected vs. uninfected Escherichia coli. Can J Microbiol/Rev Can Microbiol 51(1):29-35.

Keshavarz-Moore E, Hoare M, Dunnill P. 1990. Disruption of baker's yeast in a high-pressure homogenizer: New evidence on mechanism. Enzyme Microb Technol 12:764-70.

Khalil AS, Ferrer JM, Brau RR, Kottmann ST, Noren CJ, Lang MJ, Belcher AM. 2007. Single M13 bacteriophage tethering and stretching. Proc Natl Acad Sci USA 104(12):4892-7.

Kletch WS. 1997. Regulatory considerations. In: Goldberg E, editor. Handbook of Downstream Processing. London: Blackie. p 557-68.

Kolter R, Siegele D, Tormo A. 1993. The stationary phase of the bacterial life cycle. Annual Reviews in Microbiology 47(1):855-74.

Kondo T, Fukushima Y, Kon H, Riesz P. 1989. Effect of shear stress and free radicals induced by ultrasound on erythrocytes. Arch Biochem Biophys 269(2):381-89.

Korb LJ. 1987. Corrosion. Metals Park, OH: ASM International. 1415 p.

Kozlowski S, Swann P. 2006. Current and future issues in the manufacturing and development of monoclonal antibodies. Adv Drug Del Rev 58(5-6):707-22.

Kurosaki Y, Abe H, Morioka H, Hirayama J, Ikebuchi K, Kamo N, Nikaido O, Azuma H, Ikeda H. 2003. Pyrimidine dimer formation and oxidative damage in M13 bacteriophage inactivation by ultraviolet C irradiation. Photochem Photobiol 78(4):349-54.

Kutter E, Raya R, Carlson K. 2005. Molecular Mechanisms of Phage Infection. In: Kutter E, Sulakvelidze A, editors. Bacteriophages: CRC Press. p 165-213.

Kutzler MA, Weiner DB. 2008. DNA vaccines: ready for prime time? Nature Reviews Genetics 9(10):776-88.

Lander R, Manger W, Scouloudis M, Ku A, Davis C, Lee A. 2000. Gaulin homogenization: a mechanistic study. Biotechnol Prog 16(1):80-5.

Lander RJ, Winters MA, Meacle FJ; 2001 6/28/01. Process for the large-scale purification of plasmid DNA. Patent WO 01/46215A1.

Lander RJ, Winters MA, Meacle FJ, Buckland BC, Lee AL. 2002. Fractional precipitation of plasmid DNA from lysate by CTAB. Biotechnol Bioeng 79(7):776-84.

Lange H, Taillandier P, Riba JP. 2001. Effect of high shear stress on microbial viability. J Chem Technol Biotechnol 76(5):501-05.

Lange R, Hengge-Aronis R. 1991. Growth phase-regulated expression of bolA and morphology of stationary-phase *Escherichia coli* cells are controlled by the novel sigma factor sigma S. J Bacteriol 173(14):4474-81.

Lankes H, Zanghi C, Santos K, Capella C, Duke C, Dewhurst S. 2007. *In vivo* gene delivery and expression by bacteriophage lambda vectors. J Appl Microbiol 102(5):1337-49.

Larocca D, Burg MA, Jensen-Pergakes K, Ravey EP, Gonzalez AM, Baird A. 2002. Evolving phage vectors for cell targeted gene delivery. Curr Pharm Biotechnol 3(1):45-57.

Larocca D, Jensen-Pergakes K, Burg MA, Baird A. 2001. Receptor-targeted gene delivery using multivalent phagemid particles. Mol Ther 3(4):476-84.

Lawrence JG, Ochman H. 1998. Molecular archaeology of the *Escherichia coli* genome. Proc Natl Acad Sci USA 95(16):9413-7.

Lee SW, Mao C, Flynn CE, Belcher AM. 2002. Ordering of quantum dots using genetically engineered viruses. Science 296(5569):892-95.

Lee Y, Yi H, Kim W, Kang K, Yun D, Strano M, Ceder G, Belcher A. 2009. Fabricating Genetically Engineered High-Power Lithium-Ion Batteries Using Multiple Virus Genes. Science 324(5930):1051.

Legendre D, Fastrez J. 2002. Construction and exploitation in model experiments of functional selection of a landscape library expressed from a phagemid. Gene 290(1-2):203-15.

Levy MS, Ciccolini LAS, Yim SSS, Tsai JT, Titchener-Hooker N, Ayazi-Shamlou P, Dunnill P. 1999a. The effects of material properties and fluid flow intensity on plasmid DNA recovery during cell lysis. Chem Eng Sci 54(15-16):3171-78.

Levy MS, Collins IJ, Tsai JT, Ayazi Shamlou P, Ward JM, Dunnill P. 2000a. Removal of contaminant nucleic acids by nitrocellulose filtration during pharmaceutical-grade plasmid DNA processing. J Biotechnol 76(2-3):197-205.

Levy MS, Collins IJ, Yim SS, Ward JM, Titchener-Hooker N, Ayazi-Shamlou P, Dunnill P. 1999b. Effect of shear on plasmid DNA in solution. Bioprocess Biosystems Eng 20(1):7-13.

Levy MS, Kennedy RD, Ayazi-Shamlou P, Dunnill P. 2000b. Biochemical engineering approaches to the challenges of producing pure plasmid DNA. Trends Biotechnol 18(7):296-305.

Li ZJ, Shukla V, Fordyce AP, Pedersen AG, Wenger KS, Marten MR. 2000. Fungal morphology and fragmentation behavior in a fed-batch *Aspergillus oryzae* fermentation at the production scale. Biotechnol Bioeng 70(3):300-12.

Liang Y, Shi B, Zhang J, Jiang H, Xu Y, Li Z, Gu J. 2006. Better gene expression by (-) gene than by (+) gene in phage gene delivery systems. Biotechnol Prog 22(3).

Lievense L, van't Riet K. 1993. Convective drying of bacteria. I: The drying processes. Adv Biochem Eng/Biotechnol 50:45-63.

Lin J, Lee I, Frey J, Slonczewski J, Foster J. 1995. Comparative analysis of extreme acid survival in *Salmonella typhimurium, Shigella flexneri,* and *Escherichia coli*. J Bacteriol 177(14):4097-104.

Ling T, Loong C, Tan W, Tey B, Abdullah W, Ariff A. 2004. Purification of filamentous bacteriophage M13 by expanded bed anion exchange chromatography. The Journal of Microbiology:228-32.

Lingwood RJ. 1995. Absolute instability of the boundary layer on a rotating disk. J Fluid Mech 299(17):17-33.

Lionberger R, Lee S, Lee L, Raw A, Yu L. 2008. Quality by Design: Concepts for ANDAs. AAPS J 10(2):268-76.

Litman S. 1997. The Facility Design Process. In: Goldberg E, editor. Handbook of Downstream Processing. London: Blackie. p 509-29.

Little J. 2006. Gene Regulatory Circuitry of Phage Lambda. In: Calendar R, Abedon S, editors. The Bacteriophages. 2nd ed. Oxford: Oxford University Press. p 74-81.

Loewen P, Hengge-Aronis R. 1994. The role of the sigma factor sigmas (KatF) in bacterial global regulation. Annual Reviews in Microbiology 48(1):53-80.

Luria S. 1945. Mutations of bacterial viruses affecting their host range. Genetics 30(1):84-99.

Mackay D. 1996. Broth Conditioning and Clarification. In: Verrall M, editor. Downstream Processing of Natural Products: A Practical Handbook. Chichester: John Wiley & Sons Ltd. p 11-40.

Mahadevan H, Hall C. 1990. Statistical-mechanical model of protein precipitation by nonionic polymer. AICHE J 36(10).

Mahadevan H, Hall C. 1992. Theory of precipitation of protein mixtures by nonionic polymer. AICHE J 38(4).

Makowski L. 1992. Terminating a macromolecular helix : Structural model for the minor proteins of bacteriophage M13. J Mol Biol 228(3):885-92.

Mao C, Solis D, Reiss B, Kottmann S, Sweeney R, Hayhurst A, Georgiou G, Iverson B, Belcher A. 2004. Virus-based toolkit for the directed synthesis of magnetic and semiconducting nanowires. Nano Lett 303(5655):213-17.

March J, Clark J, Jepson C. 2004. Genetic immunisation against hepatitis B using whole bacteriophage particles. Vaccine 22(13-14):1666-71.

Marks T, Sharp R. 2000. Bacteriophages and biotechnology: A review. J Chem Technol Biotechnol 75(1):6-17.

Marvin DA, Hoffman-Berling H. 1963. Physical and chemical properties of two new small bacteriophages. Nature 197 517-18.

Marvin DA, Hohn B. 1969. Filamentous bacterial viruses. Bacteriol Rev 33(2):172-209.

Matsuzaki S, Yasuda M, Nishikawa H, Kuroda M, Ujihara T, Shuin T, Shen Y, Jin Z, Fujimoto S, Nasimuzzaman M. 2003. Experimental protection of mice against lethal *Staphylococcus aureus* infection by novel bacteriophage MR11. J Infect Dis 187(4):613-24.

Mazzotta A. 2001. Thermal inactivation of stationary-phase and acid-adapted *Escherichia coli* O157: H7, *Salmonella*, and *Listeria monocytogenes* in fruit juices. J Food Prot 64(3):315-20.

McDonnell G. 2007. Antisepsis, Disinfection, and Sterilization: Types, Action, and Resistance. London: Wiley-Blackwell. 361 p.

McGrath S, Fitzgerald G, van Sinderen D. 2007. Bacteriophages in dairy products: Pros and cons. Biotechnology Journal 2(4):450-55.

McKetta J. 1993. Chemical Processing Handbook: CRC Press. 972 p.

McLean R, Mortimer A. 1988. A cavitation and free radical dosimeter for ultrasound. Ultrasound Med Biol 14(1):59-64.

Meacle FJ, Lander R, Ayazi Shamlou P, Titchener-Hooker NJ. 2004. Impact of engineering flow conditions on plasmid DNA yield and purity in chemical cell lysis operations. Biotechnol Bioeng 87(3):293-302.

Meola A, Delmastro P, Monaci P, Luzzago A, Nicosia A, Felici F, Cortese R, Galfre G. 1995. Derivation of vaccines from mimotopes. Immunologic properties of human hepatitis B virus surface antigen mimotopes displayed on filamentous phage. J Immunol 154(7):3162-72.

Merson M. 2006. The HIV-AIDS pandemic at 25--the global response. New Engl J Med 354(23):2414.

Messing J, Vieira J. 1982. A new pair of M13 vectors for selecting either DNA strand of double-digest restriction fragments. Gene 19(3):269-76.

Miles AA, Misra SS. 1938. The estimation of the bactericidal power of the blood. J Hyg 38:732-49.

Model P, Russel M. 1988. Filamentous bacteriophage. The bacteriophages. Oxford: Oxford University Press. p 375-456.

Model P, Russel M. 2006. Filamentous bacteriophage. In: Calendar R, Abedon ST, editors. The Bacteriophages. 2nd ed. Oxford: Oxford University Press. p 375-456.

Moineau S. 1999. Applications of phage resistance in lactic acid bacteria. Anton Leeuw 76(1):377-82.

Mollet M, Ma N, Zhao Y, Brodkey R, Taticek R, Chalmers JJ. 2004. Bioprocess equipment: characterization of energy dissipation rate and its potential to damage cells. Biotechnol Prog 20(5):1437-48.

Monteiro GA, Ferreira GN, Cabral JM, Prazeres DM. 1999. Analysis and use of endogenous nuclease activities in *Escherichia coli* lysates during the primary isolation of plasmids for gene therapy. Biotechnol Bioeng 66(3):189-94.

Moreton J, Delves H. 1999. Use of Virkon as a disinfectant for clinical samples carrying a high risk of infection in inductively coupled plasma mass spectrometry. J Anal At Spectrom 14(5):893-94.

Morrison J. 1932. Bacteriophage in the treatment and prevention of cholera. London: HK Lewis & Co.

Morrison M, Bayse GS, Michaels AW. 1971. Determination of spectral properties of aqueous I2 and I3 and the equilibrium constant. Anal Biochem 42(1):195-201.

Moses PB, Boeke JD, Horiuchi K, Zinder ND. 1980. Restructuring the bacteriophage f1 genome: expression of gene VIII in the intergenic space. Virology 104(2):267-78.

Mullen L, Nair S, Ward J, Rycroft A, Williams R, Henderson B. 2007. Comparative functional genomic analysis of Pasteurellaceae adhesins using phage display. Vet Microbiol 122(1-2):123-34.

Murphy JC, Wibbenmeyer JA, Fox GE, Willson RC. 1999. Purification of plasmid DNA using selective precipitation by compaction agents. Nat Biotechnol 17(8):822.

Nagaraj N, Sampangi C, Karumanchi SMSR; 2005 03/08/05. Process for separation and recovery of polyethylene glycol (PEG) from spent aqueous two-phase systems. Patent US 6863828.

Nakai T, Park S. 2002. Bacteriophage therapy of infectious diseases in aquaculture. Res Microbiol 153(1):13-18.

Nam K, Kim D, Yoo P, Chiang C, Meethong N, Hammond P, Chiang Y, Belcher A. 2006. Virus-enabled synthesis and assembly of nanowires for lithium ion battery electrodes. Science 312(5775):885-88.

Negrete A, Ling TC, Lyddiatt A. 2007. Aqueous two-phase recovery of bio-nanoparticles: A miniaturization study for the recovery of bacteriophage T4. J Chromatogr B 854(1-2):13-19.

Odell JA, Taylor MA. 1994. Dynamics and thermomechanical stability of DNA in solution. Biopolymers 34(11):1483-93.

Oliva A, Santovena A, Farina J, Llabres M. 2003. Effect of high shear rate on stability of proteins: kinetic study. J Pharm Biomed Anal 33(2):145-55.

Overman S, Tsuboi M, Thomas Jr G. 1996. Subunit orientation in the filamentous virus Ff (fd, f1, M13). J Mol Biol 259(3):331-36.

Paithankar KR, Prasad KSN. 1991. Precipitation of DNA by polyethylene glycol and ethanol. Nucleic Acids Res 19(6):1346.

Papamichael N, Kula MR. 1987. A hydrodynamic study of the retention of polyethylene glycols by cellulose acetate membranes in the absence and presence of proteins. J Membr Sci 30(3):259-72.

Parfitt T. 2005. Georgia: an unlikely stronghold for bacteriophage therapy. Lancet 365(9478):2166-67.

Pelta J, Livolant F, Sikorav JL. 1996. DNA aggregation induced by polyamines and cobalthexamine. J Biol Chem 271(10):5656-62.

Perry RH, Green DW, Maloney JO. 1998. Perry's Chemical Engineers' Handbook: McGraw-Hill.

Petrenko V, Vodyanoy V. 2003. Phage display for detection of biological threat agents. J Microbiol Methods 53(2):253-62.

Petrides D. 2003. Bioprocess Design. In: Harrison R, Todd P, Rudge S, Pretrides D, editors. Bioseparations Science and Engineering. Oxford: Oxford University Press. p 319-72.

Pollard E, Solosko W. 1971. The thermal inactivation of T4 and bacteriophage lambda. Biophys J 11(1):66-74.

Pommier S, Gavioli M, Cascales E, Lloubes R. 2005. Tol-dependent macromolecule import through the *Escherichia coli* cell envelope requires the presence of an exposed TolA binding motif. J Bacteriol 187(21):7526-34.

Poul MA, Marks JD. 1999. Targeted gene delivery to mammalian cells by filamentous bacteriophage. J Mol Biol 288(2):203-11.

Prazeres S, Ferreira HG. 2004. Design of flowsheets for the recovery and purification of plasmids for gene therapy and DNA vaccination. Chem Eng Process 43(5):609-24.

Prouty C. 1953. Storage of the bacteriophage of the lactic acid streptococci in the desiccated state with observations on longevity. Appl Environ Microbiol 1(5):250-51.

Przybycien T, Pujar N, Steele L. 2004. Alternative bioseparation operations: Life beyond packed-bed chromatography. Curr Opin Biotechnol 15(5):469-78.

Rahn O. 1945. Physical methods of sterilization of microorganisms. Microbiol Mol Biol Rev 9(1):1-47.

Ramesh V, Fralick J, Rolfe R. 1999. Prevention of *Clostridium difficile*-induced ileocecitis with bacteriophage. Anaerobe 5(2):69-78.

Rathore AS, Winkle H. 2009. Quality by design for biopharmaceuticals. Nat Biotechnol 27(1):26-34.

Reddy P, McKenney K. 1996. Improved method for the production of M13 phage and single-stranded DNA for DNA sequencing. BioTechniques 20(5):854-60.

Reed S, Laxminarayan R, Black D, Sullivan S. 2002. Economic issues and antibiotic resistance in the community. Ann Pharmacother 36(1):148-54.

Reynolds T, Boychyn M, Sanderson T, Bulmer M, More J, Hoare M. 2003. Scale-down of continuous filtration for rapid bioprocess design: Recovery and dewatering of protein precipitate suspensions. Biotechnol Bioeng 83(4).

Rodrigues T, Carrondo MJ, Alves PM, Cruz PE. 2007. Purification of retroviral vectors for clinical application: biological implications and technological challenges. J Biotechnol 127(3):520-41.

Rossomando EF, Zinder ND. 1968. Studies on the bacteriophage f1. J Mol Biol 36:387-99.

Roy A, Mitra S. 1970. Increased fragility of *Escherichia coli* after infection with bacteriophage M13. J Virol 6(3):333-39.

Russel M. 1995. Moving through the membrane with filamentous phages. Trends Microbiol 3(6):223-28.

Russel M, Lowman HB, Clackson T. 2004. Introduction to Phage Biology and Phage Display. In: Clackson T, Lowman HB, editors. Phage Display: Oxford p1-26.

Russel M, Model P. 1989. Genetic analysis of the filamentous bacteriophage packaging signal and of the proteins that interact with it. J Virol 63(8):3284-95.

Salivar WO, Tzagoloff H, Pratt D. 1964. Some physical-chemical and biological properties of the rod-shaped coliphage M13. Virology 24:359-71.

Sambrook J, Russell DW. 2001. Molecular Cloning: A Laboratory Manual: Cold Spring Harbor Laboratory Press. A8.40 p.

Santella RM. 2006. Approaches to DNA/RNA extraction and whole genome amplification. Cancer Epidemiol Biomarkers Prev 15(9):1585-7.

Sargeant K. 1970. Large-scale bacteriophage production. Adv Appl Microbiol 13 121-37.

Sargeant K, Yeo R. 1966. The production of bacteriophage mu 2. Biotechnol Bioeng 8(2).

Sargeant K, Yeo RG, Lethbridge JH, Shooter KV. 1968. Production of bacteriophage T7. J Appl Microbiol 16(10):1483-88.

Sarli M. 2007. Regulatory Constraints on Disinfectants and Decontamination. In: Manivannan G, editor. Disinfection and Decontamination: Principles, Applications and Related Issues. New York: CRC Press.

Sathaliyawala T, Rao M, Maclean D, Birx D, Alving C, Rao V. 2006. Assembly of human immunodeficiency virus (HIV) antigens on bacteriophage T4: a novel in vitro approach to construct multicomponent HIV vaccines. The Journal of Virology 80(15):7688.

Schade A, Caroline L. 1944. The preparation of a polyvalent dysentery bacteriophage in a dry and stable form II. Factors affecting the stabilization of dysentery bacteriophage during lyophilization. J Bacteriol 48(2):179-90.

Schlichting H. 2000. Boundary Layer Theory. Berlin: Springer. 801 p.

Schmidt FG, Hinner B, Sackmann E, Tang JX. 2000. Viscoelastic properties of semiflexible filamentous bacteriophage fd. Phys Rev E 62(4):5509-17.

Schmidt FR. 2004. Recombinant expression systems in the pharmaceutical industry. Appl Microbiol Biotechnol 65(4):363-72.

Schmidt J. 1966. Observations on the adsorption of *Caulobacter* bacteriophages containing ribonucleic acid. Microbiology 45(2):347-53.

Sharma VK, Kalonia DS. 2004. Polyethylene glycol-induced precipitation of interferon alpha-2a followed by vacuum drying: development of a novel process for obtaining a dry, stable powder. AAPS PharmSci 6(1):E4.

Sherwood D. 1996. GMP and Quality Control. In: Verrall M, editor. Downstream Processing of Natural Products: A Practical Handbook. Chichester: John Wiley & Sons Ltd. p 329-46.

Shors T. 2008. Understanding Viruses: Jones & Bartlett Publishers. 639 p.

Shreir LL, Jarman RA, Burstein GT. 1994. Corrosion. Oxford: Butterworth-Heinemann. 1408 p.

Shulgin IL, Ruckenstein E. 2006. Preferential hydration and solubility of proteins in aqueous solutions of polyethylene glycol. Biophys Chem 120(3):188-98.

Siquet-Descans F, Calberg-Bacq CM, Delcambe L. 1973. Large scale production of bacteriophage Phi x 174. Biotechnol Bioeng 15 (5):927-32.

Small P, Blankenhorn D, Welty D, Zinser E, Slonczewski J. 1994. Acid and base resistance in *Escherichia coli* and *Shigella flexneri:* role of rpoS and growth pH. J Bacteriol 176(6):1729-37.

Smith G, Gingrich T. 2005. Hydroxyapatite chromatography of phage-display virions. BioTechniques 39(6):879.

Smith GP. 1985. Filamentous fusion phage: novel expression vectors that display cloned antigens on the virion surface. Science 228:1315-17.

Smith H, Huggins M. 1982. Successful treatment of experimental *Escherichia coli* infections in mice using phage: its general superiority over antibiotics. Microbiology 128(2):307.

Smith H, Huggins M. 1983. Effectiveness of phages in treating experimental *Escherichia coli* diarrhoea in calves, piglets and lambs. Microbiology 129(8):2659.

Smith H, Huggins M, Shaw K. 1987. The control of experimental *Escherichia coli* diarrhoea in calves by means of bacteriophages. Microbiology 133(5):1111.

Smrekar F, Ciringer M, Peterka M, Podgornik A, ätrancar A. 2008. Purification and concentration of bacteriophage T4 using monolithic chromatographic supports. J Chromatogr B 861(2):177-80.

Sofer G. 1995. Validation of biotechnology products and processes. Curr Opin Biotechnol 6(2):230-34.

Solomon B. 2008. Filamentous Bacteriophage as a Novel Therapeutic Tool for Alzheimer's Disease Treatment. J Alzheimer's Dis 15(2):193-98.

Songer J. 1967. Influence of relative humidity on the survival of some airborne viruses. Appl Environ Microbiol 15(1):35-42.

Steiner D, Forrer P, Stumpp MT, Pluckthun A. 2006. Signal sequences directing cotranslational translocation expand the range of proteins amenable to phage display. Nat Biotechnol 24(7):823-31.

Stryer L. 1995. Biochemistry. New York: W. H. Freeman and Company. 1064 p.

Suciu D, Inouye M. 1996. The 19-residue pro-peptide of staphylococcal nuclease has a profound secretion-enhancing ability in *Escherichia coli*. Mol Microbiol 21(1):181-95.

Sulakvelidze A, Alavidze Z, Morris J. 2001. Bacteriophage therapy. Antimicrob Agents Chemother 45(3):649-59.

Sulakvelidze A, Kutter E. 2005. Bacteriophage Therapy in Humans. In: Kutter E, Sulakvelidze A, editors. Bacteriophages: CRC Press. p 381-436.

Summers WC. 2005. Bacteriophage Research: Early History. In: Kutter E, Sulakvelidze A, editors. Bacteriophages: CRC Press. p 5-28.

Sutton R, Rockett B, Swindells P. 2000. Chemistry for the Life Sciences: CRC Press. 208 p.

Swartz JR. 2001. Advances in *Escherichia coli* production of therapeutic proteins. Curr Opin Biotechnol 12(2):195-201.

Tang JX, Janmey PA, Lyubartsev A, Nordenskiold L. 2002. Metal ion-induced lateral aggregation of filamentous viruses fd and M13. Biophys J 83(1):566-81.

Teeters M, Conrardy S, Thomas B, Root T, Lightfoot E. 2003. Adsorptive membrane chromatography for purification of plasmid DNA. J Chromatogr 989(1):165-73.

Thomas CR, Nienow AW, Dunnill P. 1979. Action of shear on enzymes: studies with alcohol dehydrogenase. Biotechnol Bioeng 21(12):2263-78.

Thommes J, Etzel M. 2007. Alternatives to chromatographic separations. Biotechnol Prog 23(1).

Thompson SS, Yates MV. 1999. Bacteriophage inactivation at the air-water-solid interface in dynamic batch systems. Appl Environ Microbiol 65(3):1186-90.

Tinnes R, Hoare M. 1992. The biocontainment of a high speed disc bowl centrifuge. Bioprocess Biosystems Eng 8(3):165-72.

Tomanee P, Hsu JT, Ito Y. 2004. Fractionation of protein, RNA, and plasmid DNA in centrifugal precipitation chromatography using cationic surfactant CTAB containing inorganic salts NaCl and NH(4)Cl. Biotechnol Bioeng 88(1):52-9.

Tsoka S, Ciniawskyj OC, Thomas OR, Titchener-Hooker NJ, Hoare M. 2000. Selective flocculation and precipitation for the improvement of virus-like particle recovery from yeast homogenate. Biotechnol Prog 16(4):661-7.

Tustian A. 2008. An Engineering Study of Key Interactions within the Process for Antibody Fragment Production. London: University College London. 272 p.

Tustian AD, Salte H, Willoughby NA, Hassan I, Rose MH, Baganz F, Hoare M, Titchener-Hooker NJ. 2007. Adapted ultra scale-down approach for predicting the centrifugal separation behavior of high cell density cultures. Biotechnol Prog 23(6):1404-10.

Twort F. 1915. An investigation on the nature of ultra-microscopic viruses. Lancet 2:1241-43.

USDA/FSIS. 2008a. *E. coli* O157:H7 targeted bacteriophages applied as a spay mist or wash on the hides of live animals in the holding pens prior to slaughter. Case Number 06-NT-0239-N-A.

USDA/FSIS. 2008b. *Salmonella* targeted bacteriophage products applied on the feathers of live poultry prior to slaughter. Case Number 08-NT-0318-N-C.

USDA/FSIS. 2008c. *Salmonella* targeted bacteriophages applied as a spray mist or wash on the hides of live animals in the holding pens prior to slaughter. Case Number 07-NT-0253-N-A.

Vajda B. 1978. Concentration and purification of viruses and bacteriophages with polyethylene glycol. Folia Microbiol 23(1):88-96.

van Houten N, Zwick M, Menendez A, Scott J. 2006. Filamentous phage as an immunogenic carrier to elicit focused antibody responses against a synthetic peptide. Vaccine 24(19):4188-200.

Wagenaar J, Bergen M, Mueller M, Wassenaar T, Carlton R. 2005. Phage therapy reduces *Campylobacter jejuni* colonization in broilers. Vet Microbiol 109(3-4):275-83.

Walker J. 1929. The protective effect of bacteriophage against the simultaneous injection of colon bacilli. Am J Dis Children 23:531.

Walsh G. 2006. Biopharmaceutical benchmarks 2006. Nat Biotechnol 24(7):769-76.

Wan Y, Wu Y, Bian J, Wang X, Zhou W, Jia Z, Tan Y, Zhou L. 2001. Induction of hepatitis B virus-specific cytotoxic T lymphocytes response *in vivo* by filamentous phage display vaccine. Vaccine 19(20-22):2918-23.

Wang L, Yu M. 2004. Epitope identification and discovery using phage display libraries: applications in vaccine development and diagnostics. Curr Drug Targets 5(1):1.

Wardlaw A. 1999. Practical Statistics for Experimental Biologists. Chichester: John Wiley & Sons Ltd. 249 p.

Watts P, Long G, Meek M. 2004. Chloroform. Geneva: World Health Organization. 58 p.

Wayment D, Casadonte D. 2002. Design and calibration of a single-transducer variable-frequency sonication system. Ultrason Sonochem 9:189-95.

Webster RE, Lopez J. 1985. Structure and Assembly of the Class I Filamentous Bacteriophage. In: Casjens S, editor. Virus Structure and Assembly: Jones and Bartlett. p 235-67.

Weissler A, Cooper H, Snyder S. 1950. Chemical effect of ultrasonic waves: Oxidation of potassium iodide solution by carbon tetrachloride. J Am Chem Soc 72(4):1769-75.

Wenger M, DePhillips P, Price C, Bracewell D. 2007. An automated microscale chromatographic purification of virus-like particles as a strategy for process development. Biotechnol Appl Biochem 47(Pt 2):131.

Wenzig E, Lingg S, Kerzel P, Zeh G, Mersmann A. 1993. Comparison of selected methods for downstream processing in the production of bacterial lipase. Chem Eng Technol 16(6).

Westwater C, Kasman LM, Schofield DA, Werner PA, Dolan JW, Schmidt MG, Norris JS. 2003. Use of genetically engineered phage to deliver antimicrobial agents to bacteria: an alternative therapy for treatment of bacterial infections. Antimicrob Agents Chemother 47(4):1301-07.

Whaley S, English D, Hu E, Barbara P, Belcher A. 2000. Selection of peptides with semiconductor binding specificity for directed nanocrystal assembly. Nature 405(6787):665-68.

Wheelwright S. 1987. Designing downstream processes for large-scale protein purification. Nat Biotechnol 5(8):789-93.

Whyte W. 1991. Cleanroom Design. Chichester: John Wiley & Sons Ltd. 357 p.

Wimo A, Winblad B, Jonsson L. 2007. An estimate of the total worldwide societal costs of dementia in 2005. Alzheimer's Dement 3(2):81-91.

Winzor DJ. 2003. Surface plasmon resonance as a probe of protein isomerization. Anal Biochem 318(1):1-12.

Withington R. 2001. Regulatory issues for phage-based clinical products. J Chem Technol Biotechnol 76 673-76.

Wright A, Hawkins C, Anggard E, Harper D. 2009. A controlled clinical trial of a therapeutic bacteriophage preparation in chronic otitis due to antibiotic-resistant *Pseudomonas aeruginosa*: a preliminary report of efficacy. Clinical Otolaryngology 34(4):349-57.

Yamamoto KR, Alberts BM, Benzinger R, Lawhorne L, Treiber G. 1970. Rapid bacteriophage sedimentation in presence of polyethylene glycol and its application to large-scale virus purification. Virology 40(3):734-44.

Yan JX, Harry RA, Spibey C, Dunn MJ. 2000. Postelectrophoretic staining of proteins separated by two-dimensional gel electrophoresis using SYPRO dyes. Electrophoresis 21(17):3657-65.

Yanisch-Perron C, Vieira J, Messing J. 1985. Improved M13 phage cloning vectors and host strains: nucleotide sequences of the M13mp18 and pUC19 vectors. Gene 33(1):103-19.

Yau S, Keshavarz-Moore E, Ward J. 2008. Host strain influences on supercoiled plasmid DNA production in *Escherichia coli*: Implications for efficient design of large-scale processes. Biotechnol Bioeng 101(3).

Yim SSS, Shamlou PA. 2000. The engineering effects of fluids flow on freely suspended biological macro-materials and macromolecules. Berlin/ Heidelberg: Springer.

Yoo PJ, Nam KT, Qi J, Lee SK, Park J, Belcher AM, Hammond PT. 2006. Spontaneous assembly of viruses on multilayered polymer surfaces. Nat Mater 5:234-40.

Zanghi CN, Lankes HA, Bradel-Tretheway B, Wegman J, Dewhurst S. 2005. A simple method for displaying recalcitrant proteins on the surface of bacteriophage lambda. Nucleic Acids Res 33(18):e160.

Zhang H, Kong S, Booth A, Boushaba R, Levy MS, Hoare M. 2007. Prediction of shear damage of plasmid DNA in pump and centrifuge operations using an ultra scale-down device. Biotechnol Prog 23(4):858-65.

Zhang Y, Cremer PS. 2006. Interactions between macromolecules and ions: The Hofmeister series. Curr Opin Chem Biol 10(6):658-63.

Zhao K, Gan Y, Zhang ZJ. 2005. A study of fermentation for human interleukin-11 with recombinant *E. coli*. International Journal of Chemical and Reactor Engineering 3(3):1281.

Zielenkiewicz U, Ceglowski P. 2001. Mechanisms of plasmid stable maintenance with special focus on plasmid addiction systems. Acta Biochim Pol 48(4):1003-24.

Zimmermann K, Hagedorn H, Heuck CC, Hinrichsen M, Ludwig H. 1986. The ionic properties of the filamentous bacteriophages Pf1 and fd. J Biol Chem 261(4):1653-55.

Interesting… but I don't agree.

– Kath Day-Knight